HSE

Health and Safety Executive

Area classification for secondary releases from low pressure natural gas systems

Prepared by the **Health and Safety Laboratory**
for the Health and Safety Executive 2008

RR630
Research Report

HSE

Health and Safety Executive

Area classification for secondary releases from low pressure natural gas systems

Dr M J Ivings, Mr S Clarke, Dr S E Gant, Mr B Fletcher, Dr A Heather, Mr D J Pocock, Dr D K Pritchard, Mr R Santon, Mr C J Saunders

Health and Safety Laboratory
Harpur Hill
Buxton
Derbyshire
SK17 9JN

The ATEX Workplace Directive (1999/92/EC) has been implemented in the UK as the Dangerous Substances and Explosive Atmospheres Regulations (DSEAR) 2002 and by similar regulations in other EU member states. These regulations require area classification to be carried out where there may be a risk of explosion due to the presence of flammable substances in the form of gases, vapours, mist or dust. Any equipment used to ensure safe operation in a classified hazardous area falls within the scope of the regulations. The regulations have major implications for all non-domestic natural gas installations. Whilst area classification has been applied to high-pressure natural gas installations in the past, it is now necessary to consider it for all pressures including distribution pressure.

Hazardous areas are classified into zones based on the frequency of the occurrence and the duration of an explosive gas atmosphere. In the case of a secondary release, the relevant zone is zone 2 and is defined as a place where an explosive atmosphere is not likely to occur in normal operation but, if it does occur, will persist for a short period only. In areas where the ventilation can be regarded as 'high' relative to the leak size, BS EN 60079:10 recommends that the area classification is zone 2 but of negligible extent (NE) such that no action is thus required to control sources of ignition within it.

This report and the work it describes were funded by the Health and Safety Executive (HSE). Its contents, including any opinions and/or conclusions expressed, are those of the authors alone and do not necessarily reflect HSE policy.

HSE Books

First published 2008

ACKNOWLEDGEMENTS

We gratefully acknowledge the funding, support and technical input provided by the sponsors of this joint industry project:

Health and Safety Executive, UK
Burgoyne Consultants, UK
Corus Construction and Industrial, UK
Danish Gas Technology Centre, Denmark
Directorate for Civil Protection and Emergency Planning, Norway
EnergieNed, The Netherlands
EON-UK, UK
Epsilon Compliance (Europe), UK
Gastec Technology, The Netherlands
Gasunie, The Netherlands
Hamworthy Combustion, UK
Knauf Insulation Ltd, UK
National Grid, UK
Northern Gas Networks, UK
SGL Technic Ltd, UK
Slough Heat and Power, UK

We also gratefully acknowledge the input provided by Barrie Church and Geoff Winckles (Global Energy Associates Ltd), Chris Lea (Lea CFD Associates) and Malcolm Howe (IGEM).

CONTENTS

EXECUTIVE SUMMARY

Background

The ATEX Workplace Directive (1999/92/EC) has been implemented in the UK as the Dangerous Substances and Explosive Atmospheres Regulations (DSEAR) 2002 and by similar regulations in other EU member states. These regulations require area classification to be carried out where there may be a risk of explosion due to the presence of flammable substances in the form of gases, vapours, mist or dust. Any equipment used to ensure safe operation in a classified hazardous area falls within the scope of the regulations. The regulations have major implications for all non-domestic natural gas installations. Whilst area classification has been applied to high-pressure natural gas installations in the past, it is now necessary to consider it for all pressures including distribution pressure.

Hazardous areas are classified into zones based on the frequency of the occurrence and the duration of an explosive gas atmosphere. In the case of a secondary release, the relevant zone is zone 2 and is defined as a place where an explosive atmosphere is not likely to occur in normal operation but, if it does occur, will persist for a short period only. In areas where the ventilation can be regarded as 'high' relative to the leak size, BS EN 60079:10 recommends that the area classification is zone 2 but of negligible extent (NE) such that no action is thus required to control sources of ignition within it.

Current methodologies available for carrying out area classification applied to low pressure indoor gas systems generally result in a zone 2 requirement, but the gas industry has maintained that the incidence of fires or explosions following foreseeable small leaks from flanges, fittings, joints etc. is so low in typical well ventilated locations that area classification is inappropriate. Recent work (Gant and Ivings, 2005) has demonstrated that these methodologies lead to a very large degree of conservatism when applied to outdoor systems.

BS EN 60079:10 defines the degree or effectiveness of the ventilation on the basis of a calculated hypothetical parameter V_z, which is also defined as the volume within which the mean concentration of flammable gas arising from a release will be (for secondary releases) 50% of the Lower Explosive Limit (LEL). The standard gives a method for the calculation of V_z, for indoor situations, using the enclosure air change rate and release rate. Subsequent to the calculation of V_z, area classification can then be associated with ventilation since the standard allows the concept of negligible extent to be applied if V_z is less than 0.1 m^3.

Objectives

The aim of this project was to devise a more soundly based methodology for defining zone 2 NE applied to the area classification of low pressure (<10 barg) equipment with the possibility of removing a significant amount of conservatism from the method given in BS EN 60079:10.

The following objectives were set to meet this aim:

- Carry out a review of methods for assessing the effectiveness of ventilation for preventing the build up of gas following a secondary leak. Also review methods for calculating the ventilation rate of naturally ventilated enclosures and make a recommendation on an approach that can be used in an area classification methodology.

- Confirm that the hazard posed by a leak giving a gas cloud with an average concentration of ½ LEL and smaller than 0.1 m^3 is low and therefore its appropriateness as the basis for defining zone 2 NE.

- Carry out a series of experiments to provide data to validate a Computational Fluid Dynamics (CFD) model for predicting gas cloud build up from low pressure, high momentum leaks in enclosures. Simulate these experimental tests using the CFD model and assess its ability to accurately predict the gas concentration field.

- Use the validated CFD model to provide data that can be used to define a methodology for area classification for low pressure secondary gas leaks in enclosures. In particular correlate the gas cloud volume against the mass release rate and ventilation rate.

- Describe how these data can be used for area classification of low pressure gas systems in enclosures and outdoors.

Main Findings

A review has been carried out on the ventilation of enclosures focusing on measures of ventilation effectiveness and how ventilation rates can be measured for input into an area classification methodology. The most accurate approach to calculating air change rates for naturally ventilated enclosures is to make measurements of the decay rate of a tracer gas within the enclosure. However, the time and expense required to do this means that it is not an approach suitable for area classification. BS 5925 describes a method for calculating air change rates that is simple to apply and should provide data of sufficient accuracy to be appropriate for area classification. The approach has been applied to two enclosures where the air change rate was measured experimentally. In the first of the two cases considered, the calculated air change rate was in good agreement with the measurements, whereas in the other case it under-predicted the ventilation rate. An appropriate conservative choice of the wind speed, say 0.5 m/s, should provide corresponding conservative estimates of the ventilation rate.

As part of the ventilation review, BS EN 60079:10 has been reviewed in detail and in this report we have made a clear distinction between the two definitions given for the gas cloud volume V_z. They are:

- a hypothetical volume that can be calculated using the formula in BS EN 60079:10 and is proportional to the mass release rate of a leak divided by the air change rate of the enclosure. V_z in this context is therefore simply a measure of ventilation effectiveness and the criterion V_z less than 0.1 m^3 is used to define zone 2 NE.

- a gas cloud that has an average gas concentration of ½ LEL.

Both of the above definitions of V_z are in BS EN 60079:10 and the current work has highlighted the differences between them. This work has shown that the two descriptions of V_z above are not equivalent, i.e. the calculation method in BS EN 60079:10 for V_z does not provide reasonable estimates of the volume of the gas cloud whose average gas concentration is ½ LEL. Furthermore, V_z calculated using BS EN 60079:10 has been found to be up to three orders of magnitude larger than the gas cloud volume V_z predicted by using a validated CFD model. The greatest differences are seen in the largest enclosures. This implies that use of BS EN 60079:10 for calculating V_z significantly over estimates the hazard and therefore leads to areas requiring a higher classification than is necessary.

The hazard associated with a leak that leads to a V_z of 0.1 m^3 has been assessed through experiments and modelling. The work has shown that the hazard is low in terms of the overpressure created on ignition of the cloud and the thermal radiation associated with the explosion and subsequent jet flame. Igniting gas clouds created by a leak leading to $V_z = 0.1$ m^3 was found to be difficult and a powerful ignition source was required. When ignition of the gas

cloud was achieved it resulted in overpressures up to 4 mbarg in a 31 m^3 enclosure. This work has shown that the V_z criterion in BS EN 60079:10, i.e. $V_z < 0.1$ m^3 is required for zone 2 NE, is appropriate for area classification, where V_z is predicted using a validated physically based model that takes into account the interaction of the leak with the ventilation flow.

However, the overpressure resulting from the ignition of a fixed volume of flammable gas (e.g. $V_z = 0.1$ m^3) increases as the enclosure volume decreases. So whilst it has been demonstrated that the V_z criterion is conservative, and can therefore be adopted as a basis for safety for large enclosures, it is not appropriate to do so for small enclosures. An appropriate cut-off would appear to be around 10 m^3 since this implies a theoretical maximum overpressure of 12.5 mbar. Below 10 m^3 the maximum value of V_z should be smaller therefore and an additional criterion has been introduced requiring that V_z should be less than 1% of the enclosure volume for zone 2NE to be applicable.

An approach to zoning outdoors has been developed based on a conservative estimate of the leak rate required to produce a gas cloud with $V_z = 0.1$ m^3 outdoors. For releases in the open air it has been shown that the largest gas cloud sizes result from conditions where the leak is aligned to the wind direction and the wind speed is low. We have therefore been able to apply an integral free jet model, GaJet, to calculate the pressure and hole size required to give a gas cloud with $V_z = 0.1$ m^3. For choked releases (for methane, where the pressure is above 0.85 barg) the gas cloud volume is dependent only on the mass release rate. It has been shown that the presence of obstructions near to the leak source can act to increase the resulting gas cloud volume compared to the equivalent unobstructed case. It has also been shown that a leak rate of 1 g/s provides a conservative estimate of the leak rate required to give $V_z = 0.1$ m^3 in an outdoor environment. However, this criterion may not be appropriate in cases where there is a high level of congestion, or an arrangement of obstacles that leads to re-entrainment of gas into the jet or reduces the dilution of the jet more significantly than for any of the cases considered in this project. Therefore, for secondary releases in locations that are not heavily congested / confined, leaks rate less than 1 g/s can be appropriately classed as zone 2 NE. For completely unobstructed releases a less conservative approach can be adopted and 2 g/s is a suitable maximum leak rate for zone 2 NE. For a given pressure and hole size, the leak rate can be estimated using standard equations that are included in this report.

The ventilation in an enclosure is not expected to be any more efficient at diluting a gas leak than if the leak occurred outdoors. By definition, releases within enclosures are likely to experience some form of confinement. Therefore, it is also appropriate to apply the mass release rate criterion for outdoor obstructed releases, 1 g/s, as an upper bound on the release rate for zone 2NE in an enclosure.

An alternative approach to measuring the ventilation effectiveness in enclosures to that in BS EN 60079:10 (i.e. V_z) has been suggested based on the average gas concentration at the outlet. It has been shown that this is equivalent to an assessment of the air entrainment requirement of the leak compared to the ventilation rate. The current approach differs significantly from BS EN 60079:10 in two key ways. Firstly, the average gas concentration at the outlet is dependent on the ventilation rate as opposed to V_z calculated using BS EN 60079:10 which is dependent on the air change rate of the enclosure. This therefore means that the measure of ventilation effectiveness (i.e. the average gas concentration at the outlet) increases as the enclosure volume increases for a fixed air change rate. Secondly, and most importantly, this new measure of ventilation effectiveness is based on a physical understanding of the behaviour of the dispersion of high momentum jets and has been evaluated here against data on gas cloud build up in enclosures.

A validated CFD model has been used to provide data on gas cloud volumes for low pressure gas leaks in enclosures. The data show that there is a strong correlation between the average gas concentration at the outlet, c_{out}, and the gas cloud volume, V_z. For the majority of cases examined, where the average concentration at the outlet was less than 10% LEL the gas cloud volume V_z was found to be less than 0.1 m^3. This suggests that the condition c_{out} < 10% LEL would provide a more suitable criterion for zone 2 NE rather than using the calculation method for V_z in BS EN 60079:10. The approach described here removes a very large degree of conservatism from the zoning methodology described in BS EN 60079:10.

The CFD model simulations have shown that for the above approach to be applicable, the leak source must not be located within a confined space within an enclosure. It has been shown that local confinement of a leak can lead to re-entrainment of gas into the jet resulting in significantly larger gas cloud volumes than would be expected in an unconfined space. Such cases are more likely to occur in large enclosures where the jet length scale is smaller relative to the enclosure and there is more opportunity for short-circuiting of the ventilation to occur leading to stagnant regions. As there are so many factors affecting gas cloud build up, it is not possible to provide specific guidelines based on the current data on when a leak location should be described as confined.

The presence of a heat source in an enclosure has been shown to lead to reduced mixing and therefore greater gas cloud build up in some cases. In particular, large gas clouds can result from cases where a strong thermal stratification exists coupled with a confined leak location. However, in the absence of a confined leak location it would appear that the c_{out} < 10% LEL criterion is still appropriate.

The CFD model for the above work has been validated against 29 experimental tests carried out in a purpose built enclosure. The experimental tests consisted of releases of simulated methane gas for a range of leak rates and ventilation rates. Three different configurations of the release location and direction were tested and measurements of the point gas concentration measurements were used as the basis for the model validation. The results of the CFD simulations showed good agreement with the experimental data.

1 INTRODUCTION

1.1 ATEX AND DSEAR

The ATEX Workplace Directive (1999/92/EC) has been implemented in the UK as DSEAR, the Dangerous Substances and Explosive Atmospheres Regulations 2002 and by similar regulations in other EU member states. These regulations require area classification to be carried out where there may be a risk of explosion due to the presence of flammable substances in the form of gases, vapours, mist or dust. Any equipment used to ensure safe operation in a classified hazardous area falls within the scope of the regulations. The regulations have major implications for all non-domestic natural gas installations. Whilst area classification has been applied to high-pressure natural gas installations in the past, it is now necessary to consider it for all pressures including distribution pressure, and it has been required for new installations since 30th June 2003. However, the regulations are retrospective and were applied to existing installations from 30th June 2006.

1.2 AREA CLASSIFICATION

Hazardous areas are classified into zones based on the frequency of the occurrence and the duration of an explosive gas atmosphere. In the case of a secondary release, the relevant zone is zone 2, i.e. a place where an explosive atmosphere is not likely to occur in normal operation but, if it does occur, will persist for a short period only. In areas where the ventilation is 'high' relative to the leak size, BS EN 60079:10 recommends that the area classification is zone 2 but of negligible extent (NE), i.e. that no action is thus required to control sources of ignition within it.

In the UK, the main sources of area classification guidance are BS EN 60079 –10[1] (general guidance) and IGEM/SR/25 (guidance specific to natural gas). The recommendations provided by these documents have been increasingly regarded by trade associations, people working in industry and consultants as unjustifiably conservative for secondary releases from low-pressure gas installations. Recent work (Gant and Ivings, 2005) has demonstrated that these recommendations lead to a very large degree of conservatism when applied to outdoor systems. The same recommendations applied to low pressure indoor gas systems generally result in a zone 2 requirement, but the gas industry has maintained that the incidence of fires or explosions following foreseeable small leaks from flanges, fittings, joints etc. is so low in typical well ventilated locations that area classification is inappropriate. Risk assessment based arguments have been applied, but in many cases area classification is still applied by suppliers, required by users, or recommended by enforcing authorities or notified bodies. In the absence of alternative well-founded technical data and suitable criteria, recommendations and enforcement are not uniform nationally or internationally.

1.3 VENTILATION

The application of ventilation to area classification was probably first discussed in detail in the seminal publication Cox, Lees and Ang (1990), which recognised that 'The dispersion of leaks by ventilation is difficult to model and more work needs to be done in this area...". Despite this recommendation, the majority of practical work has concentrated on the hazards associated with poor ventilation rather than the benefits of good ventilation.

[1] *IEC 60079-10:2002 has been adopted as a European Standard and is published as a national standard by members of CENELEC. The UK version is thus BS EN 60079-10:2003*

Guidance on ventilation assessment is given in IGE/SR/25. Naturally ventilated indoor spaces are assessed on the basis of ventilator location and relative size, buoyancy effects and overall location. However, even if 'adequate' ventilation is demonstrated in accordance with this code, it recommends zone 2 within defined distances from secondary sources for all gas pressures, without any lower limit.

Other guidance on ventilation design may be found in standards and codes unrelated to area classification, such as CIBSE (2005).

BS EN 60079-10 defines the degree of ventilation, high medium or low, on the basis of a calculated hypothetical parameter V_z, which is additionally defined as the volume within which the mean concentration of flammable gas arising from a secondary release is 50% of the Lower Explosive Limit (LEL). The standard gives a method for the calculation of V_z, for indoor situations, using the enclosure air change rate and release rate. It is based on the presumption of instantaneous and homogeneous (perfect) mixing and therefore requires the adoption of an empirical correction factor. Subsequent to the calculation of V_z, area classification can then be associated with ventilation since the standard allows the concept of negligible extent (NE) to be applied if V_z is less than 0.1 m^3, thus defining the ventilation as 'high'. In such an event, unless the ventilation availability is 'poor' as defined by the standard, secondary releases give rise to zone 2 NE in which case no further precautions are required. The concept of V_z is, in effect, a special case of dilution ventilation.

The basic assumption of the standard and its criterion of V_z is that a cloud of this size is so small and contains so little flammable material that its ignition is an insignificant event and will cause no injury to persons in the vicinity or damage to equipment.

The calculation methods for V_z in the standard have been shown (Gant and Ivings, 2005) to give an unrealistically large V_z volume for outdoor releases. For indoor applications, the methodology is limited in its scope and has been found to be similarly limited in its application. Few real situations comply. Relevant and realistic definitions of acceptable natural and mechanical ventilation are clearly required for indoor locations so that the zone 2 NE concept can be applied to low pressure natural gas situations where it is appropriate.

1.4 LEAK SIZES

Area classification is, currently, fundamentally based on an estimate of the maximum foreseeable orifice size. This concept was first discussed in detail in Cox, Lees & Ang (1990) based on data available from the organisations represented on the steering committee by which it was produced. Standard hole sizes were postulated and recommended values proposed for different equipment types. As a direct consequence of this, a value of 0.25 mm^2 has become very widely accepted for gas fittings (flanges, screwed fittings, joints and valve glands), although larger values are also used for some specific applications. Some suppliers argue that these sizes are very conservative in relation to modern equipment.

Other sources of hole size data are available. For the purposes of this project a wide range of hole sizes and pressures relevant to those used in Europe have been examined. The following were identified as being of particular interest:

Pressure: 21 mbarg – standard supply pressure in the UK
500 mbarg, 2.5 barg, and 5 barg. These are cut–off values in use for Standards development in Europe.

Hole size: 0.25mm^2, 2.5mm^2 and 5mm^2. The two smaller hole sizes (0.25 and 2.5 mm^2) are often used for area classification.

The medium pressures actually used by the gas industry vary across the EU, e.g. 7 barg in UK, 8 barg in The Netherlands. The project will span pressures in these ranges up to 10 barg in order to define the maximum pressure for given hole sizes that will still satisfy the V_z criterion.

1.5 CRITERIA FOR ZONE 2 NE

As noted above, the parameter V_z within BS EN 60079-10 may be used as a criterion to define zone 2 NE. Despite the inherent difficulties of the application of the calculation methods given in the standard, the definition of V_z gives rise to a very conservative constraint. Typically for a free unobstructed high momentum release the gas cloud volume V_z will be approximately 25 times larger than the volume of gas above the lower explosive limit. Note that EU guidance document (Communication from the Commission, 2003) suggests that "*a continuous volume of over 10 litres (0.01 m^3) of explosive atmosphere in a confined space must always be regarded as a hazardous explosive atmosphere, irrespective of the size of the room*". Therefore the BS EN 60079:10 criterion is in general more conservative.

For the purposes of this project V_z will be estimated using Computational Fluid Dynamics (CFD). The validity of the use of V_z, if calculated or estimated by other means, has been provisionally accepted by the UK Health and Safety Executive (HSE) for outdoor applications in the UK. The acceptability of the use of alternative methods of estimation of V_z has been included in the draft revision of IEC 60079-10. It has been confirmed that the definition is likely to remain unchanged for the foreseeable future. Although other definitions of the flammable gas cloud volume could be used, V_z is used in this report to maintain consistency with IEC 60079:10.

It has been indicated informally that the selection of 0.1 m^3 as the limiting volume for V_z was based on experience and pragmatism and has no experimental or formal theoretical basis. In view of the significance of the criterion in the context of this project and thus in future area classification studies, experimental work has been carried out so far as is necessary to confirm its validity.

Using defined ventilation conditions and agreed orifice size(s) and gas pressure(s), it has been possible to set up a CFD model to calculate the gas cloud size under foreseeable conditions and evaluate it against the defined V_z. This has enabled limits to be set for the application of V_z, i.e. the limits for the safe application of zone 2 NE. Experimental tests have been used to validate the CFD for this particular application.

1.6 PROJECT AIMS AND SCOPE

The primary aim of this project is to provide an appropriate technical basis for realistic hazardous area classification for foreseeable secondary gas leaks from low pressure natural gas systems. This technical basis is founded on model predictions of gas cloud volumes, which result from gas releases over a range of hole sizes and pressures in naturally and mechanically ventilated spaces. Cloud volumes are correlated against enclosure volume and defined ventilation criteria. Model predictions are validated against experimental data.

The intention is to devise a more soundly-based methodology for defining zone 2 NE with the possibility of removing a significant amount of conservatism from the method given in BS EN 60079:10 with the potential for very significant cost savings for industry and enabling any costs to be restricted to areas of genuine risk.

The overall scope of the work is limited by the following factors:

- It was concerned only with secondary releases, i.e. a release which is not expected to occur in normal operation and, if it does occur, is likely to do so only infrequently and for short periods

- Zone 0 and 1 are out of scope, i.e. the aim of this work is to differentiate between the conditions suitable for zone 2 and zone 2 NE

- It is concerned only with natural gas (although the majority of the experiments and modelling will use methane)

1.7 RESEARCH PROGRAMME

This project was carried out in three main phases as described below:

Phase 1 – Ventilation and V_z criterion

The first aim of this phase of the project was to carry out a review of different methods for assessing the effectiveness of ventilation for preventing the build up of gas following a secondary leak. The main findings of this review are summarised in Section 2 of this report.

The criterion for zone 2 NE in BS EN 60079:10 is based on a requirement that V_z is less than 0.1 m^3. Therefore, the next stage of the this project was to firstly confirm that this criterion was not likely to be changed in the foreseeable future and then experimentally demonstrate that this criterion is conservative. This has been done by creating a gas cloud with $V_z = 0.1$ m^3, igniting it and assessing the hazard. This work is described in Section 4.

Phase 2 – CFD model validation

Measuring gas cloud volumes is difficult to do experimentally, therefore CFD modelling has been used which has the ability to assess gas cloud volumes as a function of mass release rate and ventilation rates. (All CFD modelling carried out in this project has used the general purpose CFD code ANSYS CFX). The first step therefore is to demonstrate that the approach is suitably accurate for the intended purpose through a model validation study.

A series of experimental gas releases at a range of gas pressures and hole sizes has been carried out and is described in Appendix D. For the purpose of the experimental tests, natural gas was replaced with a non-flammable simulated source of tracer gas that is easily detectable and with identical density. A number of point measurements of gas concentration were made once experimental conditions had reached steady state.

A CFD model was then set up and validated against the experimental data using the point gas concentration measurements as a basis for comparison. The technical detail of the CFD modelling approach and the results of the CFD model validation study can be found in Appendix D. Note that background information on the behaviour of high momentum gas leaks, and how to model them, can be found in Section 3.

Phase 3 – Data generation and interpretation

The final phase of this project was to use the validated CFD model to provide gas cloud volume data and correlate this against mass release rate, ventilation rate, leak orientation etc.. These data can then be used as a basis for area classification. The work carried out on zoning in outdoor situations is described in Section 5 and indoors is in Section 6.

2 VENTILATION

2.1 INTRODUCTION

The aim of this Section is to provide a review of the methods available for assessing the adequacy of the ventilation of enclosed spaces for controlling the build up of gas following a leak. It begins with a general review on the characteristics of ventilation and its interaction with leaks of natural gas. There are many techniques available for measuring ventilation effectiveness, but the one in most common usage is the room air change rate which is usually measured in air changes per hour (ach). This is discussed together with a description of the methods available for calculating it including the methodology in the standard BS 5925: 1991. Additionally, the results of applying this standard to calculate air change rates for typical enclosures are compared to on-site experimental measurements.

In the context of area classification, BS EN 60079:10 and IGE/SR/25 provide some methodologies and rules for assessing the adequacy of ventilation. These methodologies are very widely used within the UK and elsewhere and are discussed in detail below.

2.2 VENTILATION

The two basic types of ventilation are ‘natural’ and ‘forced’. Natural ventilation is air movement caused by wind or temperature effects and in the cases of open and semi-open areas, is the usual method of ventilation. Natural ventilation is the movement of air through openings in the fabric of the building due to a) static pressure differences caused by temperature differences between the interior and exterior of the building, b) wind pressure or c) (more usually) a combination of the two factors. Enclosed spaces can be ventilated naturally using well-positioned inlet/outlet openings. It should be appreciated that natural ventilation depends on conditions that are variable and in general cannot be controlled. Forced ventilation is air movement caused by mechanical means such as fans or other air movers. It is usually used in enclosed spaces and can be applied in the form of general ventilation throughout the whole enclosure or local ventilation to deal with small, well-defined gas leaks. Local exhaust ventilation (LEV) is a type of forced ventilation used where there are defined localised sources of release. It is often associated with the control of hazards to health but in some cases may have an influence on area classification, e.g. in paint spray booths. It is generally not applicable to the low pressure gas releases that are the subject of this research.

In the context used here, ventilation is the movement of air through or within an enclosure in order to minimise the flammable extent of a gas released within the volume. The applications to which this research is relevant are enclosures, rooms or buildings within which low pressure gas pipes and fittings have been installed. These include, for example, low pressure district regulator enclosures, gas distribution pipework in commercial and industrial premises and boiler houses. DSEAR applies to all such cases and area classification is thus required. The majority of these applications are ventilated naturally. Forced ventilation is not normally used for safety reasons but for environmental purposes, i.e. in air conditioned buildings or for the cooling of plant or machinery. In such cases, ventilation may not be seen as a safety feature and may therefore be of limited reliability.

Natural ventilation is normally provided in accordance with civil engineering standards or specific industry standards such as CIBSE, BS 5925 or IGE/SR/25. For boiler house design for example, the requirements for cooling and the availability of combustion air dictate the ventilation design. The ventilation requirements of the current area classification standards have

not generally been applied to enclosure ventilation design in relation to low pressure gas because the requirement for zoning has not been recognised.

2.2.1 General ventilation

There are many factors that affect the mixing of a release of gas into the ventilating air. The method and size of the release, the density of the gas being released and the presence of nearby surfaces will all influence the gas cloud formation. Interaction between the release and the air movement will also be a major factor. With general ventilation, the removal of contamination occurs between two extremes cases:

1. The gaseous contaminant is well-mixed throughout the space and contaminated air is extracted or displaced by the input air. This method of ventilation is often referred to as dilution ventilation and, although all the air within the space will be contaminated, the gaseous concentration will be low if the air flow volume is sufficient.

2. The gaseous contaminant is displaced from the enclosure with a minimum of mixing. This is sometimes referred to as plug flow. The air and gas are displaced through the volume as a plug. (Note that the gas cloud contained within the plug can be at a high concentration and this situation may persist over a large distance.) This type of flow can be produced by specifically engineered systems where a horizontal flow is produced or by inducing an upward vertical displacement using cool input air at a low level.

In practice the real situation lies between these two idealised extremes. Mixing within the space is never perfect: Recirculation of air occurs in corners and in the wakes of obstructions (creating dead zones), air ‘short circuits’ between inlet and extract and leakage occurs in numerous places. There is a need to quantify not only the magnitude of the true ventilation, but to evaluate its effectiveness in dealing with small leakage at specific locations in a room.

2.2.2 Quantification of general ventilation

Ventilation Standards traditionally quote airflow requirements in one of four ways:

- Air volume flow rate.
- Air volume flow rate per unit floor area.
- Volume flow rate per person.
- Volume flow rate per unit volume of the enclosure (air changes per hour).

The emphasis in each case is slightly different. Volume flow rate would be more relevant where there is a known contaminant generation rate i.e. for dilution of the contaminant. Dependence on floor area and enclosure volume relate the likely work activity, and therefore contaminant generation rate, to the required ventilation rate. Volume flow rate per person links ventilation rate to the degree of work activity and also to the comfort of the persons. For the purpose of area classification, volume flow rate is the most appropriate as a gas leak will require a certain volume flow rate of air to dilute it to a safe level.

2.2.3 Air change measurements

Air change rates can be calculated or measured in a number of ways. When the space is mechanically ventilated, it is the air velocity in a straight section of ductwork divided by the volume of the enclosure. Alternately if the characteristics of the fan are known the flow rate can

be determined from pressure readings and information from the manufacturer's fan curve. Again, once the flow rate has been determined the air change rate is calculated by dividing by the volume of the enclosure.

For naturally ventilated spaces the task is more difficult. One method is to use tracer gas techniques. These are well documented and give accurate results, however, the measurements are time consuming and require specialist knowledge. For the purposes of hazardous area classification the most appropriate seems to be the method described in BS 5925:1991 and therefore this is described in more detail in the next Section. Whilst BS 5925 refers to occupied buildings, there is no reason why the methods described in the document cannot be used as part of an area classification methodology.

2.3 BS 5925: 1991

The natural ventilation of buildings is covered by BS 5925: 1991. This document is a Code of Practice for ventilation principles and the design of natural ventilation in buildings. It gives recommendations on the principles that should be observed when designing the natural ventilation of buildings for human occupation. The rate of natural ventilation can be estimated based on the size and distribution of openings in a building, together with certain meteorological and thermal data.

The meteorological variables to be considered are wind speed and direction, and the external temperature. Not only do these factors affect the air supply rate but they also determine whether a particular opening will act as an inlet or outlet, or both. This in turn influences the effectiveness of the ventilation in mixing a contaminant within the building.

2.3.1 Flow through openings

Openings in a building can be broadly classified as cracks/small openings, typically with dimensions less than 10 mm, and openings, typically greater than 10 mm. The latter tend to be planned openings, for example airbricks and windows. The former are usually unplanned and are difficult to quantify. When a pressure difference is applied across an opening, a flow will take place from the high to the low-pressure region. The flow rate is dependent on the pressure difference across the opening and this is generated by either the wind or a temperature difference or a combination of the two. The wind pressure on the surface of a building depends on the wind speed and direction relative to the building, the shape of the building and its location and surroundings. If the wind direction remains constant, the pressure will vary with the square of the wind speed. The mean surface pressure over a surface can be defined in terms of a reference wind speed (usually taken as the undisturbed wind speed at the height of the building) and a surface pressure coefficient (examples given in BS 5925:1991). Values of the mean surface pressure coefficient for very simple building shapes can be found in CP3 (1972). For wind pressure only, air enters the building on the windward side and leaves on the leeside.

Gas density varies with the inverse of the absolute temperature and hence where a temperature difference between the inside and outside of a building exists, there will be a pressure difference. When there are two openings at different heights in a building where the internal temperature exceeds that outside, there will be airflow in through the lower opening and out at the higher one.

When both wind and temperature differences act, the flows are more complicated. On the windward side, the effects supplement each other at the lower level openings but oppose one another at the high level ones. On the leeward side, the converse is the case.

2.3.2 Meteorological variables

Not only is the wind turbulent but its mean speed also varies with height above the ground, the stability of the atmosphere and the roughness of the terrain over which it passes. The wind speeds variation with height can be taken to be

$$u = u_m K z^a \qquad (2.1)$$

where u is the wind speed at height z, u_m is the wind speed at a reference height (10 m in open country – data from the Meteorological Office) and K and a are constants depending on the terrain (and given in BS 5925). Statistical data on wind speed and direction can be found in Caton (1976,1977) and CIBSE (1986).

Ambient air temperatures vary from day to day and also throughout the 24 hour period. Statistical data can be found in publications from the Meteorological Office (1975, 1976) and Chandler and Gregory (1976).

2.3.3 Calculating ventilation rates

Whilst BS 5925 refers to human occupancy the equations on which the standard is based are independent of human occupancy and are only a function of pressure differences applied to openings and temperature differences. So long as the geometry of the enclosure and the characteristics of the openings are known the equations described in BS 5925 are applicable.

A problem with short-term measurements of ventilation rates is the variability of wind speed. Gusting will cause pressure fluctuations that in turn can cause reversal of the flow, especially at high levels on the windward side and at low level on the leeward side. Temperature is likely to be less variable in the short term.

However, the natural ventilation rate within a building can be estimated using BS 5925 for a given wind speed and direction, provided that the following are known:

- the position and flow characteristics of the openings
- the mean surface pressure coefficient distribution
- the internal and external temperatures.

In general the calculations are relatively simple but the validity of the results depends on the accuracy of the above three pieces of data and some judgement is required in inputting appropriate wind conditions. Also the proximity of the building to other large obstacles / buildings will clearly have an effect on the natural ventilation. Consideration also needs to be given to how the wind speed is specified, for example should worst case or typical meteorological conditions be used?

To provide further confidence in the methods described in BS 5925 for application to area classification, detailed experimental measurements were made at two different enclosures and the results compared to the predicted ventilation rates. These are described in the two worked examples below. Appendix A describes the measurements in more detail and also includes qualitative flow visualisation carried out at two further, larger enclosures.

2.3.4 Worked examples

2.3.4.1 GRP Kiosk

Appendix A describes the geometry and ventilation arrangements of the enclosure in detail. The ventilation rate was measured using a tracer gas technique for two wind speeds, 3.3 m/s and 3.6 m/s, with the wind speed measured at a height of 4.7 m in both cases.

For the purpose of the calculation using the method described in BS 5925 it was assumed that the temperature difference between inside and outside the enclosure was small and therefore the airflow rate has been taken to be that from the wind induced pressure-difference alone.

The method of calculation is that given in Table 11 of BS 5925. The effective equivalent area of the openings (A_w) is obtained by adding together areas in parallel whilst those in series are obtained from the reciprocal of their squares

$$\frac{1}{A_w^2} = \frac{1}{(A_1 + A_2)^2} + \frac{1}{(A_3 + A_4)^2} \qquad (2.2)$$

where A_1 and A_2 are the areas of openings on a windward face and A_3 and A_4 are the areas of the openings on the leeward face. In this case this gives A_w = 45,378 mm^2 = 0.0454 m^2.

For a wind-driven flow, the volume flow rate is given by

$$Q_w = C_d A_w u (\Delta C_p)^{\frac{1}{2}} \qquad (2.3)$$

where C_d is a discharge coefficient taken to be 0.61 (BS 5925), u is the wind speed and ΔC_p is a differential mean pressure coefficient, values of which can be obtained from the standard. In these examples the value can be taken as 1. We therefore obtain: Q_w = 0.0277u m^3/s. The volume, V_0, of the kiosk is approximately 28 m^3 and the air change rate per hour is $Q_w \times 3600/V_0$ or 3.56u (where u is in m/s). For this example three values of u have been used for comparison:

1. A value for u of 0.5 m/s is often used for area classification to represent typical worst case conditions.

2. The actual wind speeds measured at a height of 4.7 m.

3. BS 5925 provides a method for calculating the reference wind speed at the height of the building based on Meteorological Office data. It is based on the mean wind speed for the area and in this case gives u = 2.8 m/s.

The calculated air change rates are shown in Table 2.1 together with the corresponding measured values.

Table 2.1 Air change rates in the GRP kiosk

Wind speed: m/s	***Measured air change rate (hr^{-1})***	***Calculated air change rate (hr^{-1})***		
		using measured wind speed	***using BS 5925 reference wind speed***	***using u=0.5 m/s***
3.3	11.9	11.75	9.97	1.78
3.6	15.6	12.8		

The calculated air change rate using the measured wind speed, 3.3 m/s, is close to the measured value (within 2%), whereas the calculated and measured values differ to a larger extent at the

higher wind speed (approximately 18%). In both cases the measured value is larger. This could be due to unplanned gaps in the structure and, to a small extent, temperature differences between the inside and outside of the kiosk. In this case, use of the method in BS 5925 for calculating the reference wind speed for the site gives a lower air change rate than that measured and use of u=0.5 m/s gives a conservative estimate of the air change rate, although of course wind speeds can be lower than this.

2.3.4.2 Brick Kiosk

This larger enclosure is described in Appendix A. As for the previous example, the air change rate was measured twice during which the wind speed was measured at 2.8 m/s and 2.2 m/s. The temperature difference between inside and out was small and the air flow rate has been taken to be that from the wind induced pressure-difference alone.

The method of calculation is the same as that used in the above example. Considering the air bricks as the sole source of the ventilation, the effective equivalent area of the openings is calculated as A_w = 18,102 mm^2 = 0.018 m^2, giving a volume flow rate of $Q_w = 0.011u$ m^3/s. The volume of the kiosk is approximately 112 m^3 and the air change rate per hour is therefore given by $0.35u$. As in the previous example, three different approaches were used to input the wind speed in to the calculation of the air change rate. The reference wind speed at the height of the kiosk is calculated to be 2.84 m/s. Table 2.2 summaries the calculated and measured air change rates.

Table 2.2 Air change rates in the brick kiosk

Wind speed: m/s	***Measured air change rate (hr^{-1})***	***Calculated air change rate (hr^{-1})***		
		using measured wind speed	***using BS 5925 reference wind speed***	***using u=0.5 m/s***
2.8	4.5	0.98	0.99	0.18
2.2	3.7	0.77		

The effect of taking into account the 200 mm diameter hole in the calculation would be to increase the effective equivalent area of the openings. This would now give a value of A_w = 0.0234 m^2 and hence $Q_w = 0.014u$ m^3/s. Therefore all of the calculated air change rates would increase by 27%. For example, for a wind speed of 2.8 m/s the air change rate would be 1.28 ach using the measured wind speed.

For the brick kiosk the calculated air change rates are all considerably lower than the measured ones. This is most likely due to the large number of 'unplanned' gaps in the structure. Using the measured wind speed to calculate the air change rate introduces a factor of five difference on the conservative side. Clearly using the low wind speed u=0.5 m/s input and coupled with this factor of five difference leads to a very low air change rate.

2.3.5 Conclusions

There are a number of methods available for measuring and calculating ventilation rates in enclosures. Any method applied to area classification must, out of necessity, be straightforward and give a reasonable degree of accuracy.

BS 5925 provides a relatively simple method for calculating the air change rate for naturally ventilated buildings. Although not as accurate as making measurements such as the ones described in Appendix A, it should provide a reasonable estimate of the ventilation rate / air change rate. In the two example discussed above the calculated air change rates were all less than the measured values. Use of a conservative estimate of the wind speed as an input to the

BS 5925 method will lead to an equally conservative estimate of the air change rate and would therefore be appropriate for input into a zoning methodology.

2.4 BS EN 60079-10:2003

Annex B of this standard is an informative annex, the purpose of which is to '*assess the degree of ventilation*'. The zone type is determined from the degree and availability of ventilation by the following method:

1. establish the maximum release rate of gas at the source, $\dot{m}$. The notation $(dG/dt)_{\max}$ is used in BS EN 60079:10 for the mass release rate.

2. calculate the minimum volume flow rate, $(dV/dt)_{\min}$, of fresh air required to dilute the release of flammable material to the required concentration below the LEL using a safety factor k taken as 0.5 for second grade releases.

3. from the actual ventilation rate in the volume under consideration, derive the fresh air changes per unit time, C.

4. calculate the volume which the minimum volume flow rate would occupy at this air change rate $V_k = (dV/dt)_{\min} / C$.

5. the value of V_k would hold for instantaneous and homogeneous mixing at the source of release. An additional correction factor, f, is then applied to give a hypothetical volume $V_z = f \times V_k$. The correction factor is used to account for non-homogeneous and non-instantaneous mixing at the source, due for example to impediments to the airflow, with f ranging from $f = 1$ (ideal situation) to, typically, $f = 5$ (impeded airflow).

In summary, BS EN 60079:10 provides a methodology for calculating V_z for a given release rate and air change rate given by

$$V_z = \frac{f}{C}\frac{\dot{m}}{k.LEL_m}\frac{T}{293} \qquad (2.4)$$

where LEL_m is the lower explosive limit in kg/m^3 and T is the ambient temperature.

The hypothetical volume V_z represents the volume over which the mean concentration of flammable gas will be k times the LEL, where for secondary releases $k = 0.5$. At the extremities of the hypothetical volume estimated, the gas concentration will be significantly below ½LEL, i.e. the volume where the concentration is above the LEL will be considerable less than V_z. V_z therefore provides a conservative estimate of the volume of the flammable gas cloud, but it does not normally equate to the volume of the zone. The shape of the hypothetical volume V_z, is not defined and will be influenced by the location and direction of the leak and the ventilation.

The 'type' of ventilation is then determined from this hypothetical volume V_z. BS EN 60079:10 states that "*The ventilation may be regarded as 'high' only when an evaluation of the risk shows that the extent of potential damage due to the sudden increase in temperature and/or pressure, as a result of the ignition of an explosive gas atmosphere of volume equal to V_z, is negligible. The risk evaluation should also take account of secondary effects (for example, further releases of flammables). The above conditions will normally apply when V_z is less than 0.1 m^3.*"

In addition to degree of ventilation, the availability also has to be considered. Three levels are defined: Good ventilation is defined as being present virtually continuously whilst fair is expected to be present during normal operation, discontinuities being permitted provided that

they occur infrequently and for short periods. Poor ventilation is that which does not meet the standard of good or fair. For secondary releases with a high degree of ventilation based on the value of V_z and good or fair availability, the standard recommends that the area classification is zone 2 but of negligible extent (NE), i.e. that no action is required to control sources of ignition within it.

2.4.1 Open air situations

Having established the definition of V_z and the methodology for its calculation for enclosures and subsequent application to area classification, BS EN 60079-10:2003 includes a methodology for the estimation of V_z for outdoor applications. It is based on the indoor methodology and therefore requires an approximation of the enclosure size and ventilation rate that might be regarded as equivalent to outdoor situations. Such approximations are inevitably arbitrary. An example is given in the standard, based on a hypothetical cube with side dimensions of 15 m and a wind speed of 0.5 m/s. There is no basis for the choice of this value of enclosure volume. A wind speed of 0.5 m/s is often used in generic hazard calculations. The standard correctly emphasises that the results of the use of the methodology and these example values of enclosure volume and wind speed will be conservative, but nevertheless they are often used in the absence of any guidance. Earlier work (Gant and Ivings, 2005) compared the results of the use of CFD and the outdoor methodology and showed that the methodology in the standard gave V_z results that were two to three orders of magnitude higher. It is now generally recognised that the outdoor methodology in the standard is arbitrary and of little, if any, value. The calculated value of V_z is directly proportional to the chosen notional arbitrary values of enclosure volume, wind speed and air change rate. McMillan(1998), for example, uses a volume of 1,000 m^3 and an air change rate of 0.16 s^{-1}, whilst BS EN 60079:10 uses 3,375 m^3 and 0.03 s^{-1} respectively. HSE have recommended to the IEC responsible committee that the open air methodology be removed from the next revision of the standard.

2.5 IGE/SR/25

The recommendations given in the Institution of Gas Engineers document IGE/SR/25 '*provide a procedure for hazardous area classification around installations handling natural gas*' and '*are based on good engineering practice and the use of mathematical models which have been validated by experimental work*'. The document is based on British Gas research previously made available on a restricted basis by that organisation as 'SHA1'. Much of the original research remains unpublished. However the document remains highly regarded and detailed guidance uniquely available in relation to a specific substance and, for higher pressures, will undoubtedly continue to retain this role.

The document defines adequate, inadequate and poor ventilation for natural and forced ventilation cases, and its area classification recommendations are strongly dependent upon the application of these definitions. Natural ventilation calculations assume a minimum wind speed of 0.5 m/s.

2.5.1 Outdoor naturally ventilated areas

Tables of zoning distances for secondary releases are given, based on pressure, for flanges and other fittings and distribution regulator vents. More complex methodologies are described for relief vents and gasholders.

For fittings, the maximum hole size used for leakage calculations is normally 0.25 mm^2, rising to 2.5 mm^2 in an adverse (e.g. vibrating) environment. These values have become widely used.

2.5.2 Indoor naturally ventilated areas

An enclosed space is considered to possess adequate natural ventilation if it meets certain criteria for:

- Ventilator design.
- The availability of good mixing.
- The adequacy of buoyancy-driven and wind-driven ventilation within the space, whichever is the smaller.

Criteria are given in terms of the free ventilation area and its distribution. Note that no references are given for the values/formulae used and that the mixing formula is stated as not being valid for enclosed spaces greater than 100 m^3 in volume.

In general these criteria are questionable. It does not, for example, seem reasonable to assume that dead spaces can be avoided solely by having a free ventilation area that is specified as being greater than a fraction of the volume of the enclosed space. Where there is adequate ventilation, the zoning distance is calculated by evaluating a ventilation factor based on ventilation areas and, depending on its magnitude, increasing the distances recommended for the open-air, naturally ventilated cases by up to 100%.

If the ventilation is not adequate the zoning classifications become more stringent, reaching zone 0 in extreme cases.

2.5.3 Indoor forced ventilated areas

An enclosed space possesses adequate artificial or forced ventilation if it meets certain criteria for:

- The appropriateness of ventilator design.
- Availability of good mixing.
- Adequacy of the airflow within the enclosed space.

The design is said to be adequate if the air intakes/openings are located in non-hazardous areas with a minimum clearance of 1 m (or less conditionally) from the nearest zone and '*a properly distributed airflow is provided throughout the entire enclosed space and the velocities of the air inlets are the same to within 10%.*'

The criteria for the avoidance of dead spaces by good mixing are given in terms of volume flow rates.

The airflow (volume flow rate) is said to be adequate if it is above a minimum value that is based on the total natural gas release rate within the enclosed space and on the gas density. Where there is adequate ventilation, the zoning distance is calculated by evaluating a ventilation factor based on mixing and airflow criteria and, depending on its magnitude, increasing the distances recommended for the open-air, naturally ventilated cases by up to 100%.

If the ventilation is not adequate the zoning classifications become more stringent, reaching zone 0 in extreme cases.

3 MODELLING GAS LEAKS

3.1 INTRODUCTION

This project is concerned with accidental releases of natural gas into ventilated enclosures and open spaces. Such releases are characterised by high momentum gas jets that entrain and mix with the surrounding air. Unless these releases are significantly confined, or if there is gas build-up through re-entrainment, the buoyancy of the gas plays a much smaller role in determining the gas dispersion than the jet's momentum.

The shape of the leak source is likely to have an effect on the resulting gas dispersion but for the purposes of this project, and area classification in general, it is sufficient to assume that the leak source is circular. For non-circular orifices an equivalent circular orifice with the same area can be assumed.

Natural gas is variable in its composition and so throughout this report pure methane is used as a substitute.

3.2 SOURCE CONDITIONS

The most important parameter in defining the source of a gas leak is its mass release rate. This can be easily computed based on the known upstream temperature and pressure. The method used will depend on the whether the release is subsonic or choked. Choked releases are sonic at the point of release. Figure 3.1 shows the notation that is used to denote the flow properties that define the release. The upstream or stagnation conditions are given the suffix *'0'*, the conditions at the exit use *'1'*, and the ambient conditions *'a'*.

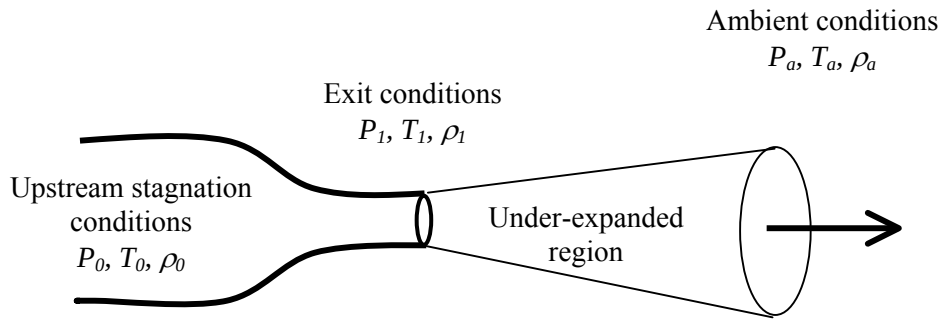

Figure 3.1 Notation used in definition of source conditions

Both the released and ambient gases are assumed to behave as ideal gases, whereby the gas density, ρ, is given by

$$\rho = \frac{PM}{RT} \qquad (3.1)$$

where P is the pressure, R the universal gas constant, M the molecular weight and T is the temperature. The local speed of sound, a, is a function of the gas thermodynamic properties:

$$a = \sqrt{\gamma RT / M} \tag{3.2}$$

where γ is the ratio of specific heats. The release will be either *sonic* or *subsonic* depending on the stagnation pressure. The critical pressure ratio is defined as

$$\frac{P_*}{P_0} = \left(\frac{2}{\gamma+1}\right)^{\frac{\gamma}{\gamma-1}} \tag{3.3}$$

where P_* is the critical pressure (i.e. the critical pressure ratio is a property of the gas only). If the pressure ratio, P_a / P_0, is less than the critical pressure ratio then the flow is 'choked' and the Mach number at the exit is unity. For methane ($\gamma = 1.3$) the critical pressure ratio is 0.55 which means that the release is sonic if the stagnation pressure is greater than 0.85 barg.

3.2.1 Sonic releases

For a sonic release, the Mach number is unity at the exit by definition and the pressure, temperature and density at the exit can be computed from the isentropic flow equations

$$\frac{P_0}{P_1} = \left(\frac{T_0}{T_1}\right)^{\frac{\gamma}{\gamma-1}} = \left(\frac{\gamma+1}{2}\right)^{\frac{\gamma}{\gamma-1}} \tag{3.4}$$

and

$$\frac{\rho_0}{\rho_1} = \left(\frac{T_0}{T_1}\right)^{\frac{1}{\gamma-1}} \tag{3.5}$$

The local speed of sound is then determined using (3.2) and the mass release rate is given by

$$\dot{m}_1 = C_d \rho_1 A_1 v_1 \tag{3.6}$$

where C_d is the coefficient of discharge, A_1 is the cross sectional area of the orifice and v_1 is the choked velocity at the orifice (i.e. the speed of sound). The mass release rate can be expressed in terms of the stagnation conditions as follows

$$\dot{m}_1 = C_d A_1 P_0 \sqrt{\frac{\gamma M}{RT_0}} \left(\frac{2}{\gamma+1}\right)^{\frac{\gamma+1}{2(\gamma-1)}}. \tag{3.7}$$

3.2.2 Subsonic releases

For subsonic releases the Mach number at the exit ($M_1 = v_1 / a_1$) can be calculated from the isentropic flow equations, noting than $P_1 = P_a$, as follows

$$M_1 = \sqrt{\frac{2}{\gamma-1}\left(\left(\frac{P_0}{P_a}\right)^{\frac{\gamma-1}{\gamma}} - 1\right)} \tag{3.8}$$

The exit temperature can then be found using the isentropic flow equation

$$\frac{T_0}{T_1} = 1 + \frac{\gamma - 1}{2} M_1^2 \qquad (3.9)$$

Again the mass release rate can be calculated in terms of the stagnation conditions using (3.6) but in this case the formula reduces to

$$\dot{m}_1 = C_d A_1 P_0 \sqrt{\frac{\gamma M}{R T_0} \frac{2}{(\gamma - 1)} \left[1 - \left(\frac{P_a}{P_0} \right)^{\frac{\gamma - 1}{\gamma}} \right]} \left(\frac{P_a}{P_0} \right)^{\frac{1}{\gamma}} \qquad (3.10)$$

3.3 GAS CLOUD VOLUMES

The cloud volume resulting from an accidental release of gas is used in area classification to determine the zone. In this report four different measures of 'gas cloud volume' are introduced as follows:

1. 100% LEL volume. This is the volume of gas that is above the lower explosive limit of the gas and is therefore directly related to the volume of gas that would be expected to take part in an explosion. Note that the volume of gas above the Upper Explosive Limit (UEL) is not subtracted from the 100% LEL volume because it is likely to be relatively small and it is possible that during an explosion this gas could become diluted and therefore also take part in the explosion.

2. 50% LEL volume. This is the volume of gas above half LEL and is the volume that is often used as part of a risk assessment to allow for uncertainty in the calculation of the 100% LEL volume.

3. V_z. As discussed previously, and defined in BS EN 60079:10, this is the volume of gas that has an average concentration of ½ LEL. The boundary of the gas cloud is undefined in BS EN 60079:10. We assume that the cloud boundary is at a constant concentration. This concentration will be less than ½ LEL and will typically be around one third LEL although it will vary from case to case.

4. The Equivalent Stoichiometric Volume (ESV) is defined to be the volume of a uniform stoichiometric mixture of gas and air containing the same number of moles of gas as that enclosed by an iso-surface at a given gas concentration. For example, we could take the 100% LEL volume, calculate the number of moles of gas within that volume and then work out the volume of gas and air that would be required to mix that number of moles of gas to a uniform stoichiometric concentration. See Section 4.1 for further details.

Figure 3.2 shows the results of a CFD simulation of a free gas jet and shows how the gas cloud volumes defined by an iso-surface at 100% LEL and 50% LEL compare to the V_z gas cloud volume. For a further discussion on the relative size of the 100% LEL volume and V_z see Section 6.4.2.

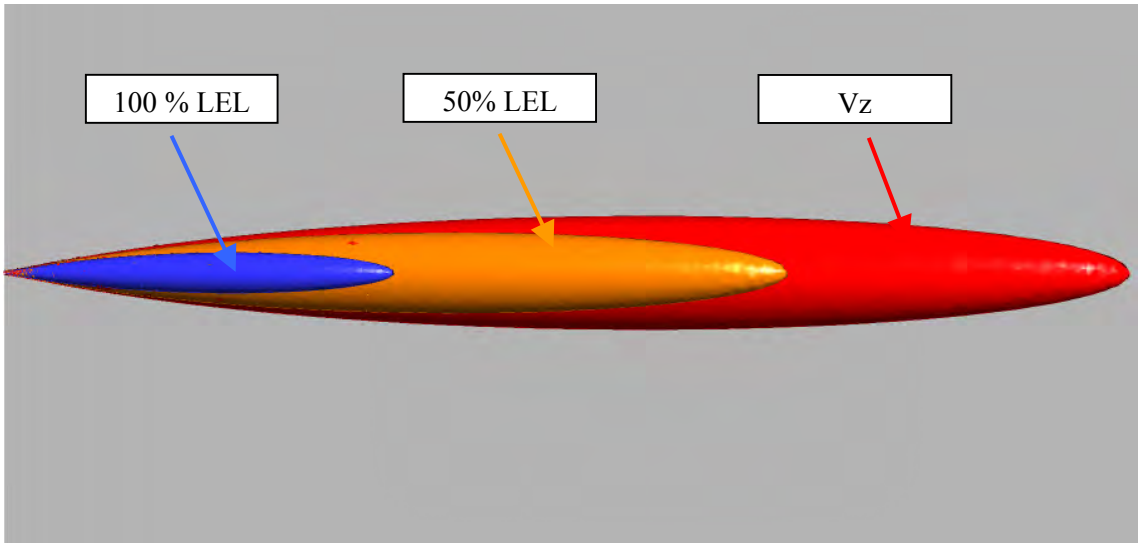

Figure 3.2 Relative sizes of gas cloud volumes for a free jet

3.4 PREDICTING GAS CLOUD VOLUMES

There are a number of different ways of varying complexity of calculating the above volumes. The method used in BS EN 60079:10 for calculating V_z is described in Section 2.4 above. For free unobstructed gas jets simple correlations can be used to construct a one-dimensional integral model. HSL have developed such a model called GaJet which is applicable to both sonic and sub-sonic releases based on the work of Ewan and Moodie (1986) and List (1982). As the model is empirically based it provides a very good basis for assessing the hazards associated with gas leaks. A firm understanding of the behaviour of free jets and their associated gas cloud volumes then provides a basis for studying gas leaks that interact with obstructions, enclosures and ventilation.

For subsonic releases, List (1982) provides a correlation for the gas concentration (volume fraction) on the jet centreline

$$c_c = c_1 \frac{D_1}{0.194z} \qquad (3.11)$$

where c_1 is the concentration at the exit (usually assumed to be 1, i.e. pure gas), D_1 is the hole diameter and z is the distance downstream from the exit. This is important in that it shows that the gas concentration, and hence gas cloud volume, does not depend on the upstream pressure. Therefore the gas cloud volume depends only on the leak area for low Mach number flows. As the upstream pressure is increased to that required to produce a choked flow (0.85 barg for methane) the pressure will start to have an effect on the gas cloud volume.

For gas leaks in enclosures, where a complex interaction between the jet and ventilation is likely to occur, CFD provides the only practical means for estimating gas cloud volumes. The CFD modelling approach taken in this report is described in detail in Appendix D. In general, it would be reasonable to assume that the presence of obstacles in the path of a jet in the open would lead to a decrease in the gas cloud volume as the obstacles would lead to increased mixing and therefore the gas would dilute more quickly (Cooper, 2001). The report by Lewis (1998) describes a model for jets impinging normally onto a plane surface and highlights why

the resulting gas cloud volume will be smaller than the equivalent free jet. In Section 5.3 a few idealised scenarios are modelled which shows that in some cases (particularly large flat surfaces such as walls parallel to the jet direction) the interaction between a jet and an obstacle can lead to larger gas cloud volumes.

3.5 ENTRAINMENT OF AIR INTO A FREE JET

An important parameter in determining whether the ventilation within an enclosure is sufficient to dilute a given gas leak is the volume of air that is entrained by the turbulent jet. List (1982) provides a method for calculating this entrained volume for subsonic free jets. However, to provide a more widely applicable model the GaJet model has been extended to compute the volume numerically. The entrained gas volume flux at a distance z downstream of the orifice is given by

$$Q_{ent} = \int_{r=0}^{\infty} (1 - c_c(z,r)) v(z,r) dr \qquad (3.12)$$

where r is the radial distance and v is the gas velocity. GaJet is used to compute this integral numerically in a similar fashion to which the cloud volume is calculated. Numerical experiments have shown that this approach gives identical results to the method described by List (1982) for subsonic releases.

To use this approach a downstream location, z, or a centreline concentration, c_c, needs to be chosen at which to evaluate Q_{ent}. For example in Figure 3.3 the vertical black line indicates the plane on which the centreline concentration is 50% LEL. Therefore, Q_{ent} represents the volume of air that moves through this plane. Note that it is assumed that the ambient air is still. In practice the entrained volume of fresh air is a linear function of the mass release rate of gas (List, 1982).

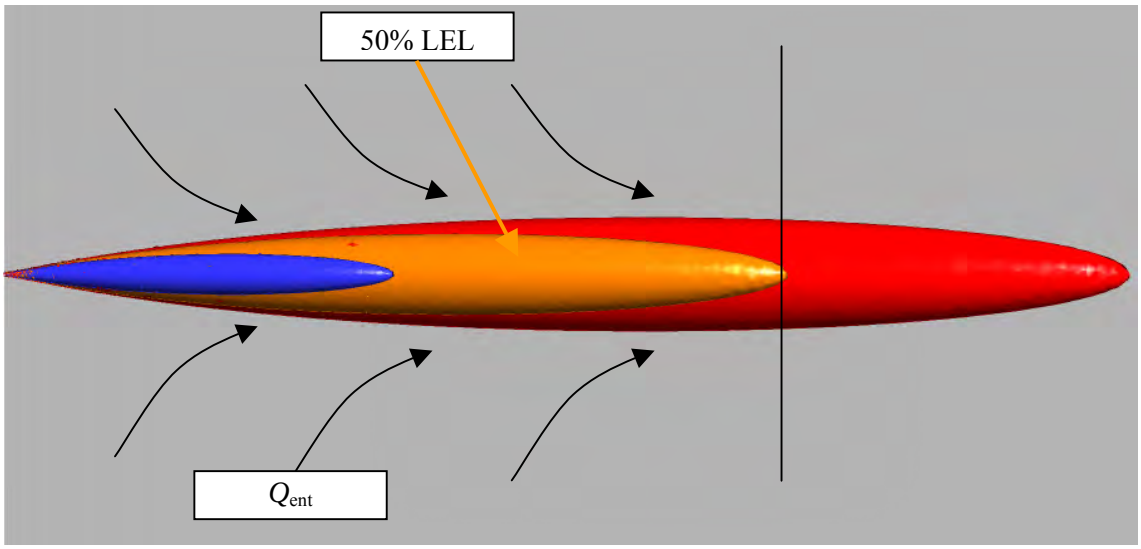

Figure 3.3 Entrainment of air into a free jet

4 A SAFETY CRITERION FOR ZONE 2 NE

4.1 INTRODUCTION

In BS EN 60079:10 the assumption is made that a gas cloud with $V_z < 0.1$ m^3 poses very little hazard to people or equipment. It is understood that when this V_z concept was introduced it was based on expert opinion rather than sound scientific data. Therefore, this Section of the report describes experimental work carried out to create gas clouds with $V_z = 0.1$ m^3, to ignite them and to assess the hazard. The concept of V_z was originally developed for the purpose of assessing the ventilation effectiveness rather than representing a measure of the hazard the result of trying to ignite V_z was never considered. The hazard associated with a gas cloud with $V_z = 0.1$ m^3 is assessed here so that this criterion can continue to be used as part of a zoning methodology, with the confidence that if this criterion is met then indeed the hazard is appropriately low. First, however, the theoretical overpressure that can be created by such a gas cloud is considered.

4.2 EQUIVALENT STOICHIOMETRIC VOLUME

4.2.1 Definition

The concept of an equivalent uniform stoichiometric gas cloud volume is used here to help quantify the likely overpressure generated from the ignition of a non-uniform flammable gas cloud. This volume is defined to represent the potential energy available to create overpressure.

As mentioned in Section 3.3, the ESV is defined to be 'the volume of a uniform stoichiometric mixture of gas and air containing the same number of moles of gas as that enclosed by an iso-surface at a given gas concentration'.

As an example, consider a leak of gas and then assume that it is possible to measure the total 'amount' of flammable gas within the iso-surface at, say, LEL. The amount of gas is given by the average volume fraction multiplied by the volume of the iso-surface. Then assume that this amount of pure gas is mixed with just enough air to give a stoichiometric concentration. The volume of this stoichiometric volume is then defined as the equivalent stoichiometric volume.

This example gives a straightforward approach to defining the ESV and it can be clearly seen how this may relate to the expected overpressure. However, a more conservative approach would be to assume that the flammable gas down to ½ LEL could contribute to the explosion, in which case the ESV could be calculated based on the number of moles of gas within the iso-surface at ½ LEL. An even more conservative approach would be to assume that all of the gas within the V_z volume contributes to the explosion overpressure.

Quantitatively the ESV can be seen to be the volume averaged mole fraction within a given iso-surface multiplied by the volume of the iso-surface divided by the stoichiometric concentration.

In the case of the V_z volume, it is trivial to compute the ESV as the average concentration within the cloud is ½ LEL by definition. For methane (which has a stoichiometric concentration of 0.0948 by volume), with ½ LEL=0.022 and $V_z = 0.1$ m^3 the equivalent stoichiometric volume is simply:

$$V_{stoich} = 0.1 \times \frac{0.022}{0.0948} = 0.023 m^3 \quad (4.1)$$

The ESV of a gas cloud defined by an iso-surface at LEL or ½ LEL is more difficult to compute as the gas concentration within the iso-surface is non-uniform and its average molar fraction is unknown. However, it is relatively easy to compute from the results of a CFD simulation or in the case of a free unobstructed jet from the results of a one-dimensional integral model such as GaJet.

4.2.2 Theoretical Overpressure Produced by V_z = 0.1 m^3

A closed vessel completely filled with a stoichiometric mixture of methane will be subjected to a hypothetical maximum uniform overpressure of 8 barg on ignition. If only 1% of the enclosure volume is filled with a stoichiometric mixture, then, as a first approximation, the over pressure generated is simply 1% of 8 barg, i.e. 80 mbarg. This can be expressed in the following simple formula:

$$P = \frac{8V_{stoich}}{V_{room}} \quad (4.2)$$

where P is the overpressure in barg, V_{stoich} is the volume of the gas cloud at stoichiometric conditions and V_0 is the room volume. This simple model does not take account of any cooling effects, the effects that obstacles may have in creating turbulence and accelerating the flame or of the shape of the enclosure, which can lead to locally higher or lower overpressures.

The enclosure used in the explosion test (see Section 4.3.2) is 2.5 × 2.5 metres in cross-section and 4.9 metres long with a volume of 31 m^3. As shown above, a methane gas cloud with V_z = 0.1 m^3 is equivalent to a stoichiometric gas cloud with volume 0.023 m^3. This fills 0.075% of the enclosure volume. The simple theoretical model suggests that this would give rise to an overpressure of 6.0 mbar when ignited. CFD simulations of the gas release in the test enclosure that gives rise to a V_z = 0.1 m^3 gas cloud have been carried out and have shown that the ESV of the ½ LEL and LEL iso-surfaces are 0.0128 m^3 and 0.0031 m^3, respectively. Such gas clouds would give rise to an overpressure of 3.3 mbarg and 0.8 mbarg respectively. Therefore, we have a predicted theoretical maximum overpressure in the range 0.8 to 6.0 mbarg depending on the level of conservatism in the approximation of the flammable gas cloud size.

Figure 4.1 shows the results of applying this theoretical model to a range of enclosure sizes. Here we have used the ESV of the V_z = 0.1 m^3 cloud with a volume of 0.023 m^3 which is a very conservative assumption. In smaller rooms the percentage of the space occupied by the gas cloud increases and the overpressure increases. The theoretical model predicts that an overpressure of 100 mbarg is generated when the room has a volume of 1.8 m^3 (a cube with sides of 1.2 metres, approximately).

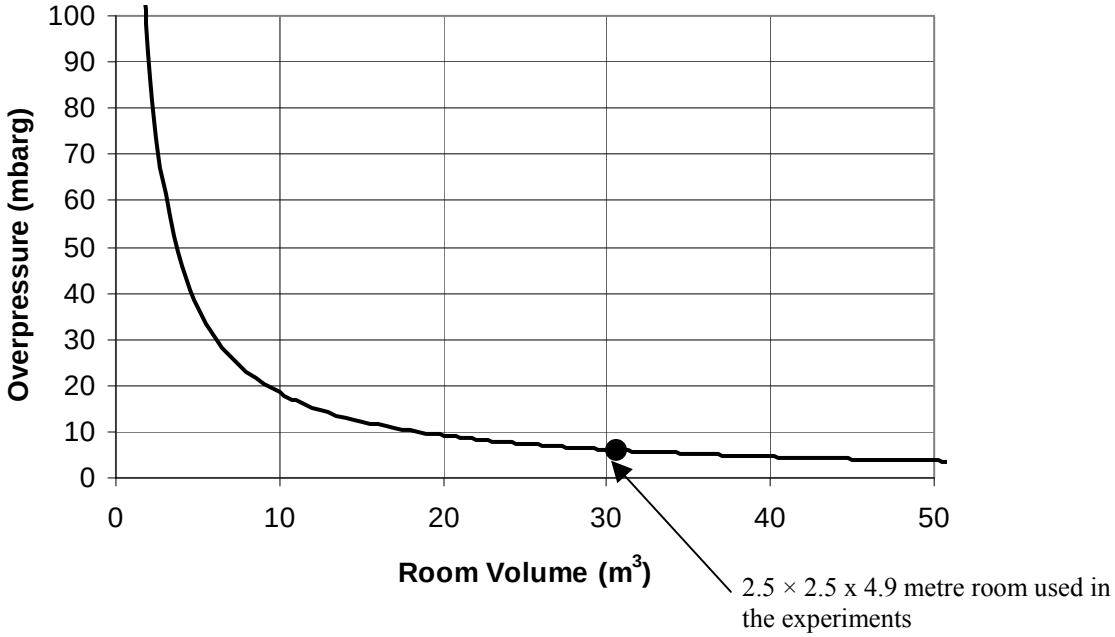

Figure 4.1 Variation of overpressure in enclosures of different sizes filled with a methane cloud at stoichiometric conditions with content equivalent to V_z = 0.1 m^3

4.3 EXPLOSION TEST

4.3.1 Determination of Leak Size

Clearly it would not be possible to ignite a gas cloud in which the concentration was uniform at ½ LEL. Therefore, the experimental test is based on a high-pressure gas leak which results in a gas jet with varying methane concentration confined within an enclosure.

Simulations of a methane jet have been performed to calculate the hole size and pressure required to give a gas cloud with V_z = 0.1 m^3. Both CFD and the integral model, GaJet, have been used. Preliminary simulations were made of a methane jet flowing into unobstructed, open space (a free-jet) and this was followed by CFD simulations using a more realistic geometry, based on the experimental enclosure.

4.3.1.1 Free-jet simulations

Free-jet simulations have been performed using both CFD and GaJet for mass release rates of methane ranging from 0.1 to 6.0 g/s. This is equivalent to pressures ranging from 21 mbarg to 13 barg for a 2.5 mm^2 orifice (assuming an orifice discharge coefficient of unity[2]). The CFD methodology used in these simulations is similar to that used in the earlier study by Gant & Ivings, 2005. For pressures above 0.85 barg, the flow is choked and instead of resolving the complex shockwave patterns close to the orifice, the 'resolved sonic source approach' has been used (see Gant and Ivings, 2005). As with the previous study, a co-flow of air with velocity 0.5 m/s has been used in all cases. This has been shown to produce slightly larger (i.e. more conservative) predictions of the gas cloud volume compared to counter- or cross-flow ventilation (for details, see Section 5.2). The leak rate conditions used in the CFD simulations are summarised in Table 4.1.

[2] *It doesn't make any difference what loss coefficient is used here, as it is just the mass release rate that we are really interested in.*

A comparison of the predicted V_z against the volume of the gas cloud enclosed by 50% and 100% LEL iso-surfaces is given in Figure 4.2. The CFD model predicts the ratio of the V_z to the 100% LEL volume to be on average around 19. This compares to a ratio of 26.5 predicted by GaJet and in this case the ratio is independent of pressure and hole size. The flammable volume, defined by the LEL iso-surface, is clearly considerably smaller than that defined by the V_z criterion. The results show that a V_z of 0.1 m^3 is achieved with a release pressure of around 12 barg.

Table 4.1 CFD inlet boundary conditions

Case	**Leak conditions**			**CFD model boundary conditions**		
	Pressure (barg)	**Area (mm^2)**	**Leak rate (g/s)**	**Temp. (K)**	**Area (mm^2)**	**Velocity (m/s)**
1	0.021	2.5	0.1	291.8	2.5	79.0
2	0.5	2.5	0.6	267.2	2.5	341.6
3	2	2.5	1.3	254.9	4.1*	415.0
4	5	2.5	2.6	254.9	8.1*	415.0
5	10	2.5	4.7	254.9	14.8*	415.0
6	11	2.5	5.1	254.9	16.2*	415.0
7	12	2.5	5.6	254.9	17.5*	415.0
8	13	2.5	6.0	254.9	18.9*	415.0

* Note: in the CFD model a pseudo-source approach has been used to define an equivalent area at atmospheric pressure, for all choked releases.

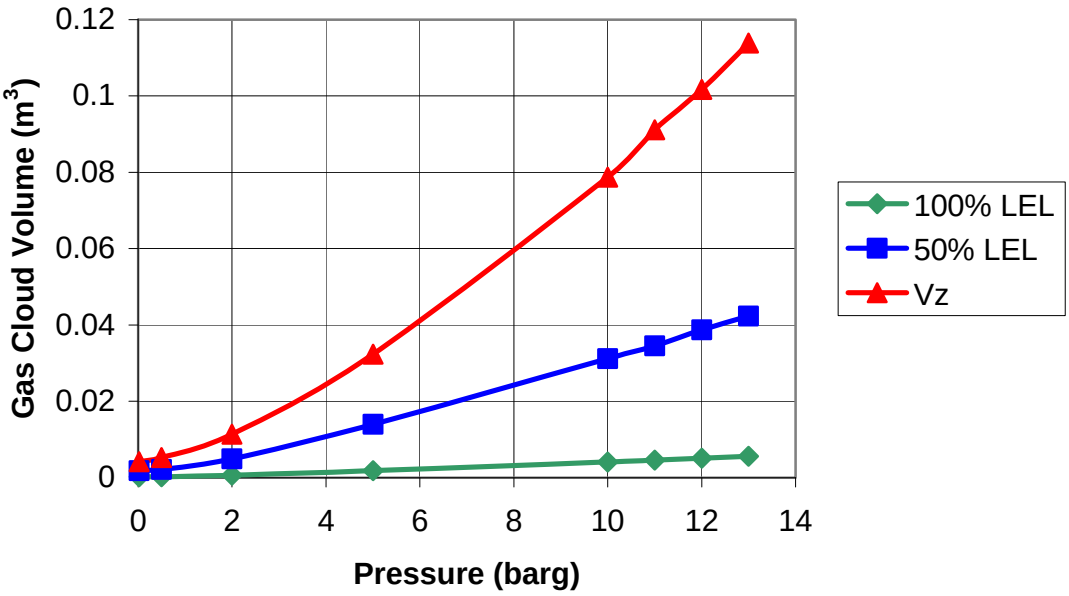

Figure 4.2 Variation of gas cloud volume with pressure in CFD simulations of methane free-jets with hole size 2.5 mm^2

In the free-jet CFD simulations, the method for calculating the gas cloud volume is conservative, resulting in gas cloud volumes which may be over-estimated. Whilst this

conservatism can be considered desirable in the context of area classification, in the present work CFD simulations are being used to estimate the range of pressures to be tested in the experimental validation of the V_z criterion. Here, an over-estimation of the gas cloud volume could potentially lead to the experiments igniting gas clouds smaller than a V_z of 0.1 m^3.

As a quick check on the CFD results, GaJet has been used to estimate V_z cloud volumes for a range of pressures. The model is based on experimental correlations for the axial and radial decay of gas concentration and velocity for turbulent free-jets. A comparison of the CFD and GaJet results is presented in Figure 4.3. The GaJet results are on average around 40% lower than the CFD results for a given pressure. This behaviour is consistent with the use of a conservative method for the calculation of the gas cloud volume in the CFD approach. As a consequence, GaJet predicts a V_z = 0.1 m^3 to be obtained at a mass release rate of 7.7 g/s as opposed to 5.6 g/s with the CFD. This is equivalent to a release pressure of approximately 17 barg, compared to around 12 barg.

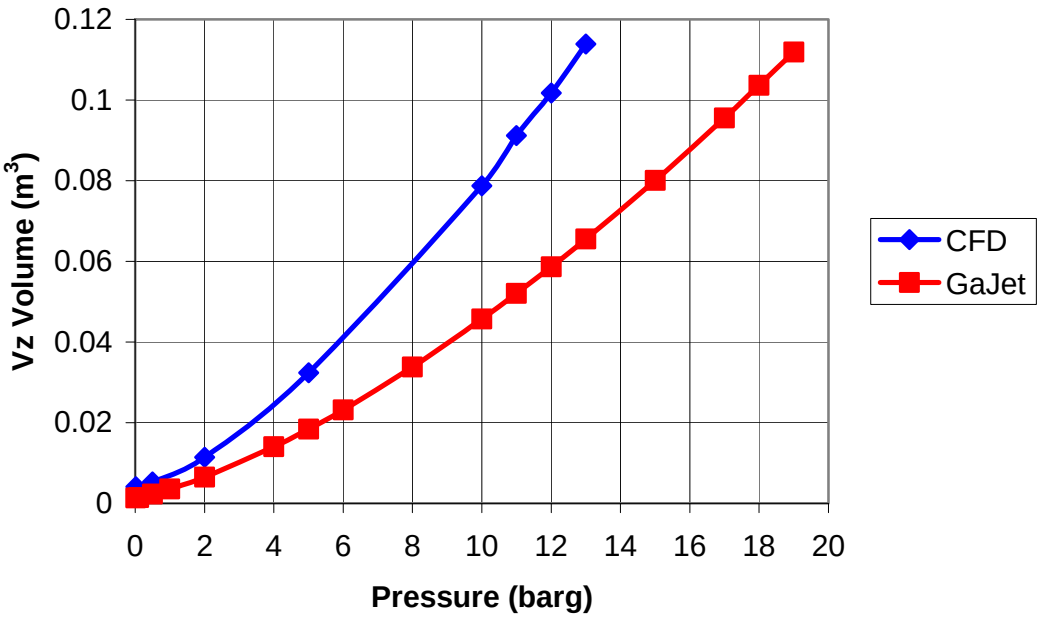

Figure 4.3 Comparison of CFD and GaJet predictions of V_z volume with pressure in methane free-jets with hole size 2.5 mm^2

4.3.1.2 CFD simulations with realistic enclosure geometry

Further CFD simulations have been performed of a methane jet in an enclosure with the same dimensions as the steel box used in the explosion experiments. The aim of these simulations was to find the release pressure necessary to produce a gas cloud with V_z = 0.1 m^3 for an orifice with open area of 2.5 mm^2.

The enclosure used in the experimental releases was not fully sealed; there were some gaps in the walls for instrumentation and other small cracks (see Section 4.3.2.1). To prevent the build-up of pressure in the CFD model of the container as the gas was released, two 40 mm diameter holes were modelled in one of the walls near the orifice (see Figure 4.4). As the gas was released into the container, air was expelled through these two holes. Tests showed that the location of the holes did not have a significant effect on the flow field around the jet.

Three release rates were tested in the CFD model: 5.6, 6.8 and 7.7 g/s, equivalent to supply pressures of 12, 15 and 17 barg assuming a 2.5 mm^2 orifice and a discharge coefficient of unity. All three releases were choked and, as with the earlier free-jet studies, the 'resolved sonic source' approach was used to set inlet conditions for the CFD model.

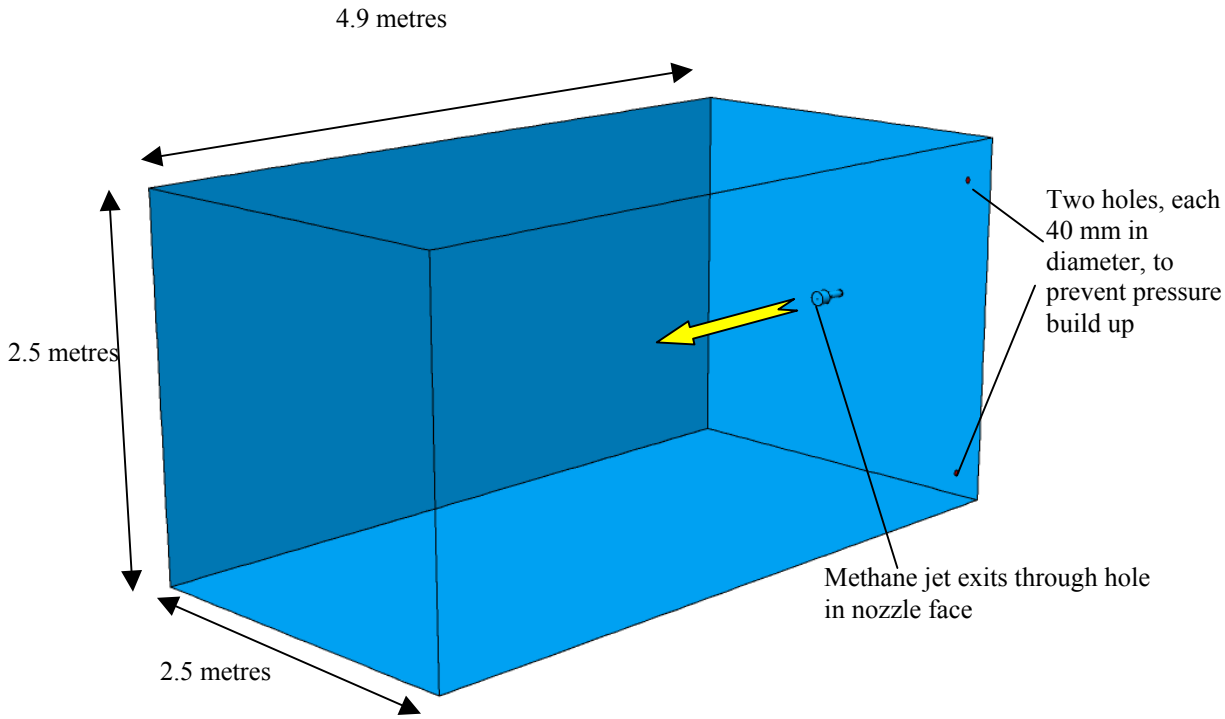

Figure 4.4 Flow Domain and boundary conditions

The computational mesh used in the CFD simulations was composed of mainly tetrahedral cells with prism layers on the walls, comprising in total around 192,000 grid nodes. Since the evolution of the jet flow was of primary interest, a transient simulation was performed with time-step of 0.005 s.

Figure 4.5 gives the V_z volume against time from the start of the 7.7 g/s release. There is a rapid increase over the first 1 to 2 seconds and thereafter it reaches a plateau with V_z remaining constant at approximately $V_z \approx 0.11$ m^3 for the next 12 seconds. During this time the flow field is essentially fully-developed and the jet is entraining clean air from within the container. After 14 seconds, the jet starts entraining a mixture of methane and air and the size of the V_z cloud increases. This behaviour is fortunate in that it suggests that the timing of ignition in the experiments is not crucial and provided it occurs after approximately 2 seconds and before 14 seconds, the gas cloud should be of constant size.

For the smaller releases at 5.6 g/s and 6.8 g/s, the CFD model predicted the V_z to reach a plateau at around $V_z \approx 0.07$ m^3 and 0.09 m^3, respectively.

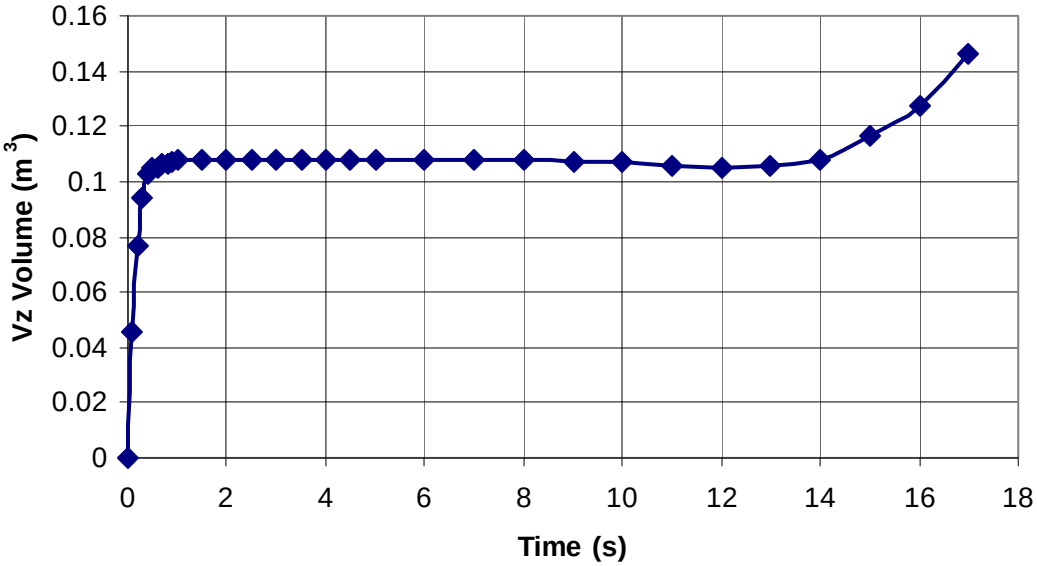

Figure 4.5 Variation of V_z with time from the start of the 7.7 g/s methane release

4.3.1.3 Summary of CFD Results

The CFD model predicted that a release rate of approximately 7.7 g/s will produce a methane gas cloud in the enclosure with $V_z \approx 0.1$ m^3. The gas cloud was predicted to remain roughly the same size with $V_z \approx 0.1$ m^3 between 2 and 14 seconds after the start of the release.

Note that the post-processing method used to calculate V_z in these CFD simulations is conservative and tends to over-estimate the gas cloud volume. This means that in reality a V_z of 0.1 m^3 may be produced from a larger release than that predicted by the CFD model. For this reason, although the explosion experiments first attempted to ignite clouds produced by releases of around 7.7 g/s, tests were also undertaken with larger releases.

4.3.2 Experiment

4.3.2.1 Experimental arrangement

A schematic of the experimental rig used for the tests is shown in Figure 4.6. The test enclosure was a nominally unventilated rectangular steel box constructed from two 2.5 m by 2.5 m by 2.5 m cubic modules to give an enclosure of internal volume 31.3 m^3. The enclosure was not completely gastight as there were small gaps in the joins between the two modules and the end plates and modules. Thus the ventilation rate will be negligible but not zero and its magnitude will depend on the external weather conditions at the time of the tests.

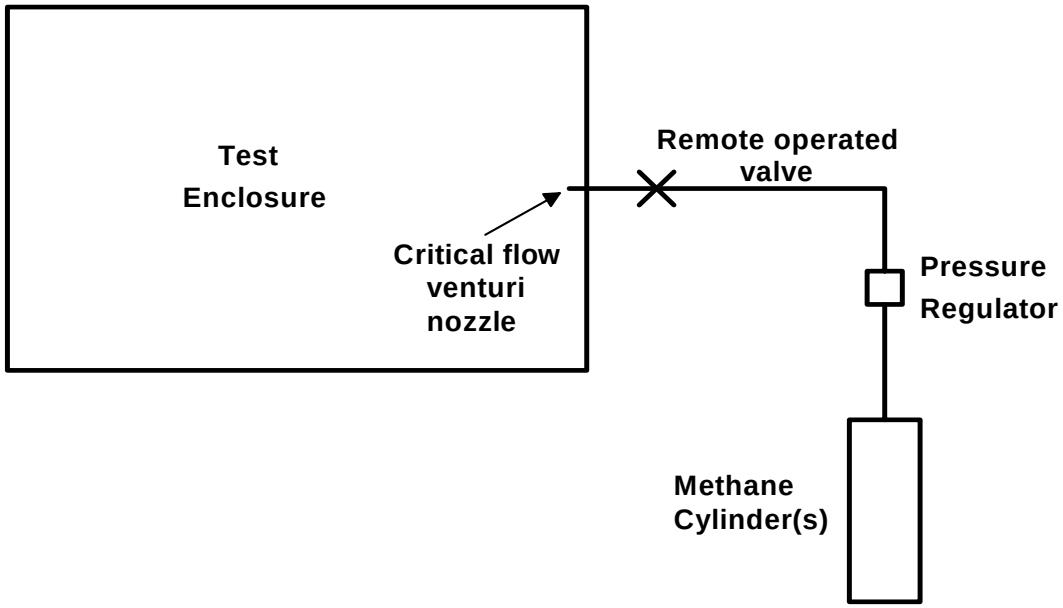

Figure 4.6 Schematic of the experimental rig

The methane was supplied from a cylinder supply, either a single cylinder or in the latter tests a bank of 12 cylinders, via a high pressure regulator, to a critical flow venturi nozzle. A venturi nozzle was used to simulate the leak source rather than a hole drilled in a blanking plate, as the flow characteristics, e.g. discharge coefficient, are well defined. From the measured pressure and temperature upstream of the venturi nozzle it is possible to calculate the mass flow through the nozzle by the method given in BS EN ISO 9300:2005. For the tests a venturi nozzle of 1.70 mm diameter was used that had an open area of 2.27 mm^2 (see Figure 4.7). The open area of the nozzle is slightly less than the representative leak size of 2.5 mm^2 but of those available this nozzle had an open area closest to 2.5 mm^2. For upstream conditions of 20 bar absolute and 15 ^oC the nozzle would give a leakage rate of 7.95 g/s of methane.

To allow continuous monitoring of the gas pressure, the methane supply pressure and temperature on the upstream side of the critical flow nozzle, a pressure transducer (0-25 bar absolute) and a thermocouple (Type T, stainless steel sheathed) were mounted in the 50 mm diameter pipe upstream of the nozzle. The pressure transducer was calibrated against a standard test gauge and the temperature monitoring system calibrated with a thermocouple simulator unit.

Figure 4.7 Critical flow venturi nozzle

For the measurement of the explosion pressures generated in the enclosure by ignition of the released methane, two Kistler Model 4043A1 piezo-resistive transducers (0 to 1 bar absolute) were mounted in the enclosure walls. These were calibrated against a standard test gauge.

An electric match head or a chemical igniter was used for the ignition source. The match heads contain a very small amount of pyrotechnic composition which is ignited by passing an electric current through the composition. It is the resulting burning particles of composition that ignite the methane. The chemical igniters were similar to the match heads but contained more composition. They have a nominal strength of 1 kJ. The match head or igniters was located in the test enclosure so it fired the burning particles into the jet to ensure optimum conditions for igniting the methane.

4.3.2.2 Procedure

The test procedure was to open the remotely operated valve to allow the methane leak to start. After a delay (the ignition delay time) the match head or igniter was fired and after a further delay the remotely operated valve closed to stop the methane leak. Both the ignition delay and the release duration, i.e. the time between the remotely operated valve opening and closing, can be varied. Release durations were kept to 15 seconds or less, so as to prevent build-up of a flammable atmosphere throughout the bulk of the test enclosure, in line with the CFD simulations.

4.3.2.3 Results

An initial series of tests were carried out with methane supply pressures of about 20 bar absolute giving rise to a leak rate of about 8 g/s. No ignitions were achieved using a match head for the ignition source. It is not possible to say whether this was because the match heads were not powerful enough to ignite the methane or because the burning particles from the match head did not pass through a flammable region of the methane jet. More energy is usually required to ignite a flowing gas with a hot particle than a stationary gas as the gas flow increases the heat loss from a particle. Thus it is possible that a match head, that would readily ignite a stationary methane mixture, could fail to ignite a jet of methane, especially if it was located too close to the leak source.

Ignitions were achieved using a chemical igniter, a much more powerful ignition source. Tests with ignition delays of 4, 9 and 14 s, with the methane release terminated 1 s after the igniter fired, gave peak pressures ranging from about 1.5 to 4 mbar. Figure 4.8 shows the pressure-time history for the 9 s delay test which gave the highest peak overpressure.

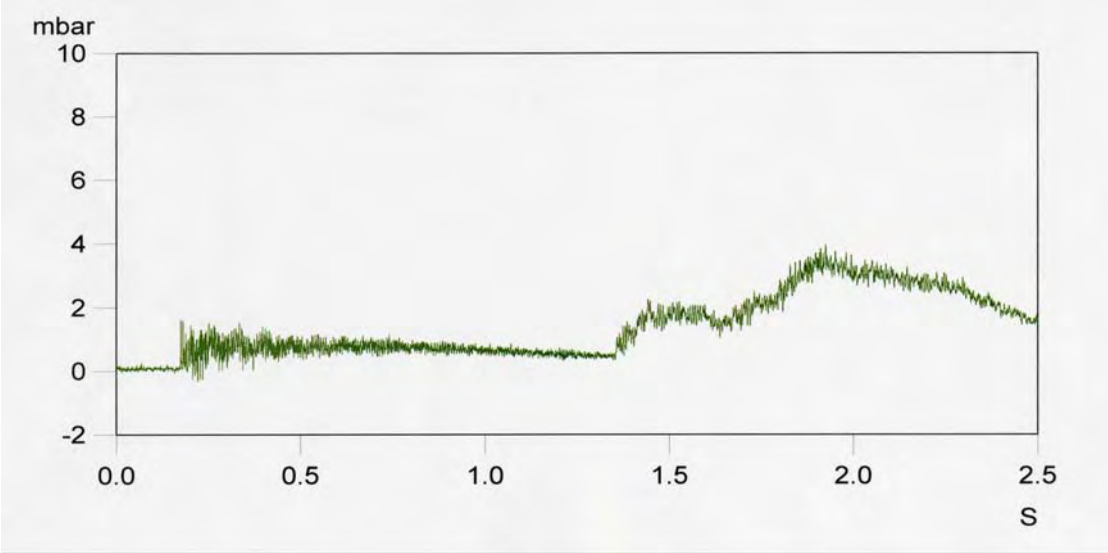

Figure 4.8 Pressure-time plot for 9 s ignition delay test (leakage rate of 8.2 g/s)

A further series of tests were then carried with the same leakage rate of about 8 g/s, but with different ignition locations, release durations and ignition delays. No ignitions were obtained even when a chemical igniter was used as the ignition source. When tests from the first series, which resulted in ignitions, were repeated, no ignitions were obtained. No satisfactory explanation can be offered for why these repeat tests no longer resulted in an ignition.

In the final series of tests the leakage rate was increased to about 9.6 g/s. CFD modelling predicts that this leakage rate should give a V_z of 0.15 m^3. Again, no ignitions were obtained in any of the tests.

4.3.2.4 Conclusions

From the results it can be concluded that ignitions of small volumes of flammable gas mixture, with a V_z of the order of 0.1 m^3, generated by a leak are difficult to achieve but not impossible. The measured explosion over-pressures from the tests in which ignition occurred indicate that the V_z criterion is safe since, as defined, its ignition has negligible effect for all but small enclosures (see below). Measured explosion pressures in the test chamber (internal volume of 31.3 m^3) ranged from about 1.5 to 4 mbar for a nominal V_z of 0.1 m^3. However, note that it would be appropriate to apply a safety factor in deciding the maximum leak size that can be given zone 2 NE classification and therefore leak rates as high as 8 g/s should not occur (In Section 5.2.3 it is argued that about a maximum of about 1 to 2 g/s would be more appropriate).

It has been shown that a conservative theoretical estimation of the overpressure resulting from the explosion of a gas cloud with V_z = 0.1 m^3 is equal to 0.184 barg.m^3 divided by the volume of the enclosure (c.f. Equation 4.2 with V_{stoich} = 0.023 m^3, see Section 4.2.2). Therefore, for the experimental enclosure with a volume of 31.3 m^3 this would predict an over-pressure of 6 mbar. In the experiments a maximum overpressure of 4 mbar was recorded, which is in reasonable agreement with our theoretical calculation given our conservative assumptions.

As a first approximation, these experimental results would translate to explosion pressures of about 9.5 to 25 mbar for an enclosure of 5 m^3 internal volume and about 47 to 125 mbar for a 1 m^3 enclosure. The predicted pressures for the 1 m^3 enclosure are high enough to cause extensive damage to most designs of enclosure and likely to cause serious injury from flying fragments to anybody close to the enclosure.

So whilst the above has demonstrated that the V_z criterion is conservative, and can therefore be adopted as a basis for safety for large enclosures, it cannot be used for small enclosures. An appropriate cut-off would appear to be around 10 m^3, since this implies a maximum overpressure of 12.5 mbar. Below 10 m^3 an additional criterion could be introduced maintaining V_z below some fraction of the enclosure volume. Clearly as V_z gets smaller still, the possibility of the release being ignited reduces rapidly (as demonstrated by the difficulty of igniting a gas cloud with $V_z = 0.1$ m^3). Such a criterion for zone 2 NE could take the following form:

$$\begin{aligned} V_0 > 10\ m^3 \qquad & V_z < 0.1\ m^3 \\ 1\ m^3 < V_0 < 10\ m^3 \qquad & V_z < 0.01\ V_0 \\ V_0 < 1\ m^3 : \qquad & V_z < 0.01\ m^3 \end{aligned} \tag{4.3}$$

where V_0 is the enclosure volume.

4.4 THERMAL RADIATION

Overpressure is not the only hazard that would arise should the leaking gas ignite. There is also a thermal radiation hazard from the explosion resulting in possible burn injuries and if the leaking gas continues to burn and a jet flame is established. The Shell FRED (version 5.0) hazard consequence modelling package has been used to estimate the likely thermal radiation levels resulting from a jet flame.

Figure 4.9 and Figure 4.10 show the predicted thermal radiation contours for a 8 g/s leak of natural gas from a 2.5 mm^2 hole (1.78 mm diameter). The leak was located 1 m above ground level and the leak orientation was horizontal into still air conditions.

The predicted flame lift-off was 0.56 m and the flame length about 1 m.

Figure 4.11 and Figure 4.12 show the predicted thermal radiation contours for the same release conditions but with the gas jet orientated vertically.

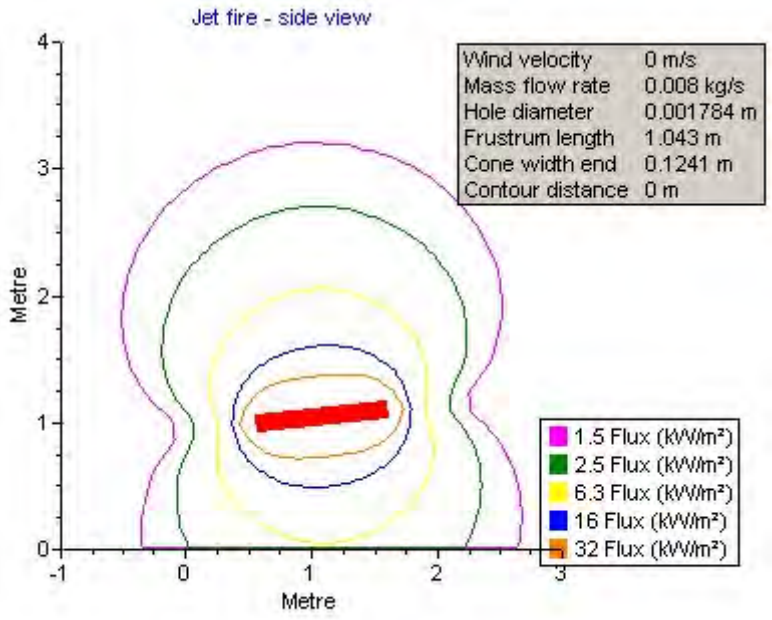

Figure 4.9 Side view for 0.008 kg/s horizontal leak

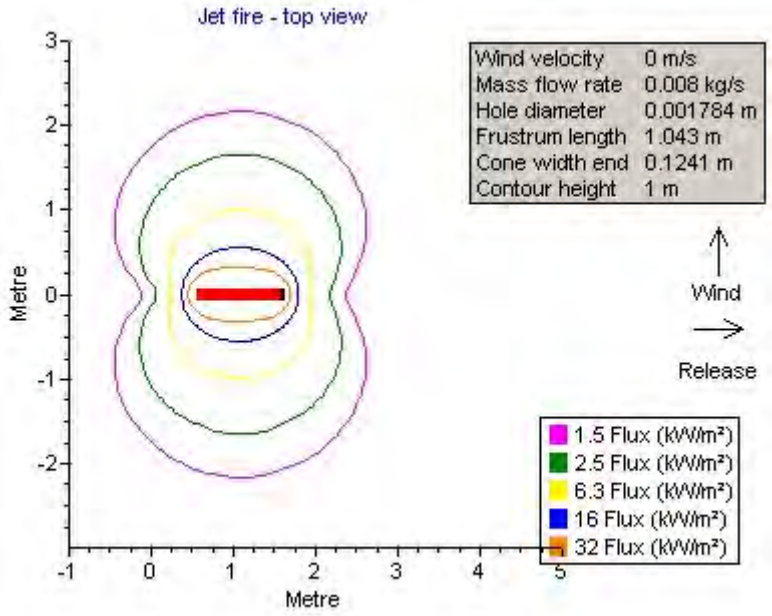

Figure 4.10 Plan view (1 m above ground level) for 0.008 kg/s horizontal leak

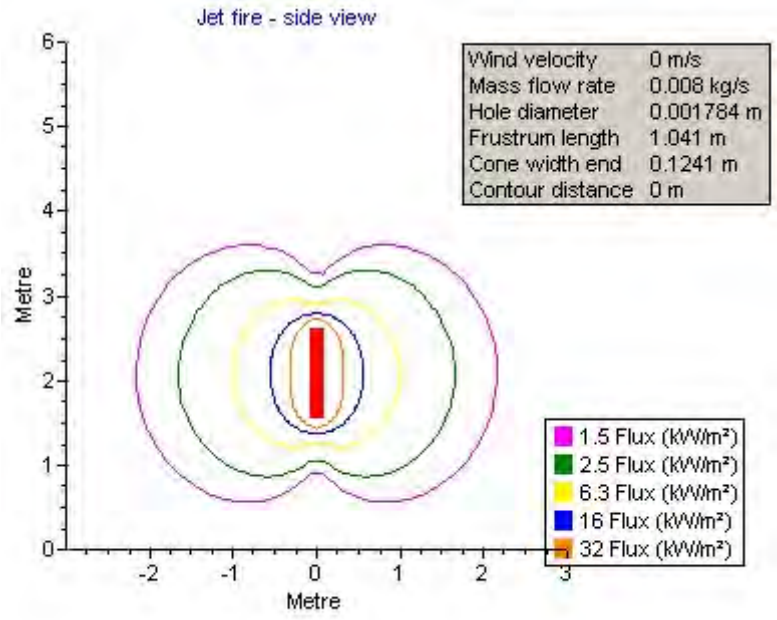

Figure 4.11 Side view for 0.008 kg/s vertical leak

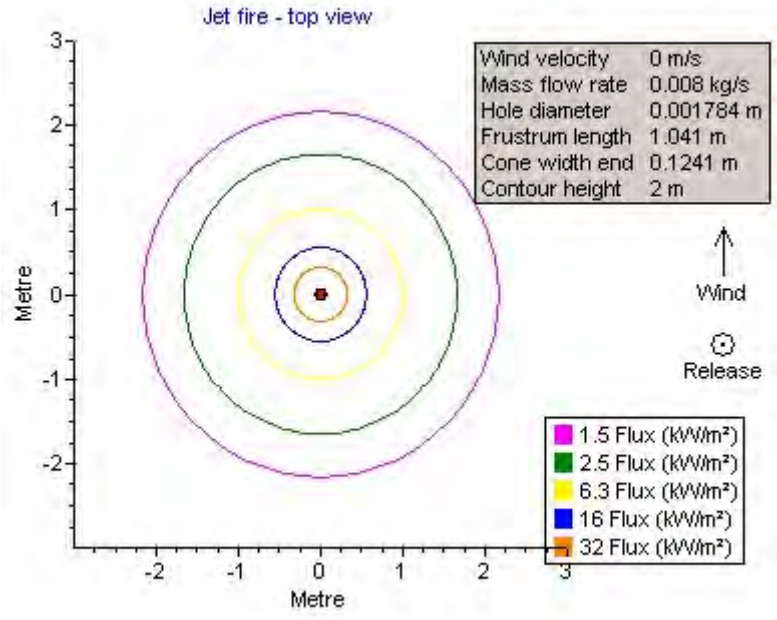

Figure 4.12 Plan view (2 m above ground level) for 0.008 kg/s vertical leak

It was not possible to undertake estimates for a 0.25 mm^2 hole size (diameter 0.564 mm) as this size was below the lower limit (1 mm diameter) at which FRED operates. Reducing the hole size to 1 mm in diameter (area of 0.785 mm^2), for a 8 g/s leakage rate, resulted in a negligible change to the predicted flame lift-off, flame length and thermal radiation levels.

Values in the technical literature for the time to pain for exposed bare skin are about 10 s for a thermal radiation intensity of 6.3 kW/m^2. This level is generally considered tolerable for

clothed personnel able to quickly move away from the flame. On this basis any persons further away than about 1 m from flame, provide they were not trapped or unconscious, are unlikely to suffer any burn injuries from the burning jet resulting from a 8.0 g/s leak. Even at closer distances burn injuries are likely to be negligible provided the person can move quickly away from the flame.

The predicted thermal radiation levels need to be treated with some caution as some of the input parameters for the calculations were outside the validated range of the 'pressurised release scenario' used to obtain Figure 4.9 to Figure 4.12. It is considered, however, that the predicted thermal radiation levels are conservative and thus over-predict the hazard from the jet flame as the predicted fraction of heat radiated from the flame (the F-factor) is very high. Using an alternative 'gas jet scenario', where again some of the input parameters were outside the validated range, a larger flame lift-off but shorter flame and lower thermal radiation levels were predicted.

5 ZONING OUTDOORS

5.1 INTRODUCTION

The application and limitations of the methodology in BS EN 60079:10 for zoning in the open air has been described in Section 2.4.1. Previous work (Gant and Ivings, 2005) has shown that the application of the standard to free unobstructed jets in the open air leads to predictions of the gas cloud volume V_z that are two to three orders of magnitude too large. This means that areas that could otherwise be classified as zone 2 NE would be classified as zone 2.

A gas leak in the open air generally leads to the formation of an unobstructed gas jet that interacts with the ambient wind field. Examination of this simple case provides a good insight into the gas cloud volume that can be expected to arise from a leak outdoors. These simple cases are described in Section 5.2 below, followed in Section 5.3 by a discussion on the interaction of jets with obstacles.

5.2 FREE JETS

The gas cloud volume resulting from an unobstructed leak is determined simply by the characteristics of the leak source (predominately the leak rate), the wind angle relative to the leak direction and the wind speed. Such leaks will generally be diluted quickly and lead to only very modest gas cloud sizes. This is due to the shear induced turbulence generated by the jet momentum, the jet interaction with the wind and the lack of re-entrainment. The worst case scenario, in terms of leading to the largest gas cloud volume, can be seen to be where the leak direction is aligned with the wind and the wind speed is low. Figure 5.1 shows a gas release interacting with wind fields of differing direction and speed simulated using CFD. Although these modelled gas leaks are from pressures higher than considered in this study, the general observations can be applied to leaks of any size. The figure clearly shows, with all plots shown on the same scale, that the greatest gas cloud volume results from the case with the lowest wind speed and the wind aligned with the leak direction. This observation makes it very much easier to calculate worst case gas cloud volumes for releases in the open air because simple free jet models can be used. Such models have been described earlier in Section 3.

1 m/s 3m/s 5m/s

coflow

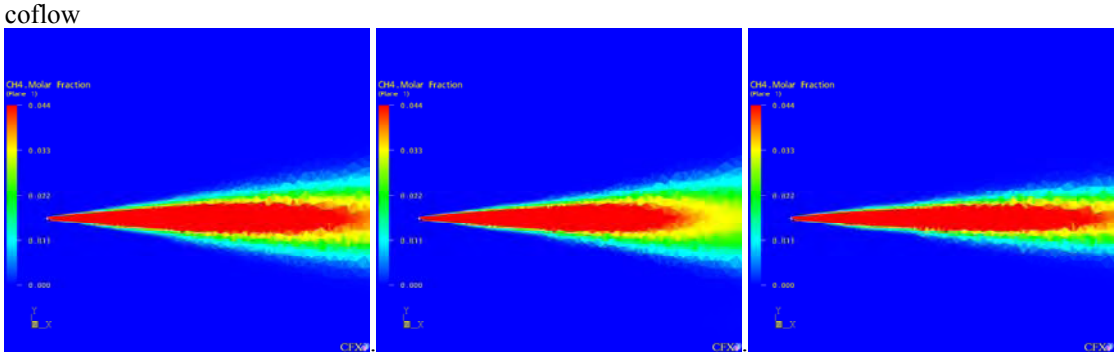

counter flow

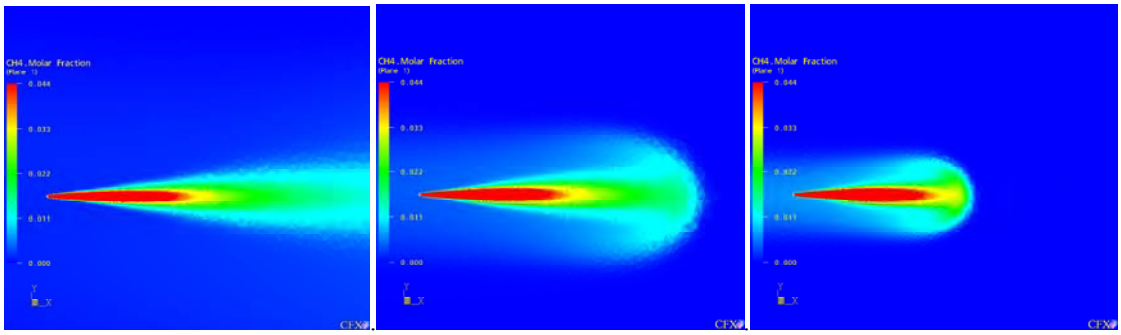

crossflow

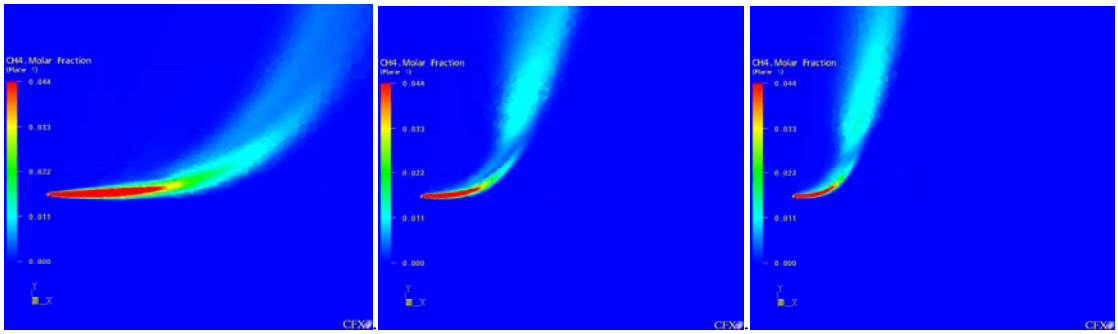

Figure 5.1 The interaction of a free jet with different wind fields: From top to bottom co-flow, counter flow and cross flow; from left to right 1 m/s, 3 m/s and 5 m/s.

Clearly, given the V_z criterion for zone 2 NE presented in Section 4, we are interested in the leak conditions required to give a gas cloud volume of V_z = 0.1 m^3. Below, a number of methods are presented for calculating these conditions, including the methodology in BS EN 60079:10, GaJet and CFD.

5.2.1 Leak rates that meet the V_z criterion

5.2.1.1 BS EN 60079:10 Methodology

The expression for calculating the gas cloud volume V_z as a function of the mass release rate and air change rate in BS EN 60079:10, see equation (2.4), can be rearranged to calculate the mass release rate required to give a specified V_z as follows

$$\dot{m} = V_z \frac{C\,k.LEL_m}{f} \frac{293}{T} \qquad (5.1)$$

In the calculations presented below the air change rate $C = 0.03\ s^{-1} = 108$ ach has been used as suggested in BS EN 60079:10 which is described as a conservative estimate of an outdoor air change rate. Note that despite arguing earlier that the methodology of calculating V_z outdoors in BE EN 60079:10 is not appropriate, it is still worth considering here simply as a comparison to the other methods. BS EN 60079:10 describes how an outdoor air change rate can be derived in terms of a hypothetical cube. However, this means that any air change rate can effectively be chosen by selecting an appropriate cube volume. For the time being we will continue to simply use $C = 0.03\ s^{-1}$, which is based on a hypothetical cube of side 15 m and a wind speed of 0.5 m/s.

The results of carrying out this calculation are shown along with the other model predictions in Section 5.2.1.2.

5.2.1.2 GaJet and CFD predictions

The free jet integral model GaJet has been used to determine the range of pressures and hole sizes that are required to produce a gas cloud with $V_z = 0.1\ m^3$. Since GaJet is so quick to run, it is possible to calculate the pressure required to give $V_z = 0.1\ m^3$ for a range of hole sizes. The same calculations are difficult with CFD as the pressure and hole size need to be specified first and then it takes some time to run the model to compute V_z. However, by reviewing the results of previous CFD simulations (including those in Section 4.3.1.1 and Gant and Ivings, 2005), cases have been identified where the predicted V_z is very close to $0.1\ m^3$.

The GaJet and CFD predictions and BS EN 60079:10 estimates of pressure and hole sizes required to give $V_z = 0.1\ m^3$ are shown in Figure 5.2. A detailed description of the content of the Figure follows.

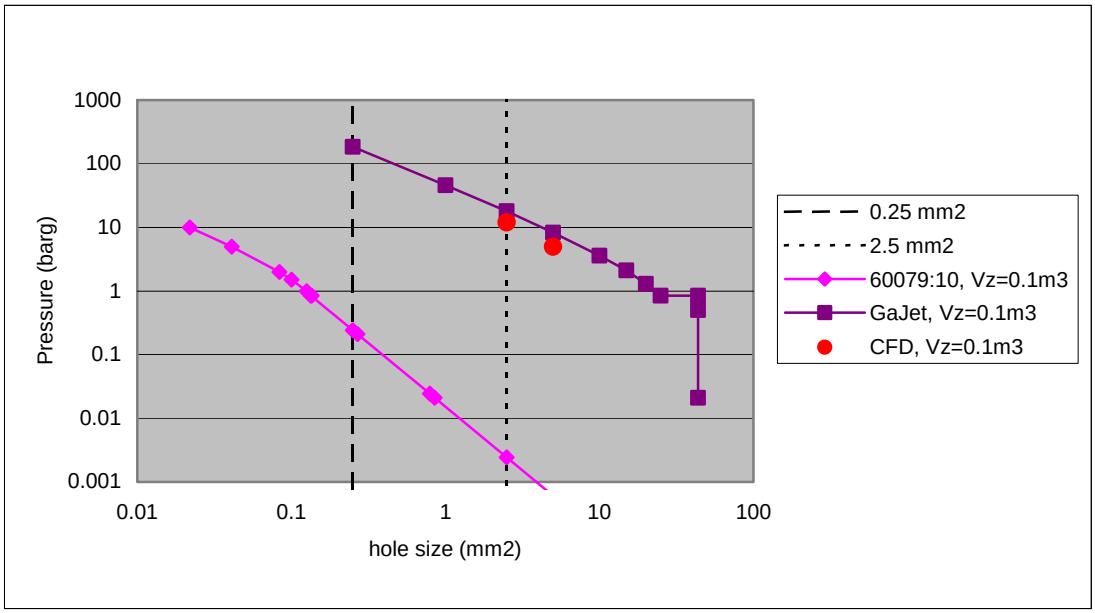

Figure 5.2 Graph of constant $V_z = 0.1m^3$ as a function of supply pressure and hole size, pink line-60079:10 calculation, purple line-GaJet calculation, red dots CFD predictions

The pink (lower) line in Figure 5.2 shows the results of applying the methodology in BS EN 60079:10:2003 for outdoor releases to determine the hole size and pressures required to give a gas cloud $V_z = 0.1$ m^3. This means that, according to the BS EN 60079:10 methodology, hole sizes / pressures below the line can be given zone 2 NE classification; e.g. for a hole size of 0.25mm^2, zone 2 NE can be applied for pressures below 0.24 barg. Due to the way that the methodology is derived, all of the leaks defined on this curve have the same leak rate, namely 0.044 g/s, see equation (5.1). Note that this mass release rate is derived assuming that the efficiency of ventilation, *f*, has a value of 1 in ideal situations – which is the case for a free jet and $C = 0.03$ s^{-1} as suggested by BS EN 60079-10. However, in applying the BS EN 60079:10 methodology, *f* could take a value up to 5 (impeded flow) which would mean that the leak rate to give a V_z of 0.1 m^3 would then be 5 times smaller (i.e. 0.009 g/s) and the pink line would be further to the bottom left of the chart than appears in Figure 5.2

The purple line represents a curve of pressures / holes sizes required to give a gas cloud with $V_z = 0.1$ m^3 as predicted by the integral model GaJet. For choked releases (i.e. for pressures greater than 0.85 bar) this curve represents leaks with a constant leak rate of 8.0 g/s. Note that the pressures and hole sizes are calculated assuming a discharge coefficient of unity. If a discharge coefficient of 0.8 were applied (as suggested by IGE/SR/25) then higher pressures would be required to give the same leak rate and the curve would move upwards. For subsonic releases GaJet assumes that the gas cloud volume, V_z, is independent of the supply pressure and depends only on the hole size (this assumption may not be strictly true for Mach numbers greater than about 0.3, but is valid at lower Mach numbers, see List, 1982). The model predicts that a subsonic leak with a hole size of 44 mm^2 will lead to a gas cloud with $V_z = 0.1$ m^3, independent of the supply pressure. Clearly there is some uncertainty in the model predictions in the transition from subsonic to choked releases. GaJet makes different assumptions for these two cases, which are likely to be valid away from this transition region.

To provide an additional check that the GaJet predictions are reasonable, the results of two CFD simulations have also been plotted in Figure 5.2 (red dots). These show the results of CFD simulations of free jets that give a value of V_z very close to 0.1 m^3. The CFD model generally

predicts larger gas cloud volumes for the same leak rate compared to GaJet. Overall the agreement is reasonable and it provides confidence in both models' predictions. The discrepancy between the two models is likely to be partly due to the way in which the gas cloud volume is calculated (post-processed) from the CFD model solution.

Clearly there is a very significant difference between the models and the BE EN 60079:10 methodology for estimating the pressure and hole size required to give a gas cloud with V_z = 0.1 m^3 and therefore the circumstances in which zone 2 NE can be applied. The data presented above can be used as a basis for determining the pressure and hole sizes for unobstructed leaks in the open air that can be classified as zone 2 NE. The next Section discusses how a reasonable safety factor can be adopted to account for modelling uncertainty and other variable factors.

5.2.2 Conservative leak rates

In the previous Section it was shown that to a reasonable approximation for unobstructed, choked releases the gas cloud size is dependent on the mass release rate only. Therefore it is appropriate to use a mass release rate as the cut off for zone 2 NE classification for unobstructed choked releases in the open air. We have shown above that for unobstructed releases a mass release rate of 8 g/s, or a hole size of 44 mm^2 for subsonic releases, will produce a gas cloud with V_z = 0.1 m^3. To account for modelling uncertainty and other variable factors it is appropriate to use a smaller leak rate. The yellow curve in Figure 5.3 shows a line of constant leak rate of 2 g/s which could be adopted as such a cut off.

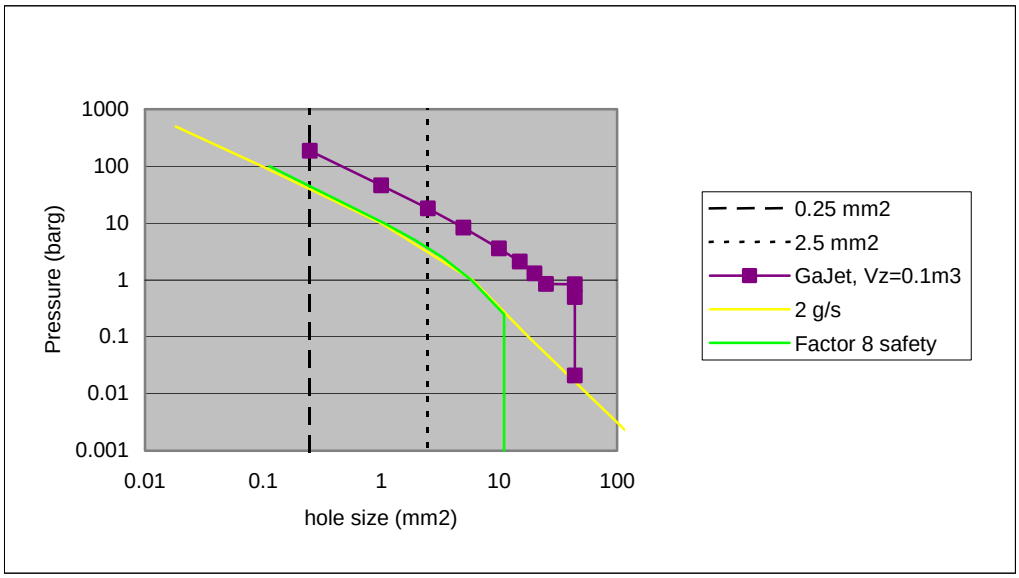

Figure 5.3 GaJet predictions of hole size and pressure required to give V_z = 0.1 m^3 (purple line). Curve of constant leak rate (yellow) and GaJet predictions of hole size and pressure required to give V_z = 0.0125 m^3

To assess how much of a safety factor this adds compared to the GaJet predictions for V_z = 0.1 m^3, the gas cloud volumes for a range of leak rates have been calculated using GaJet and are shown in Table 5.1. Commonly adopted zoning hole sizes have been used along with a discharge coefficient of unity. The data show that the predicted gas cloud volumes for leak rates of 1, 2 and 4 g/s are approximately 22, 8 and 3 times smaller than the 0.1 m^3 criterion. As these factors relate to differences in gas cloud volume they provide a direct relationship with the hazard. The sponsors of this project agreed that a factor of 8 would be a reasonable basis of

safety and therefore it would be appropriate to classify unobstructed leaks in the open air as zone 2 NE if the leak rate is less than 2 g/s.

To maintain the same factor of 8 safety for subsonic releases, an additional requirement that the hole size must be less than 11 mm^2 would also be required. The green line in Figure 5.3 shows the value of pressures and hole sizes that meet these two criteria, i.e. pressures and hole sizes that fall below and to the left of the green line could be classified as zone 2 NE. This cut-off therefore incorporates a factor of eight safety compared to the GaJet model predictions.

Table 5.1 Pressures required to give leak rate of 0.5, 1, 2 and 4 g/s and the corresponding GaJet predictions for V_z.

Hole size	***0.5 g/s***		***1 g/s***		***2 g/s***		***4 g/s***	
	Pressure (barg)	***V_z (10^{-3} m^3)***	***Pressure (barg)***	***V_z (10^{-3} m^3)***	***Pressure (barg)***	***V_z (10^{-3} m^3)***	***Pressure (barg)***	***V_z (10^{-3} m^3)***
0.25 mm^2	10.5	1.58	22.0	4.46	45	12.6	91	35.6
2.5 mm^2	0.31	1.37	1.3	4.46	3.6	12.6	8.2	35.6

5.2.3 Summary and implications for indoor zoning

GaJet has shown that a choked release of 8 g/s or a subsonic release from a hole of 44 mm^2 will give V_z = 0.1 m^3. To use these data as part of zoning methodology a degree of conservatism would be required. A safety factor of eight, for example, applied to the gas cloud volume would suggest that a maximum leak rate of 2 g/s and hole size of 11 mm^2 would be suitable as a criterion for zone 2 NE.

5.3 OBSTRUCTED JETS

5.3.1 Introduction

Obstacles in the path of a release, or obstructions to the free spreading of a jet release, have the potential to increase or decrease the gas cloud volume. For example, normal impingement of a jet release onto a flat surface, such as the ground, can generally be expected to decrease the gas cloud volume compared to that of a free jet since the area for entrainment of air, and thus dilution, is greatly increased by the radial spreading which occurs following impingement. However, in other circumstances the cloud volume can be increased by a jet's interaction with obstacles.

Here the results of a series of CFD simulations are presented which are used to investigate the circumstances and extent to which obstructions can increase the cloud volume. This information can therefore be used as the basis for guidance on the configurations in which an outdoor release can be treated as an unobstructed free jet, in which case the data presented in the previous Section can be used or where additional safety factors should be employed.

Two main classes of interaction are considered. Firstly, gas leaks constrained by one or two walls parallel to the leak direction and secondly gas jets interacting with obstacles. The details of the CFD modelling are presented in Appendix B. Here a brief summary of the cases examined is presented along with a discussion on the results and conclusions.

For all of the cases considered, a single size of gas leak is used with a hole size of 2.5 mm^2 and a leak rate of 0.86 g/s. GaJet was used to define the parameters for the CFD simulations. An axial length scale, L, and radial length scale, R (=D/2), are used to define the location and size of the obstructions relative to the jet (see Appendix B).

A parametric study varied the position and size of the wall(s) and obstruction, as summarised in Table 5.2. The radial offset was taken relative to the jet axis and the downstream location is the distance from the jet source to the upwind side of the obstruction.

Table 5.2 Summary of conditions used in CFD model simulations of constrained and impinging jets

Obstruction	*Radial offset*	*Downstream location*	*Obstruction size*
Single wall	0.5*R*, 0.8*R*, 1.0*R*, 1.2*R*	n/a	n/a
Twin walls	0.8*R*, 1.0*R*, 1.2*R*	n/a	n/a
Sphere	0	*L*	Diameter *D*
Cube	0	*L*	Side length *D*
Pipe	0	0.8*L*, 1.0*L*, 1.2*L*	Diameter 1.0*D*, 1.2*D*

5.3.2 Results

The full results for the CFD simulations are presented in Appendix B; here the gas cloud volumes for the obstructed cases are compared to the equivalent free jet results.

Table 5.3 shows the effect on the gas cloud volume of a wall parallel to the release axis. The results of four simulations are shown with the wall at different distances from the jet axis. The results show that the presence of the wall increases the cloud volumes by up to a factor of 4. The largest increase is seen where the jet is located closest to the wall.

Table 5.3 Relative size of gas cloud volume for a jet parallel to a wall compared to a free jet

Volume	*Free jet*	*0.5 R*	*0.8 R*	*1.0 R*	*1.2 R*
100% LEL	1.00	2.47	1.95	1.55	1.09
50% LEL	1.00	4.03	3.35	3.02	2.66
V_z	1.00	3.66	3.04	2.71	2.37

The effect of two walls on the 100% LEL gas cloud volume is shown in Table 5.4. In this case the gas cloud volumes are between 1.7 and 3.9 times greater than the equivalent single wall case and in turn between 1.8 and 7.6 times larger than the equivalent free jet. Data is unavailable for the 50% LEL and V_z volume as they extended beyond the end of the computational domain, see Appendix B.

Table 5.4 Relative size of gas cloud volume for a jet parallel to two walls compared to a free jet

Case	*Free jet*	*0.8 R*	*1.0 R*	*1.2 R*
100% LEL	1.00	7.55	4.62	1.82

The effect on the gas cloud volume of the jet interaction with a cube and a sphere compared to a free jet are shown in Table 5.5. The results show that the sphere and cube have roughly the same effect on the gas cloud volume, increasing it by a factor of 1.3 to 2.1.

Table 5.5 Relative size of gas cloud volume for a jet interacting with obstacles compared to a free jet

Case	*Free jet*	*Sphere*	*Cube*
100% LEL	1.00	1.25	1.27
50% LEL	1.00	1.68	1.53
V_z	1.00	1.50	2.09

Table 5.6 shows the CFD predictions of the effect of a pipe on the gas cloud volume. In all cases, the computed cloud volumes can be seen to increase due to the jet interaction with the pipe compared to the free jet case, except for one case where it stays the same. The increases in gas cloud volume compared to the free jet case are relatively modest with the largest increase being a factor of 1.5.

Table 5.6 Relative size of gas cloud volume for a jet interacting with a pipe compared to a free jet

Case	*Free jet*	*1.2D 1L*	*1D 0.8L*	*1D 1L*	*1D 1.2L*
100 % LEL	1.00	1.30	1.49	1.28	1.19
50 % LEL	1.00	1.21	1.11	1.18	1.23
V_z	1.00	1.08	1.00	1.08	1.14

5.3.3 Summary

The above results have shown the significance of obstacles, walls and blockages in determining the gas cloud volume resulting from a low pressure gas leak. Zoning for obstructed locations outdoors will need to take these factors into account. For the cases considered, the CFD simulations have shown a maximum increase in gas cloud volume of a factor of about 8 compared to that for a free jet. The case that led to this large gas cloud volume, the jet running parallel to two walls, could be seen to be an unlikely scenario in practice, i.e. the chances of a jet running exactly parallel to two walls is small. However, none of the cases considered here have taken into account the possibility of gas becoming re-entrained through the jet's interaction with more complicated obstacles and the wind field.

5.4 CONCLUSIONS

The results above indicate that for a given size of release an obstructed jet could give a gas cloud about 8 times the size of the equivalent free jet. Therefore, to define a cut-off for zone 2 NE that is applicable to obstructed as well as unobstructed releases, it is appropriate to calculate the leak rate which will give a free jet gas cloud volume of $V_z = \frac{0.1}{8} = 0.0125$ m^3. GaJet predicts that for choked releases a leak rate of 2 g/s, or for subsonic releases a hole size of 11 mm^2, will provide this, as has been shown earlier in Section 5.2.2. Therefore, the integral and CFD models predict that for release rates less than 2 g/s and hole sizes smaller than 11 mm^2 the gas cloud volume V_z will be less than 0.1 m^3 even if the jet interacts with simple obstacles as described above. However, this criterion may not be appropriate in cases where there is a significant amount of congestion, or an arrangement of obstacles that leads to re-entrainment of gas into the jet or reduces the dilution of the jet more significantly than for any of the cases considered above.

(Note that a limitation of the work described here is that the obstructed leak simulations have all been carried out with a choked release and therefore the extension of the findings to subsonic releases with large hole sizes need to be approached with caution. However, hole sizes greater than 5 mm^2 are rarely used for area classification).

The criteria set out above do not include a safety factor for obstructed cases. Such a safety factor can be introduced in a similar way to that described for free jets (see Section 5.2.2, and in particular Table 5.1) by examining the release rate required to produce a smaller V_z. For example, reducing the cut-off to 1 g/s (or 5.5 mm^2 for subsonic releases) would introduced a safety factor of ($\frac{12.6}{4.46}$ =) 2.8 for obstructed leaks and a cut-off of 0.5 g/s (or 2.8 mm^2 for subsonic releases) would give a safety factor of ($\frac{12.6}{1.58}$ =) 8.0.

The above suggests two possible approaches for zoning outdoor equipment. The simplest would be to specify a single, low mass release rate (and corresponding hole size for sub-sonic releases) that could be applied to both unobstructed and obstructed leak locations, e.g. 1 g/s and 5.5 mm^2. An alternative approach would be to use the lower rate in the majority of cases and then use a higher value, 2 g/s and 11 mm^2 say, for leak locations that are completely free from obstructions. In either case a judgement would be required to confirm that the leak is not in an area that is either heavily congested or confined to such an extent that significant gas cloud build-up could occur, which may make the above approach inappropriate.

Table 5.7 below shows the mass release rate for a range of hole sizes and supply pressures and indicates which of these meet the suggested criteria for zone 2 NE above. The data takes account of the limit on the pressure of 10 barg which is defined in the scope of this project.

Recall that BS EN 60079:10 implies that for outdoor releases of methane, assuming a hypothetical cube volume of side 15 m and an air change rate of 0.03 s^{-1}, a zone 2 NE classification is appropriate for leak rates less than 0.044 g/s. Table 5.7 therefore shows the reduction in conservatism implied by the proposed criteria. For example, for a hole size of 0.25 mm^2 the BS EN 60079:10 methodology would lead to a zone 2 classification above 400 mbarg, whereas the current approach would imply that zone 2 NE is appropriate up to 10 barg.

Table 5.7 Leak rates (calculated using equations (3.7) and (3.10) using C_d=0.8) that meet the following criteria: red <2 g/s, <11mm^2 and blue <1 g/s, <5.5mm^2

Leak rates (g/s)		Hole Size (mm^2)						
		0.1	**0.25**	**1**	**2.5**	**5**	**10**	**25**
Pressure (barg)	**0.021**	0.00	0.01	0.04	0.11	0.21	0.43	1.07
	0.1	0.01	0.02	0.09	0.23	0.47	0.93	2.33
	0.2	0.01	0.03	0.13	0.33	0.65	1.31	3.27
	0.5	0.02	0.05	0.20	0.51	1.02	2.03	5.08
	1.0	0.03	0.07	0.28	0.70	1.40	2.80	7.01
	2.0	0.04	0.10	0.42	1.05	2.10	4.20	10.49
	4.0	0.07	0.17	0.70	1.75	3.49	6.98	17.46
	5.0	0.08	0.21	0.84	2.09	4.19	8.38	20.94
	8.0	0.13	0.31	1.26	3.14	6.28	12.56	31.40
	10.0	0.15	0.38	1.53	3.84	7.67	15.35	38.36
	20.0	0.29	0.73	2.93	7.32	14.64	29.28	73.20
	50.0	0.71	1.78	7.11	17.77	35.54	71.09	177.72

5.4.1 Implications for indoor zoning

Note that the criteria for the use of zone 2 NE for outdoor obstructed releases should also apply as upper limits to all releases within enclosures. By definition, releases within enclosures are likely to experience some form of confinement. It is unreasonable to expect that the ventilation of an enclosure should be more effective at diluting a gas cloud than if that leak were outdoors (unless it was specifically designed to do so, such as in a gas turbine enclosure). Therefore, if the above suggestion of using 1 g/s is applied for outdoor obstructed releases then all releases greater than 1 g/s in an enclosure should be classed as at least zone 2.

6 ZONING INDOORS

6.1 INTRODUCTION

6.1.1 Zoning in enclosures

The two main methodologies employed in the UK for zoning indoor spaces, BS EN 60079:10 and IGE SR 25, are described in Section 2. In this Section we describe how data has been generated within the current project and how it can be used to produce a transparent and soundly based zoning methodology appropriate for low pressure gas systems. The data therefore needs to be utilised in such a way that a fairly simple and practical methodology can be derived.

In this Section the assumption is made that the specification of the zone is based on an assessment of the adequacy of the ventilation to dilute secondary releases down to acceptably low levels. This low level is defined by $V_z < 0.1$ m^3 and the small enclosure criterion, equation (4.3), discussed in Section 4. Additional requirements, for example on the availability of the given ventilation condition, are also appropriate and the current procedures on this in BE EN 60079:10 are applicable. As defined in the scope of this project, we are only concerned with pressures less than 10 barg and generally with holes sizes smaller than 5 mm^2, paying particular attention to the hole sizes 0.25 mm^2 and 2.5 mm^2 that are commonly used for area classification.

In this project we are interested in ventilation that is used to prevent the build up of gas within the enclosure as opposed to ventilation that is designed to locally limit the size of a flammable gas cloud. For this reason we do not expect ventilation to be any better at limiting the size of a flammable gas cloud than if the same leak were in a completely un-obstructed environment with no possibility of re-entrainment (i.e. outdoors). Therefore an upper limit can be placed on the leak rate that should be considered for area classification in enclosures based on the size of a free jet that leads to a gas cloud with a volume of $V_z = 0.1$ m^3. Section 5 of this report describes how such a leak rate can be defined.

6.1.2 Development of data

The main objective of this project was to generate data that can be used as part of a zoning methodology for low pressure gas equipment in naturally or mechanically ventilated enclosures. The data required will therefore need to allow for correlation of the gas cloud volume, and in particular V_z, resulting from a secondary gas leak against the gas supply pressure, hole size and other factors. The only practical approach to developing such data is through CFD modelling. However, before this data can be used with confidence the modelling approach needs to be validated against experimental measurements of gas cloud build up in enclosures. These data then need to be used to derive a practical measure or methodology for assessing the ventilation effectiveness.

In the next Section ventilation effectiveness is discussed and two new methods for measuring it are introduced. In Section 6.3 an overview of the work that has been carried out to validate the CFD model is presented. The details of this validation exercise can be found in Appendices C and D that describe the experiments and CFD modelling respectively. In Section 6.4, the additional CFD modelling that has been carried out to create further data for zoning in enclosures is described. This additional CFD modelling expands on the simulations carried out during the CFD model validation by examination of a wider range of parameters as well as other factors that can have an influence on gas cloud build-up such as enclosure volume and the effects of heat transfer. The gas cloud volumes from all of the CFD simulations are also presented in Section 6.4, along with a description of the effect of these different parameters on the gas cloud volume. Section 6.4 concludes with discussions on how these data can be used for

area classification of indoor spaces and the implications for large and small enclosures. Section 6.4.3 draws some conclusions on the use of these data and examples of how they can be applied are provided in Section 6.6.

6.2 VENTILATION EFFECTIVENESS

The key factor that determines the zone for a particular piece of equipment is the effectiveness of the ventilation at diluting a potential leak. BS EN 60079:10 provide a methodology by which the ventilation effectiveness in an enclosure can be assessed. This is achieved through calculation of the size of the hypothetical volume V_z which is dependent on the ratio of the mass release rate of flammable gas to the enclosure air change rate. Clearly this makes the assumption that the air change rate is known. However, BS EN 60079:10 does not make any recommendation or suggestion as to how the air change rate, or equivalently the ventilation rate, can be measured or calculated. In Section 2.2.3 methods for estimating air change rates are discussed. The measures of ventilation effectiveness introduced below assume that one of these methods has been used.

The second observation regarding the methodology in BS EN 60079:10 is that the ventilation effectiveness, and hence the zone, is dependent on the air change rate (measured in air changes per hour or per second) rather than the ventilation rate. This means that for large enclosures, where the ventilation rate is likely to be relatively high, the air change rate could still be quite small, leading to the conclusion that the ventilation is not effective. However, in general it would be expected that even with relatively low air change rates, the dispersion of gas following a secondary release in increasingly large enclosures would be likely to behave in a similar manner to a release outdoors and therefore be far less hazardous than the BS EN 60079:10 methodology would suggest.

Two alternative measures of the ventilation effectiveness will now be introduced. They are similar in their level of complexity to the method used in BS EN 60079:10 but are instead based on a physical understanding of the behaviour of the dispersion of high momentum jets in an enclosure. Furthermore, in Section 6.4 these measures are assessed by applying them to the cases for which we have gas cloud volume data provided by CFD simulations. By providing these measures of ventilation effectiveness we aim to establish a practical and soundly-based methodology to differentiate between situations where V_z gas cloud volumes greater and smaller than 0.1 m^3 can arise.

6.2.1 Entrainment requirement

The first method of assessing ventilation effectiveness is to compare the volume of clean air entrained by a free gas jet to the ventilation rate of the enclosure. Clearly if the rate of air entrainment required for a leak to dilute down to a given level is less than the ventilation rate, then a gas cloud would be expected to build up in the enclosure. In these circumstances V_z would very likely exceed 0.1 m^3 and the ventilation rate would not be sufficient.

Methods that can be used to calculate the entrainment volume supply rate for a free jet are described in Section 3.5. Therefore, assuming that this value can be computed for a given supply pressure and hole size this measure of ventilation effectiveness can be calculated as follows

$$VE_1 = \frac{Q_{ent}}{\dot{V}} \qquad (6.1)$$

where Q_{ent} (m^3/s) is the total volumetric air entrainment requirement of a free jet (up to a specified location downstream from the point of release), $\dot{V} = CV_0$ is the enclosure ventilation rate, V_0 is the enclosure volume and C is the air change rate. Therefore, high values of VE_1 imply poor ventilation, i.e. the ventilation is not supplying enough fresh air to permit the jet to entrain and dilute the flammable gas to a safe level.

It is worth noting the similarity between this measure of ventilation effectiveness and that used in BS EN 60079:10, namely V_z – see equation (2.4). The air entrainment requirement of a free jet is essentially a linear function of the mass release rate of gas (List, 1982), therefore, like BS EN 60079:10, this measure of ventilation effectiveness is proportional to the gas mass release rate. However, a key difference is that VE_1 is inversely proportional to the ventilation rate, $\dot{V}$, whereas the BS EN 60079:10 calculated V_z is inversely proportional to the air change rate, C. This means that the proposed measure of ventilation effectiveness, VE_1, can be more readily met for large enclosures with low air change rates than is the case with BS EN 60079:10.

6.2.2 Flammable gas concentration at the ventilation outlets

The second method for assessing the ventilation effectiveness is to calculate the average flammable gas concentration at the outlets from the enclosure. The idea behind this approach can be seen by considering an example in which the gas concentration at the outlet is above LEL, which would clearly imply that the ventilation is insufficient to dilute the gas leak and therefore that zone 2 NE would be inappropriate.

In practice the gas concentration as it leaves an enclosure will not be uniform across the ventilation opening (in fact it is likely to also vary with time). However, the average gas concentration across the ventilation outlets can be simply calculated if the ventilation rate and mass release rate of flammable gas is known. The latter can be used to calculate the volume flow rate of flammable gas leaving the enclosure by assuming that it is diluted to such an extent that it has reached ambient temperature and pressure. The average volumetric concentration at the outlets can therefore be calculated using

$$c_{out} = \frac{\dot{m}}{CV_0\rho_{amb}} = \frac{\dot{m}}{\dot{V}\rho_{amb}} \qquad (6.2)$$

where ρ_{amb} is the density of the flammable gas at ambient temperature and pressure. It is often more convenient to express this concentration in terms of the LEL (by volume) in which case c_{out} is divided by LEL and expressed as a fraction.

The practical application of an average concentration at the enclosure outlet as a measure of ventilation effectiveness requires that some acceptable upper limit is placed on this value. For example, $c_{out} < 20\%$ LEL could be used as a necessary requirement for the application of zone 2 NE. This approach is similar to the guidance in the Energy Institute code IP15 (2003) which states that the average concentration of gas within a building should be less than 20% LEL in a well mixed atmosphere for continuous releases. Clearly the average concentration at the outlet is equivalent to the average concentration within the building.

6.2.3 Discussion

The two methods described above are essentially the same in practice as they both provide a measure of the ratio of the gas mass release rate to the enclosure ventilation rate. Note that taking $VE_1 = 1$, which represents the point at which the ventilation is only just providing enough clean air to dilute the gas release, is equivalent[3] to an outlet concentration of c_{out} = 31% LEL (based on calculations carried out using GaJet).

Given the simplicity of the second of these two measures of ventilation effectiveness, only the average volumetric gas concentration at the outlet will be used from here on. The data presented in Section 6.4 enables us to assess whether we can use this measure of ventilation effectiveness to distinguish between cases that lead to large gas clouds (and in particular where $V_z > 0.1$ m^3) and those that don't. Clearly in practice there are many factors that will affect gas cloud build-up. Therefore all we can expect is to be able to predict the general trends and be able to implement a methodology that is conservative. Having created such suitable data it will then be possible to decide on values for c_{out} which would be appropriate for the definition of zone 2 NE.

Finally, it is worth recapping on the similarity, and differences, between the measure of ventilation effectiveness proposed here, i.e. c_{out}, and that used in BS EN 60079:10, i.e. the hypothetical volume V_z. If we ignore all of the constants in the equations used to calculate these two measures of ventilation effectiveness they can be written as follows

$$c_{out} \propto \frac{\dot{m}}{CV_0}; \qquad V_z \propto \frac{\dot{m}}{C} \tag{6.3}$$

This highlights that for a constant air change rate and mass release rate, c_{out} reduces as the enclosure volume increases but the BS EN 60079:10 calculated V_z remains constant. In Section 6.4 both of these values are calculated and then plotted against V_z volumes as predicted with a validated CFD model. We will therefore ensure that we make the distinction between the BS EN 60079:10 calculated V_z, i.e. using formula (2.4), and V_z predicted by a CFD model that takes into account the physical interaction of the leak with the ventilation within the enclosure.

6.3 CFD MODEL VALIDATION

6.3.1 Validation programme of tests

The aim of the validation exercise was to generate sufficient confidence in the CFD model so that it can be applied to a wide range of scenarios relevant to this project. Ideally the validation exercise would include test cases with a very wide range of parameters including differing enclosure sizes, pressures from 21 mbarg to 10 barg, a range of hole sizes, a wide range of ventilation rates and arrangements, different configurations of equipment in the enclosure and different leak locations and directions. Clearly, to carry out a series of experiments that covers all of these conditions would be prohibitively time consuming and expensive. The experimental programme therefore includes a degree of compromise in the number and range of tests cases carried out. Nevertheless, tests do cover an extensive and challenging set of conditions.

All of the experimental tests were undertaken in a purpose-built enclosure using leak hole sizes of 0.25 mm^2 and 2.5 mm^2. Isothermal conditions were maintained throughout the tests as

[3] *Assuming that Q_{ent} is calculated based on the total volume of air entrained in the jet to the plane at which the centreline concentration is 50% LEL – see Section 3.5*

previous experience has shown that defining appropriate boundary conditions for non-isothermal flows can be difficult and any errors in doing this can have a significant effect on the results. The effects of non-isothermal conditions on gas cloud build-up are explored in Section 6.4.

Three configurations of the leak location and direction were used. The first and simplest case consisted of a leak directed towards the middle of the enclosure such that the gas dispersion was not affected greatly by the interaction of the resulting gas jet with obstacles or walls. This case was used to make an initial assessment of the effect of the ventilation rate on the gas cloud size compared to the equivalent free jet. Since there was little possibility of re-entrainment of gas into the jet, gas cloud volumes were expected to be relatively small for this configuration.

The second configuration chosen was based on the results of the obstructed jet simulations described in Section 5.3. In this case the jet was close to and directed parallel to one of the side walls, with the anticipated effect of decreasing the volume of air available for dilution, thereby increasing the gas cloud volume. The final configuration was chosen on the basis of the results of a series of CFD simulations to find a credible 'worst case' scenario. A range of leak directions and locations relative to a large obstacle in the enclosure were modelled and the case which led to the largest gas cloud was chosen as the basis of configuration 3. This scenario consisted of a leak located in a corner of the enclosure with a large rectangular obstacle positioned to one side.

For each of the three configurations, a range of ventilation conditions and leak rates were considered. The cases were chosen by considering the average gas concentration at the outlet, the gas cloud volume V_z as determined by applying BS EN 60079:10 and the gas cloud volume for the equivalent free jet calculated using GaJet (see Section 3.4). In particular, the tests were chosen to give gas cloud sizes both greater and smaller than $V_z = 0.1$ m^3.

Table 6.1 provides a summary of the test programme for the CFD model validation study. The third column shows the approximate pressure required to give the specified leak rate. The values are based on an assumed atmospheric pressure of 1.01 bar, a stagnation temperature of 20 °C and a discharge coefficient through the orifice of unity. The ventilation rates are based on the specified air change rate and take into account the reduced volume of the enclosure due to the obstacle. The final three columns provide information that can be used to indicate the expected level of gas build-up in the enclosure. Note that the concentration at the outlet is expressed as a percentage of LEL and the two methods used to calculate V_z use different units (the last two columns). There was some variation from this test programme when the experimental tests were carried out, these details are given in Appendix C.

Table 6.1 Validation programme of tests

Test	*Hole size* A mm^2	*Approx pressure* P_0 *barg*	*Leak rate* $\dot{m}$ *g/s*	*Air change rate* C */hour*	*Ventilation rate* $\dot{V}$ *Litres/s*	*Average conc. at outlet* c_{out} *% LEL*	*Gas cloud volume calculated using 60079:10* V_z m^3	*Equivalent free jet gas cloud volume* V_z *Litres*
Configuration 1								
C1-1	0.25	2.5	0.15	6	74.53	6.9	6.1	0.25
C1-2	2.5	0.06	0.22	12	149.07	5.0	4.5	1.37
C1-3	0.25	5	0.26	6	74.53	11.9	10.6	0.56
C1-4	0.25	10	0.47	2	24.84	64.7	57.8	1.38
C1-5	0.25	10	0.47	6	74.53	21.6	19.3	1.38
C1-6	0.25	10	0.47	12	149.07	10.8	9.6	1.38
C1-7	2.5	0.3	0.49	12	149.07	11.2	10.0	1.37
C1-8	2.5	1	0.86	2	24.84	118.3	105.6	3.41
C1-9	2.5	1	0.86	6	74.53	39.4	35.2	3.41
C1-10	2.5	1	0.86	12	149.07	19.7	17.6	3.41
C1-11	2.5	1	0.86	24	298.13	9.9	8.8	3.41
C1-12	2.5	3	1.72	12	149.07	39.4	35.1	9.60
Configuration 2								
C2-3	0.25	5	0.26	6	74.53	11.9	10.6	0.56
C2-4	0.25	10	0.47	2	24.84	64.7	57.8	1.38
C2-5	0.25	10	0.47	6	74.53	21.6	19.3	1.38
C2-6	0.25	10	0.47	12	149.07	10.8	9.6	1.38
C2-7	2.5	0.3	0.49	12	149.07	11.2	10.0	1.37
C2-8	2.5	1	0.86	2	24.84	118.3	105.6	3.41
C2-9	2.5	1	0.86	6	74.53	39.4	35.2	3.41
C2-10	2.5	1	0.86	12	149.07	19.7	17.6	3.41
C2-12	2.5	3	1.72	12	149.07	39.4	35.1	9.60
Configuration 3								
C3-3	0.25	5	0.26	6	74.53	11.9	10.6	0.56
C3-4	0.25	10	0.47	2	24.84	64.7	57.8	1.38
C3-5	0.25	10	0.47	6	74.53	21.6	19.3	1.38
C3-6	0.25	10	0.47	12	149.07	10.8	9.6	1.38
C3-7	2.5	0.3	0.49	12	149.07	11.2	10.0	1.37
C3-8	2.5	1	0.86	2	24.84	118.3	105.6	3.41
C3-9	2.5	1	0.86	6	74.53	39.4	35.2	3.41
C3-10	2.5	1	0.86	12	149.07	19.7	17.6	3.41

6.3.2 Experimental Programme

The aim of the experimental programme was to provide sufficient data to validate the CFD model. Due to the difficulty in estimating gas cloud volumes based on a finite number of gas concentration measurements, the experimental programme was not used to establish gas cloud volumes for input into a zoning methodology. However, the results of the CFD simulations

carried out as part of the validation exercise provide V_z data (in addition to the data required to validate the model).

The experiments were carried out in a purpose built enclosure at HSL with internal dimensions of approximately $4 \times 4 \times 3$ m. A total of 29 different tests were carried out using a range of ventilation conditions, gas supply pressures, obstacle configurations, hole sizes and leak locations and orientations. A non-flammable tracer gas with the same density as methane was used in the tests. Point gas concentration measurements were made at 14 locations within the enclosure. The CFD results were compared against these point measurements and this comparison provides the basis for the model validation. Temperature measurements were also made within the enclosure and these demonstrated that the tests were essentially isothermal. The ventilation was carefully controlled and monitored to ensure that the ventilation conditions were known and stayed constant throughout each test.

The experimental programme is described in detail in Appendix C.

6.3.3 CFD model validation

The ability of the CFD model to predict the dispersion behaviour following a high momentum leak of methane into a ventilated enclosure has been assessed by comparing the results of the CFD simulations against each of the 29 experimental tests. In addition to these 29 tests, a number of other simulations have been carried out to assess the sensitivity of the results to various modelling parameters. The details of the CFD model validation study can be found in Appendix D.

Overall, the simulations show good agreement with the experimental data. The vast majority of point gas concentrations are predicted to within 0.5% vol/vol. It has been estimated that this equates to an error in the V_z predictions of roughly +/- 30%. With the application of a suitable safety factor into the area classification methodology to be based on these data, this level of accuracy is judged sufficient for the required purpose.

6.4 DATA FOR ZONING IN ENCLOSURES

This Section of the report presents one of the key elements of this project. It discusses the results of the CFD simulations used to generate data for area classification, the physical factors that affect the gas cloud volume, and hence the hazard, and describes how the data can potentially be used as part of an area classification methodology.

6.4.1 Gas cloud volume data

Having established in the model validation study that the CFD simulations predict V_z to an acceptable degree of accuracy, the validated CFD model has been applied to assess the effect of a wider range of factors that affect gas cloud build up following a secondary leak in a ventilated enclosure. The aim of these further tests is not to model a very large number of realistic cases accurately, but instead to consider the factors that may have an effect on gas cloud build-up and to assess the magnitude of their effect on V_z. In summary, the factors that have been taken into account and the range of parameters considered are:

- Ventilation rate
  - 2 – 24 ach / 0.3 – 1300 litres/s

- Hole size
  - 0.25 mm^2 and 2.5 mm^2

- Leak rate / supply pressure
  - Leak rates 0.01 g/s to 1.7 g/s
  - Supply pressures 21 mbarg to 10 barg

- Enclosure volumes
  - Large enclosure ($10 \times 10 \times 4.25$ m)
  - Medium enclosure ($4 \times 4 \times 3.96$ m)
  - Small enclosure ($2 \times 2 \times 2$ m)
  - Very small enclosure ($1 \times 1 \times 1$ m)

- Leak location, direction and location of large obstruction(s) in enclosure
  - Approx. 20 different configurations across the different enclosures

- Heat transfer
  - Heat sources representative of a boiler
  - Cold floors
  - Heat loss to walls

In total 66 CFD simulations have been carried out (including those done for the validation study) leading to predictions of V_z that can be used as input to a methodology for zoning in enclosures. Many more CFD simulations have also been undertaken as additional sensitivity tests to provide confidence in the CFD predictions, although not all the results are described in this report. Details of the simulations can be found in Appendix E.

The CFD results are discussed in three Sections below, starting with the simplest cases in which the leak is not greatly affected by any obstructions or heat transfer effects. To fully understand the discussions on the data presented below we recommend that the interested reader consults Appendix E.

6.4.1.1 Enclosure volume, leak + ventilation rate

The results of the CFD simulations for cases in which the leak issues without obstruction into the centre of the enclosure and in which the jet runs parallel to the side wall (for the medium size enclosure only) are summarised in Table 6.2. These results cover the four enclosure sizes discussed in Appendix E, but do not include the cases in which the leak was located in a confined space or where there were significant temperature variations within the enclosure.

For all of the enclosure sizes and mass release rates in the range examined, the gas cloud volume correlates strongly with the average gas concentration at the outlet, c_{out}, see Figure 6.1. The results show that low levels of c_{out} correlate with small values of V_z, and, as c_{out} increases, V_z increases more and more rapidly until V_z reaches the enclosure volume. The latter can be seen clearly for the small enclosure by the four horizontal green diamonds.

Figure 6.1 can be considered as consisting of four areas: Data points in the bottom left of the graph indicate cases where the measure of ventilation effectiveness, c_{out}, indicate a negligible hazard and is confirmed by a small predicted V_z. Conversely, points in the top right of the graph show where c_{out} and the predicted V_z gas cloud volumes are both high. A data point in the bottom right hand portion of the graph would indicate areas where the measure of ventilation effectiveness is indicating a high hazard but the actual hazard is low. This indicates that the use of c_{out} as a measure of ventilation effectiveness is conservative in this case. Finally, points in the top left portion of the graph (if there were any) would indicate where c_{out} is suggesting that the ventilation is adequate to control the leak but the gas cloud volume is in fact large. Any points in this area would present some concern as it would suggest that c_{out} is not a conservative

measure of the ventilation effectiveness. Clearly, all of this depends on where the line is drawn between each of these portions of the graph. The $V_z = 0.1$ m^3 criterion is the obvious division between the top and bottom parts of the graph as it has been shown in Section 4 that gas cloud volumes with $V_z < 0.1$m^3 are not hazardous. Based on the data presented here, a vertical division at c_{out} at 39% LEL would avoid any of the data points appearing in the top left portion of the graph.

Figure 6.1 shows a significant overlap between the data for the different enclosure volumes. For a given average gas concentration at the outlet, the predicted gas cloud volume V_z is roughly of the same order of magnitude for each enclosure volume. In general though, for a given c_{out}, V_z tends to be smaller in the smaller enclosures. This means that a zoning methodology based on c_{out} will be more conservative for smaller enclosure volumes. See the further discussion on this in Section 6.4.5.

Having compared the predicted gas cloud volume V_z against the proposed measure of ventilation effectiveness c_{out}, it is interesting to do the same for the measure of ventilation effectiveness used in BS EN 60079:10, i.e. V_z calculated using equation (2.4) (see Section 6.2.3). Figure 6.2 plots the CFD predictions of gas cloud volume V_z on the *y*-axis against the V_z calculated using equation (2.4) on the *x*-axis, for the same cases as in Figure 6.1. It is clear that the calculated V_z is greater than 0.1 m^3 for all cases considered which reaffirms that BS EN 60079:10 is extremely conservative. Moreover it is obvious that there is nowhere near a one-to-one correspondence between the BS EN 60079-10 calculated[4] V_z and the CFD predictions of V_z. More importantly, the correlation between the calculated and predicted V_z volumes is far weaker across the different size of enclosures. This means that use of the 'calculated V_z' as a measure of ventilation effectiveness leads to an approach which is far more conservative for large enclosures than it is for small enclosures. However, despite being far less conservative for small enclosure volumes, even for the smallest leak considered at just 0.013 g/s, the calculated V_z is still greater than 0.1 m^3 for the smallest enclosure volume whereas the CFD model predicts that it would be nearly 1,000 times smaller than that! For a **fixed** enclosure volume, consider only the square symbols say in Figures 6.1 and 6.2: the correlation between the two measures of ventilation effectiveness (c_{out} and calculated V_z) and the predicted V_z using CFD, is the same in both cases (i.e. the relative distribution of squares is the same, it's just that they are in a different position compared to the results for the other enclosure volumes). The reason for this is made clear by considering the definition of the two measure of ventilation effectiveness (see equation (6.3) which, apart from a number of linear factors, differ only by a factor of the enclosure volume.

[4] *We are making a clear distinction here between the 'calculated Vz', which refers to the Vz calculated using BS EN 60079:10, and the Vz that has been physically modelled and experimentally assessed in Section 4.*

Table 6.2 Results of CFD simulations for non-confined, iso-thermal cases. C1 and C2 refer to Configurations 1 and 2 (see Appendix D)

Enclosure volume	*Hole size (mm^2)*	*Approx. Pressure (barg)*	*Leak Size (g/s)*	*Air change rate (ach)*	*Configuration*	*Average conc. at outlet (% LEL)*	*CFD V_z Volume (m^3)*
1	0.25	0.021	0.013	12	C1	13.3	0.00016
1	0.25	0.021	0.013	1	C1	159.7	0.80
8	0.25	0.5	0.06	13	C1	7.5	0.00020
8	0.25	1	0.09	6.9	C1	20.0	0.00051
8	0.25	2.5	0.15	3.07	C1	75.0	8.00
8	0.25	2.5	0.15	6.45	C1	35.7	0.00949
8	2.5	0.06	0.22	7.5	C1	45.0	0.134
8	0.25	10	0.47	6	C1	120.3	8.00
8	2.5	0.3	0.49	8.36	C1	90.0	8.00
8	2.5	1	0.86	22	C1	60.0	8.00
45	0.25	2.5	0.15	6	C1	6.9	0.00048
45	2.5	0.06	0.22	12	C1	5.0	0.0041
45	0.25	5	0.26	2	C1	35.3	0.024
45	0.25	5	0.26	6	C1	11.9	0.0015
45	0.25	10	0.47	2	C1	64.7	45.00
45	0.25	10	0.47	6	C1	21.6	0.0082
45	0.25	10	0.47	12	C1	10.8	0.0039
45	2.5	0.3	0.49	12	C1	11.2	0.0075
45	2.5	1	0.86	2	C1	118.3	45
45	2.5	1	0.86	6	C1	39.4	0.240
45	2.5	1	0.86	12	C1	19.7	0.015
45	2.5	1	0.86	24	C1	9.9	0.008
45	2.5	3	1.72	12	C1	39.4	0.68
45	0.25	5	0.26	2	C2	35.3	0.063
45	0.25	5	0.26	6	C2	11.9	0.0017
45	0.25	7.9	0.38	6	C2	17.4	0.0084
45	0.25	10	0.47	2	C2	64.7	0.14
45	0.25	10	0.47	6	C2	21.6	0.011
45	0.25	10	0.47	12	C2	10.8	0.0048
45	2.5	0.3	0.49	12	C2	11.2	0.0122
45	2.5	1	0.86	2	C2	118.3	33
45	2.5	1	0.86	6	C2	39.4	0.380
45	2.5	1	0.86	12	C2	19.7	0.033
45	2.5	3	1.72	12	C2	39.4	0.57
400	0.25	10	0.47	2	C1	7.2	0.00220
400	2.5	1	0.86	6	C1	4.4	0.00593
400	2.5	1	0.86	12	C1	2.2	0.00530
400	2.5	3	1.72	3	C1	17.6	0.02526
400	2.5	3.6	2.00	1.72	C1	35.7	0.04663

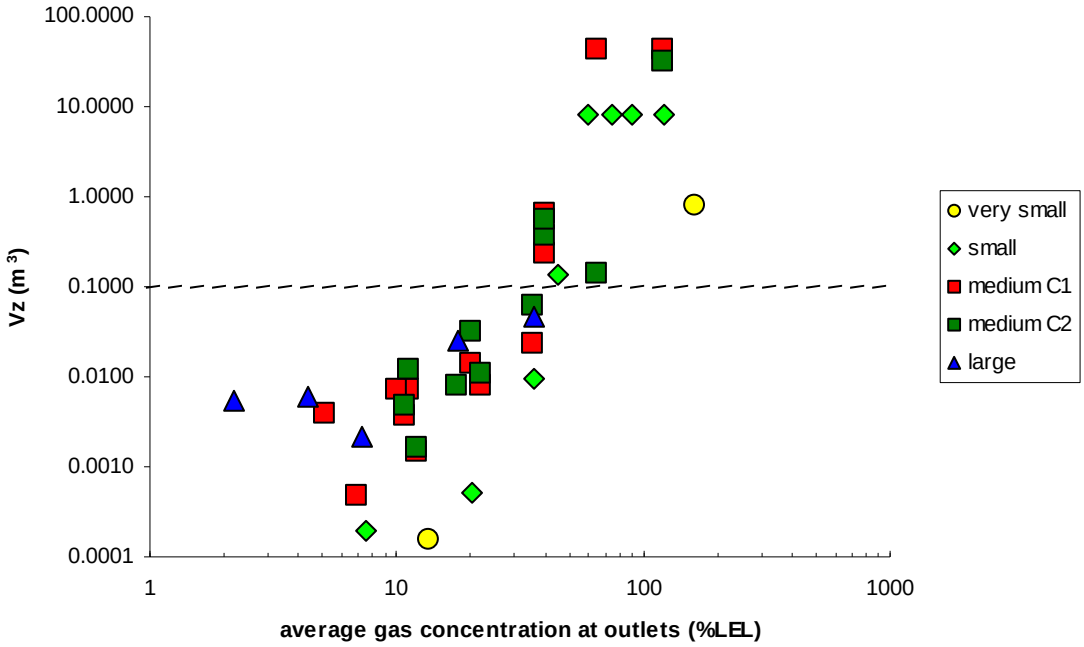

Figure 6.1 Correlation between CFD predictions of V_z and the average gas concentration at the outlet for different enclosure sizes. Data points do not include cases where the leak is confined or non-adiabatic cases

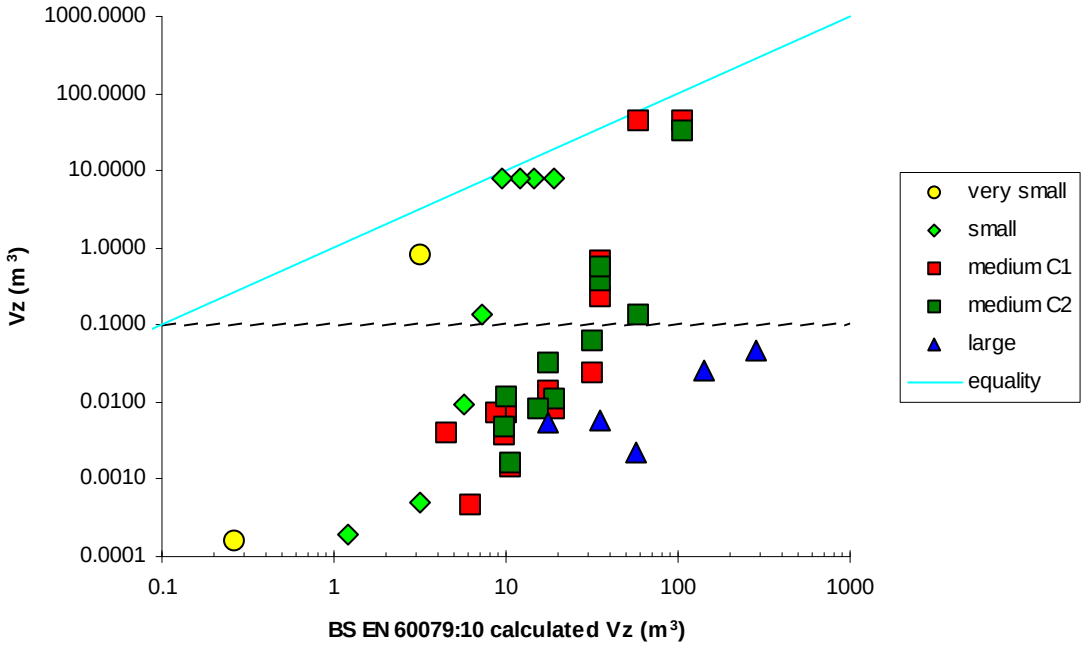

Figure 6.2 Correlation between CFD predictions of V_z and BS EN 60079:10 measure of ventilation effectiveness, V_z (see equation (2.4)), for different enclosure sizes

6.4.1.2 Leak location / local confinement

The results presented in the previous Section summarised all of the CFD simulations for cases where there were no significant obstructions in the path of the jet that could lead to significant gas cloud build up. Here we examine those cases described in Appendix E (Section 12.3) which considered various orientations of the gas leak relative to a large obstruction, the Configuration 3 simulations from the validation study and two similar confined releases in the large enclosure. These cases are listed in Table 6.3 using the same labelling scheme, D1-D13, as used in Appendix E and Appendix D (C1-1 etc.). Test cases D1-D13 were used to design a 'worst-case scenario' in terms of leak location and this was then used as Configuration 3 in the validation study. The gas cloud volumes for all of these cases are plotted in Figure 6.3 against the average concentration at the outlet, c_{out}. Also shown in the graph are the unconfined results discussed in the previous Section. The results labelled 'medium D#' shows the results of moving the leak location relative to the large obstruction for the same leak rate and ventilation conditions.

Note that Configuration 3 was chosen as a worst case leak location based on a series of gas leak simulations in which the gas release rate and ventilation rate were fixed (0.86 g/s and 12 ach). Therefore, for different leak rates / ventilation rates this arrangement may be far from the worst case. Consider for example the case with the smallest leak rate in Table 6.3 (0.029 g/s). In this case the leak location is relatively far away from the opposite wall and therefore the jet is likely to become dilute before it gets a chance to start re-entraining. It is therefore possible that a larger V_z could result in this case if the release was nearer to the wall. Similarly for other cases under different conditions.

The CFD results in Figure 6.3 show that by varying the leak location the resulting gas cloud volume can change by two orders of magnitude. Hence leak location is a key factor that needs to be taken into consideration in a zoning methodology. The other new results in Figure 6.3, which are all based on Configuration 3, show much larger gas cloud volumes compared to their non-obstructed counterparts. So, whereas before c_{out} < 39% LEL was required to keep V_z below 0.1 m^3, now we require that c_{out} < 19% LEL to take into account the increased gas cloud volume resulting from the effect of possible obstructions near the leak source.

Table 6.3 Results of CFD simulations for cases with varying leak location. C3 refers to leak locations based on Configurations 3 (see Appendix D)

Enclosure volume	*Hole size (mm^2)*	*Approx. Pressure (barg)*	*Leak Size (g/s)*	*Air change rate (ach)*	*Configuration*	*Average conc. at outlet (% LEL)*	*V_z Volume (m^3)*
45	2.5	1	0.86	12	D1	19.7	0.015
45	2.5	1	0.86	12	D2	19.7	0.033
45	2.5	1	0.86	12	D3	19.7	0.89
45	2.5	1	0.86	12	D4	19.7	0.092
45	2.5	1	0.86	12	D5	19.7	0.13
45	2.5	1	0.86	12	D6	19.7	0.044
45	2.5	1	0.86	12	D7	19.7	0.013
45	2.5	1	0.86	12	D8	19.7	0.018
45	2.5	1	0.86	12	D9	19.7	0.016
45	2.5	1	0.86	12	D10	19.7	0.028
45	2.5	1	0.86	12	D11	19.7	0.031
45	2.5	1	0.86	12	D12	19.7	0.017
45	2.5	1	0.86	12	D13	19.7	0.20
45	0.25	0.1	0.029	2	C3	4.0	0.00011
45	0.25	5	0.26	6	C3-3	11.9	0.0017
45	0.25	10	0.47	2	C3-4	64.7	44
45	0.25	10	0.47	6	C3-5	21.6	0.17
45	0.25	10	0.47	12	C3-6	10.8	0.011
45	2.5	0.3	0.49	12	C3-7	11.2	0.020
45	2.5	1	0.86	2	C3-8	118.3	45
45	2.5	1	0.86	6	C3-9	39.4	34
45	2.5	1	0.86	12	C3-10	19.7	0.89
45	2.5	1	0.86	12	C3a	19.7	0.092
45	2.5	1	0.86	12	C3b	19.7	0.13
45	2.5	1	0.86	12	C3c	19.7	0.044
400	2.5	1	0.86	6	C3	4.4	0.026
400	2.5	1	0.86	6	C3b	4.4	0.012

Key: C3-# – Configuration 3 validation case (see Appendix D); C3 – Configuration 3 geometry; C3a – same as C3 but with obstacle 0.75 m from back wall; C3b – same as C3 but with obstacle 1.0 m from back wall; C3c – same as C3 but with obstacle 0.2 m from side wall.

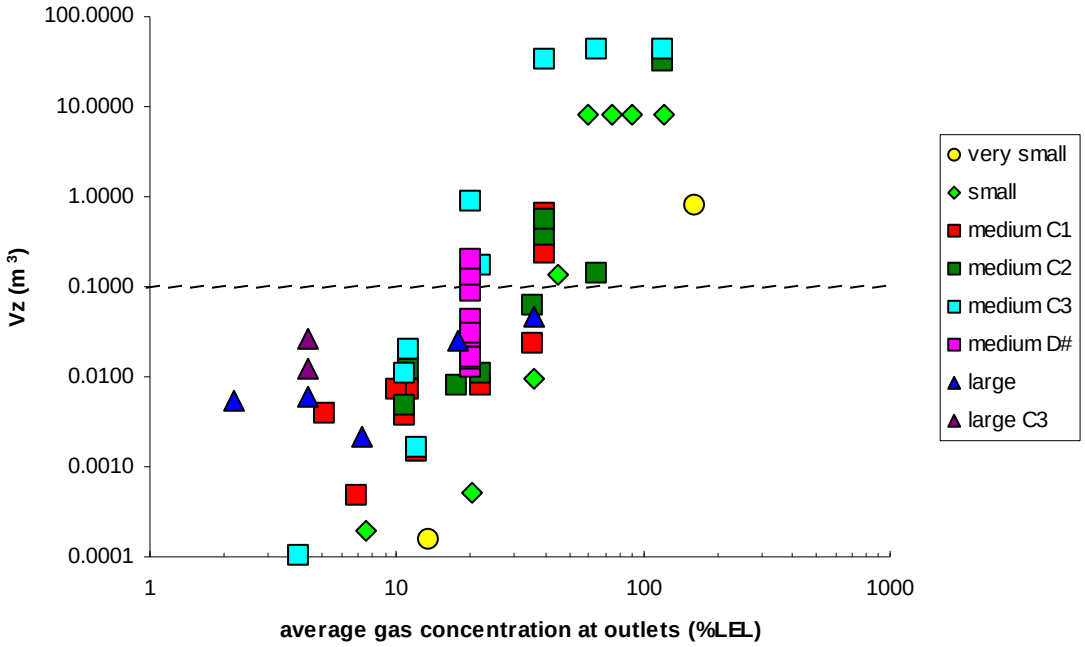

Figure 6.3 Correlation between CFD predictions of V_z and the average gas concentration at the outlet for releases into a confined space (Configuration 3 and D# series of tests) for different sizes of enclosure. Data points do not include non-isothermal cases

6.4.1.3 Heat transfer

The final set of CFD simulations take into account the effect of non-isothermal conditions within the enclosure. This is an important factor to take into consideration as it is well understood that thermal stratification within an enclosure can significantly reduce the level of mixing. Table 6.4 shows a summary of all of the CFD simulations that have been undertaken to investigate the effects of non-isothermal conditions. The corresponding predictions of V_z plotted against the average gas concentration at the outlet are shown in Figure 6.4. Two heat transfer effects have been considered: heat loss to the floor and walls and heating within the enclosure, for example caused by a hot boiler. Appendix E discusses the results of these simulations and describes in detail the behaviour of the gas dispersion. The CFD simulations show that heat loss to the floor or walls has relatively little effect on the gas cloud volume. However, the results show that heat sources can cause stratification within the enclosure and, when coupled with a confined leak location, they can lead to significantly larger gas cloud volumes compared to releases under isothermal conditions.

It must be noted that the stratified cases that have been examined could be regarded as rather extreme for a couple of reasons. Firstly, and perhaps most significantly, the existence of large heat sources in a room will induce increased ventilation rates compared to an equivalent non-heated naturally ventilated enclosure. For example given an 8 °C difference between internal and external temperatures in the large enclosure, the BS 5925 methodology would predict an air change rate of approximately 20 ach. However, the largest air change rate that has been considered here is 12 ach. Secondly, the strong thermal stratification that has been modelled in the large enclosure may not be wholly realistic as heat loss to the roof has not been modelled and heat loss to the walls may have been under-estimated. Both of these factors would be likely to reduce the strength of the thermal stratification. The above two factors therefore are likely to

lead to conservative estimates of the gas cloud size and this should be taken into account when reviewing the data presented below.

Figure 6.4 clearly shows that some of the results from CFD simulations that include the effect of heat transfer do not follow the trends found for the previous isothermal conditions. In particular, the combination of a confined leak and a thermally stratified enclosure, leads to gas clouds in excess of 0.1 m^3 even when the average gas concentration at the outlet is relatively low. In fact the most surprising result occurs for the 12 ach case in the large enclosure where the predicted V_z is 1.6 m^3, which is bigger than the equivalent 6 ach case. It is worth noting that some effort was put into designing a scenario that would lead to such a large gas cloud volume. The series of tests described in Section 12.3 tested a number of geometries and this configuration led to a significantly larger gas cloud than the others. This series of tests was carried out with the leak rate held constant and so higher or lower leak rates, with a corresponding ventilation rate set to keep c_{out} the same, could lead to smaller gas clouds. However, an even more extensive set of simulations is almost certain to lead to some cases that may produce even bigger gas cloud volumes. Therefore our analysis has focussed on assessing the general trends.

Table 6.4 Results of CFD simulations for non-isothermal cases

Enclosure volume	***Hole size (mm^2)***	***Approx. Pressure (barg)***	***Leak Size (g/s)***	***Air change rate (ach)***	***Configuration***	***Average conc. at outlet (% LEL)***	***V_z Volume (m^3)***
8	0.25	0.5	0.06	6	CF	16.1	0.00029
45	0.25	10.0	0.47	6	C3, CF	21.6	0.092
45	0.25	10.0	0.47	12	C3, CF	10.8	0.05
45	0.25	10.0	0.47	12	C2, X70C	10.8	0.0047
45	2.5	1.0	0.86	12	C2, CF	19.7	0.038
45	2.5	1.0	0.86	12	C3, CF	19.7	1.228
400	2.5	1.0	0.86	6	C3, B70C	4.4	1.0
400	2.5	1.0	0.86	6	C3, B84W	4.4	0.95
400	2.5	1.0	0.86	6	C3, B84W, W20C	4.4	0.89
400	2.5	1.0	0.86	6	C3, B84W, W-2.7W	4.4	1.0
400	2.5	1.0	0.86	6	C3, B70C, X40C	4.4	0.23
400	2.5	1.0	0.86	6	C3b, B84W	4.4	0.15
400	2.5	1.0	0.86	12	C3, B70C	2.2	1.6

Key: C2/3 – Configuration 2/3; CF – cold floor; B70C – hot boiler at 70 °C; B84W – hot boiler with heat flux 84 W/m^2; X40C – hot box at 40 °C; W20C walls at 20 °C; W-2.7W walls extracting heat flux of 2.7W/m^2.

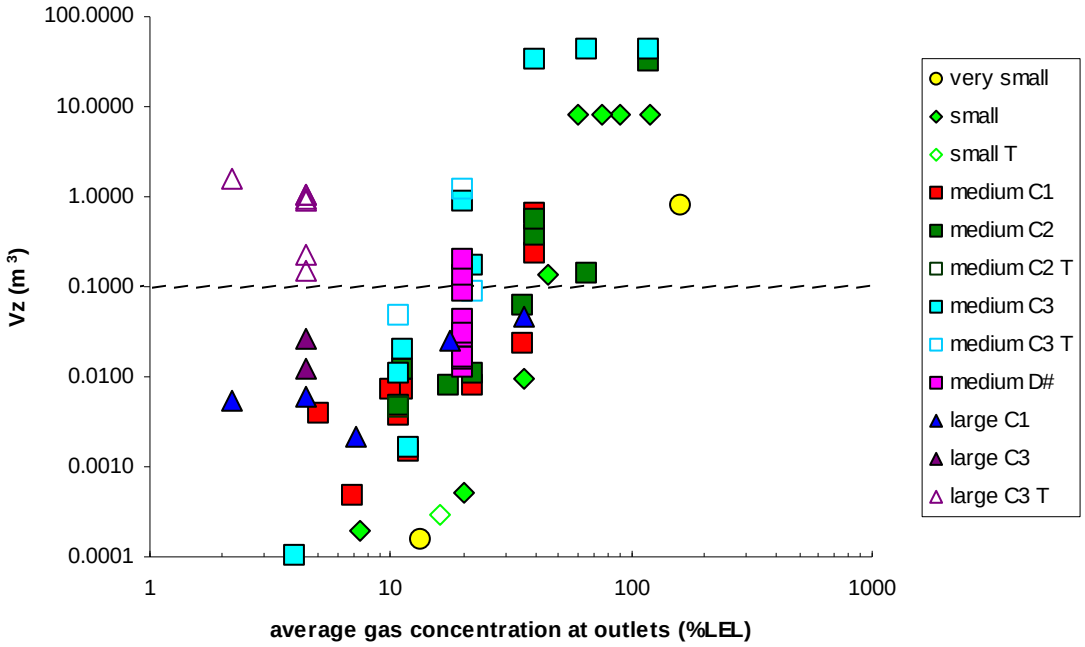

Figure 6.4 Correlation between CFD predictions of V_z and the average gas concentration at the outlet including releases into a confined space (Configuration 3 and D# series of tests) and non-isothermal conditions

6.4.2 Flammable gas cloud volume

The above analysis is based on the calculation of the gas cloud volume V_z. However, as discussed in Section 4, V_z is a conservative estimate of the actual flammable gas cloud volume i.e. the volume of gas enclosed within the 100% LEL iso-surface. Therefore, the 100% LEL volume has also been computed for all of the above CFD simulations to provide a better understanding of the hazard associated with the modelled gas leaks.

For a free jet, the V_z gas cloud volume is typically between 19 to 26 times bigger than the 100% LEL volume (Section 4.3.1.1). However, for releases in enclosures this ratio is generally expected to be larger, as the gas disperses more slowly. This was confirmed by the results from the CFD simulations. For the relatively unobstructed releases, i.e. Configurations 1 and 2, the ratio is mostly around 30-50, but in some cases is as high as 670 (except when the V_z gas cloud filled the enclosure, for which the ratio is less meaningful).

For gas leaks that experience a greater level of confinement (Configuration 3) the ratio of V_z to the 100% LEL volume is significantly greater, mostly in excess of 100. Including the effects of heat transfer to these confined releases produces the largest ratios of all, with values of around 700. This means that the use of V_z as a measure of the flammable gas cloud volume, and hence the hazard, is likely to be **very** conservative in these cases.

The 100% LEL volumes are given in Figure 6.5 against the average gas concentration at the outlet. A volume of 10 litres is also indicated in Figure 6.5 which according to (Communication from the Commission, 2003) represents the volume above which '*a continuous volume of explosive atmosphere in a confined space must always be regarded as a hazardous explosive atmosphere, irrespective of the size of the room*'. Comparison of these data against that

presented in Figure 6.4 shows that this criterion is less conservative than using the $V_z < 0.1$ m^3 criterion. There are many similarities between the results in Figures 6.4 and 6.5 and in particular the expected general trend is seen that the gas cloud volume increases as the average gas concentration at the outlet increases. However, the results for the 100% LEL gas cloud volume indicate a different assessment of the relative hazard. In particular the Configuration 3 cases in the large enclosure with thermal stratification give smaller gas cloud volumes than some of the releases in isothermal conditions.

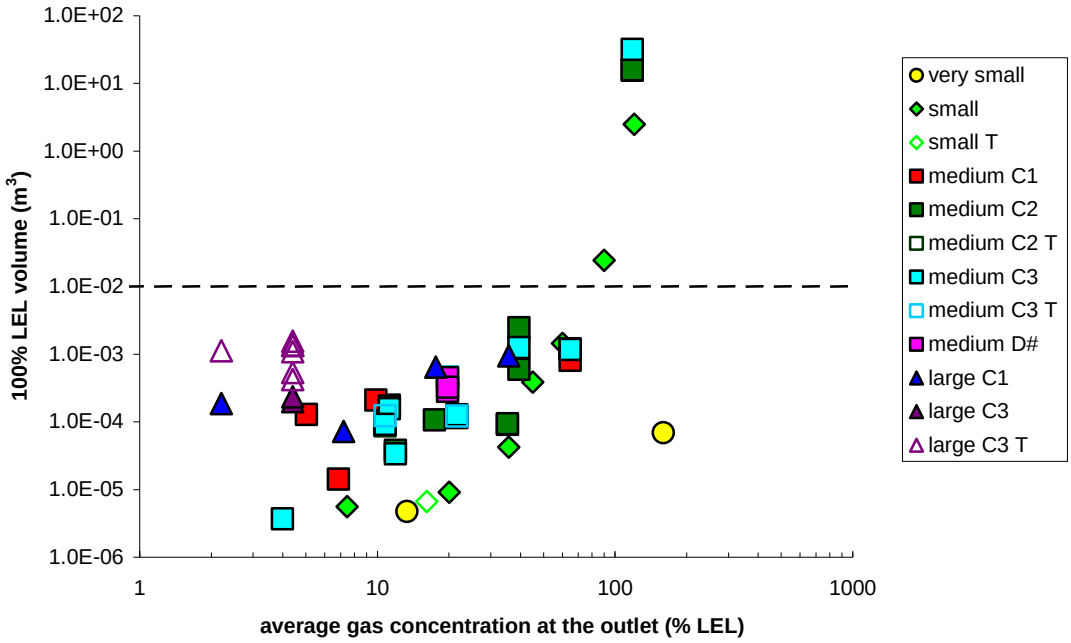

Figure 6.5 Correlation between CFD predictions of 100% LEL volumes and the average gas concentration at the outlet

6.4.3 How this data can be used

The data presented in Section 5 and in the above two Sections can be used to help develop a methodology for area classification in enclosures for low pressure natural gas systems. The starting point for any such methodology is the leak rate that leads to $V_z = 0.1$ m^3 in a well-ventilated enclosure which provides effectively the same level of dilution as an outdoor obstructed release. A conservative estimate of this leak rate, taking into account interactions with simple obstacles, is 1 g/s (see Section 5.2.2). Therefore any leak rate greater than 1 g/s would not be suitable for classification of zone 2 NE in an enclosure. For a hole size of 0.25 mm^2 the leak rate will always be less than 1 g/s up to 10 barg and for a hole of 2.5 mm^2 a pressure of approximately 1.3 barg will give a leak rate of 1 g/s.

The results presented in Figure 6.4 show a strong correlation between the gas cloud volume V_z and the average gas concentration at the outlet, c_{out}. In the vast majority of cases if $c_{out} < 19\%$ LEL, V_z will be less than 0.1 m^3. However, there are a number of cases in which values of V_z were obtained that were greater than 0.1 m^3 and in which c_{out} was significantly less than 19% LEL. The lowest value of c_{out} for which a V_z is obtained that is greater than 0.1 m^3 is 2.2% LEL. This means that it would be appropriate for a zoning methodology to take such cases into account (see below). In the majority of cases the correlation between c_{out} and V_z is strong

enough that the data can be used, with a suitable safety factor, to determine whether or not it is appropriate to apply a classification of zone 2 NE. The data suggest that c_{out} < 10% LEL would be a reasonable necessary condition for zone 2 NE. This would cover the majority of cases considered here and also many variations on these. However, this would still leave the possibility of leak scenarios that could lead to V_z volumes greater than 0.1 m^3 where the average gas concentration at the outlet is less than 10% LEL.

The data have shown that a fairly specific set of conditions is required to generate a large V_z when c_{out} is small. The two key factors appear to be strong thermal stratification (which is frequently likely to be case in practice) and / or the leak location is sheltered from the ventilation flow in the room to such an extent that gas is re-entrained into the jet.

An area classification assessment will therefore need to take into account whether or not a secondary source location is confined to such an extent that the application of the c_{out} < 10% LEL criterion is appropriate or not. The results clearly show that the location of the jet within the enclosure has a very significant effect on the resulting gas cloud volume. For example, cases D1 to D13, which all had the same leak and ventilation rates, led to a two order of magnitude variation in the gas cloud volume. The case which led to the largest gas cloud volume, Configuration 3, consisted of the leak location being confined on four sides by walls and a large obstruction. The gap between the wall and obstruction, where the leak was located, was just 50 cm. Increasing this to 1 m resulted in an eight-fold reduction in the gas cloud volume. However, there isn't enough data available for to provide specific guidance on how to defined a confined location such that the c_{out} < 10% criterion can or can't be applied.

Further analysis of the data has shown that in many cases where V_z is large, the actual volume of gas above LEL is still very small. Comparison of the 100% LEL volumes against the 'rule of thumb' (Communication from the Commission, 2003) that these should be less than 0.01 m^3, indicates that they can satisfy this requirement even when they do not satisfy the V_z criterion. However, we are not aware of any supporting evidence for this rule of thumb.

The following two Sections look in more detail at the implications of the above findings for large and small enclosures.

6.4.4 Implications for large enclosures

The work on outdoor area classification presented in Section 5.3 suggests a maximum allowable leak rate for zone 2 NE of 1 g/s for obstructed releases. As discussed above, it is appropriate to use this leak rate as the maximum allowable leak for zone 2 NE in enclosures, irrespective of the ventilation rate. This is because we do not expect that the ventilation in an enclosure will be any better at diluting a leak than if that leak were outdoors. The CFD simulations of gas leaks in enclosures suggest that if the average gas concentration at the outlet, c_{out}, is less than 10% LEL and the gas leak is in a relatively unobstructed location V_z will be less than 0.1 m^3.

The ventilation rate required to dilute a 1 g/s leak down to 10% LEL at the ventilation outlets can be calculated using equation (6.2) to be 0.341 m^3/s (and this is independent of the enclosure volume). Therefore, if the ventilation rate in an enclosure is greater than this then (assuming that other criteria are met such as confinement of the leak location and availability of the ventilation etc.) zone 2 NE can be applied for any leak rate up to 1 g/s in that enclosure.

Table 6.5 shows how this ventilation rate corresponds to air change rates for a range of enclosure volumes. For example, for an enclosure with a volume of 500 m^3 an air change rate of 2.5 ach would be required to dilute the gas down to an average concentration of 10% LEL at the ventilation outlets.

Table 6.5 Air change rates required to dilute a 1 g/s leak down to an average of 10% LEL at the ventilation outlets

Enclosure volume (m^3)	*Air change rate(ach)*
10	122.9
20	61.4
50	24.6
100	12.3
200	6.14
500	2.46
1,000	1.23
10,000	0.12
100,000	0.01

For large enclosures this approach suggests that very low air changes rates are sufficient to classify areas as zone 2 NE. In practice therefore, in large enclosures the indoor methodology described above (i.e. the requirement that c_{out} < 10% LEL) automatically reduces to the outdoor methodology described in Section 5.4 (i.e. the requirement that $\dot{m}$ < 1 g/s) because the air change rate requirement is low.

However, the current work has shown that if the leak location is in a confined space within the enclosure then, even if the average gas concentration at the outlet is low, significant gas cloud build-up can occur. This is less likely in small enclosures where well-mixed conditions will usually exist throughout the enclosure and the high momentum of a gas leak may contribute to this. Therefore, it is important that in large enclosures the **local** ventilation is assessed in determining the zone. If the leak location is in a confined space and the airflow is stagnant then zone 2 NE is not appropriate. An assessment of the local ventilation conditions can be made by using a hand held anemometer or smoke although it will rely invariably on an element of judgement. Clearly, significantly higher ventilation rates than those suggested in Table 6.5 will help to reduce the risk.

6.4.5 Implications for small enclosures

For small enclosures the work in Section 4 suggests that using the V_z < 0.1 m^3 criterion is not sufficiently conservative. Therefore for the zone 2 NE criteria to be met in small enclosures the limit set on the V_z volume should be smaller, see equation (4.3). In the light of this different V_z criterion is interesting to review the data in Figure 6.4. This shows that where the average gas concentration at the outlet is less than 10% LEL then V_z is smaller than 0.01 m^3 in all of the CFD simulations in the two smaller enclosures. This can be expected in the vast majority of realistic cases as the small size of the enclosure is likely to lead to the flow within the volume being well-mixed, particularly when there is a high momentum source present, such as a gas leak. However, exceptions to this could occur, for example, where the ventilation short-circuits the majority of the enclosure volume.

6.5 CONCLUSIONS

The work on zoning in outdoor locations has suggested an upper bound on the leak rate of 1 g/s that can be considered for a classification of zone 2 NE. Examples of the pressures and hole sizes required to generate this mass leak rate are provided in Table 5.7.

The data presented in this Section have shown that there is a strong correlation between the average gas concentration at the outlet, c_{out}, and the gas cloud volume, V_z. For the majority of

cases examined where the average concentration at the outlet is less then 10% LEL then the gas cloud volume V_z was less than 0.1 m^3. Therefore, the requirement that c_{out} <10% LEL would be suitable for the definition of zone 2 NE as an alternative to calculating V_z using the method described in BS EN 60079:10 and requiring that this is less than 0.1 m^3. The approach described here removes a very large degree of conservatism from the zoning methodology described in BS EN 60079:10.

For the above approach to be applicable, the leak source must not be located within a confined space within the enclosure. It has been shown that local confinement of a leak can lead to re-entrainment of gas into the jet resulting in significantly larger gas cloud volumes than would be expected in an unconfined space. Such cases are more likely to occur in large enclosures as there is more opportunity for short-circuiting of the ventilation to occur and the ventilation is more effective in some part of the enclosure than others. Defining a 'confined space' in this context is difficult as there are many factors influencing the gas build up. To do this would require a great deal more data that has been generated in the current project.

6.6 EXAMPLE APPLICATION OF THIS DATA

In this Section two examples are used to demonstrate how this data could be used. These cases are similar to the worked examples used in BS EN 60079:10.

Calculation No. 1

Characteristics of release		
Flammable material	methane gas	
Molecular mass of methane	16,05 (kg/kmol)	
Source of release	pipe fitting	
Lower explosion limit (*LEL*)	0.044 vol/vol	
Grade of release	secondary	
Hole size	0.25 mm^2	
Orifice discharge coefficient	0.8	
Ambient temperature, *T*	10 °C	
Enclosure characteristics		
Length	1.12 m	
Width	1.12 m	
Height	1.12 m	
Volume	1.405 m^3	
No heat sources in the enclosure		
Ventilation openings		
Two openings, one on opposite sides:		
A1	0.073 m^2	
A3	0.073 m^2	
A_w	0.0516 m^2	(equation (2.2))
Wind speed	0.5 m/s	
Differential mean pressure coefficient, ΔC_p	0.95	(see BS 5925, Table 13)
Volume flow rate, Q_w	0.0153 m^3/s	(equation (2.3))
Air change rate, *C*	39.3 ach	

Calculation 1a

Supply pressure	250 mbar	
Release rate, $\dot{m}$	0.04 g/s	(equation (3.10))
Average gas concentration at the outlet, c_{out}	7.7 % LEL	(equation (6.2))

Calculation 1b

Supply pressure	1 barg	
Release rate, $\dot{m}$	0.07 g/s	(equation (3.7))
Average gas concentration at the outlet, c_{out}	14.8 % LEL	(equation (6.2))

Conclusion

In Calculation 1a the average gas concentration at the outlet is below 10 % LEL. Due to the size of the enclosure it is unlikely that there will be any significant stagnant areas and therefore if the availability of the ventilation is good (see BS EN 60079:10) then zone 2 NE is likely to be appropriate.

In Calculation 1b the average gas concentration at the outlet is above 10 % LEL and therefore zone 2 NE is not appropriate.

Calculation No. 2

Characteristics of release		
Flammable material	methane gas	
Molecular mass of methane	16,05 (kg/kmol)	
Source of release	pipe fitting	
Lower explosion limit (*LEL*)	0.044 vol/vol	
Grade of release	secondary	
Hole size	2.5 mm^2	
Orifice discharge coefficient	0.8	
Ambient temperature, *T*	10 °C	
Enclosure characteristics		
Length	15.6 m	
Width	7.2 m	
Height	3.0 m	
Volume	337.0 m^3	
No heat sources in the enclosure		
Ventilation openings		
Two openings, one on opposite sides:		
A1	5.76 m^2	
A3	5.76 m^2	
A_w	4.07 m^2 (equation (2.2))	
Wind speed	0.5 m/s	
Differential mean pressure coefficient, ΔC_p	0.95	(see BS 5925, Table 13)
Volume flow rate, Q_w	1.211 m^3/s	(equation (2.3))
Air change rate, *C*	12.9 ach	

Calculation 2a

Supply pressure	1 barg	
Release rate, $\dot{m}$	0.69 g/s	(equation (3.7))
Average gas concentration at the outlet, c_{out}	1.9 % LEL	(equation (6.2))

Calculation 2b

Supply pressure	3 barg	
Release rate, $\dot{m}$	1.4 g/s	(equation (3.7))
Average gas concentration at the outlet, c_{out}	3.8 % LEL	(equation (6.2))

Conclusion

In Calculation 2a the average gas concentration at the outlet is below 10 % LEL. An assessment will need to be made on whether the leak source location is in a confined space. If not, and the availability of the ventilation is good (see BS EN 60079:10) then zone 2 NE is likely to be appropriate.

In Calculation 2b the mass release rate is above 1 g/s and therefore, even though the average gas concentration at the outlet is below 10% LEL, zone 2 NE is inappropriate.

7 CONCLUSIONS

A review has been carried out on the ventilation of enclosures focusing on measures of ventilation effectiveness and how ventilation rates can be measured for input into an area classification methodology. The most accurate approach to calculating air change rates for naturally ventilated enclosures is to make measurements of the decay rate of a tracer gas within the enclosure. However, the time and expense required to do this means that it is not an approach suitable for area classification. BS 5925 describes a method for calculating air change rates that is simple to apply and should provide data of sufficient accuracy to be appropriate for area classification. The approach has been applied to two enclosures where the air change rate was measured experimentally. In the first of the two cases considered, the calculated air change rate was in good agreement with the measurements, whereas in the other case it under-predicted the ventilation rate. An appropriate conservative choice of the wind speed, say 0.5 m/s, should provide corresponding conservative estimates of the ventilation rate.

As part of the ventilation review, BS EN 60079:10 has been reviewed in detail and in this report we have made a clear distinction between the two definitions given for the gas cloud volume V_z. They are:

- a hypothetical volume that can be calculated using the formula in BS EN 60079:10 and is proportional to the mass release rate of a leak divided by the air change rate of the enclosure. V_z in this context is therefore simply a measure of ventilation effectiveness and the criterion V_z less than 0.1 m^3 is used to define zone 2 NE.

- a gas cloud that has an average gas concentration of ½ LEL.

Both of the above definitions of V_z are in BS EN 60079:10 and the current work has highlighted the differences between them. This work has shown that the two descriptions of V_z above are not equivalent, i.e. the calculation method in BS EN 60079:10 for V_z does not provide reasonable estimates of the volume of the gas cloud whose average gas concentration is ½ LEL. Furthermore, V_z calculated using BS EN 60079:10 has been found to be up to three orders of magnitude larger than the gas cloud volume V_z predicted by using a validated CFD model. The greatest differences are seen in the largest enclosures. This implies that use of BS EN 60079:10 for calculating V_z significantly over estimates the hazard and therefore leads to areas requiring a higher classification than is necessary.

The hazard associated with a leak that leads to a V_z of 0.1 m^3 has been assessed through experiments and modelling. The work has shown that the hazard is low in terms of the overpressure created on ignition of the cloud and the thermal radiation associated with the explosion and subsequent jet flame. Igniting gas clouds created by a leak leading to $V_z = 0.1$ m^3 was found to be difficult and a powerful ignition source was required. When ignition of the gas cloud was achieved it resulted in overpressures up to 4 mbarg in a 31 m^3 enclosure. This work has shown that the V_z criterion in BS EN 60079:10, i.e. $V_z < 0.1$ m^3 is required for zone 2 NE, is appropriate for area classification, where V_z is predicted using a validated physically based model that takes into account the interaction of the leak with the ventilation flow.

However, the overpressure resulting from the ignition of a fixed volume of flammable gas (e.g. $V_z = 0.1$ m^3) increases as the enclosure volume decreases. So whilst it has been demonstrated that the V_z criterion is conservative, and can therefore be adopted as a basis for safety for large enclosures, it is not appropriate to do so for small enclosures. An appropriate cut-off would appear to be around 10 m^3 since this implies a theoretical maximum overpressure of 12.5 mbar. Below 10 m^3 the maximum value of V_z should be smaller therefore and an additional criterion

has been introduced requiring that V_z should be less than 1% of the enclosure volume for zone 2NE to be applicable.

An approach to zoning outdoors has been developed based on a conservative estimate of the leak rate required to produce a gas cloud with $V_z = 0.1$ m^3 outdoors. For releases in the open air it has been shown that the largest gas cloud sizes result from conditions where the leak is aligned to the wind direction and the wind speed is low. We have therefore been able to apply an integral free jet model, GaJet, to calculate the pressure and hole size required to give a gas cloud with $V_z = 0.1$ m^3. For choked releases (for methane, where the pressure is above 0.85 barg) the gas cloud volume is dependent only on the mass release rate. It has been shown that the presence of obstructions near to the leak source can act to increase the resulting gas cloud volume compared to the equivalent unobstructed case. It has also been shown that a leak rate of 1 g/s provides a conservative estimate of the leak rate required to give $V_z = 0.1$ m^3 in an outdoor environment. However, this criterion may not be appropriate in cases where there is a high level of congestion, or an arrangement of obstacles that leads to re-entrainment of gas into the jet or reduces the dilution of the jet more significantly than for any of the cases considered in this project. Therefore, for secondary releases in locations that are not heavily congested / confined, leaks rate less than 1 g/s can be appropriately classed as zone 2 NE. For completely unobstructed releases a less conservative approach can be adopted and 2 g/s is a suitable maximum leak rate for zone 2 NE. For a given pressure and hole size, the leak rate can be estimated using standard equations that are included in this report.

The ventilation in an enclosure is not expected to be any more efficient at diluting a gas leak than if the leak occurred outdoors. By definition, releases within enclosures are likely to experience some form of confinement. Therefore, it is also appropriate to apply the mass release rate criterion for outdoor obstructed releases, 1 g/s, as an upper bound on the release rate for zone 2NE in an enclosure.

An alternative approach to measuring the ventilation effectiveness in enclosures to that in BS EN 60079:10 (i.e. V_z) has been suggested based on the average gas concentration at the outlet. It has been shown that this is equivalent to an assessment of the air entrainment requirement of the leak compared to the ventilation rate. The current approach differs significantly from BS EN 60079:10 in two key ways. Firstly, the average gas concentration at the outlet is dependent on the ventilation rate as opposed to V_z calculated using BS EN 60079:10 which is dependent on the air change rate of the enclosure. This therefore means that the measure of ventilation effectiveness (i.e. the average gas concentration at the outlet) increases as the enclosure volume increases for a fixed air change rate. Secondly, and most importantly, this new measure of ventilation effectiveness is based on a physical understanding of the behaviour of the dispersion of high momentum jets and has been evaluated here against data on gas cloud build up in enclosures.

A validated CFD model has been used to provide data on gas cloud volumes for low pressure gas leaks in enclosures. The data show that there is a strong correlation between the average gas concentration at the outlet, c_{out}, and the gas cloud volume, V_z. For the majority of cases examined, where the average concentration at the outlet was less than 10% LEL the gas cloud volume V_z was found to be less than 0.1 m^3. This suggests that the condition $c_{out} < 10\%$ LEL would provide a more suitable criterion for zone 2 NE rather than using the calculation method for V_z in BS EN 60079:10. The approach described here removes a very large degree of conservatism from the zoning methodology described in BS EN 60079:10.

The CFD model simulations have shown that for the above approach to be applicable, the leak source must not be located within a confined space within an enclosure. It has been shown that local confinement of a leak can lead to re-entrainment of gas into the jet resulting in

significantly larger gas cloud volumes than would be expected in an unconfined space. Such cases are more likely to occur in large enclosures where the jet length scale is smaller relative to the enclosure and there is more opportunity for short-circuiting of the ventilation to occur leading to stagnant regions. As there are so many factors affecting gas cloud build up, it is not possible to provide specific guidelines based on the current data on when a leak location should be described as confined.

The presence of a heat source in an enclosure has been shown to lead to reduced mixing and therefore greater gas cloud build up in some cases. In particular, large gas clouds can result from cases where a strong thermal stratification exists coupled with a confined leak location. However, in the absence of a confined leak location it would appear that the c_{out} < 10% LEL criterion is still appropriate.

The CFD model for the above work has been validated against 29 experimental tests carried out in a purpose built enclosure. The experimental tests consisted of releases of simulated methane gas for a range of leak rates and ventilation rates. Three different configurations of the release location and direction were tested and measurements of the point gas concentration measurements were used as the basis for the model validation. The results of the CFD simulations showed good agreement with the experimental data.

8 APPENDIX A – VENTILATION MEASUREMENTS

8.1 INTRODUCTION

To get a better understanding of the type and range of enclosures that are used in industry, visits were made to four enclosures. The intention was to measure the natural ventilation rate in each enclosure, whilst monitoring the external weather conditions. However, due to operational reasons it was not possible to do this for two of the enclosures.

8.2 ENCLOSURE 1: BOOSTER HOUSE

This was the largest enclosure visited and was of approximately 2800 m^3 (21.4 m(l) × 11.5 m(w) × 11.5 m(h)). The building was naturally ventilated with an open mesh floor of approximately 70% open area, and openings at roof level. Within the space there were 3 large cooling fans and each created a jet of air with a cross section of approximately 1 m by 0.35 m travelling at a speed of 6 ms^{-1}.

The air movement within the space was driven by external wind conditions, but also by the air jets. Flow visualisation using smoke showed that air entered the enclosure via the floor and left the space via the roof openings. There were areas of re-circulation close to the walls at high level (see Figure 8.1). In addition some air left the room via the floor grating on the upwind side of the building. The air jets created significant air movement in the lower half of the room. The smoke was seen to clear in just a few minutes.

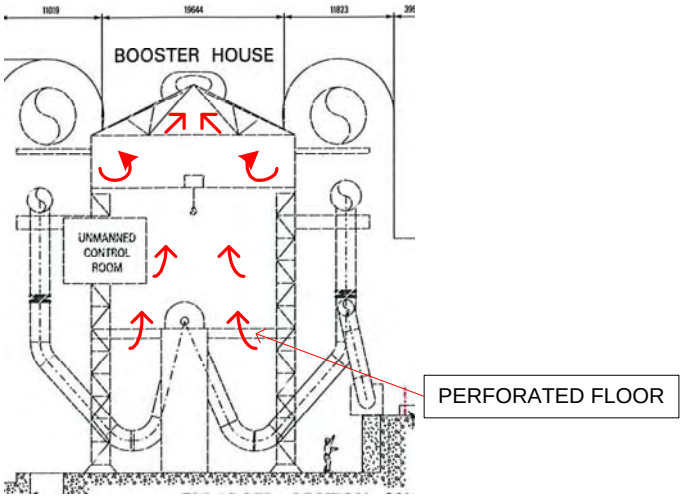

Figure 8.1 Schematic of the booster house showing observed air movement

8.3 ENCLOSURE 2: EXHAUSTER HOUSE

The second building was an exhauster house. It was naturally ventilated like the booster house but had a smaller volume and was on two levels. Again smoke was used to visualise air movement. Air tended to enter at a low level before being drawn upwards. Strong thermal plumes were noted around the exhausters. The least well-ventilated space was the area on the left of Figure 8.2.

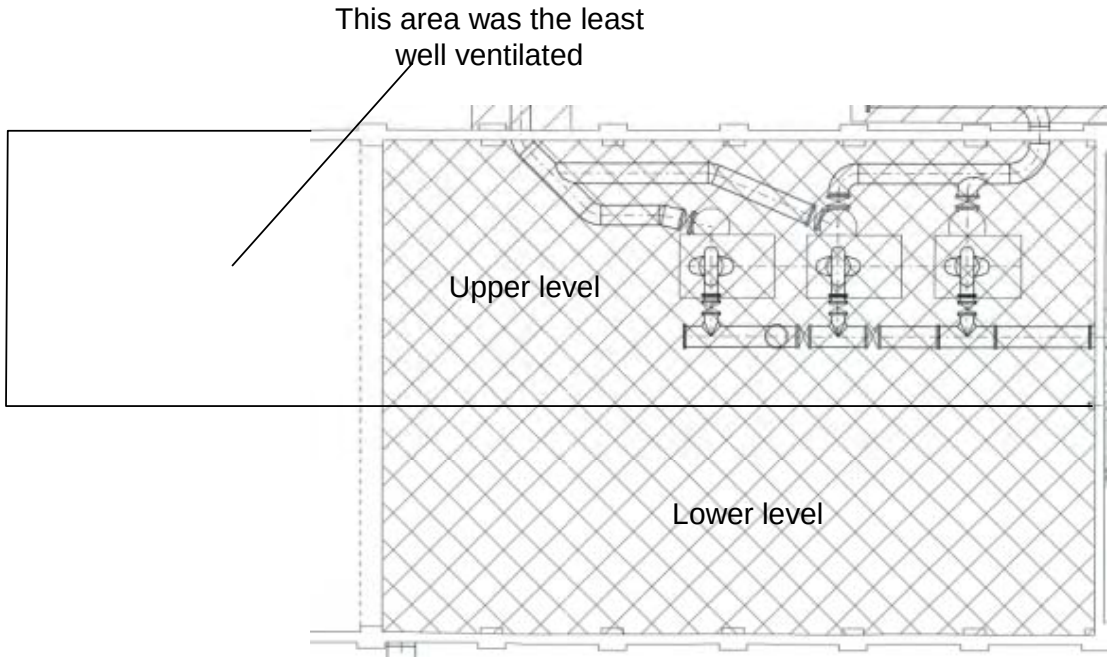

Figure 8.2 Plan view of the exhauster house

8.4 ENCLOSURE 3: GRP KIOSK

The third enclosure was a new GRP Kiosk housing a low pressure district regulator. The dimensions were 3.9 m(l) × 3 m(w) × 2.42 m(h) (28 m^3), giving a volume of approximately 28 m^3, see Figure 8.3.

Figure 8.3 GRP kiosk. Grilles can be seen at low level

The kiosk was naturally ventilated having two grilles (each 0.20 m × 0.265 m) on each wall at low level. Each grille had a total free air space of 12,580 mm^2, giving a total area of approximately 0.1 m^2. In addition, there was high-level ventilation created by a small continuous gap between the roof and walls. There were no hot surfaces within the kiosk.

To observe how air entered and left the kiosk it was filled with smoke and the leakage observed. It was noted that leakage was not steady at any of the openings and none behaved exclusively as an inlet or an outlet, but rather oscillated between the two.

To measure the rate of ventilation, tracer gas tests were carried out using the decay method (or step down method). Tracer gas comprising 10% sulphur hexafluoride and 90% nitrogen was released in the kiosk and mixed with the existing air using a small fan. Once the gas concentration had reached about 60 ppm the gas release was stopped and the decay of the tracer gas logged. The mixing fan was left on for the duration of the tests. Figure 8.4 shows the log-linear plot of tracer gas concentration with time. From the negative slope of the graph the air change rate can be calculated.

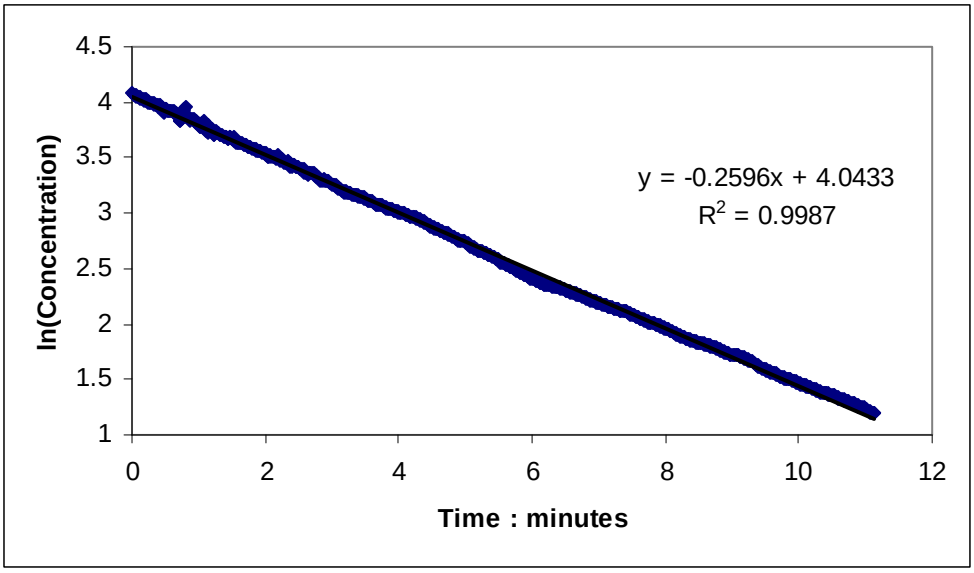

Figure 8.4 Log-linear plot of tracer gas concentration with time

As the ventilation rate was driven by external weather conditions, the wind velocity was logged with an ultrasonic anemometer positioned adjacent to the kiosk at a height of approximately 4.7 m, see Figure 8.5. The logged wind velocity is shown in Figure 8.6.

Figure 8.5 Ultrasonic anemometer positioned adjacent to the kiosk

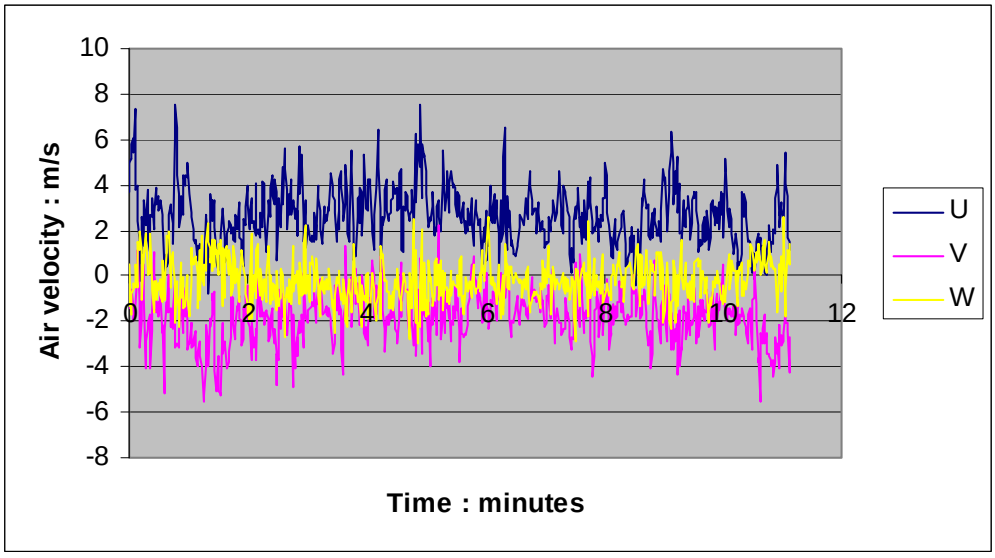

Figure 8.6 Data obtained from the ultrasonic anemometer. The three components of the wind speed are shown

Two tests were carried out using the 'decay method' described above. The results are given in Table 8.1 along with the average wind velocity during the test. As expected the higher air change rate occurred during the higher wind velocities.

Table 8.1 Measured air change rates in the GRP Kiosk

Test number	*Air change rate (h^{-1})*	*Wind velocity (ms^{-1})*
1	11.9	3.3
2	15.6	3.6

8.5 ENCLOSURE 4: BRICK BUILT ENCLOSURE

The enclosure was brick built and housed a low-pressure twin stream district regulator, see Figure 8.7. The building had a volume of approximately 112 m^3 (8.3 m(l) × 5.09 m(w) × 2.65 m(h)). There were no hot surfaces within the enclosure. There were double doors on both ends of the building and a single door on the long front side of the building. Again the building was naturally ventilated, with four air bricks on each of the two long sides of the building; two at high and two at low positions. However, there were numerous other unplanned openings including around the door and doorframe, between the walls and the roof, and in particular, openings created by the removal of equipment that had once passed through the wall of the building, see Figure 8.8. There were no hot surfaces inside the building and the air temperature inside the building was similar to the outside air temperature.

Figure 8.7 Brick built Kiosk housing a low-pressure twin stream district regulator. Four air vents can be seen; two at high level and two at low level. This pattern was repeated on the opposite wall

Figure 8.8 Photo taken from inside the building of the rear long side of the building. The circular opening has been created by the removal of equipment that once passed through the wall

For the air change range calculations described in the main body of this report using the method described in BS 5925 the following assumptions have been made:

(i) Airbricks: terra-cotta with an overall size of 225 x 225 mm and square holes. These each have an equivalent open area of 6400 mm^2.

(ii) In addition to the unplanned gaps in the structure, there was a circular hole in one of the long sides where equipment had been removed. This hole was approximately 200 mm in diameter and a calculation has been included to show the effect of this opening.

Smoke visualisation tests were carried out and showed that, as expected, leakage from the openings was not steady with each opening oscillating between an air inlet and an outlet.

To determine the air change rate, tracer gas measurements were made using the method described above. The results are detailed in Table 8.2. As expected the higher air change rate occurred during the higher wind velocities.

Table 8.2 Measured air change rates in the Brick built enclosure

Test	*Air change rate (h^{-1})*	*Wind velocity (ms^{-1})*	*Temp inside (^oC)*	*Temp outside (^oC)*
1	4.5	2.8	18.4	17.5
2	3.7	2.2	19.4	17.1

9 APPENDIX B – CFD MODELLING OF OBSTRUCTED RELEASES

9.1 INTRODUCTION

In this Section the CFD modelling that has been carried out to assess the effect of obstacles on the dispersion of a gas leak is described. The main conclusions of this work are summarised in the main body of the report in Section 5.3. All of the CFD simulations are based on a release rate of 0.86 g/s methane through a 2.5 mm^2 hole generated by a pressure of approximately 1 barg. To provide a basis for comparison, calculations first considered an unobstructed release into open air. CFD simulations were then set up of the jet interaction with obstacles as described below.

9.2 METHODOLOGY

The application of the GaJet model to free unobstructed releases showed that the gas cloud defined by the 50% LEL isosurface reached a maximum width of 6.2 cm at a downstream distance of 35 cm from the point of release. These values were subsequently applied as representative length scales in the following calculations, where:

- Length, L = 35 cm
- Diameter, D = 6.2 cm.

The computational domain and arrangement of the walls / obstacles for the test cases are shown in Figure 9.1 and 9.2. The first cases considered a bounded jet, constrained by either a single wall or two walls arranged orthogonal to each other. In each case, the release is directed parallel to the wall(s) and the initial distance from the wall is measured as a multiple of the radius $R=D/2$. The second set of simulations considered the impingement of the jet onto a range of obstacles. The obstacles comprised a sphere, a cube or a cylindrical pipe. The distance between the jet source and the upwind face is expressed as a multiple of L and the obstacle size is scaled by R. A summary of all the tests cases is shown in Table 9.1.

The source of the jet was modelled using the same approach as described in Appendix D.

Table 9.1 Summary of conditions used in CFD model simulations of constrained an impinging jets

Feature	**Radial offset**	**Downstream location**	**Obstruction size**
Single wall	0.5R, 0.8R, 1.0R, 1.2R	N/A	N/A
Twin walls	0.8R, 1.0R, 1.2R	N/A	N/A
Sphere	0	L	Diameter D
Cube	0	L	Side length D
Circular bar	0	0.8L, 1.0L, 1.2L	Diameter 1.0D, 1.2D

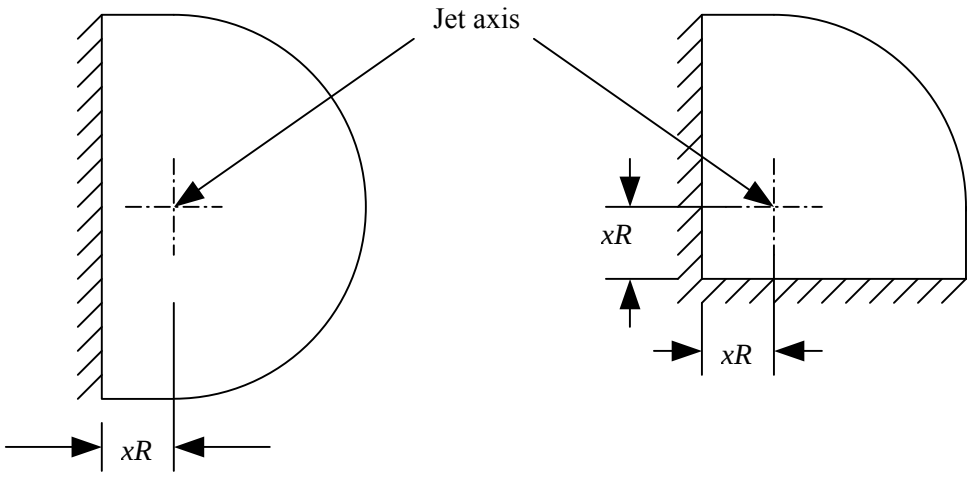

(a) Single wall. (b) Two walls.

Figure 9.1 Arrangement of CFD simulations of a jet parallel to one or two walls.

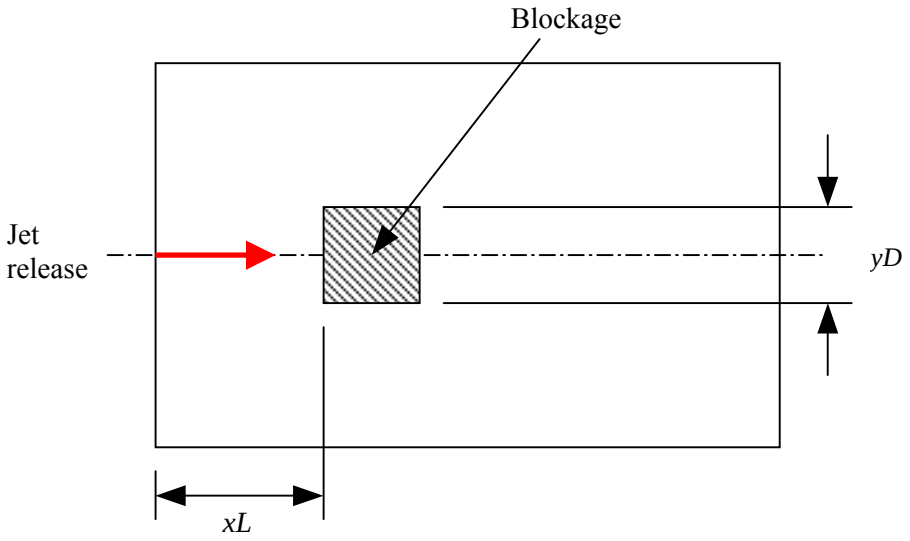

Figure 9.2 Arrangement of CFD simulations of a jet interacting with obstacles.

To improve confidence in the results of the CFD simulations two sensitivity tests were undertaken. The first investigated the dependence of the solution on the mesh size. Four levels of mesh refinement were used to model a free jet with meshes ranging from 126,000 to 529,000 cells. The resulting gas cloud volume was found to be largely grid independent.

9.3 RESULTS

Table 9.2 shows the effect on the gas cloud volume of a leak directed parallel to a wall. The results of four simulations are shown with the jet axis at different distances from the wall. The calculation domain was extended to a distance of 20L (equivalent to 7 m) to accommodate the larger gas cloud volumes compared to the results from the free jet calculation. Three measures

of the gas cloud volume are presented: the volume of gas above LEL, the volume above ½ LEL and V_z. The (constant) concentration on the boundary of the V_z gas cloud volume varies from cases to case and for these calculations an iterative procedure was used to calculate it using the CFX post-processing tool 'POST'. The number of computational cells is also given for each case.

The results show that the presence of the wall significantly increases the gas cloud volume compared to the equivalent free jet. This is because the wall restricts the rate of air entrainment into the jet, resulting in lower rates of dilution by the ambient air. The gas cloud volumes are increased by a factor of approximately two to three in most cases. The largest gas cloud volumes arise from cases where the distance to the wall is smallest, i.e. 0.5R = 1.5 cm. As the distance between the wall and the release axis is increased, the cloud volumes tend to the values obtained for the free jet calculations.

Table 9.2 CFD predictions of gas cloud volumes for a jet parallel to a wall compared to a free jet

Case	*Units*	*Free jet*	*0.5 R*	*0.8 R*	*1.0 R*	*1.2 R*
100% LEL	10^{-3} m^3	0.283	0.700	0.552	0.439	0.308
50% LEL	10^{-3} m^3	2.207	8.903	7.398	6.668	5.867
V_z	10^{-3} m^3	6.243	22.870	18.990	16.925	14.810
Nodes	-	229918	538294	471834	469819	476886

The results of the simulations of a jet running parallel to two walls are shown in Table 9.3. In this case high gas concentrations are maintained along the length of the computational domain such that the centreline concentration remains above ½ LEL even at the end of the domain, 7 m from the source. This means that the gas cloud volume V_z and the volume enclosed by the 50% LEL isosurface could not be calculated. For the 100% LEL case, the gas cloud volumes are between 1.7 and 3.9 times greater than the equivalent single wall case and again, the largest cloud volume is predicted when the walls are located closest to the release axis. Compared to the free jet, the maximum increase in gas cloud volume is by a factor of 7.5 for the case where the jet is nearest to the two walls.

Table 9.3 CFD predictions of gas cloud volumes for a jet parallel to two walls compared to a free jet

Case	*Units*	*Free jet*	*0.8 R*	*1.0 R*	*1.2 R*
100% LEL	10^{-3} m^3	0.283	2.136	1.308	0.514
50% LEL	10^{-3} m^3	2.207	N/A	N/A	N/A
V_z	10^{-3} m^3	6.243	N/A	N/A	N/A
Nodes	-	229918	448189	465970	482317

The results of the CFD simulations of the jet interaction with a cube and sphere are shown in Table 9.4 where the width of the cube and diameter of the sphere are equal to *D*. For these cases the diameter of the cylindrical computational domain was set to 12*D* (74 cm) to ensure that the boundary conditions did not effect the gas cloud volume predictions. The results show that the predicted gas cloud volumes are similar for each blockage configuration, and are approximately one third greater than the equivalent free jet. The greatest difference is seen for V_z, where the cube leads to a larger gas cloud volume than the sphere.

Table 9.4 CFD predictions of gas cloud volumes for a jet interacting with obstacles

Case	*Units*	*Free jet*	*Sphere*	*Cube*
100% LEL	10^{-3} m^3	0.283	0.354	0.359
50% LEL	10^{-3} m^3	2.207	3.710	3.385
V_z	10^{-3} m^3	6.243	9.385	13.035
Nodes	-	229918	486818	600914

Finally, the predicted gas cloud volumes for a jet interacting with a pipe are shown in Table 9.5. The effect on the cloud volume of both the pipe diameter and its position downstream of the release were considered. Pipe diameters equal to 1.0*D* and 1.2*D* were considered and the distance of the pipe from the release was varied between 0.8*L* and 1.2*L*. As for the previous cases described above, the flow was assumed to be steady state. However, the results indicated weak flapping downstream of the pipe either side of the jet axis. Although this assumption may prove an over simplification the computed volumes can still serve to provide general trends.

In all cases, the computed cloud volumes were seen to increase due to the jet interaction with the pipes when compared to the free jet case, except for the V_z cloud volume relating to the 1D 0.8*L* set-up where the gas cloud volume is marginally smaller.

The predicted cloud volume within the 100% LEL iso-surface decreases as the distance from the release to the pipe is increased. Conversely, the calculations suggest that V_z and the volume within the 50% LEL iso-surface increase as the distance from the release to the pipe increases. This behaviour is consistent with the obstacle having relatively little effect on the flow upstream of impingement. Lastly, it appears that increasing the diameter of the pipe by 20 % had little effect on the computed cloud volumes.

Table 9.5 CFD predictions of gas cloud volumes for a jet interacting with a pipe

Case	*Units*	*Free jet*	*1.2D 1L*	*1D 0.8L*	*1D 1L*	*1D 1.2L*
100 % LEL	10^{-3} m^3	0.283	0.367	0.422	0.362	0.338
50 % LEL	10^{-3} m^3	2.207	2.661	2.456	2.611	2.710
V_z	10^{-3} m^3	6.243	6.728	6.233	6.753	7.125
Nodes	-	229918	1146890	1260948	1261592	1292289

10 APPENDIX C – GAS CLOUD BUILD-UP EXPERIMENTS

10.1 INTRODUCTION

This aim of the experimental phase of the project was to validate and provide confidence in the CFD model of gas leaks in enclosures The variables investigated covered the range of conditions of interest in terms of hole size, gas pressures, ventilation rates, leak rates and leak location/orientation.

Testing took place in a specially constructed chamber with the ability to vary mechanical ventilation rates between 2 and 24 air changes per hour (ach). Three configurations were investigated; an unobstructed jet directed into the centre of the room, an unobstructed jet located a small distance from and parallel to one wall and a jet impinging directly onto a wall in a confined space. For each configuration the hole sizes, ventilation rates and gas leak rates were varied.

During each test the temperature and volume flow rate of air into and out of the room was logged. Gas concentration measurements were made at 14 locations and temperatures were also logged at a further eight locations.

10.2 APPROACH AND EXPERIMENTAL DETAILS

A tracer gas was released at a specified rate through a nozzle of cross sectional area 0.25 or 2.5 mm^2 into a test enclosure with a known ventilation rate. The tracer gas was a mixture of 1 % isobutylene (iso-C_4H_8), 48 % nitrogen and 51 % helium. The gas mixture was selected to have the same mean molecular mass and density as methane. The isobutylene was the detectable component of the tracer gas and could be measured to an accuracy of 0.1 ppm at concentrations below 100 ppm and 1 ppm above 100 ppm.

All tests were conducted within a specially constructed enclosure, with internal dimensions 4 m $\times$ 4 m $\times$ 2.92 m high, located within a climate controlled laboratory, see Figure 10.1. The enclosure had two inlets and two outlets with dimensions 0.4 m by 0.4 m located 0.5 m from the sidewalls, one at 2.3 m and one at 0.3 m from the floor and diagonally opposed on opposite walls. The volume flow rate at each inlet/extract was monitored using flow grids or orifice plates, both measuring differential pressure. To produce a uniform velocity at the two air inlets the airflow in the 0.4 by 0.4 m square section needed to be conditioned. This was achieved by including a perforated plate (25 % open area), with the central portion blocked off, followed by a layer of porous foam and finally by a section of honeycomb flow straightener. The latter ensured that the air entered the room perpendicular to the wall, see Figure 10.3. The uniformity of the airflow was verified by velocity measurements. Air exhausted from the enclosure was ducted out of the laboratory in order to prevent the re-entrainment of tracer gas into the test enclosure. The enclosure included an obstruction 2 m $\times$ 1 m $\times$ 1 m, which was positioned according to the configuration being investigated.

The temperature in the enclosure was monitored at twelve locations using nine thermistors and three platinum (Pt) resistance sensors. One thermistor was placed in each inlet/extract, the remaining five were located on a vertical rake to monitor for any thermal stratification within the room. So that temperature measurements were directly comparable to one another, the thermistors were calibrated against one of the Pt-sensors. In addition, Pt-sensors were positioned in the lower extract and on the vertical rake in order to give comparison temperature measurements in real time. The third Pt-sensor measured the temperature of the incoming tracer gas.

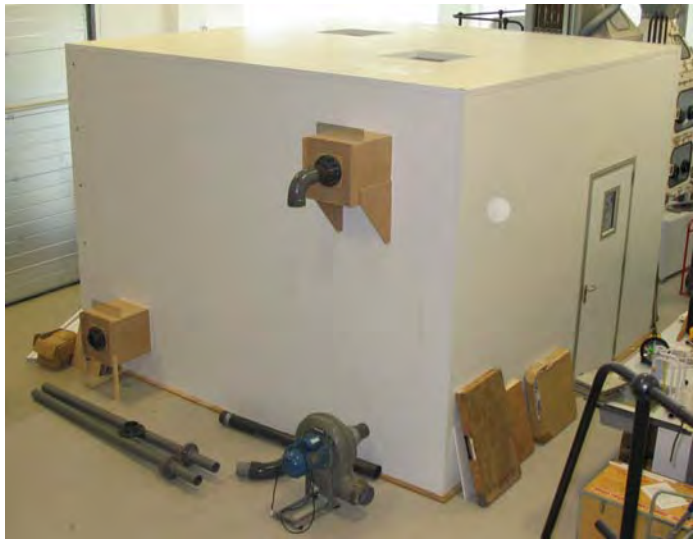

Figure 10.1 Test enclosure during commissioning showing ventilation extracts on near side

Test gas was supplied from the cylinder through a mass flow controller to the release head. Two release heads were used; a 2.5 mm^2 venturi designed nozzle and a 0.25 mm^2 nozzle. Due the small cross-sectional area of the 0.25 mm^2 nozzle, the orifice consisted of a hole with parallel sides. Figure 10.2 shows the release head with the large 2.5 mm^2 nozzle and a pressure transducer attached. The Pt-sensor measuring the temperature of the incoming gas is located beneath the wooden mount.

Before sampling of the tracer gas, the gas concentrations in the enclosure were allowed to reach equilibrium. To determine when steady state conditions had been reached, gas concentrations were measured in real-time at two positions, one in the lower extract duct and the second inside the enclosure. Once steady state was reached, gas was sampled from twelve predetermined positions for each configuration for ten minutes into gas sample bags. After the sampling period the concentration in each bag was then measured to determine the mean concentration of tracer gas at each point for comparison to the CFD model.

Measurements of gas concentrations in the sample bags were made using two MiniRae 2000 photo ionisation detectors (PIDs) and averaged. Each PID was calibrated with 100 ppm 'isobutylene in air' span gas on each day of testing and then checked against the span gas before and after each test.

A summary of the 33 tests carried out across the three configurations is shown in Table 10.1 to 10.3. Test C1-5a was a repeat of Test C1-5 which was undertaken to investigate the reproducibility of the data, see section 10.3.5.

Figure 10.2 Tracer gas release head with 2.5 mm^2 nozzle and pressure transducer attached

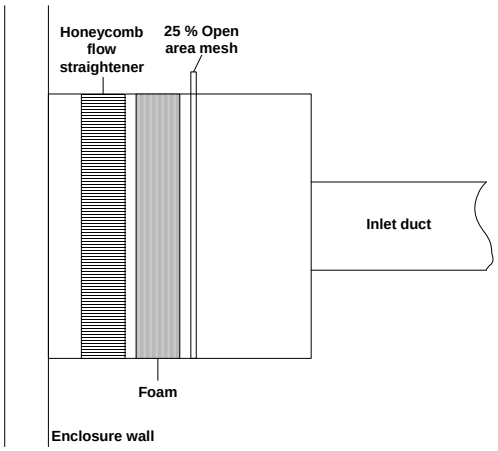

Figure 10.3 Cross section diagram of the ventilation inlet flow conditioning

Table 10.1 Test details for configuration 1 (unobstructed jet)

Test No.	*Target Release Rate* gs^{-1}	*Tracer Release Rate* gs^{-1}	*Nozzle Size* mm^2	*Ventilation Rate ach*
C1-1	0.15	0.16	0.25	6
C1-2	0.22	0.24	2.5	12
C1-3	0.26	0.25	0.25	6
C1-4	0.47	0.41	0.25	2
C1-5	0.47	0.42	0.25	6
C1-5a	0.47	0.40	0.25	6
C1-6	0.47	0.47	0.25	12
C1-7	0.49	0.46	2.5	12
C1-8	0.86	0.86	2.5	2
C1-9	0.86	0.79	2.5	6
C1-10	0.86	0.79	2.5	12
C1-11	0.86	0.79	2.5	24
C1-12	1.72	1.76	2.5	12

Table 10.2 Test details for configuration 2 (wall jet)

Test No.	*Target Release Rate* gs^{-1}	*Tracer Release Rate* gs^{-1}	*Nozzle Size* mm^2	*Ventilation Rate ach*
C2-3	0.26	0.28	0.25	6
C2-4	0.47	0.42	0.25	2
C2-5	0.47	0.38	0.25	6
C2-6	0.47	0.41	0.25	12
C2-7	0.49	0.51	2.5	12
C2-8	0.86	0.93	2.5	2
C2-9	0.86	0.93	2.5	6
C2-10	0.86	0.93	2.5	12
C2-12	1.72	1.84	2.5	12

Table 10.3 Test details for configuration 3 (obstructed and confined jet)

Test No.	*Target Release Rate* gs^{-1}	*Tracer Release Rate* gs^{-1}	*Nozzle Size* mm^2	*Ventilation Rate ach*
C3-3	0.26	0.26	0.25	6
C3-4	0.47	0.47	0.25	2
C3-5	0.47	0.47	0.25	6
C3-6	0.47	0.47	0.25	12
C3-7	0.49	0.49	2.5	12
C3-8	0.86	0.86	2.5	2
C3-9	0.86	0.86	2.5	6
C3-10	0.86	0.86	2.5	12
C3-12	1.72	1.72	2.5	12

10.2.1 Configuration 1: Unobstructed jet

Configuration 1 was an unobstructed jet directed into the middle of the room. The nozzle orifice was located 0.26 m from the air inlet wall on the centreline of the room 1.5 m from the floor as shown in Figure 10.4. The obstruction was placed centrally within the enclosure.

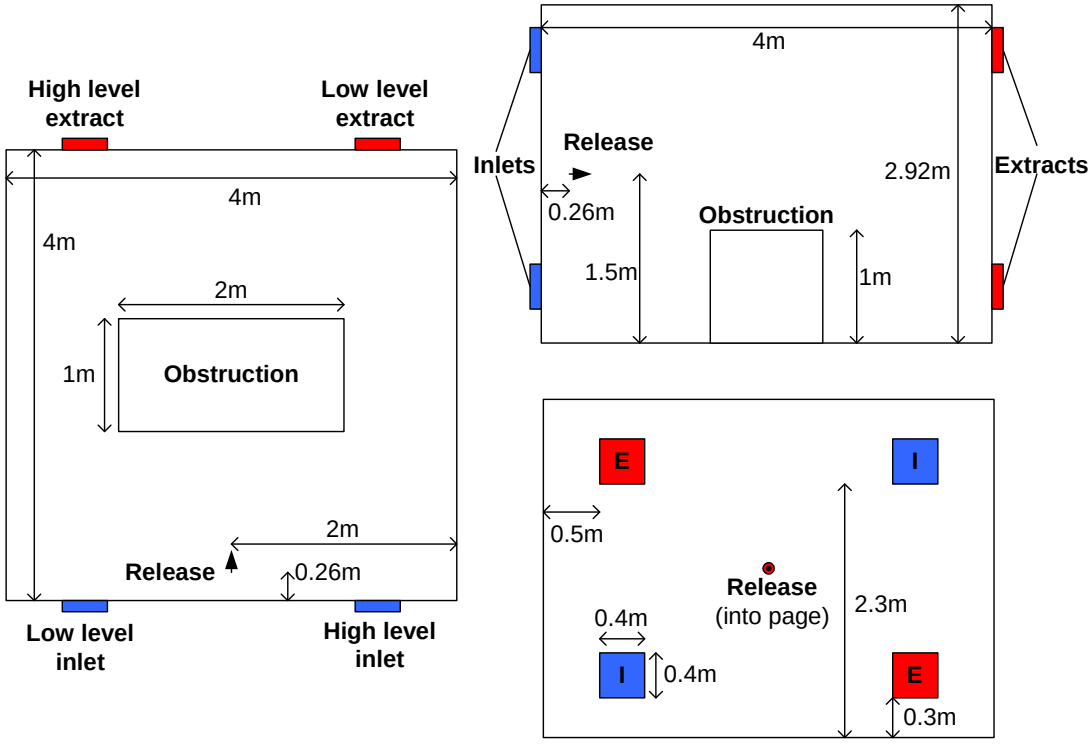

Figure 10.4 Test enclosure layout and tracer release position for configuration 1, plan view (left), side view (top right) and end view (bottom left).

The sample grid was located in front of the nozzle with positions on the centreline, to either side, above and below the jet as shown in Figure 10.5. The sample grid was arranged with two spacing dimensions dependent on the nozzle and gas release rate used. Sample positions for tests C1-2, C1-3 and C1-1 were separated by 0.25 m along the axis of the jet and 0.10 m

perpendicular to the axis of the jet. All other tests had spacings of 0.50 m along the axis of the jet and 0.20 m perpendicular to the axis of the jet. The sample grid was composed of stainless steel tubes 1.2 mm in diameter connected via Tygon plastic tubing to pumps and gas sample bags. Tygon tubing was selected because it is chemically inert and adsorption of the tracer gas onto the surface of the tubing would therefore be negligible.

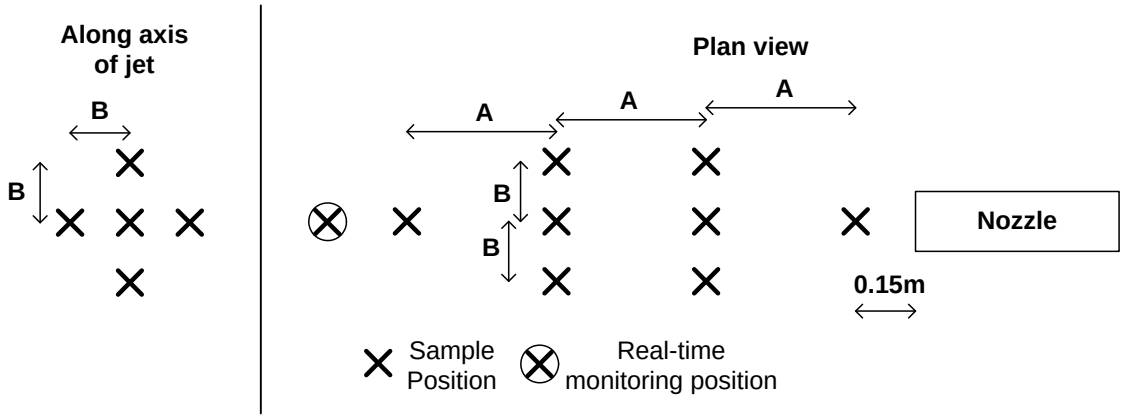

Figure 10.5 Sample grid for configuration 1. The real-time monitoring position is located 1.9m from the nozzle. For tests C1-2, C1-3 and C1-1, A = 0.25m and B = 0.10m. For all other tests A = 0.50m and B = 0.20m.

The sample tubes were mounted in steel frames 0.7 m × 0.7 m square, which in turn were mounted on a wooden frame such that the gas jet passed through the centre of the frames as shown in Figure 10.6. The real-time monitoring position within the enclosure was located on the centreline of the jet 1.9 m from the nozzle and the second real-time position was located in the lower extract duct. The sample grids were aligned using a laser making the positions accurate to +/- 5 mm.

Figure 10.6 Configuration 1 sample grid alignment

10.2.2 Configuration 2: Wall jet

Configuration 2 consisted of an unobstructed jet located 0.056 m from and parallel to a wall, 1.5 m above the floor and 1 m from the air inlet wall, see Figure 10.7.

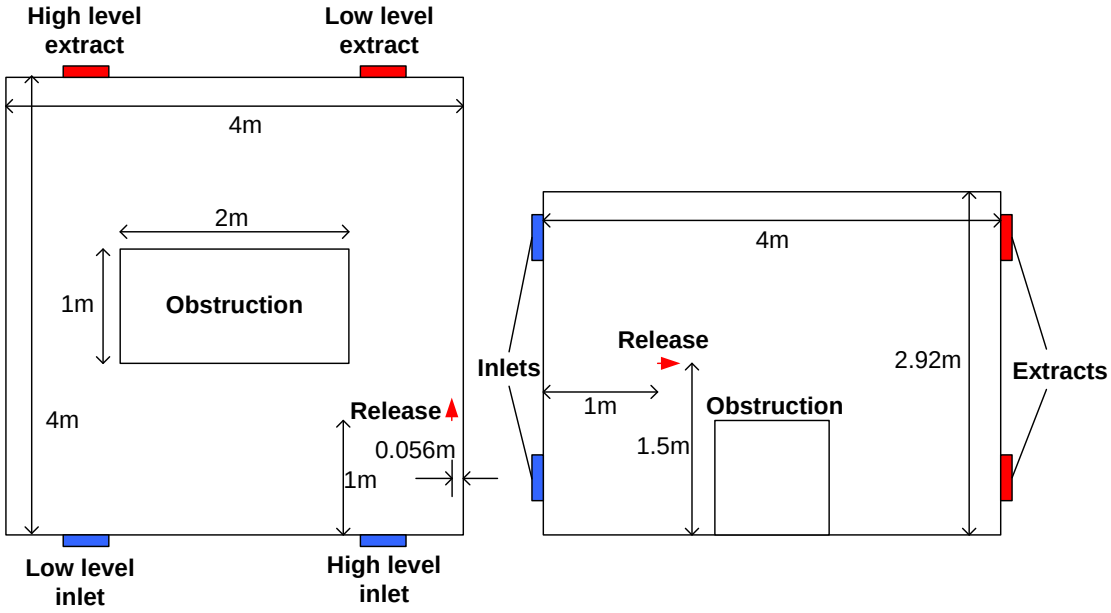

Figure 10.7 Test enclosure layout and tracer release position for configuration 2, plan view (left) and side view (right)

The sample grid was located in front of the nozzle with positions on the centreline, to one side, above and below the jet as shown in Figure 10.8. As with configuration 1, two sets of grid spacing dimensions were used depending on the hole size and release rate. Sample positions for test C2-4 were separated by 0.25 m along the axis of the jet and 0.50 m for all the other C2 tests. As with configuration 1 the sample grid was composed of 1.2 mm diameter sample tubes connected to the pumps and sample bags by Tygon tubing.

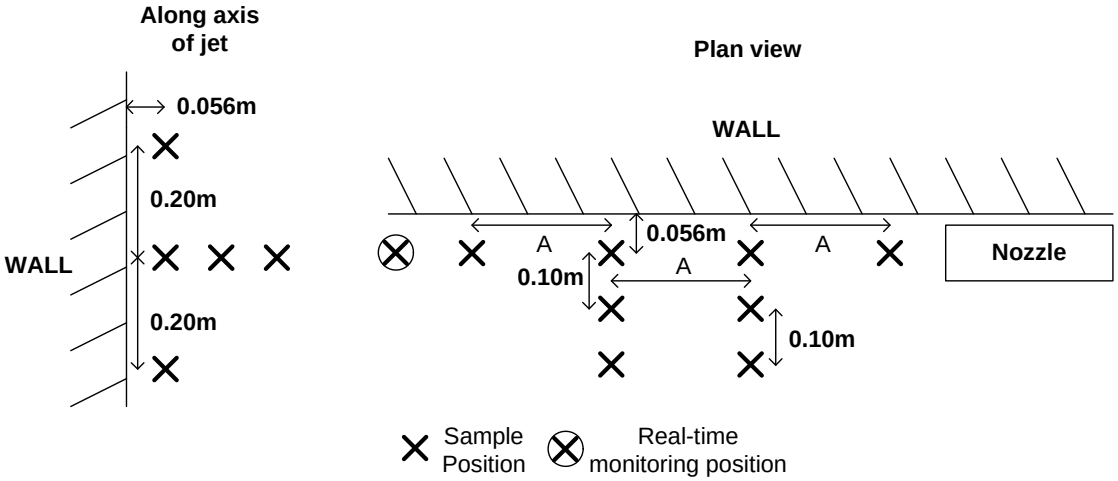

Figure 10.8 Sample grid for configuration 2, real-time monitoring position was located 1.9 m from the nozzle. For tests C2-4, A = 0.25m, otherwise A = 0.50m.

The sample grid was mounted through the wall of the enclosure as shown in Figure 10.9 and again the sample positions were aligned using a laser. The real-time monitoring position was located at 1.9 m from the nozzle and on the centreline of the jet. The obstruction was placed centrally within the enclosure, the same position as in configuration 1

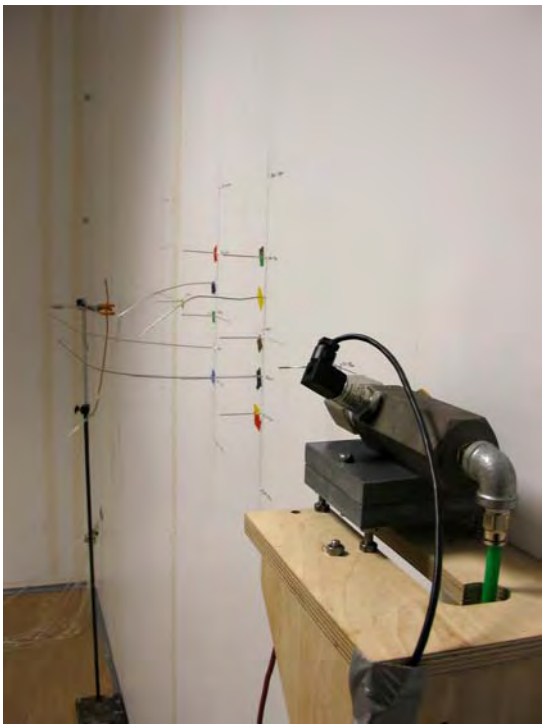

Figure 10.9 Nozzle position and sample grid for configuration 2

10.2.3 Configuration 3: Obstructed jet in a restricted space

Configuration 3 was a jet impinging directly onto a wall in a restricted space as shown in Figure 10.10. For this configuration the obstruction was moved from the centre of the room so that the short side was placed against one sidewall and the long side was 0.5 m from the extract wall thus creating a confined space into which the gas was released. The nozzle was positioned mid-way between the wall and obstruction, 0.5 m from the floor and 0.5 m from the side wall.

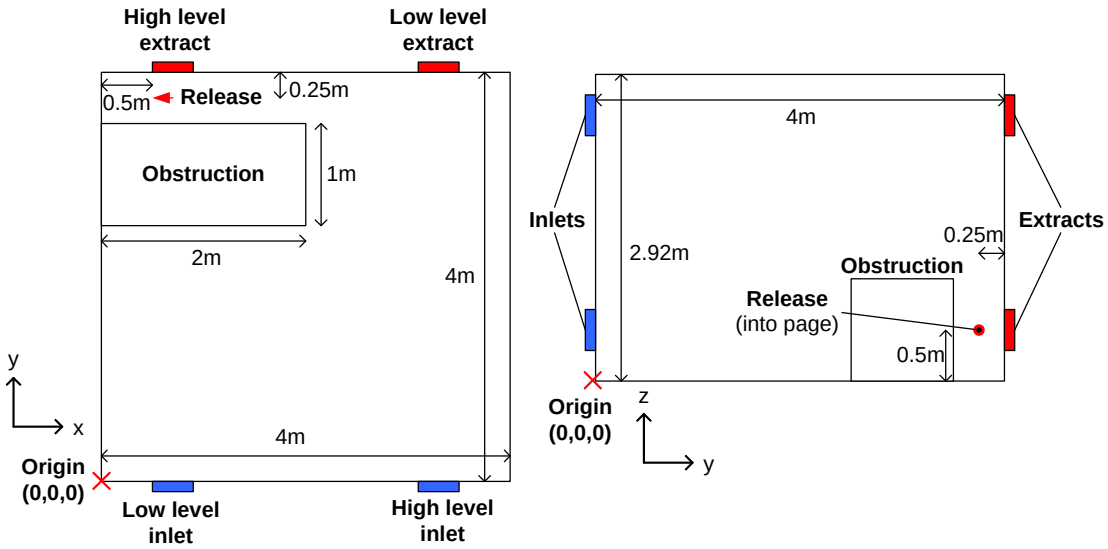

Figure 10.10 Test enclosure layout and tracer release position for configuration 3, plan view (left) and side view (right)

Configurations 1 and 2 had sample positions laid out on a regular grid, whereas since in configuration 3 the jet impinged directly onto a wall the sample positions were more widely spaced. Table 10.4 below gives the coordinates of each sample point and a brief description of the position. The origin for the coordinate system is shown in Figure 10.10.

Table 10.4 Sample grid positions and descriptions for configuration 3

Position	*x / m*	*y / m*	*z / m*	*Description relative to nozzle*
1	0.10	3.75	0.50	Centreline of jet 0.40 m from nozzle
2	0.35	3.75	0.50	Centreline of jet 0.15 m from nozzle
3	0.10	3.75	1.00	Above and in front of nozzle in y = 3.75 m plane
4	0.45	3.75	1.00	Above and in front of nozzle in y = 3.75 m plane
5	0.80	3.75	1.00	Above and behind nozzle in y = 3.75 m plane
6	0.80	3.75	0.70	Above and behind nozzle in y = 3.75 m plane
7	0.80	3.75	0.30	Below and behind nozzle in y = 3.75 m plane
8	1.50	3.75	0.50	Level with and behind nozzle in y = 3.75 m plane
9	2.00	2.04	2.83	Centre of ceiling
10	0.25	3.75	2.80	In front of nozzle at ceiling height in y = 3.75 m plane
11	0.25	3.75	1.50	Above and in front of nozzle in y = 3.75 m plane
12	0.50	3.50	1.50	Above nozzle in y = 3.50 m plane
13	0.75	3.25	1.50	Above and behind nozzle in y = 3.25 m plane
Nozzle	0.50	3.75	0.50	-

To minimise disruption to the jet, positions 1 and 2 used the same 1.2 mm diameter steel tubes as used in configurations 1 and 2. All other sample positions used 4 mm diameter annealed copper tube, which presented a smaller pressure drop to the sample pumps. Position 11 was monitored in real-time. All sample positions, except the two at ceiling height, were aligned using a laser. The release nozzle and part of the sampling grid are shown in Figure 10.11.

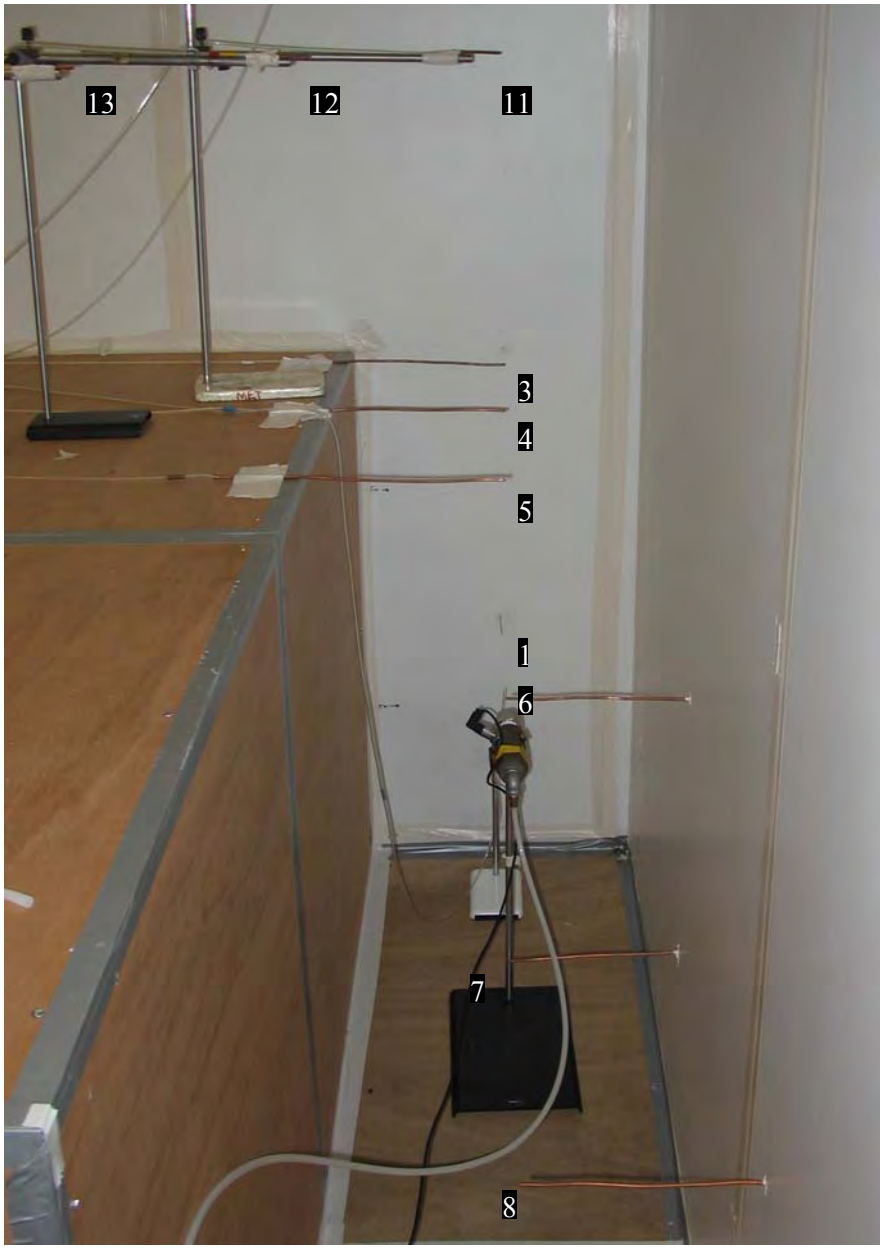

Figure 10.11 Configuration 3 nozzle and sample positions

10.3 DISCUSSION

10.3.1 Sampling accuracy

10.3.1.1 Leaks in sample lines during configuration 1

Several sampling problems were encountered, the first of which was sampling gas from within or very close to the gas jet. Sampling was a compromise between obtaining a representative sample at a given position whilst causing minimum disruption to the jet. To solve this, narrow bore 1.2 mm diameter steel tubes were used to obtain the samples from within the gas jet. However, the narrow bore tubes increased the pressure drop across the sample lines and this

resulted in air entering the sample lines at positions other than via at the sample position. The leaks occurred where the flexible plastic lines were attached to the steel tubes as shown in Figure 10.12, and where the lines attach to the sample pumps.

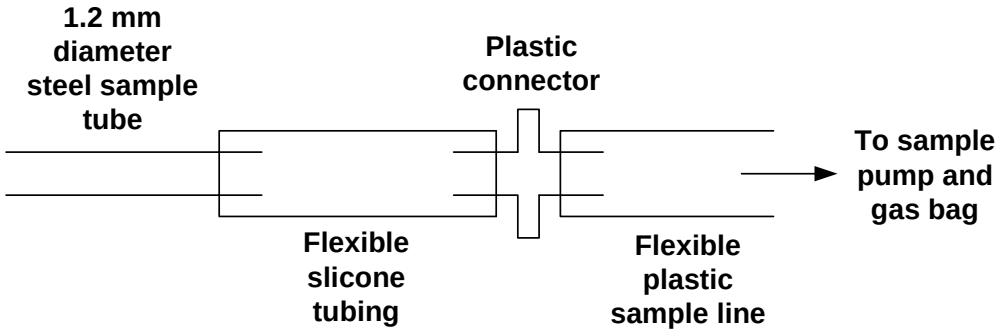

Figure 10.12 Schematic of the connection between the steel sample tube and the flexible plastic sample line.

To quantify these leaks, tracer gas of a known concentration was sampled through each line and into the sample bag. Analysis of the gas samples showed that the resultant concentrations were 16% lower than it should have been and therefore the data from configuration 1 was corrected accordingly.

In addition, it was noted that samples taken 150 mm from the nozzle orifice on the centreline collected a smaller volume of gas than at other positions. Sample tubes on the centreline were oriented such that the axis of the tube was perpendicular to the axis of the jet, as shown on the left in Figure 10.13.

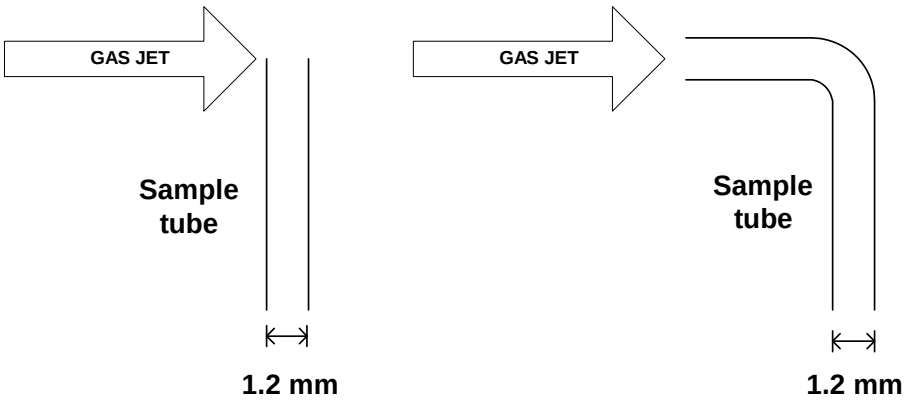

Figure 10.13 Sample tube orientation at 150 mm from nozzle orifice on the centreline. Tube axis perpendicular to jet during configuration 1 (left) and aligned with jet during configuration 2 and 3 (right).

The centreline velocities of the jets at 150 mm from the nozzle were measured to be above 20 ms^{-1} for leak rates of 0.86 and 1.72 gs^{-1} using the 2.5 mm^2 nozzle and 0.47 gs^{-1} for the 0.25 mm^2 nozzle. These leak rates constituted the majority of the tests performed. It was thought that the high velocity jet passing across the opening of the sample tube was creating a venturi effect, opposing the suction action of the sampling pump. To investigate this further the sample tube at 150 mm was oriented such that the axis was aligned with the gas jet see Figure 10.13. This sample tube orientation was tested and compared to the sample flow rate with the tube perpendicular to the flow. At tracer gas flow rates of 0.47 and 0.86 gs^{-1}, used with the 0.25 and 2.5 mm^2 nozzles respectively, the flow into the sample tube oriented perpendicular to the jet

was found to be less than 50 % of that when aligned with the jet. This value fell to less than 20 % with the highest flow rate of 1.72 gs^{-1}. This effect was only apparent at 150 mm from the nozzle orifice as the velocity of the jet decreased rapidly with distance from the nozzle. The consequence was that the sample tube 150 mm from the nozzle under-sampled by an unknown amount and was test condition dependent. Therefore, data at this sample position have not been included in the results for configuration 1.

For both configurations 2 and 3 the sample position at 150 mm from the nozzle was orientated such that the axis of the sample tube was aligned with the axis of the jet.

10.3.1.2 Leaks in sample lines during configuration 2

Setting up the sampling system for configuration 2 necessitated doubling the required length of flexible plastic tubing as the grid had to be mounted through the far wall of the enclosure. The extra length of tubing presented a larger pressure drop to the sample pumps and increased the likelihood of entraining air into the sample line. To overcome this the seal between the sample line and sample tube was improved by removing the flexible silicone tubing and attaching the plastic connector directly to the steel tube using adhesive. Unlike configuration 1 the sample tubes were not all of the same length or shape. The tube at 150 mm from the nozzle had a 90º bend and the positions offset from the centreline used longer tubes with a bend in order to position them correctly. The system was then tested for leaks at each position using the same method as for configuration 1 and these were found to vary between 24% under-sampled for the position 150 mm from the nozzle to 9% under-sampled for the positions above and below the centreline which utilised shorter lengths of steel tube. These leakage rates were then taken into account when calculating tracer concentrations at specific points.

10.3.1.3 Leaks in sample lines during configuration 3

Constructing the sampling system for configuration 3 was significantly simpler than for configurations 1 and 2. This was because there were only two measurement positions on the centreline of the jet before it impinged directly onto a wall. The sample tubes at these positions were of a similar construction to those used previously, i.e. 1.2 mm diameter steel tubes. The remainder of the positions were away from the jet and therefore there was no need to use such small diameter tubes. In order to minimise any leaks the rest of the sample positions used large 4 mm bore annealed copper tube. This presented a lower sample line pressure drop and reduced leakage at these positions to approximately 5 %.

10.3.2 Actual versus target leak rates

Some problems were encountered in achieving the correct mass release rate of tracer gas. For the first five tests carried out for configuration 1 (C1-10, C1-11, C1-7, C1-9 and C1-8) the release rate was calculated by measuring the static pressure inside the release head. However this method caused a slight under-read in the true mass release rate which was measured at a later date using the mass flow controller. Note, the release rate was correct for test C1-8 as the pressure in the gas line was set slightly too high. For the other tests a direct mass flow controller was available and this device directly controlled the rate of gas release. The device was calibrated to control the flow of propane gas and therefore a correction factor or gas constant was required as the tracer gas density was that of methane.

The gas constants for the mass flow controller are calculated at standard temperature and pressure (STP, 273 K, 1 atm) but the gas was being delivered to the mass flow controller at normal temperature and pressure (NTP, 293 K, 1 atm). Since gas density is a function of temperature, and the mass flow controller assumed that the gas is at STP, the discrepancy in

temperature caused the mass flow controller to deliver gas at too high a rate by 7 %. This accounts for the high release rates in tests C1-2 and C1-12.

A second problem occurred when using the 0.25 mm^2 nozzle, for the highest release rate of 0.47 gs^{-1}, as a pressure of approximately 10 barg was required in the release head. This proved difficult to obtain with the regulator available and generally a low release rate was achieved. This was not rectified until the start of configuration 3. This meant that for tests C1-5, C1-4, C1-5a, C2-6, C2-5, and C2-4, the mass release rate of tracer gas fell short of the target value. The release rate for tests C2-9, C2-8, C2-10, C2-7, C2-12 and C2-3 was too high because of the temperature discrepancy. For configuration 3 both these problems had been rectified and all of the target release rates were met.

10.3.3 Other uncertainties in data

As with all experimental data, there are other uncertainties. For instance, whilst the flow conditioning at the inlets produced a uniform velocity, it did increase the pressure drop across the enclosure. Consequently it proved difficult to fully seal the enclosure and therefore there were leakage through small, unplanned openings in the fabric of the enclosure. These leakage paths were probably via the joints between walls and ceiling and around the door.

In the CFD simulations replacement air entering via the two inlets was divided equally. In practice this was achieved by manually balancing the flow through the two inlets using dampers on the ducts. In every test but one this was achieved to within 2 % (i.e. <48 % of the inlet air via one inlet and <52 % via the second), in test C1-8 the flow was divided between the lower and upper inlets in the ratio 45:55.

As was discussed earlier, once a test had started the gas concentrations in the room were allowed to reach steady state. The approach to steady state was monitored by measuring the tracer gas concentration in real-time at one location within the room and at the lower extract. Before testing, a calculation based on perfect mixing was made for each ventilation rate to estimate the time required for concentrations to reach 95 % of steady state. Then, during each test the concentration at the two real-time positions was noted at regular intervals of 1, 2 or 5 minutes depending on the ventilation rate. Analysing the logs of the concentrations measured at the real-time positions showed that the calculated times to reach a steady state concentration were very close and the concentration did not change significantly during the sampling period. Figure 10.14 shows a plot of the logged concentrations measured at the real-time position within the enclosure during test C3-3. The concentration can be seen to fluctuate considerably, but the overall trend towards steady state is clear. The calculated $t_{95\%}$ time was accurate, as indicated by the quasi-steady profile of the concentration history during the 10 minute gas sampling period.

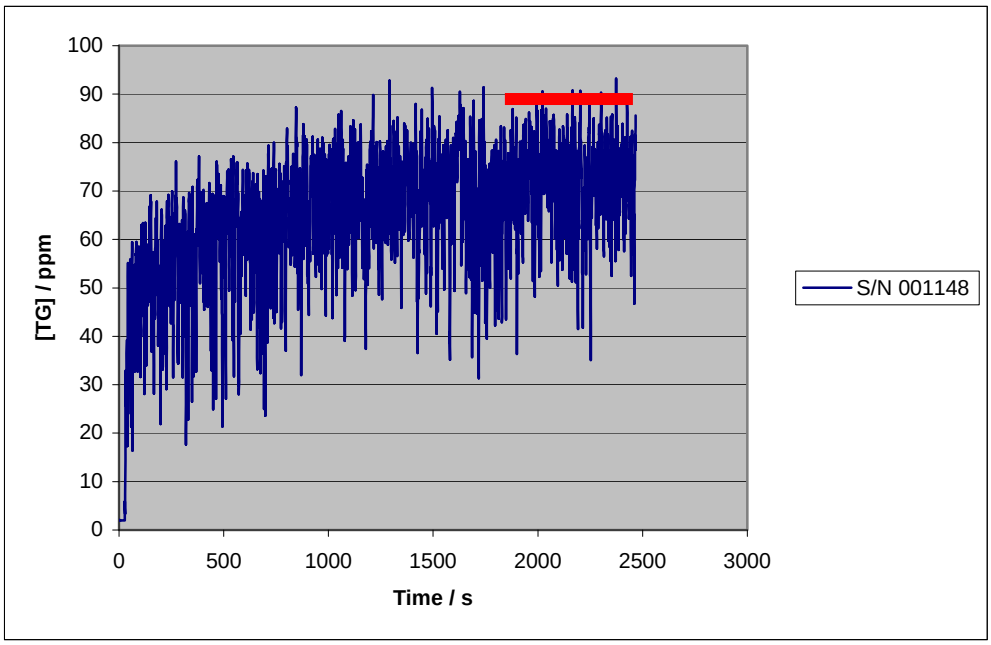

Figure 10.14 Logged plot of tracer concentration at the real-time monitoring position within the enclosure during configuration 3 test C3-3. The red bar shows the ten minute gas sampling period.

10.3.4 Results of temperature measurements

The temperature within the room was monitored and logged by a rake of thermistors at 485, 963, 1460, 1963 and 2440 mm from the floor to check for any thermal stratification. A small temperature gradient was detected, generally rising from floor to ceiling. The maximum temperature difference between the thermistors was generally 0.1 – 0.3 ºC with one test having a maximum difference of 0.54 ºC. The logs showed that the temperature inside the enclosure remained constant during a test. The temperature inside the enclosure was generally lower than within the laboratory, by up to 2.0 ºC in some cases but generally 0.5 – 1.0 ºC. A typical plot of the logged temperatures during a test is shown below in Figure 10.15.

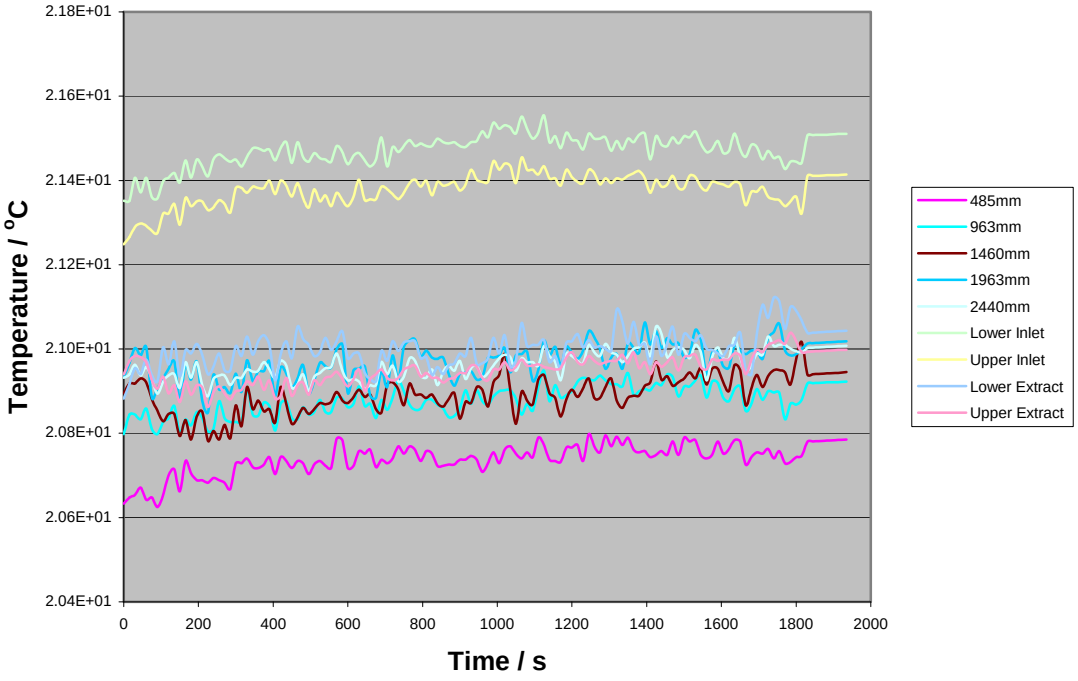

Figure 10.15 Plot of logged temperature during configuration 1 test 2.

10.3.5 Reproducibility and Repeatability

Due to experimental variations it is expected that replicating or reproducing a test will not exactly produce the same data at each measurement position. To investigate the reproducibility of the experiments test C1-5 was repeated as test C1-5a, see Table 10.1. After test C1-5 had been completed the set-up in the room was dismantled (including removing all the sample tubes from the frame and dismantling of the ventilation system). The test was then reconstructed and repeated as C1-5a. Both tests were carried out on different days. Strictly speaking it was not a full reproducibility test as the same scientists performed both tests and the same equipment was used.

Table 10.4 shows the measured concentrations expressed as a percentage of the tracer gas concentration released. Note the mass release rates were slightly different. Overall the comparison between the test data is good, particularly between the centre line data which is closer than 4%. There is a larger discrepancy for the off-axis measurements, with the greatest differences at the measurement plane furthest from the nozzle. Measurements at the lower extract were closer, differing by approximately 5%.

Table 10.4 Comparison of data from test 5 and test 5a

Position w.r.t centre line (mm)	*Distance from nozzle (mm)*	*Test 5 (0.42 gs^{-1}) (%vol/vol)*	*Test 5a (0.40 gs^{-1}) (%vol/vol)*	*Difference between tests (%vol/vol)*	
0	650	1.68	1.65	-0.03	(-1.8%)
200 above	650	0.67	0.68	0.01	(1.5%)
200 below	650	0.74	0.68	-0.06	(-8.1%)
200 left	650	0.69	0.69	0.00	(0.0%)
200 right	650	0.73	0.82	0.09	(12.3%)
0	1150	1.26	1.26	0.00	(0.0%)
200 above	1150	0.75	0.77	0.02	(2.7%)
200 below	1150	0.90	0.80	-0.10	(-11.1%)
200 left	1150	0.79	0.61	-0.18	(-22.8%)
200 right	1150	0.83	0.70	-0.13	(-15.7%)
0	1650	1.09	1.08	-0.01	(-0.9%)
0	1900	1.05	1.08	0.03	(2.9%)
Lower extract		0.59	0.56	-0.03	(-5.1%)

10.4 SUMMARY

A programme of experimental work has been carried out in a purpose built ventilated enclosure located within a climate-controlled laboratory. During each test the ventilation rate was held constant and the temperature and flow rate at the two inlets and two outlets were monitored. In addition, five thermisters were arranged in a vertical rake and temperatures logged during each test.

Tests were carried out with a tracer gas that had the same buoyancy characteristics as methane. The tracer gas was released at a range of pressures through two nozzles with different hole sizes. The tracer gas concentration in the enclosure was allowed to reach steady state before air samples were collected simultaneously at 14 different positions in the room.

Three configurations were investigated; an unobstructed jet directed into the centre of the room, an unobstructed jet located a small distance from and parallel to one wall and a jet impinging directly onto a wall in a confined space.

For configuration 1 and 2 the target gas release rate was not always met. For configuration 1 the release rate was within 10% of the target value for 11 of the 15 tests and of the four remaining tests the largest error was 15%. For configuration 2, the release rate was within 10% of the target value for six of the nine tests. The largest error of the remaining three was 19%. For configuration 3 the target values were all achieved.

Leakage on sample lines was a recurring problem. However, these were identified and the leakage and dilution rates were quantified and the data were corrected.

Repeat tests showed that the reproducibility of the tests was very good and measurement uncertainties were low.

11 APPENDIX D – CFD MODEL VALIDATION

11.1 INTRODUCTION

This section documents the validation tests that have been undertaken to determine whether the CFD model is capable of predicting the behaviour of low-pressure gas releases in ventilated enclosures to an acceptable degree of accuracy.

Comparisons are made between the CFD model predictions and measurements of gas concentration for three different enclosure arrangements with a number of different leak rates and ventilation rates, which provide in total 29 separate scenarios.

The first section describes the CFD methodology used in the validation study. This includes discussion of the different room geometries tested, an overview of the predicted flow behaviour and results from a grid dependence study. The unsteady nature of the flow and the approach taken to account for this in the CFD model are also discussed. This is followed by the presentation of the validation results where CFD predictions of gas concentration are compared against measured values. Finally, there are some conclusions.

11.2 METHODOLOGY

11.2.1 Room and Nozzle Configurations

Three different nozzle configurations have been examined, as shown in Figure 11.1. In all three cases, the enclosure was 4 metres wide, 4 metres long and 2.92 metres high. Two ventilation inlets were located diagonally opposite on one face of the room (upper-left and lower-right) and on the opposite face of the room were located two ventilation outlets, also positioned diagonally and staggered with respect to the inlets to prevent the flow "short-circuiting" directly from the inlets to the outlets.

A rectangular box obstruction (coloured blue in Figure 11.1) of dimensions 2 × 1 × 1 metres was placed inside the room. For Configurations 1 and 2 it was placed centrally, while in Configuration 3 it was moved against one wall in a corner of the room to create a narrow cavity 50 cm wide between the box and the wall.

In Configuration 1, the nozzle directed the gas release into the centre of the room, in Configuration 2 it was aimed along a wall and in Configuration 3 the nozzle was placed inside the narrow cavity formed between the box and the wall.

The detailed design of the third configuration was agreed upon following a series of CFD simulations with different room configurations (described in more detail in Appendix E). It can be considered as representing a credible "worst-case" scenario, i.e. the leak location / direction leading to the largest gas cloud for given ventilation conditions and leak rate.

More details of the experimental tests and measurement procedures are given in Appendix C.

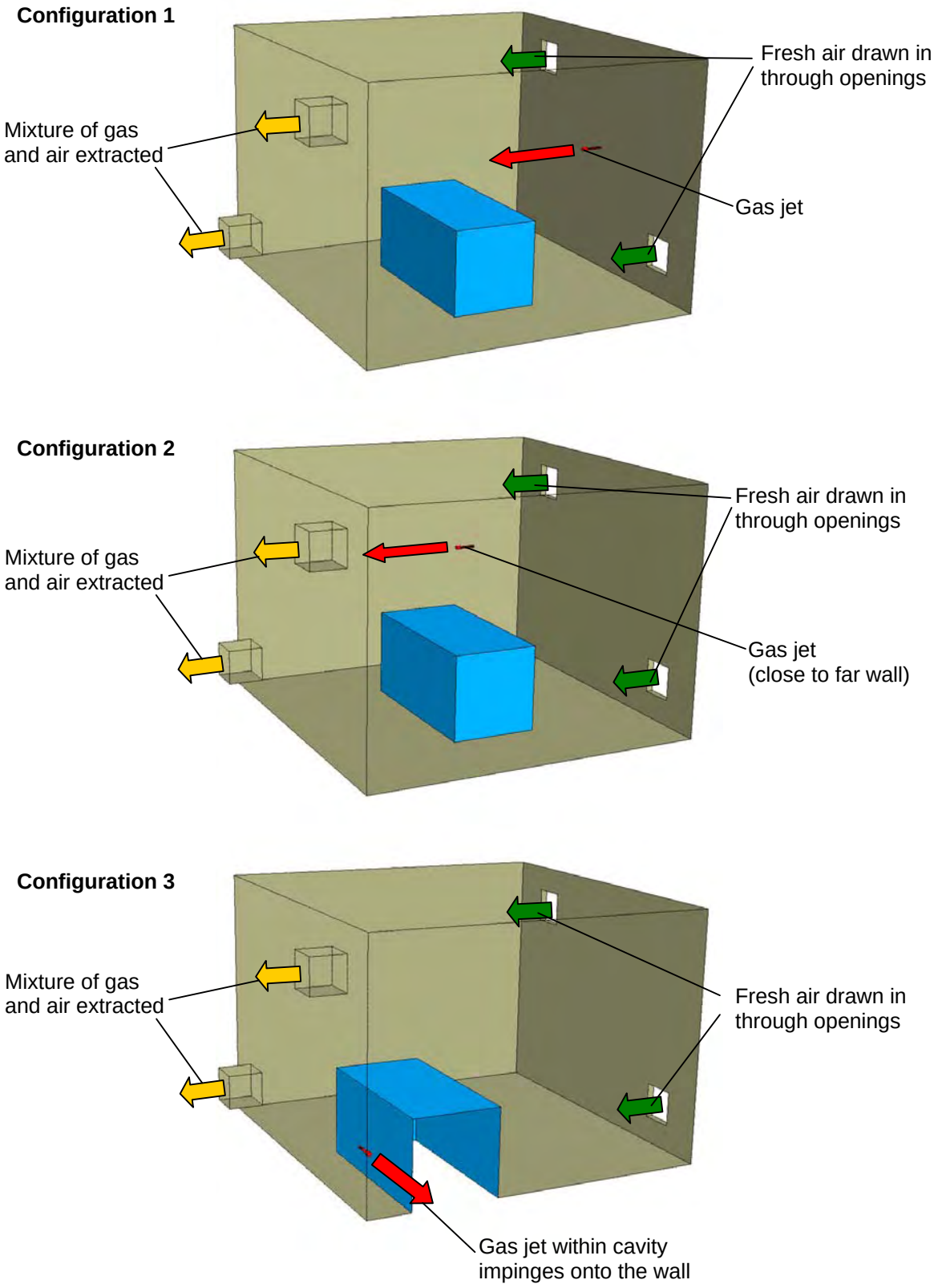

Figure 11.1 Arrangements of the room, nozzle and box for Configurations 1, 2 and 3

11.2.2 CFD Model

The model geometry for each of the configurations is shown in Figure 11.1. To match the experimental arrangement, the ventilation velocity was specified at the face of the extract ducts and air was pulled in through the two inlets. The extract velocity was calculated from the prescribed air change rate, the room volume and the cross-sectional area of the inlets/outlets, taking into account the 2 × 1 × 1 metre blockage in the room volume. For a ventilation rate of 12 ach, this gave an inlet velocity of 0.47 m/s. In the scenarios modelled where the ventilation rate was low (only 2 ach), in order to balance the flow rate through the two inlets the ventilation rate through the upper inlet was fixed in addition to the ventilation rate through the two outlets.

For the simulations involving choked gas releases (above 0.85 barg), a pseudo-source approach was used where the gas was released at the speed of sound through an opening downstream[5] of the actual orifice at the point at which the pressure had dropped to ambient. For details of this approach see Ivings *et al*. (2004) in which the methodology for modelling the gas leak is referred to as a "resolved sonic source". A close up view of the nozzle is shown in Figure 11.2. For the 0.86 g/s release through a 2.5 mm^2 orifice, which will subsequently be referred to as the baseline release, the cross-sectional area of the pseudo-source was 2.7 mm^2.

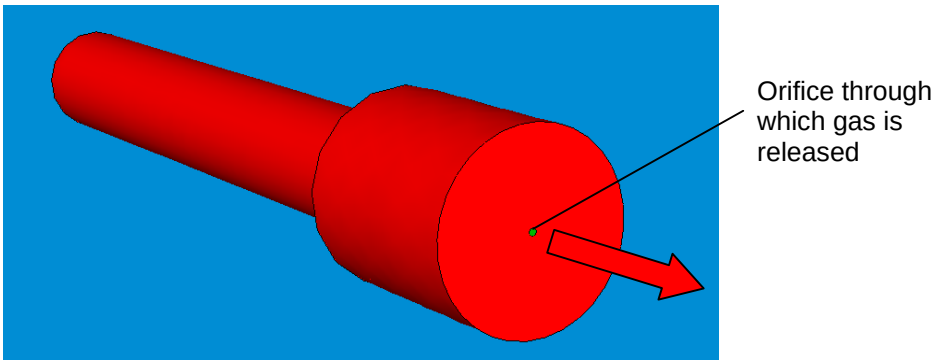

Figure 11.2 Close-up view of the modelled nozzle and orifice

All walls were treated as adiabatic (i.e. perfectly insulated) and air entered the room at a temperature of 20 °C. Depending on the nature of the gas release (choked/subsonic), the gas was released into the room at different temperatures. For the 0.86 g/s baseline case, the gas temperature was -18 °C.

Turbulence was modelled using the industry-standard Shear-Stress Transport (SST) model in conjunction with ANSYS CFX's automatic wall treatment, which switches from a low-Reynolds-number treatment to a wall function approach depending upon the near-wall resolution. Variation of fluid parameters (density, viscosity etc.) due to changes in temperature and gas composition were accounted for in the model. In addition to the buoyancy force term in the momentum equations, buoyancy modifications were also incorporated into both production and dissipation terms in the turbulence transport equations.

[5] *Actually this downstream distance is so small for the cases considered here that it has been ignored*

The V_z was calculated iteratively by first defining an iso-surface based on an estimated gas concentration and then determining the average of the gas concentration within that iso-surface. If the mean gas concentration was below 50% LEL then the iso-surface value was increased by a small amount. Conversely, if the gas concentration was above 50% LEL then the iso-surface value was decreased by a small amount. The average gas concentration was then recalculated and the process repeated until the mean gas cloud concentration was exactly 50% LEL. This iterative process was automated in CFX so that one iteration of the V_z calculation was performed for each iteration of the CFD calculation. Relatively few iterations of the V_z calculation were required for it to converge upon an average concentration of 50% LEL (usually less than 20). This approach had the advantage that the V_z volume could be monitored as the CFD calculation iterated towards a converged solution. Unlike the previous CFD approach discussed in Section 4, this iterative calculation method to find the V_z is not inherently conservative and should not over- or under-predict the gas cloud volume.

11.2.3 Overview of Predicted Flow Behaviour

Figure 11.3 shows the general flow pattern for the three room configurations. The figures show streamlines tracing the paths of imaginary mass-less particles in the flow, and V_z clouds for the three baseline cases involving a 0.86 g/s gas release and 12 ach ventilation rate.

In Configuration 1 the flow is dominated by the unobstructed jet flowing into the centre of the room and impinging onto the far wall. Complex flow patterns are generated from the interaction of the room ventilation flow on the periphery of the jet and the influence of the box obstruction. The V_z cloud for this case has an appearance similar to that of an unobstructed outdoor release.

In Configuration 2, the high-momentum gas release flows along the wall and impinges on the end face producing large unsteady flow recirculation in the bulk of the room. The V_z cloud again behaves in a similar manner to that observed in simulations of a gas release outdoors where the jet is located parallel to a wall (see Appendix B).

In contrast to the other two cases, in Configuration 3 the velocity reduces rapidly close to the nozzle as the jet impinges onto the end wall and spreads radially. The relatively slow moving gas is then redirected by the adjacent obstacle and sidewalls, and readily re-entrains into the jet, giving rise to locally high gas concentrations. The natural buoyancy of this gas-rich cloud generated within the cavity produces a low-momentum plume which rises towards the ceiling. The large V_z cloud for this case extends from the cavity where the jet is located, all the way to the ceiling and across the ceiling to the far corner.

Configuration 1

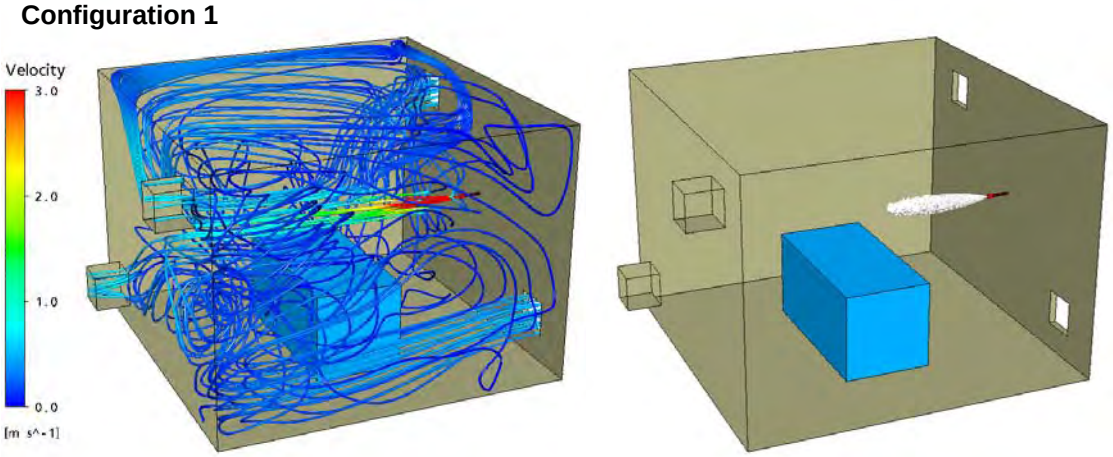

Configuration 2

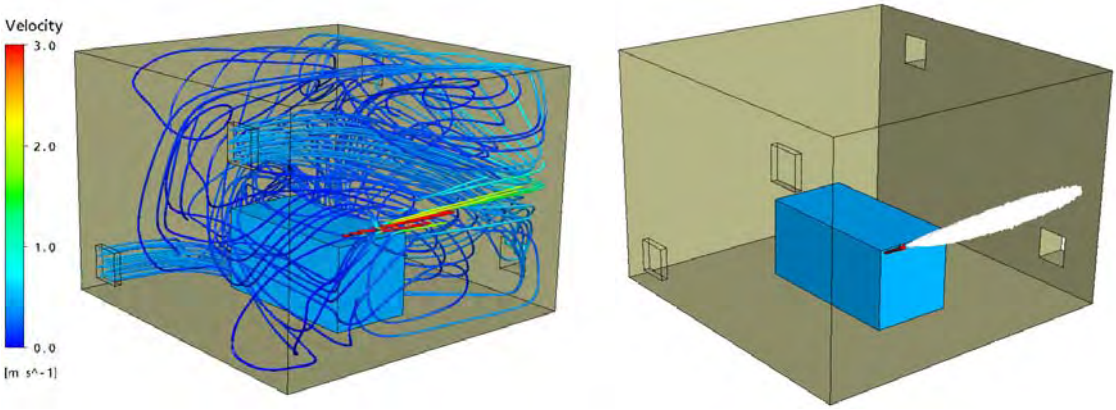

Configuration 3

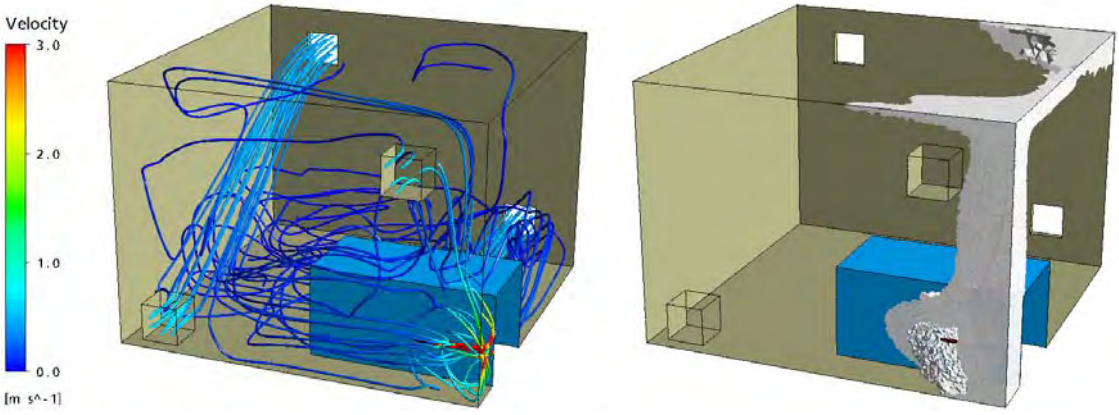

Figure 11.3 Predicted streamlines (left) and V_z cloud (right) for baseline cases (0.86 g/s gas release, 12 ach ventilation) in the three room configurations. Streamlines are coloured according to the velocity.

11.2.4 Steady and Transient CFD Simulations

In all three configurations, the predicted flow pattern in the CFD simulations was unsteady, i.e. the flow behaviour varied over time, especially in the regions of the room where the flow velocity was low. In Configuration 1, this unsteadiness led to the gas jet moving slightly up and down relative to the primary horizontal jet axis (as demonstrated in the snapshots shown in Figure 11.4). The size of the V_z cloud also changes over time, as shown in the graph in Figure 11.5. A similar degree of unsteadiness is also observed in the simulations for Configuration 2 and 3. There is reason to suspect that the flow in the test enclosure may also have been unsteady; witness the large variations in real-time gas concentration shown in Figure 10.14. In general, many flows are inherently unsteady over a relatively long time-scale. Therefore it is very likely that the CFD model is responding to a real physical effect.

The manifestation of time-dependent behaviour in these CFD simulations introduces some challenges from a practical computing standpoint. There are two different ways in which CFD simulations can be undertaken. In a "steady" approach, the flow field is initialised with some assumed values – usually zero flow velocities and zero gas concentrations everywhere – and the calculation then starts iterating. Over many successive iterations the simulated flow field evolves until it reaches a state where it no longer changes, whereupon it is said to have "converged" to a steady state. The alternative "transient" approach is usually adopted for time-dependent flows. Here the calculation iterates towards a solution at one snapshot in time. Once a converged solution has been reached for this instant in time, the time-step is incremented by a small amount and the calculation iterates to find a converged solution at this new point in time, and so on, for the duration of the simulation.

If a "steady" approach is adopted for an inherently unsteady flow, the calculation continues to iterate to find a steady-state solution but this state is never reached and the flow continues to change over successive iterations indefinitely. If the unsteadiness exhibits some periodic oscillations (such as an organised flapping motion), the steady approach cannot discern the time-period or wavelength of the motion since unlike the transient approach it does not produce a converged solution at intervals in time.

The predicted flow behaviour in Configurations 1, 2 and 3 is clearly unsteady, and therefore it might initially seem prudent to adopt a "transient" approach for the CFD simulations. However, due to the number of iterations required to reach a converged solution at each instant in time and the number of time-steps required to reach a fully-developed flow, transient simulations can be very lengthy in terms of computing time. In tests undertaken for Configuration 1, transient calculations were found to take 10 to 15 times longer than steady calculations to reach a fully-developed state. This indicated that it would not be practical to run transient simulations for all the different release scenarios, since even the steady calculations took on average 3 days to run[6]. Instead, a steady approach was used in all cases and some limited checks with transient simulations were made to ensure that the unsteadiness observed in gas cloud volumes was physically realistic. Figure 11.6 shows the results for one of these checks for Configuration 1. The calculation begins by using a steady approach and the V_z volume is shown varying over successive iterations. Once the flow has become fully-developed, the calculation is changed to run using a transient approach. Nearly the same variations in V_z magnitude are observed using the transient approach as for the previous steady method. This suggests that it is justifiable to use a "steady" calculation method for these cases.

[6] *based on calculations running on two processors of 3.8GHz Xeon desktop computer.*

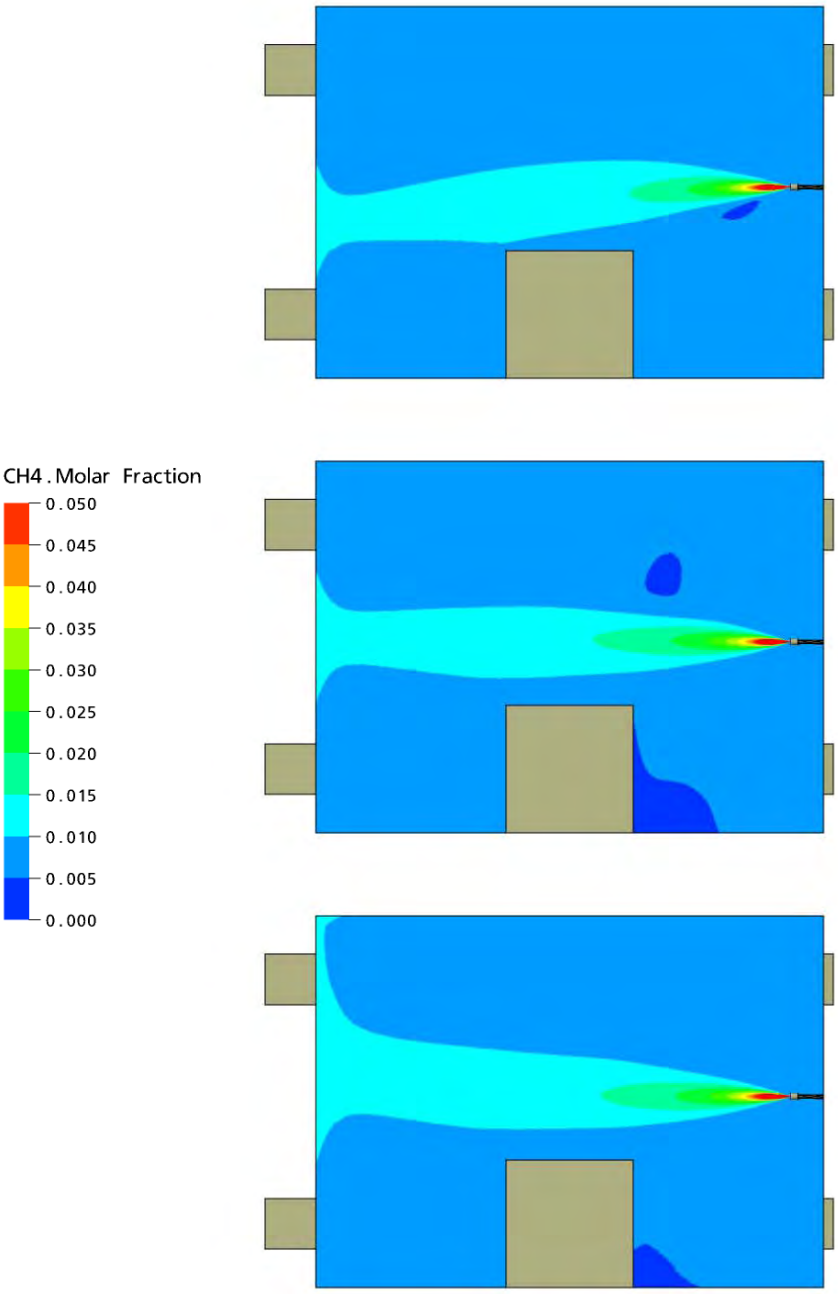

Figure 11.4 Three snapshots of the gas concentration contours on the room mid-plane taken at different stages as the CFD calculation is progressing, once the flow has reached a fully-developed state. The results shown are for Configuration 1 with a ventilation flow rate of 12 ach and release rate of 0.86 g/s.

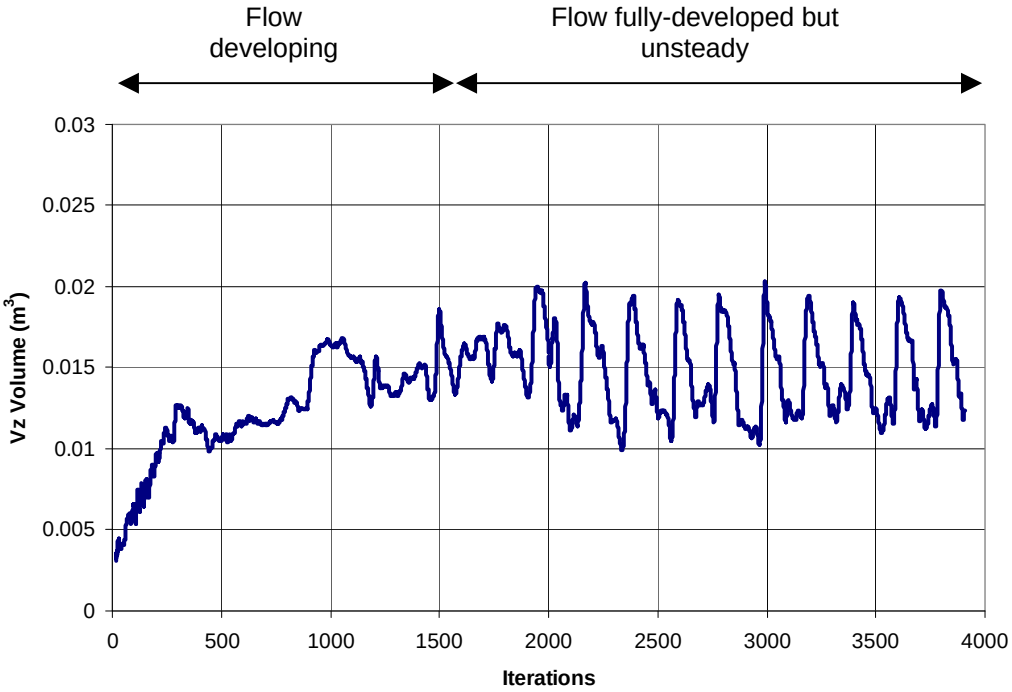

Figure 11.5 Evolution of the predicted V_z gas cloud volume using a "steady" CFD method. The result shown is for Configuration 1 with a ventilation flow rate of 12 ach and release rate of 0.86 g/s.

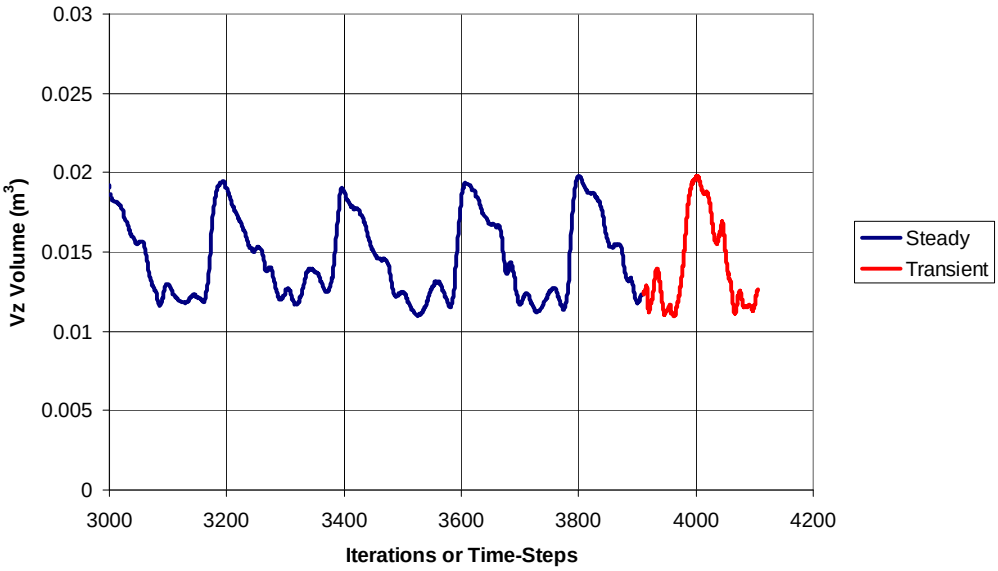

Figure 11.6 Evolution of the V_z volume using steady and transient CFD models. The transient simulation is initialised with the results from the steady model simulation. The result shown is for Configuration 1 with a ventilation flow rate of 12 ach and release rate of 0.86 g/s.

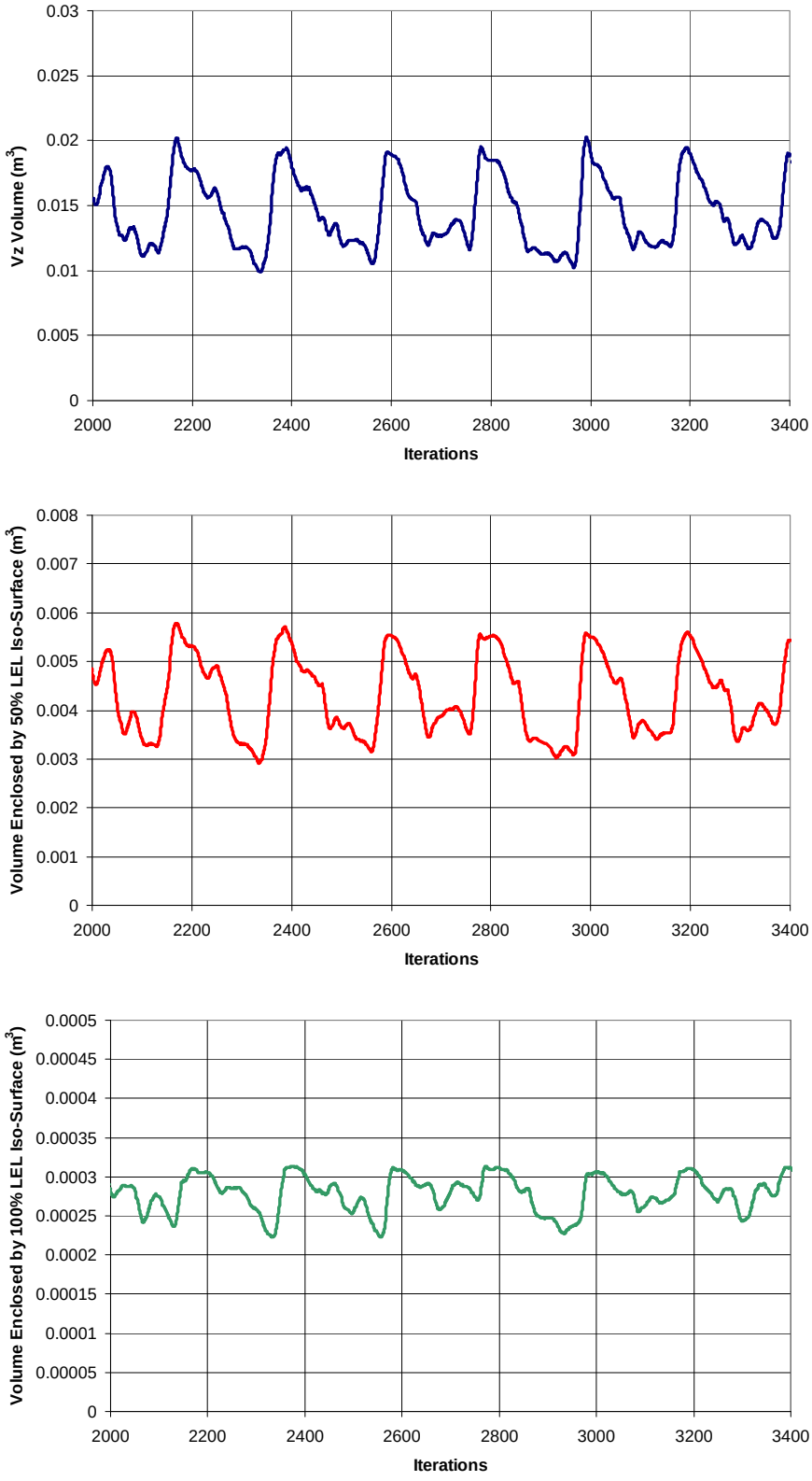

Figure 11.7 Evolution of the cloud volume defined from the V_z criterion (top), the 50 % LEL iso-surface (middle) and 100 % LEL iso-surface (bottom). The result shown is for Configuration 1 with a ventilation flow rate of 12 ach and release rate of 0.86 g/s.

The results presented in Figures 11.7 and 11.8 show the behaviour of a gas cloud using the definition for V_z, i.e. a cloud with mean concentration of 50 % LEL. In practice, this cloud is equivalent to the gas enclosed within an isosurface at a concentration of roughly 1.8 % vol/vol (although this will vary depending on the dispersion behaviour). Figure 11.7 compares the volume of V_z against that of the 50 % LEL and 100 % LEL volumes, i.e. gas volumes enclosed by iso-surfaces at 2.2 % and 4.4 % vol/vol respectively. All three volumes show some degree of unsteadiness. In terms of absolute values (in m^3), the 50 % and 100 % LEL volumes show less variation than V_z. However, in terms of percentage of the mean value (Figure 11.8), the variation in V_z and 50 % LEL volumes are roughly equivalent at around +35 % and -30 %, whilst the 100 % LEL volume shows less variation of roughly +10 % and -20 %.

Later in this Section and in Section 12 the gas cloud volume V_z is calculated for a wide range of conditions. The V_z volumes quoted are mean values which have been calculated by averaging over a number of iterations once the flow has reached a fully-developed state.

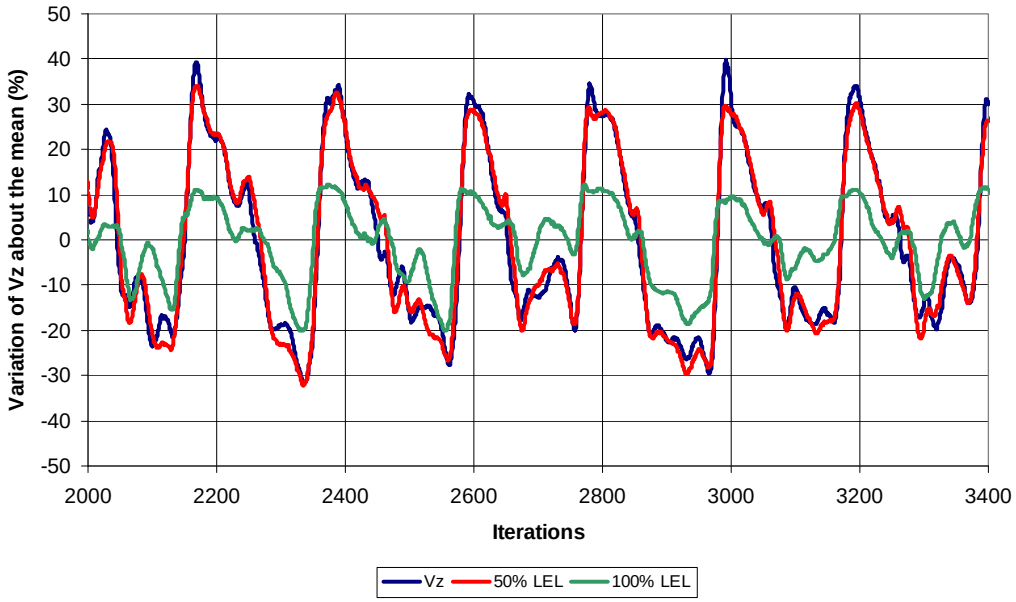

Figure 11.8 Predicted deviation from the mean V_z, 50 % LEL and 100 % LEL cloud volumes for Configuration 1 with a ventilation flow rate of 12 ach and release rate of 0.86 g/s.

11.2.5 Computational Meshes

The CFD method is based on the solution of the equations governing fluid flow behaviour at a large number of discrete points or cells throughout the room. These points are arranged using a "grid" or "mesh", and are shown on the room surfaces for Configuration 1 in Figure 11.9. In order to have confidence in the model results, the mesh must be sufficiently fine to resolve the spatial variations in flow velocity, temperature and gas concentration within the enclosure. To confirm that the grid used is sufficiently fine, it is good practice to run CFD tests using a number of different grids with an increasingly large number of cells, until further refinement of the grid leads to no appreciable difference in the results.

For each of the three configurations considered, three different grids have been tested which are referred to as 'coarse', 'medium' and 'fine'. Table 11.1 summarises the number of nodes used in each mesh. The evolution over successive iterations of the predicted V_z gas cloud volumes using the different grids is shown in Figure 11.10. For each configuration, the medium grid resolution was considered adequate. Although the results produced using these meshes may not be fully grid-independent, the choice of mesh resolution was based on balancing the increase in computing time needed for finer meshes against the possible loss in predictive accuracy from using overly coarse meshes. The magnitude of errors associated with insufficient grid resolution for the meshes adopted is considered to be small in comparison to other sources of uncertainties, such as those arising from the turbulence model or the simplification of certain geometric details in the model. Cross-sections through each of the medium meshes adopted for the three configurations are shown in Figure 11.11.

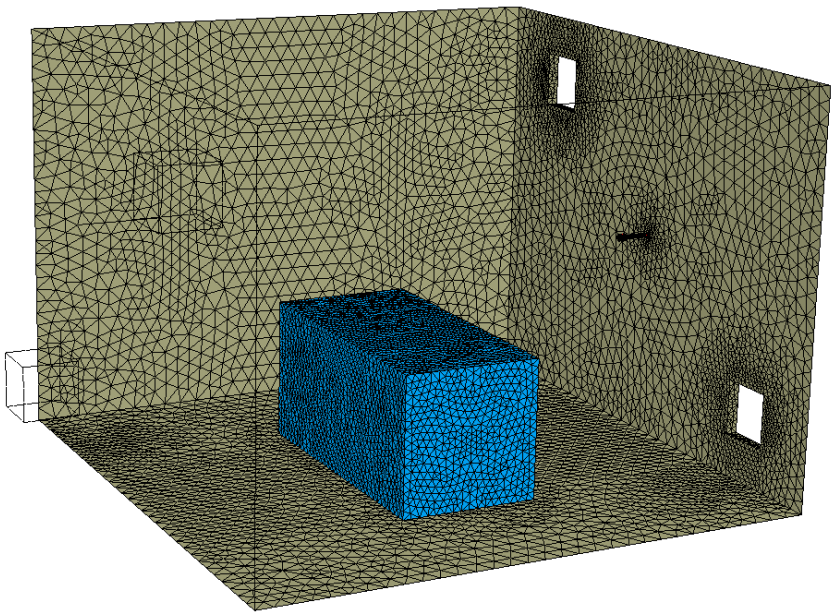

Figure 11.9 Surface mesh used in Configuration 1

Table 11.1 Number of grid nodes used in the coarse, medium and fine meshes for each room configuration

	Coarse	***Medium***	***Fine***
Configuration 1	156,000	267,000	583,000
Configuration 2	234,000	445,000	1,325,000
Configuration 3	266,000	560,000	939,000

Configuration 1

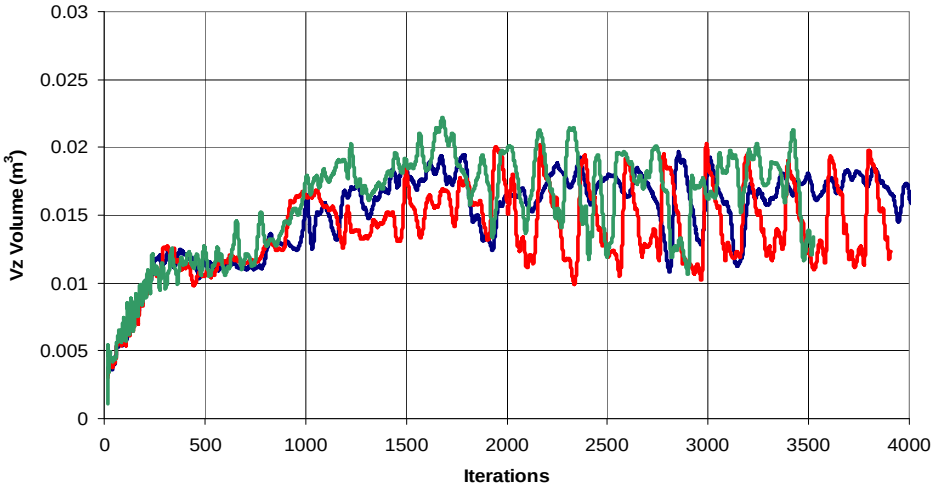

Configuration 2

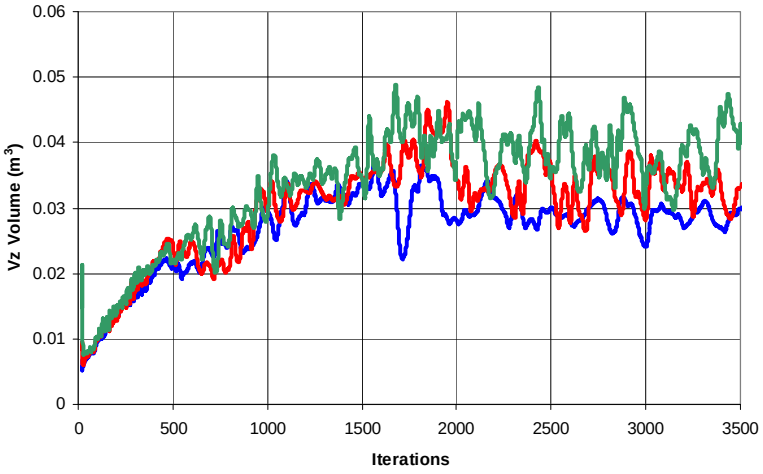

Configuration 3

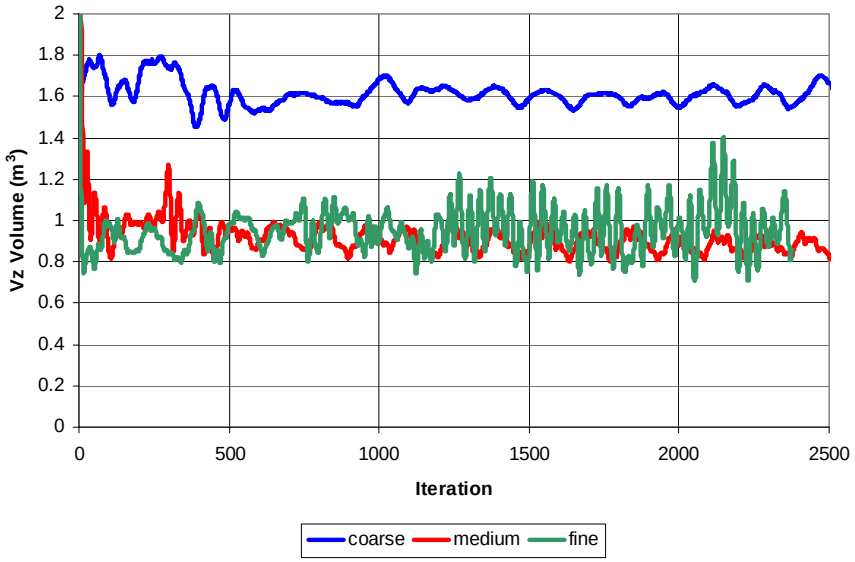

Figure 11.10 Mesh sensitivity analyses for the three configurations. The graphs show the evolution of the V_z cloud volume for three different meshes for each configuration for the baseline case of 0.86 g/s release rate and 12 ach.

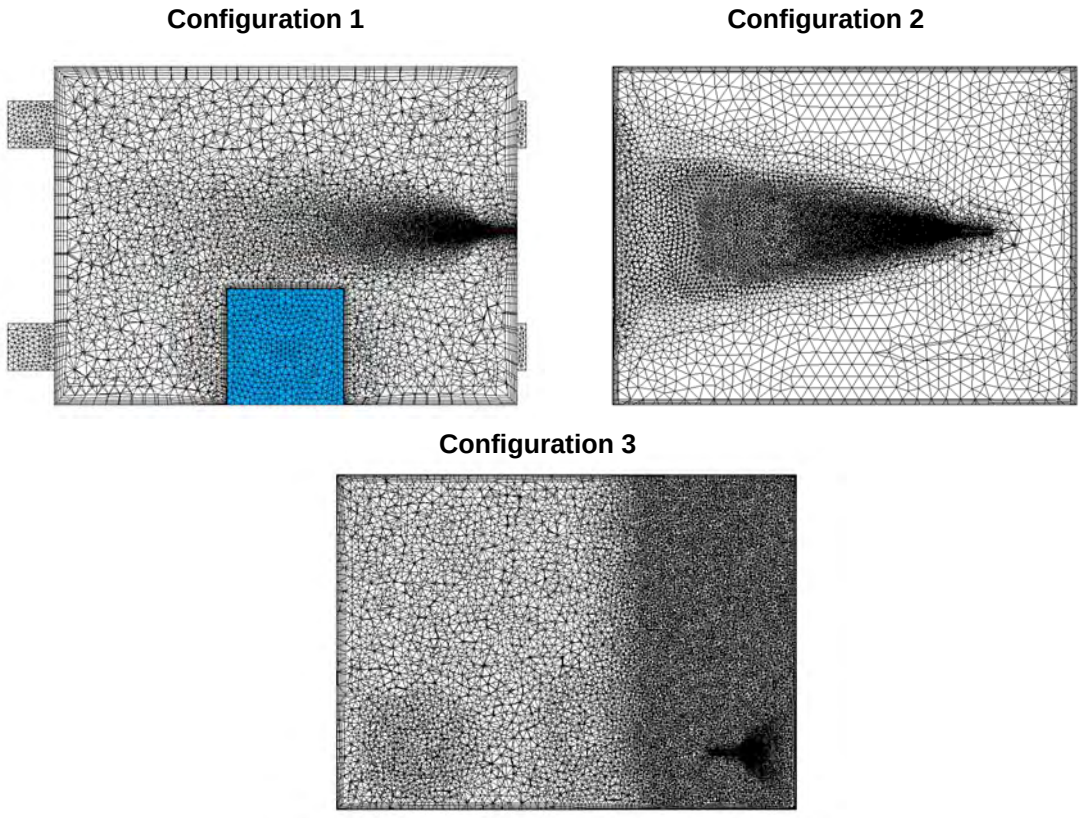

Figure 11.11 Cross-sections through the meshes on the mid-plane of the gas jet.

11.3 VALIDATION TEST RESULTS

Tables 11.2 – 11.4 summarise the validation tests undertaken for each configuration. In some of the experiments the mass release rate achieved was less than the target value modelled by CFD owing to issues with the pressure regulator and mass flow meter (for details see Appendix C). The actual mass release rate in the experimental tests is therefore also provided in the tables for comparison. In Configuration 2, test C2-5 was originally intended as a 0.47 g/s release but in the experiments a release rate of only 0.38 g/s was achieved. CFD simulations were repeated for this case using the same release rate as the experiments (0.38 g/s) to provide a direct comparison and the results for this case are denoted C2-5x.

Also provided in the tables are the room ventilation rate in air-changes-per-hour (ach), the predicted mean V_z cloud volumes obtained from the CFD model and the relevant figure number where the results are presented.

The position of the measurement probes used to sample the gas concentration in the majority of the experiments is shown in Figure 11.12. As described in Appendix C, in some tests for Configuration 1 and 2 some of the probes were moved nearer to the release source to obtain the best coverage, given the size of the release and the ventilation rate. The position of the probes in these tests will become clear in subsequent figures. Not all the measurement positions were used in all tests.

Table 11.2 Summary of validation tests for Configuration 1

Test no.	*Modelled Mass Release Rate (g/s)*	*Experimental Mass Release Rate (g/s)*	*Hole Size (mm^2)*	*Ventilation Rate (ach)*	*Predicted V_z Volume (m^3)*	*Results Shown in Figure*
C1-1	0.15	0.16	0.25	6	0.00048	11.13, 11.42
C1-2	0.22	0.24	2.5	12	0.0041	11.14, 11.43
C1-3	0.26	0.25	0.25	6	0.0015	11.15, 11.44
C1-4	0.47	0.41	0.25	2	45	11.16, 11.45
C1-5	0.47	0.42	0.25	6	0.0082	11.17, 11.46
C1-6	0.47	0.47	0.25	12	0.0039	11.18, 11.47
C1-7	0.49	0.46	2.5	12	0.0075	11.19, 11.48
C1-8	0.86	0.86	2.5	2	45	11.20, 11.49
C1-9	0.86	0.79	2.5	6	0.24	11.21, 11.50
C1-10	0.86	0.79	2.5	12	0.015	11.22, 11.51
C1-11	0.86	0.79	2.5	24	0.008	11.23, 11.52
C1-12	1.72	1.76	2.5	12	0.68	11.24, 11.53

Table 11.3 Summary of validation tests for Configuration 2

Test no.	*Modelled Mass Release Rate (g/s)*	*Experimental Mass Release Rate (g/s)*	*Hole Size (mm^2)*	*Ventilation Rate (ach)*	*Predicted V_z Volume (m^3)*	*Results Shown in Figure*
C2-3	0.26	0.28	0.25	6	0.0017	11.25, 11.54
C2-4	0.47	0.42	0.25	2	0.14	11.26, 11.55
C2-5x	0.38	0.38	0.25	6	0.0084	11.27, 11.56
C2-6	0.47	0.41	0.25	12	0.0048	11.28, 11.57
C2-7	0.49	0.51	2.5	12	0.012	11.29, 11.58
C2-8	0.86	0.93	2.5	2	33	11.30, 11.59
C2-9	0.86	0.93	2.5	6	0.38	11.31, 11.60
C2-10	0.86	0.93	2.5	12	0.033	11.32, 11.61
C2-11	1.72	1.84	2.5	12	0.57	11.33, 11.62

Table 11.4 Summary of validation tests for Configuration 3

Test no.	*Modelled Mass Release Rate (g/s)*	*Experimental Mass Release Rate (g/s)*	*Hole Size (mm^2)*	*Ventilation Rate (ach)*	*Predicted V_z Volume (m^3)*	*Results Shown in Figure*
C3-3	0.26	0.26	0.25	6	0.0017	11.34
C3-4	0.47	0.47	0.25	2	44	11.35
C3-5	0.47	0.47	0.25	6	0.17	11.36
C3-6	0.47	0.47	0.25	12	0.011	11.37
C3-7	0.49	0.49	2.5	12	0.020	11.38
C3-8	0.86	0.86	2.5	2	45	11.39
C3-9	0.86	0.86	2.5	6	34	11.40
C3-10	0.86	0.86	2.5	12	0.89	11.41

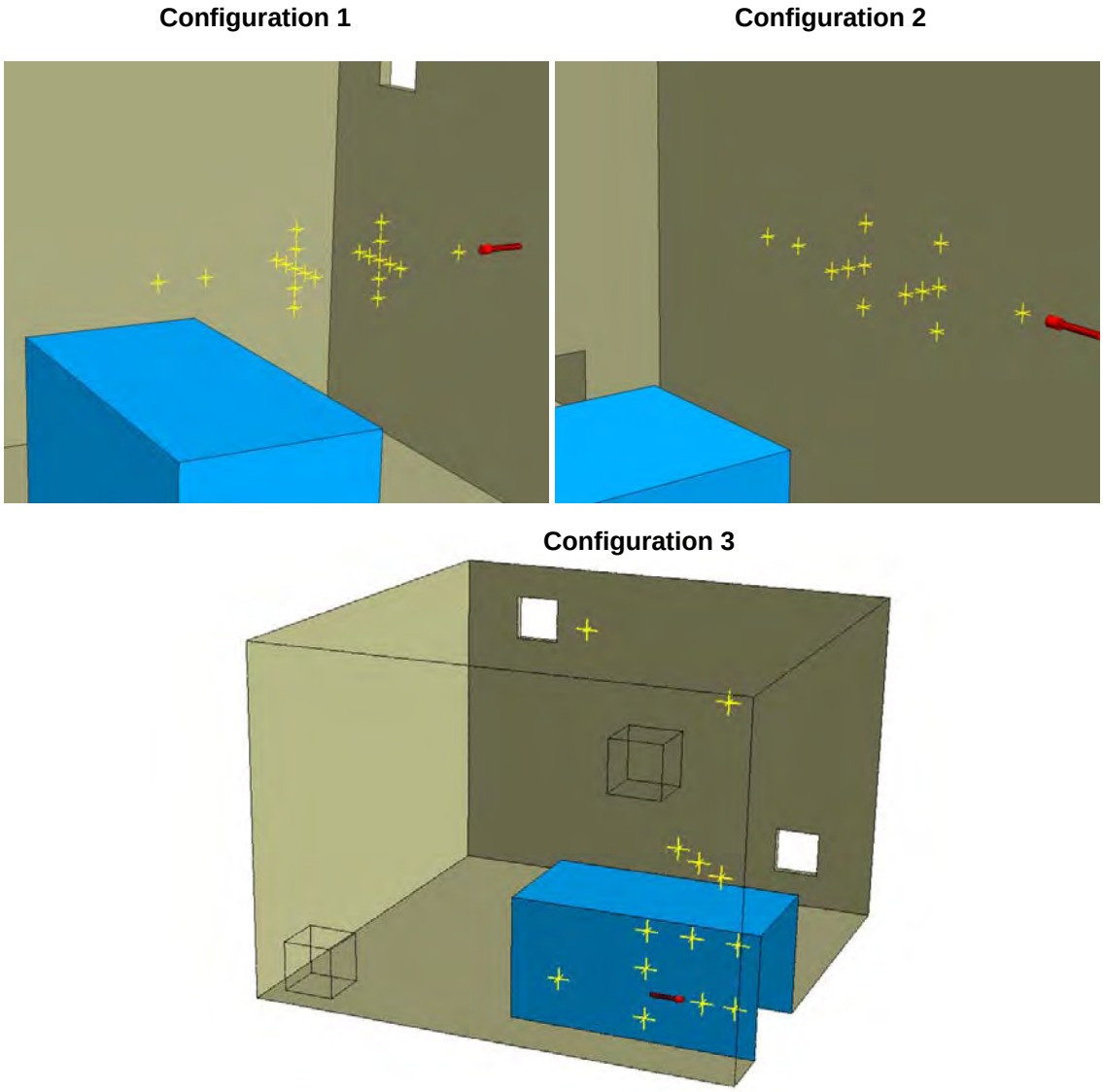

Figure 11.12 Yellow crosses marking the position of the gas measurement probes used in the majority of the validation tests.

The V_z volumes predicted by the CFD model in Configuration 1 (shown in the sixth column of Table 11.2) increases as the average gas concentration at the outlet increases. For cases C1-1, 2 , 3, 5, 6, 7, 10 and 11 the ventilation is sufficient to maintain average gas concentrations at the outlet below 20% LEL. For these cases, the V_z's obtained from the CFD model are less than 6 times that predicted by the free-jet model GaJet, which simulates outdoor unobstructed releases. For the lower ventilation cases, where the average gas concentration at the outlet is higher, the CFD V_z increases significantly and exceeds that predicted by the GaJet model. In the 2 ach cases C1-4 and C1-8, the CFD model predicts the V_z to fill the entire enclosure (V_z = 45 m^3) but the equivalent free-jet GaJet model predicts the V_z to be less than 0.01 m^3.

Comparisons of CFD results versus experimental measurements are presented as coloured contours of gas concentration in Figures 11.13 – 11.41. In each of these plots, black dots mark the location of the experimental measurements. Around each black dot is a circular fringe, the colour of which denotes the gas concentration measured experimentally. The coloured contours in the background are the CFD results, taken from one snapshot once the simulations have reached a fully-developed state. Adjacent to each black dot in the plots are given the gas

concentrations in terms of percentage gas by volume for both the experimental and mean CFD values. The CFD numerical value of concentration is a time-averaged mean value since this provides the appropriate basis for comparison against the measurements, which were also time-averaged. There are a large number of plots and to help navigate through them they have generally been ordered by increasing leak rate and ventilation rate (figure numbers are also summarised in Tables 11.2 – 11.4).

Overall, the plots show that good agreement is obtained between the experimental measurements and the CFD predictions. In some cases the coloured fringes representing the measurement values are indistinguishable from the background CFD contours indicating that the results are in very good agreement with the measurements. The good agreement is particularly encouraging in Configuration 3 (Figures 11.34 – 11.41) which represents the most challenging scenario for the CFD model.

However, there are some notable discrepancies. In Configuration 2, the CFD results for a 0.47 g/s release with a ventilation rate of 2 ach consistently overpredict the measured values (Figure 11.26). The maximum difference occurs on the centreline of the jet at a position 0.65 m downstream from the nozzle, where the predicted gas concentration was 4.0 % vol/vol and the measured value 2.9 % vol/vol. This error may be partly due to the mass release rate in the experiments being only 0.42 g/s, instead of the target value of 0.47 g/s (see Table 11.3). However, another test in Configuration 2 with a release rate of 0.47 g/s and ventilation rate of 12 ach suffered from similarly low mass release rate in the experiments but the CFD results are in reasonable agreement in that case. Another possible source of the error could have been from increased leakage between the steel measurement probes and plastic flexible sampling lines used in the experiments for this case. It was the only Configuration 2 case to use probes with a 25 cm spacing, which required some of the sampling lines to be reconfigured. However, the probes at the 0.65 m position were not moved between this and the other Configuration 2 cases, so this does not appear to explain fully the discrepancy.

The point comparisons shown in Figures 11.13-11.41 are a stringent test for a model, especially at the edge of a jet or plume where concentration gradients are large. This may explain, in part, some of the behaviour which leads to greater discrepancies between measured and experimental values off the axis of the jet in Configuration 2 (e.g. Figures 11.24, 11.26 and 11.31) and is also relevant for Configuration 3, where the CFD concentration is very different from the experimental value behind and above the nozzle (e.g. Figures 11.34, 11.36, 11.37 and 11.41).

Further comparisons of CFD results versus experimental measurements are presented in Figures 11.42 – 11.61, which show the decay of gas concentration with distance along the centreline of the jet for Configurations 1 and 2. The red lines are instantaneous values of the CFD results[7] and the symbols the experimental data points.

In the vast majority of cases for Configuration 1 (Figures 11.42 – 11.53), the differences between measured and predicted concentration on the jet axis is consistent with the difference between the target (simulated) mass release rate and actual release rate achieved in the experiments (see Table 11.2).

Overall, Figures 11.42 – 11.61 show that good agreement is obtained between the CFD and experimental measurements in terms of point gas concentrations on the jet axis. Excluding a few

[7] *Along the axis of the jet up to 2 metres from the source, the gas concentration does not vary significantly and the "instantaneous" or snapshot values of gas concentration are very similar to the mean gas concentrations. Most of the fluctuations observed in the CFD results are on the periphery of the gas jets.*

particular cases discussed above, in the vast majority of tests the model predicts the gas concentration to within 0.5 % vol/vol and in many cases to within 0.2 % vol/vol.

To help explore what this comparison between predictions and measurements signifies in terms of the ultimate quantity of interest in this work, namely the V_z, it is helpful to compare two different CFD calculations, where the predicted V_z in each case is known. By examining two CFD runs which show a similar difference to each other to that between the typical CFD predictions and experiments it is possible to infer what the likely difference may be between typical CFD and experimental V_z volumes, and hence draw some conclusions about the accuracy with which the CFD model predicts the V_z. Figure 11.63 compares the CFD results for the 0.38 g/s release against the 0.47 g/s release for Configuration 2 using the same presentation format as used previously for the comparisons of CFD versus experiments. Both of the tests involved a ventilation rate of 6 ach. A plot of the gas concentration along the axis of the jet for these two cases is also provided in Figure 11.64. The level of agreement between these two sets of results appears to be roughly typical of the general level of agreement between the CFD results and experimental data. The predicted mean V_z volumes for these two cases were 8.4 litres and 11.3 litres for the 0.38 and 0.47 g/s release respectively, a difference of around 30 %. While at first this figure may seem high, it needs to be assessed in context. Due to the unsteady nature of the flow, the size of the V_z changes over time. In the 0.47 g/s case, the V_z varied by up to 20 % above and below the mean value of 11.3 litres. The size of the V_z cloud volume is also sensitive to the release rate and ventilation rate, and the orientation of the jet or its position in the room. For the 0.47 g/s release with a ventilation rate of 6 ach, the V_z volume produced in Configuration 3 was 21 times that produced by Configuration 1. Compared to this difference of more than one order of magnitude, a difference in the V_z predictions of around 30 % is relatively small.

11.4 CONCLUSIONS

The validation study presented in this Appendix was undertaken to establish whether or not CFD models are capable of modelling gas releases in enclosures to an acceptable degree of accuracy such that the results can be used as an input to an area classification methodology. CFD predictions were compared against measured gas concentration data for 29 separate cases, involving 3 different room geometries and a range of different leak rates and ventilation rates. With a few exceptions, the majority of the CFD predictions were within 0.5 % gas concentration by volume of the measured values, and in many cases within 0.2 % vol/vol. By comparing two different CFD simulations, it appears that differences between the CFD model predictions and the measurements typically will give rise to a difference in the V_z volume of around 30 %. Although an over- or under-prediction of the V_z volume by 30 % may appear at first somewhat large, it is relatively small in comparison to the differences of more than one order-of-magnitude that can be produced for the same leak rate and ventilation rate with differing leak and obstacle locations in the enclosure. The overall conclusion is that CFD models can provide reasonably good predictions of the gas cloud volume resulting from a leak in a ventilated enclosure.

The validation exercise has considered only isothermal conditions where there are no heat sources in the enclosure. The level of agreement between CFD and experiments could potentially be different for thermally-induced ventilation flows.

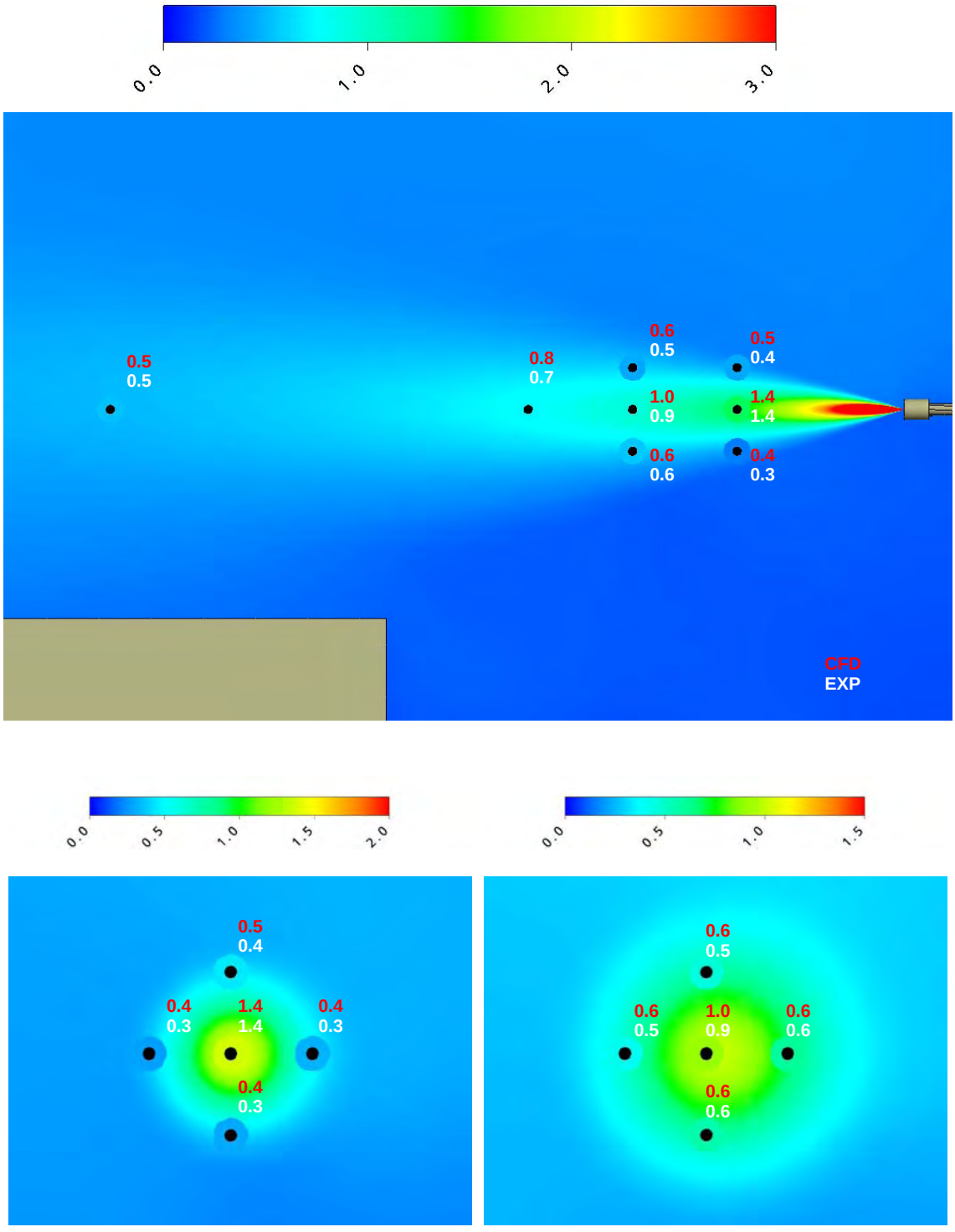

Figure 11.13 Methane concentrations in % vol/vol for case C1-1: Configuration 1 with a leak rate of 0.15 g/s and a ventilation rate of 6 ach

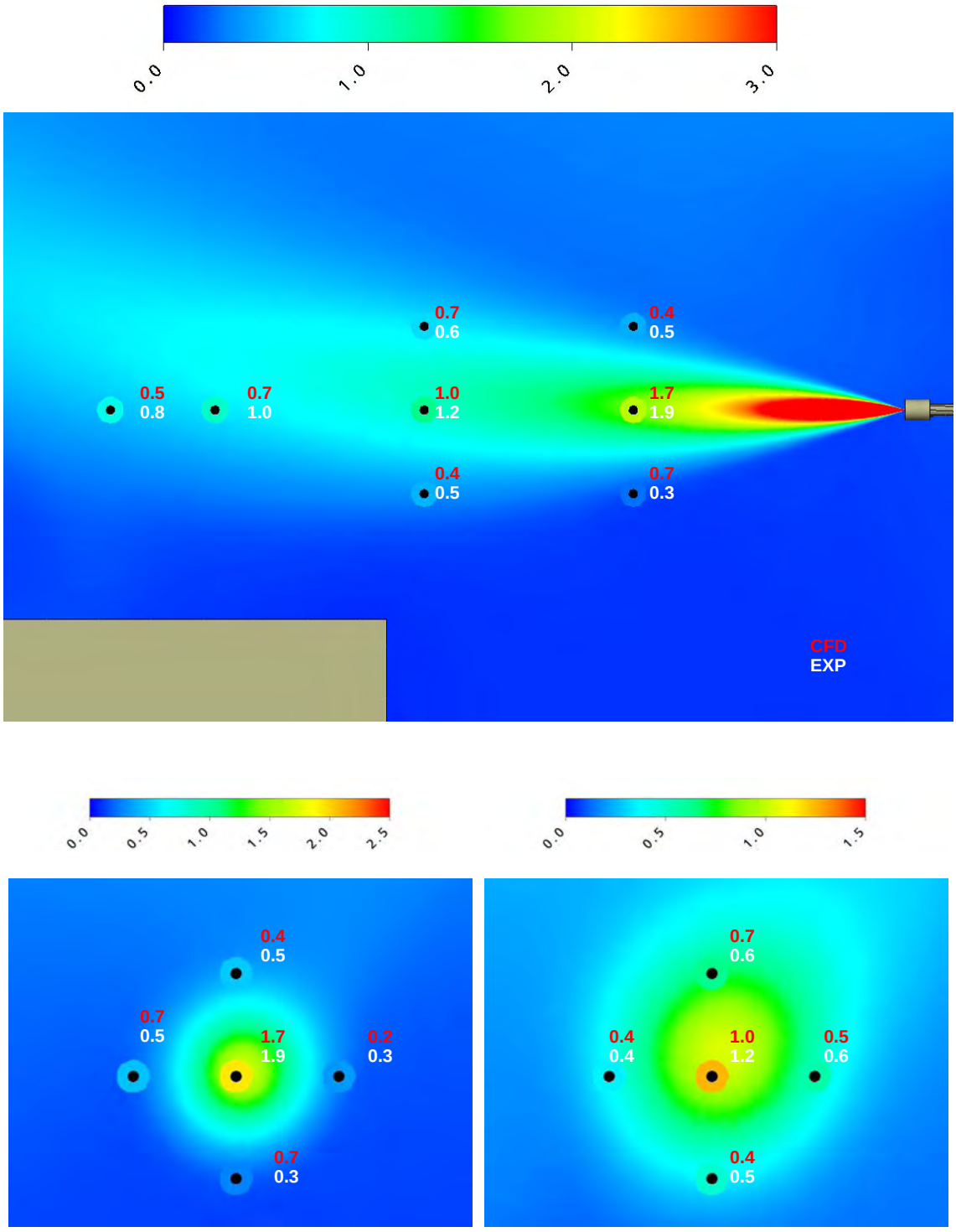

0.65 m from nozzle

1.15 m from nozzle

Figure 11.14 Methane concentrations in % vol/vol for case C1-2: Configuration 1 with a leak rate of 0.22 g/s and a ventilation rate of 12 ach.

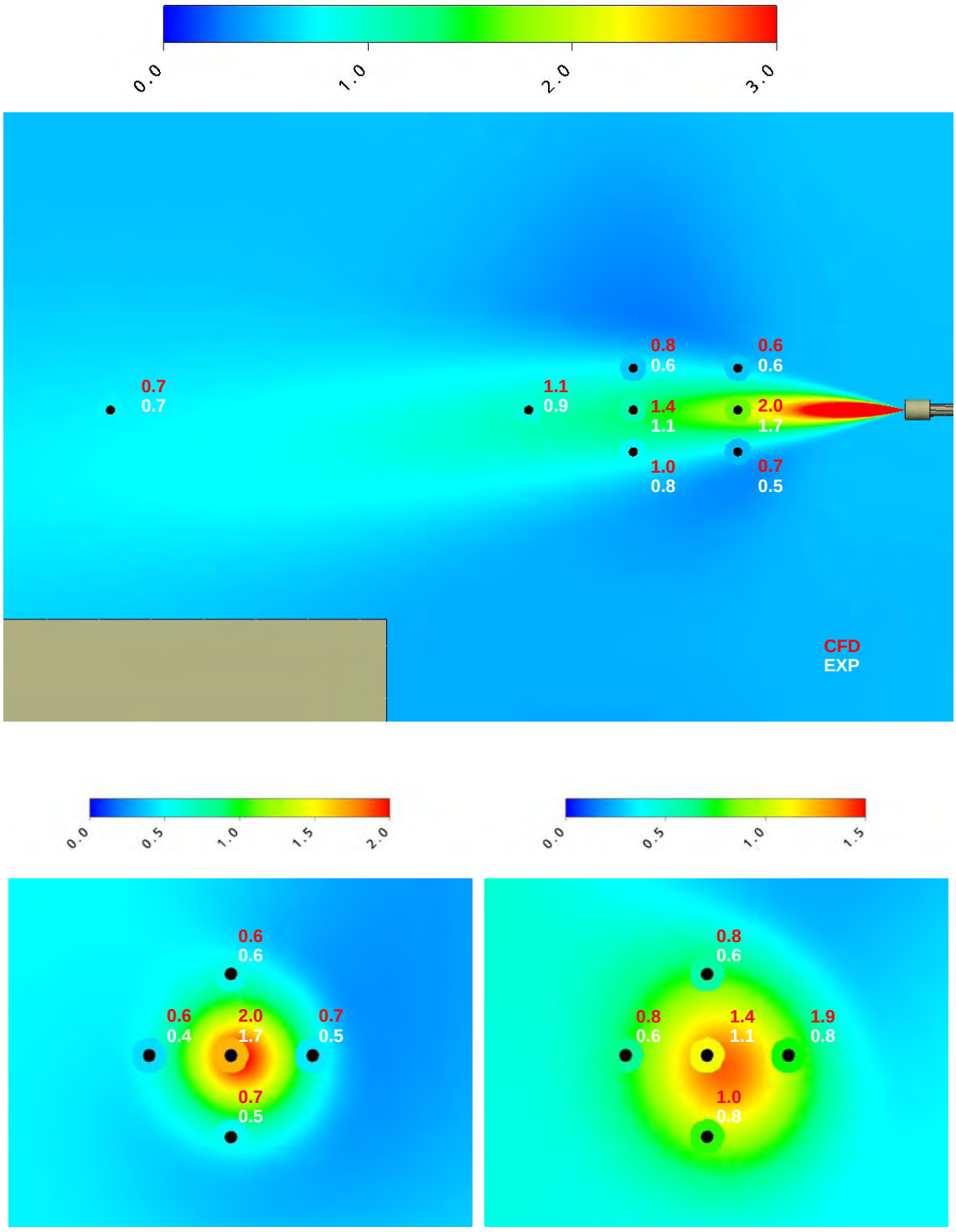

0.40 m from nozzle

0.65 m from nozzle

Figure 11.15 Methane concentrations in % vol/vol for case C1-3: Configuration 1 with a leak rate of 0.26 g/s and a ventilation rate of 6 ach.

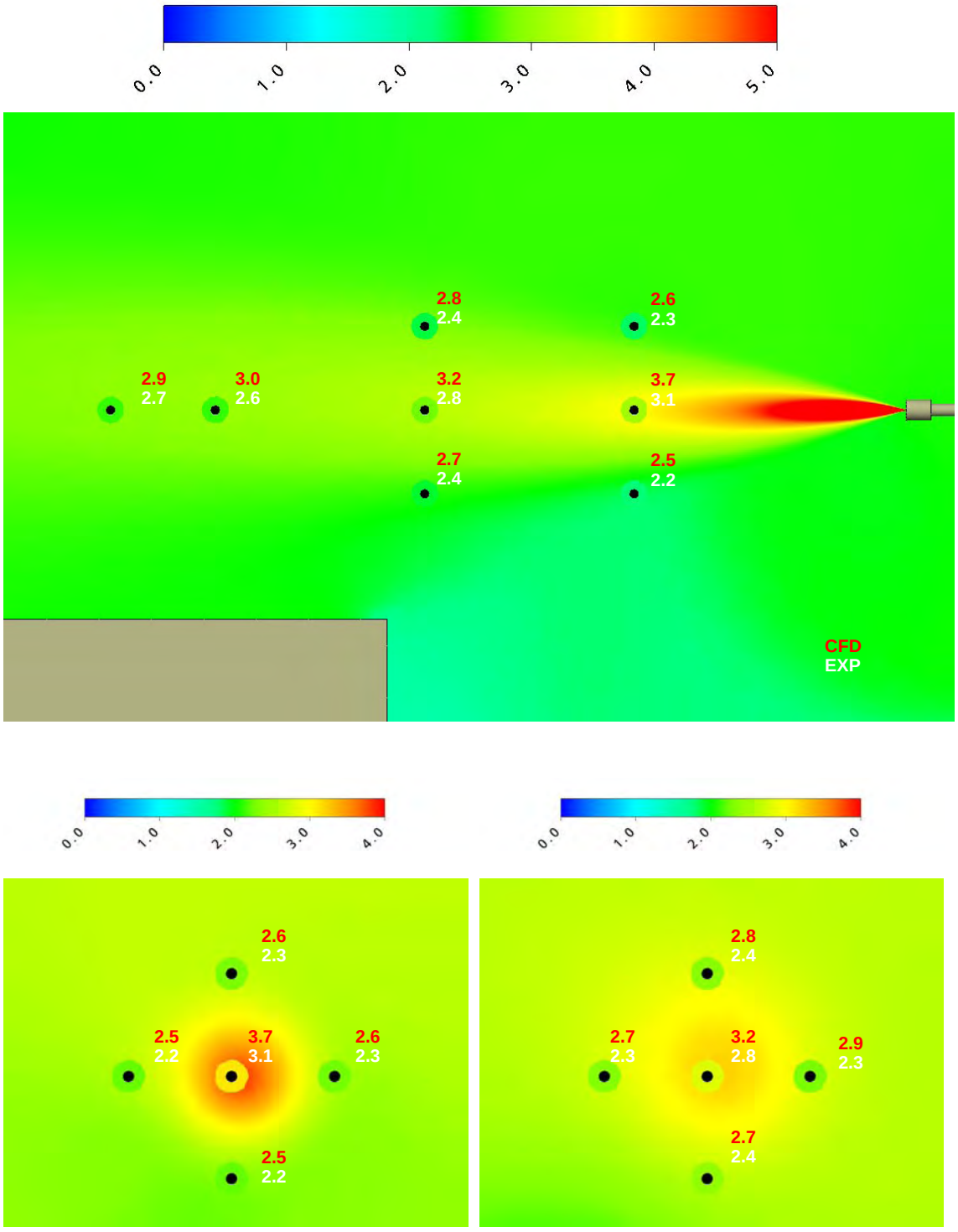

0.65 m from nozzle

1.15 m from nozzle

Figure 11.16 Methane concentrations in % vol/vol for case C1-4: Configuration 1 with a leak rate of 0.47 g/s and a ventilation rate of 2 ach.

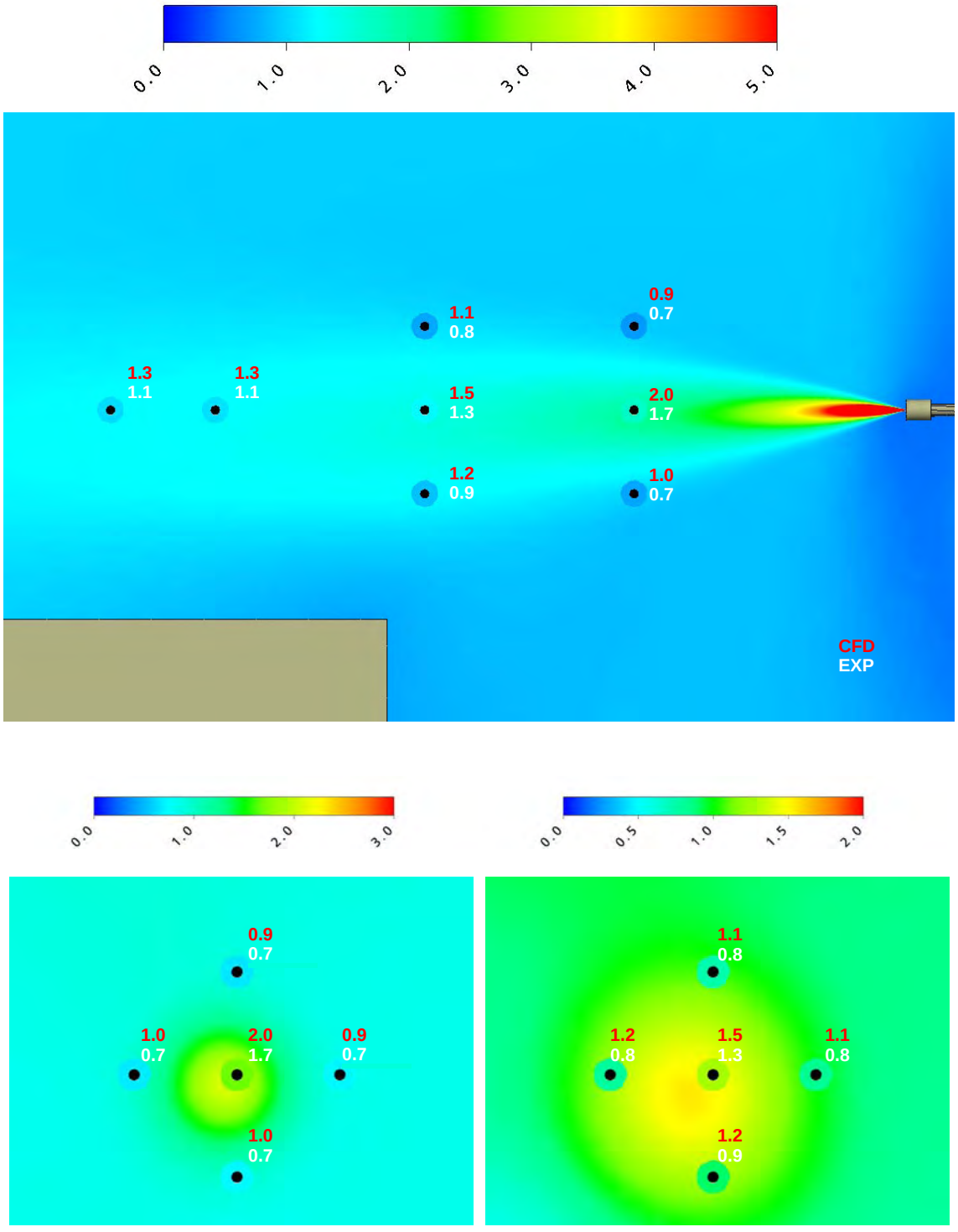

0.65 m from nozzle

1.15 m from nozzle

Figure 11.17 Methane concentrations in % vol/vol for case C1-5: Configuration 1 with a leak rate of 0.47 g/s and a ventilation rate of 6 ach.

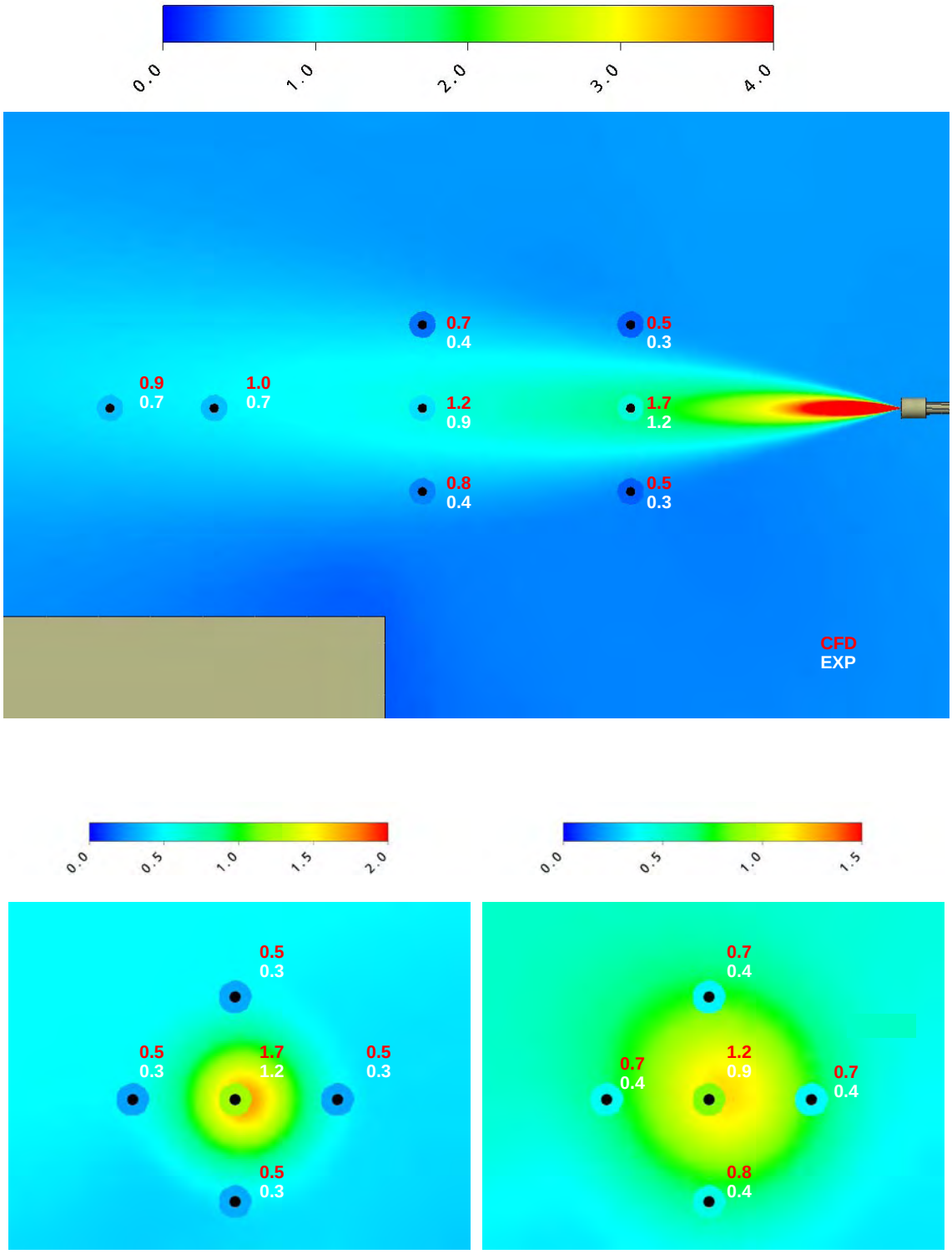

0.65 m from nozzle

1.15 m from nozzle

Figure 11.18 Methane concentrations in % vol/vol for case C1-6: Configuration 1 with a leak rate of 0.47 g/s and a ventilation rate of 12 ach.

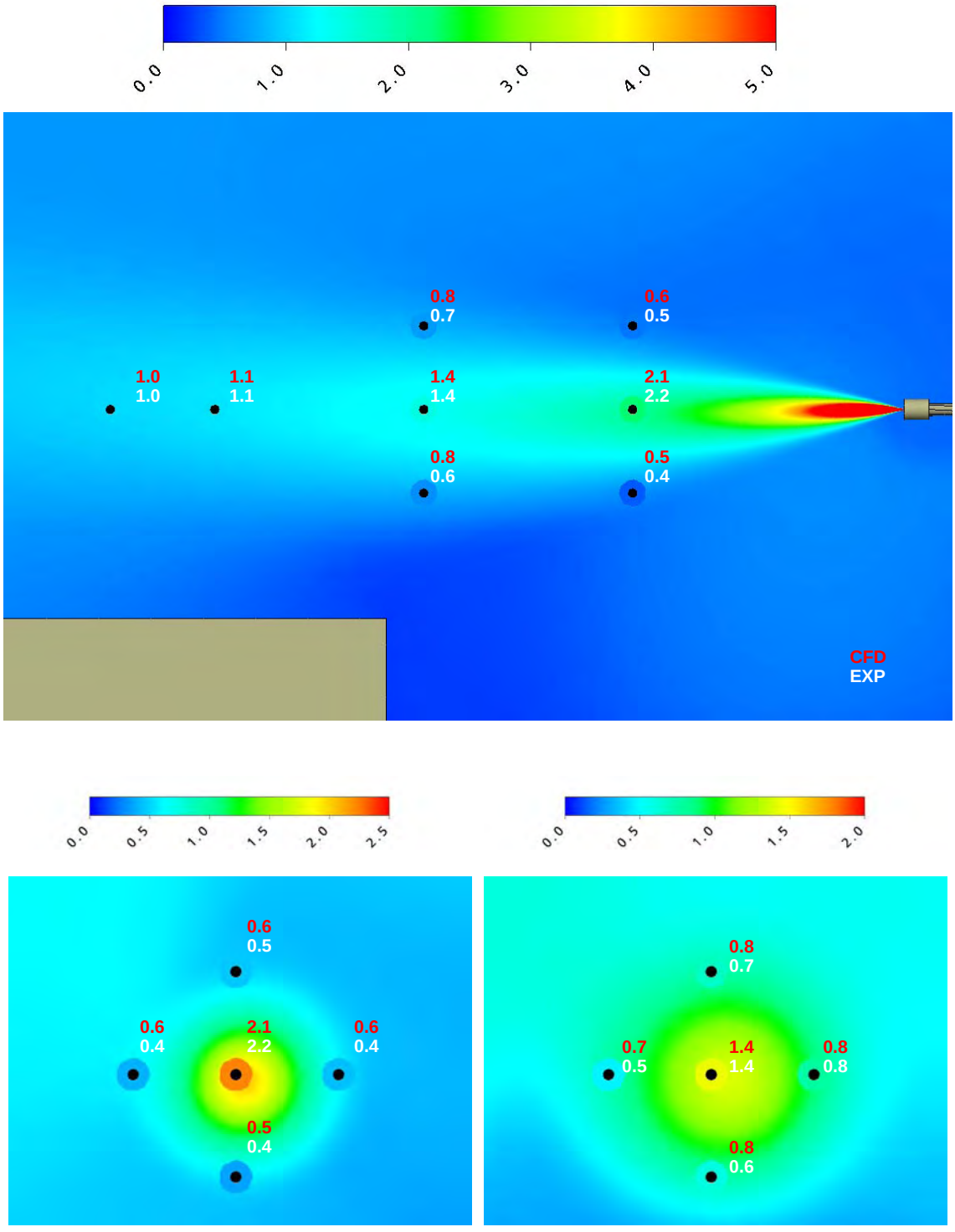

0.65 m from nozzle

1.15 m from nozzle

Figure 11.19 Methane concentrations in % vol/vol for case C1-7: Configuration 1 with a leak rate of 0.49 g/s and a ventilation rate of 12 ach.

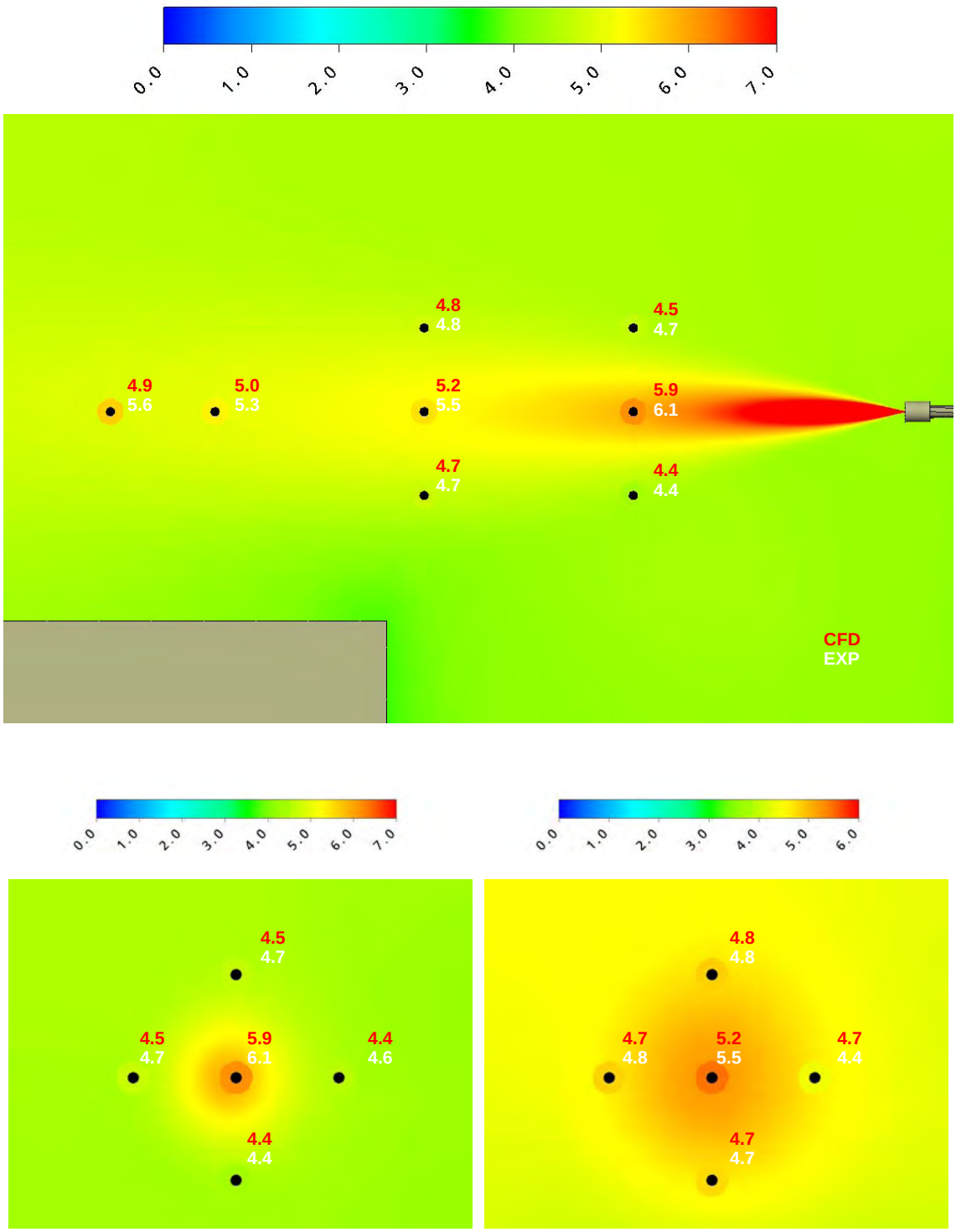

0.65 m from nozzle 1.15 m from nozzle

Figure 11.20 Methane concentrations in % vol/vol for case C1-8: Configuration 1 with a leak rate of 0.86 g/s and a ventilation rate of 2 ach.

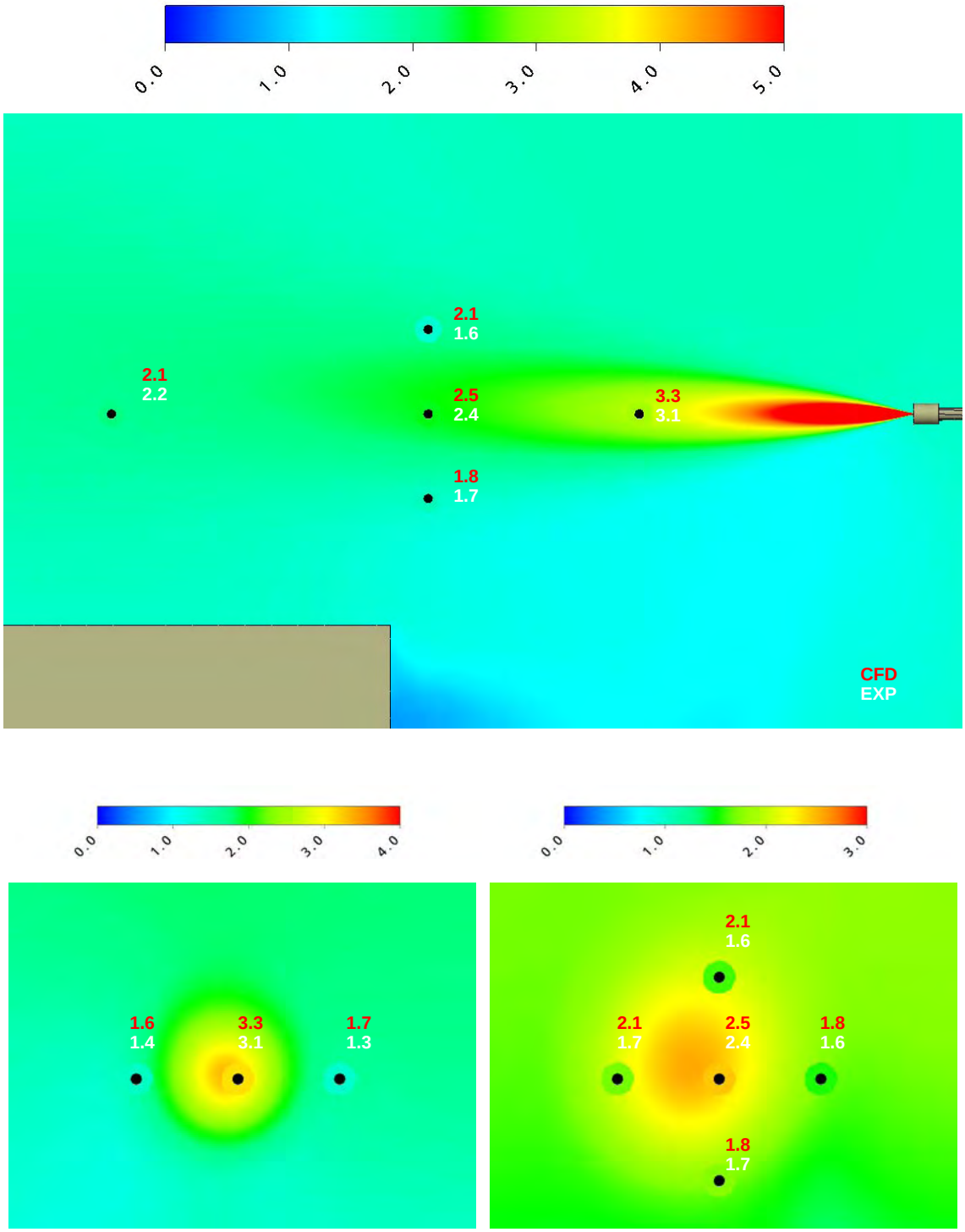

0.65 m from nozzle

1.15 m from nozzle

Figure 11.21 Methane concentrations in % vol/vol for case C1-9: Configuration 1 with a leak rate of 0.86 g/s and a ventilation rate of 6 ach.

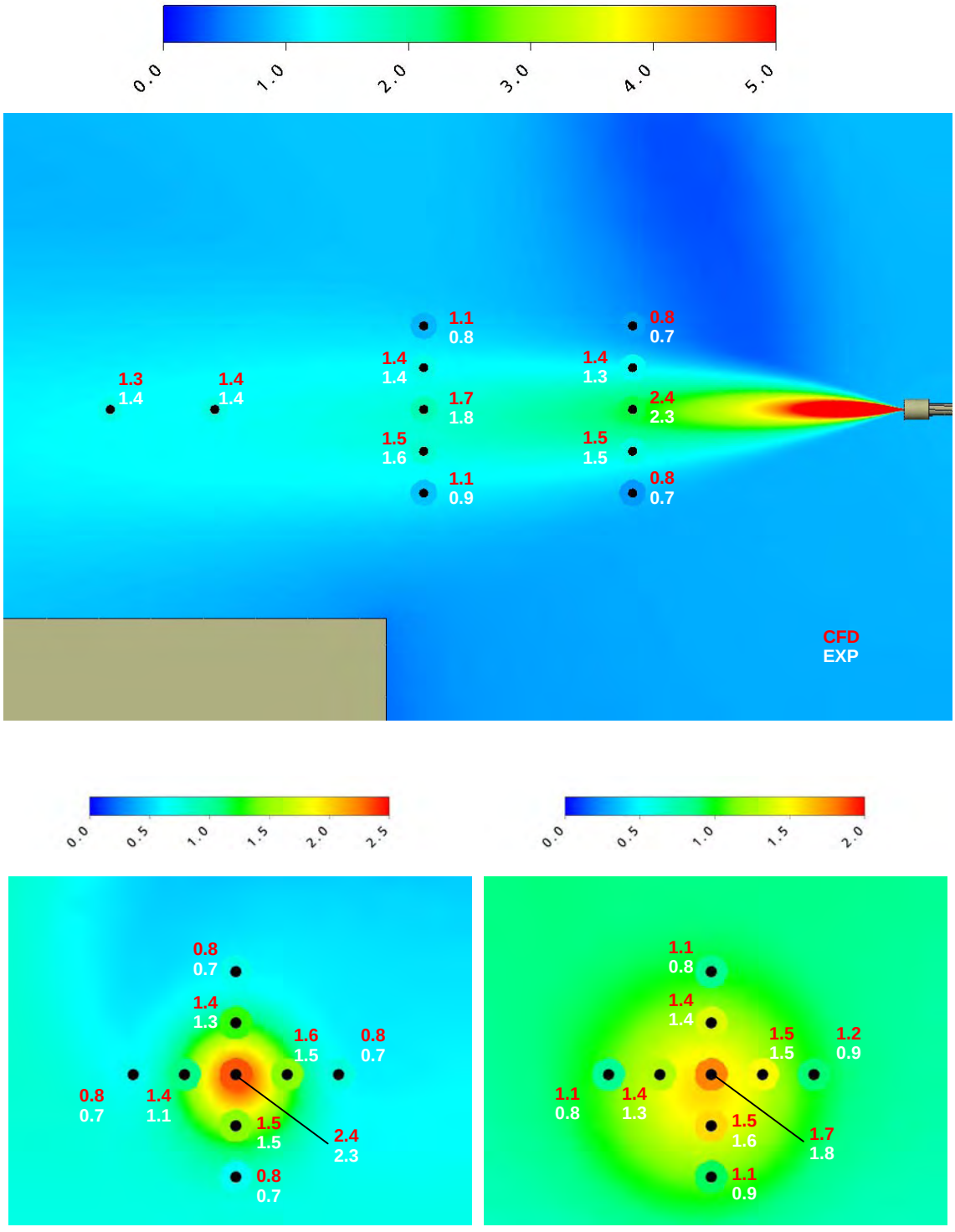

0.65 m from nozzle

1.15 m from nozzle

Figure 11.22 Methane concentrations in % vol/vol for case C1-10: Configuration 1 with a leak rate of 0.86 g/s and a ventilation rate of 12 ach.

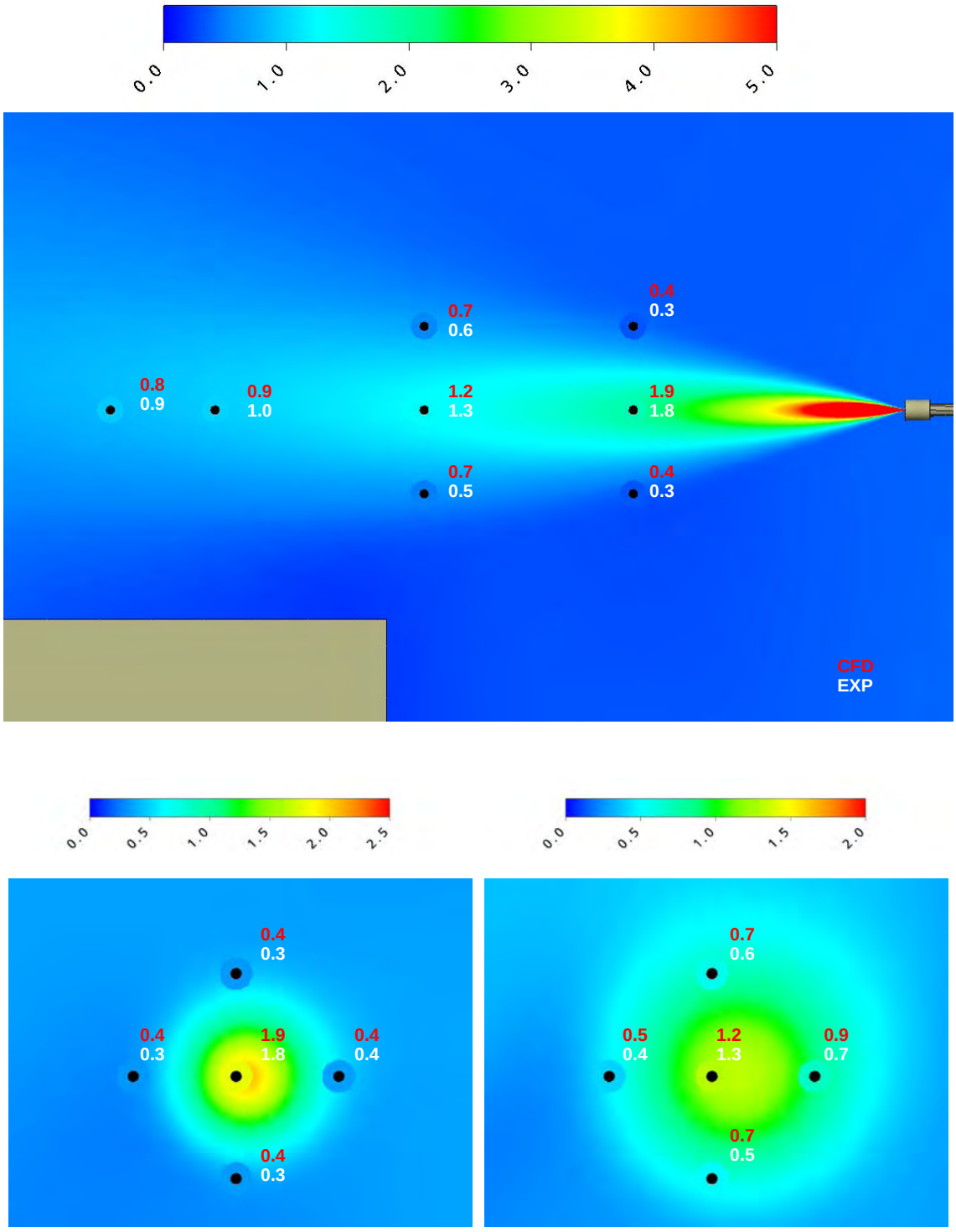

0.65 m from nozzle

1.15 m from nozzle

Figure 11.23 Methane concentrations in % vol/vol for case C1-11: Configuration 1 with a leak rate of 0.86 g/s and a ventilation rate of 24 ach.

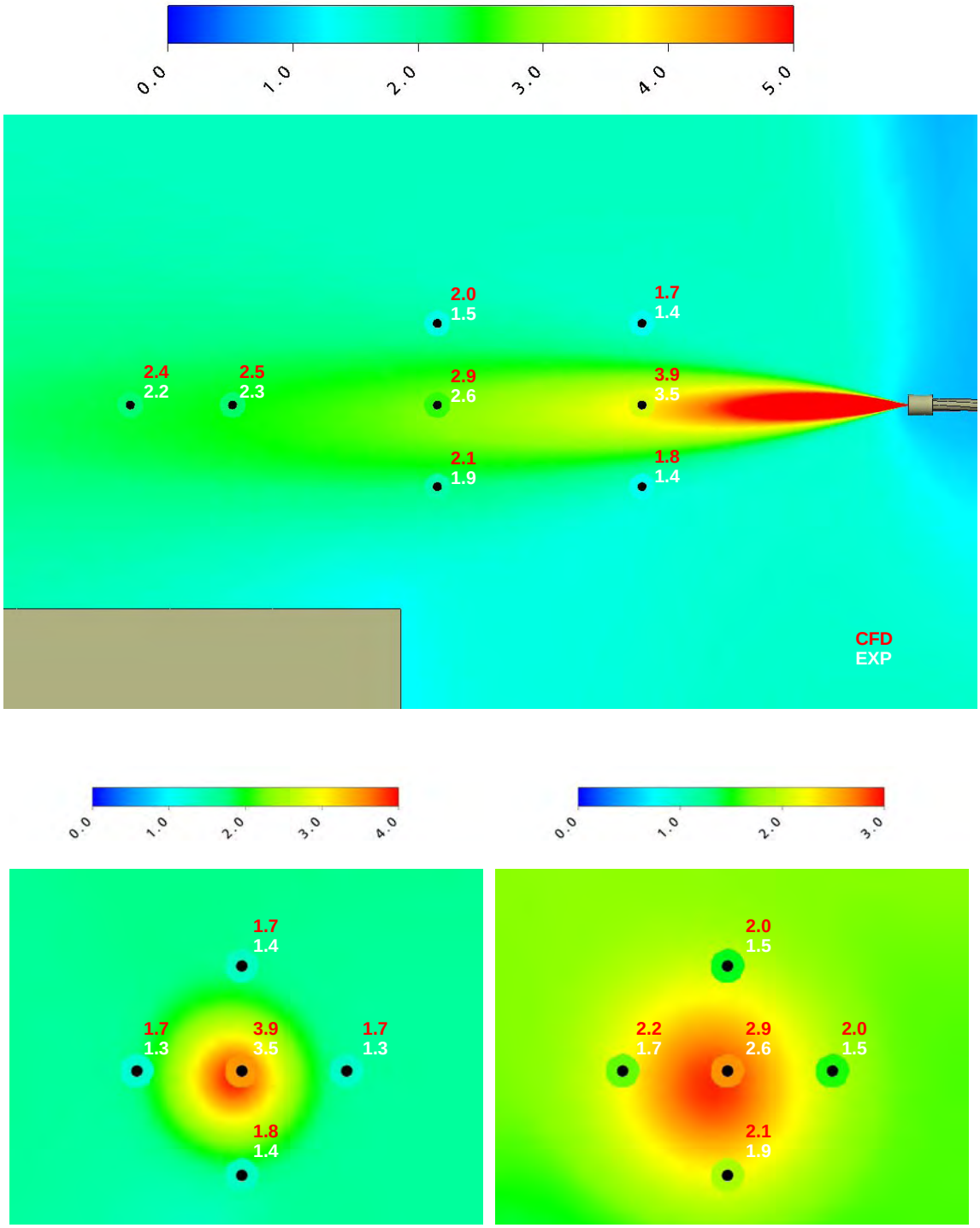

0.65 m from nozzle

1.15 m from nozzle

Figure 11.24 Methane concentrations in % vol/vol for case C1-12: Configuration 1 with a leak rate of 1.72 g/s and a ventilation rate of 12 ach.

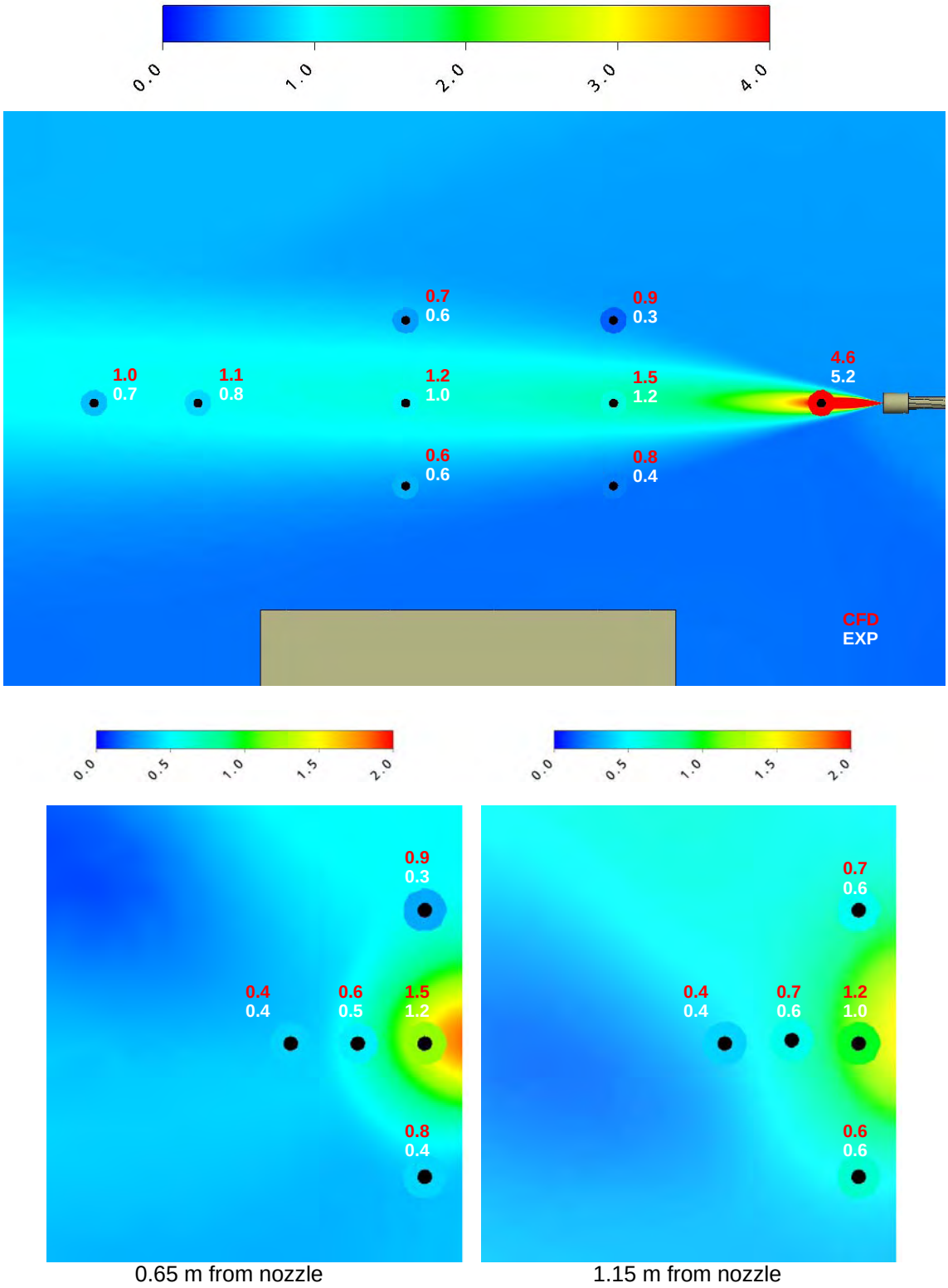

0.65 m from nozzle

1.15 m from nozzle

Figure 11.25 Methane concentrations in % vol/vol for case C2-3: Configuration 2 with a leak rate of 0.26 g/s and a ventilation rate of 6 ach.

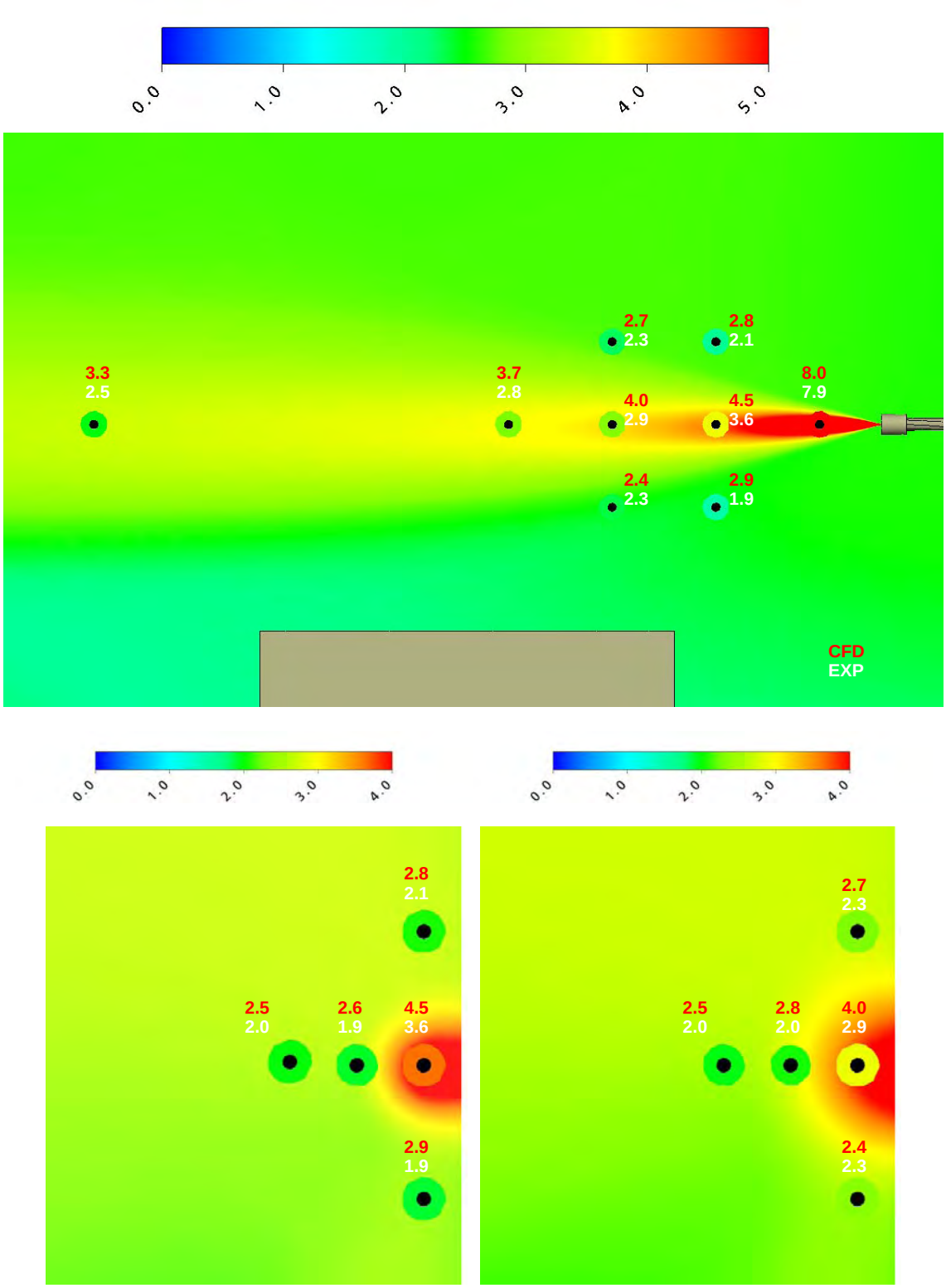

0.40 m from nozzle 0.65 m from nozzle

Figure 11.26 Methane concentrations in % vol/vol for case C2-4: Configuration 2 with a leak rate of 0.47 g/s and a ventilation rate of 2 ach.

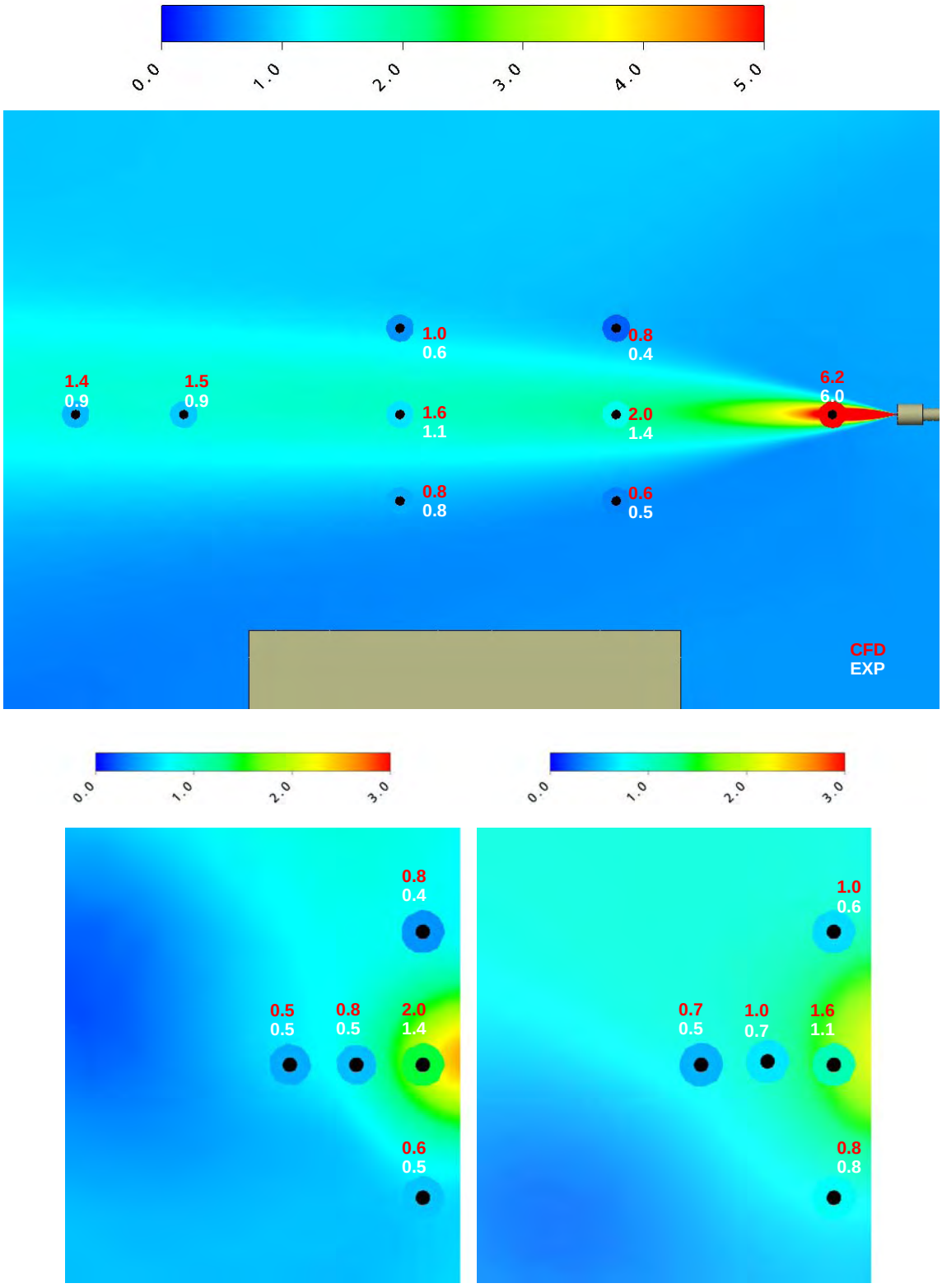

0.65 m from nozzle

1.15 m from nozzle

Figure 11.27 Methane concentrations in % vol/vol for case C2-5x: Configuration 2 with a leak rate of 0.38 g/s and a ventilation rate of 6 ach.

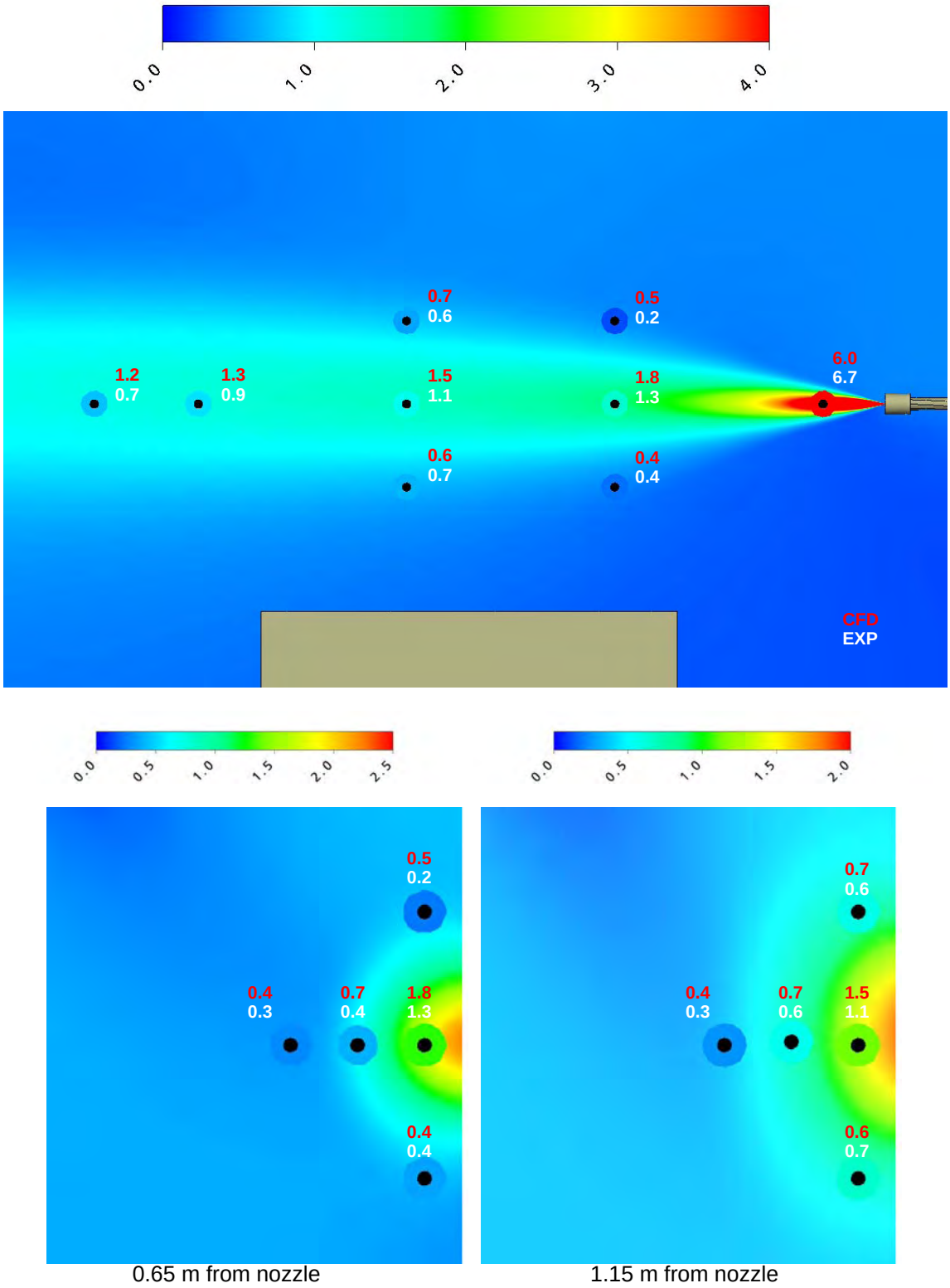

0.65 m from nozzle

1.15 m from nozzle

Figure 11.28 Methane concentrations in % vol/vol for case C2-6: Configuration 2 with a leak rate of 0.47 g/s and a ventilation rate of 12 ach.

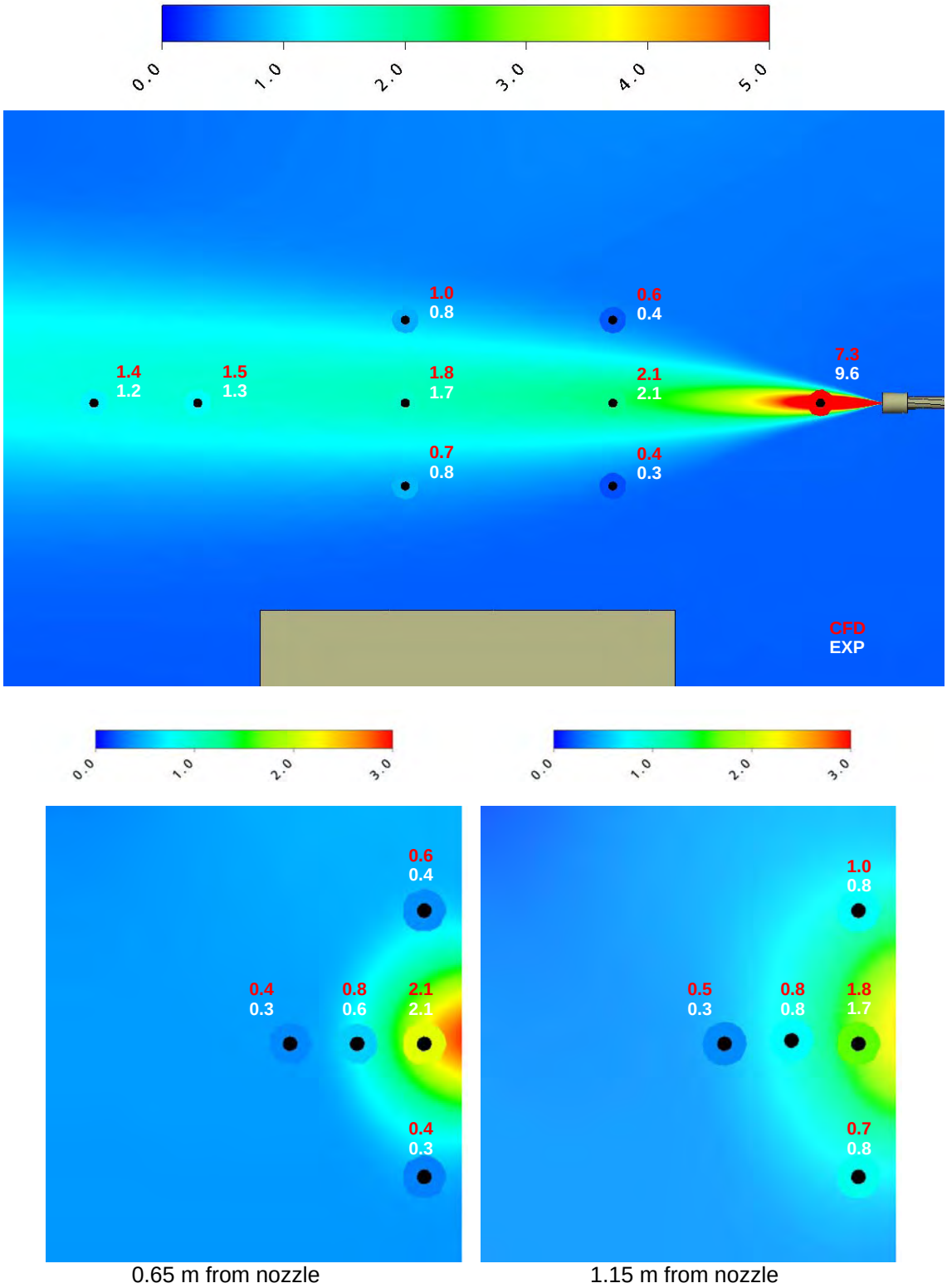

0.65 m from nozzle

1.15 m from nozzle

Figure 11.29 Methane concentrations in % vol/vol for case C2-7: Configuration 2 with a leak rate of 0.49 g/s and a ventilation rate of 12 ach.

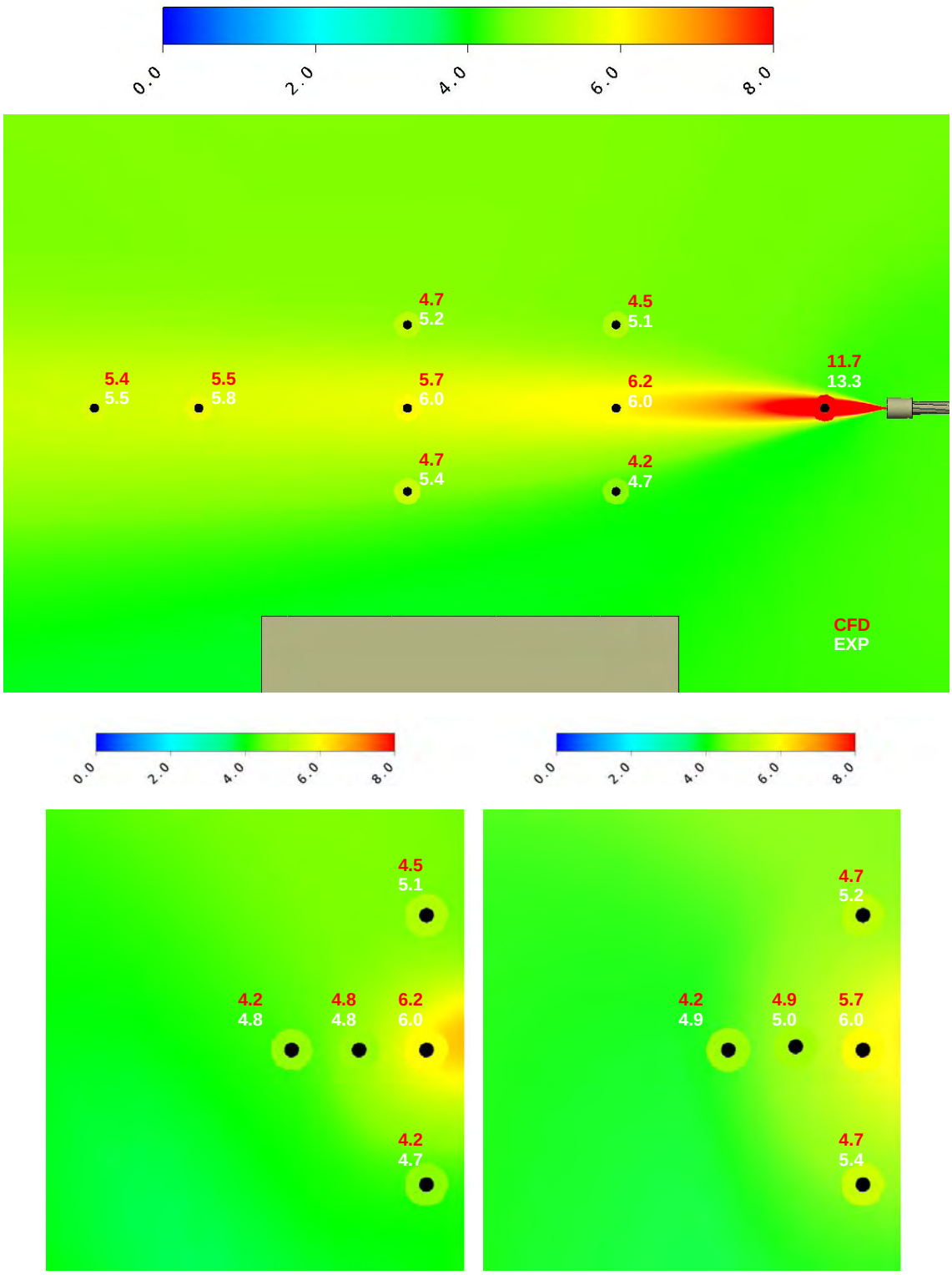

0.65 m from nozzle

1.15 m from nozzle

Figure 11.30 Methane concentrations in % vol/vol for case C2-8: Configuration 2 with a leak rate of 0.86 g/s and a ventilation rate of 2 ach.

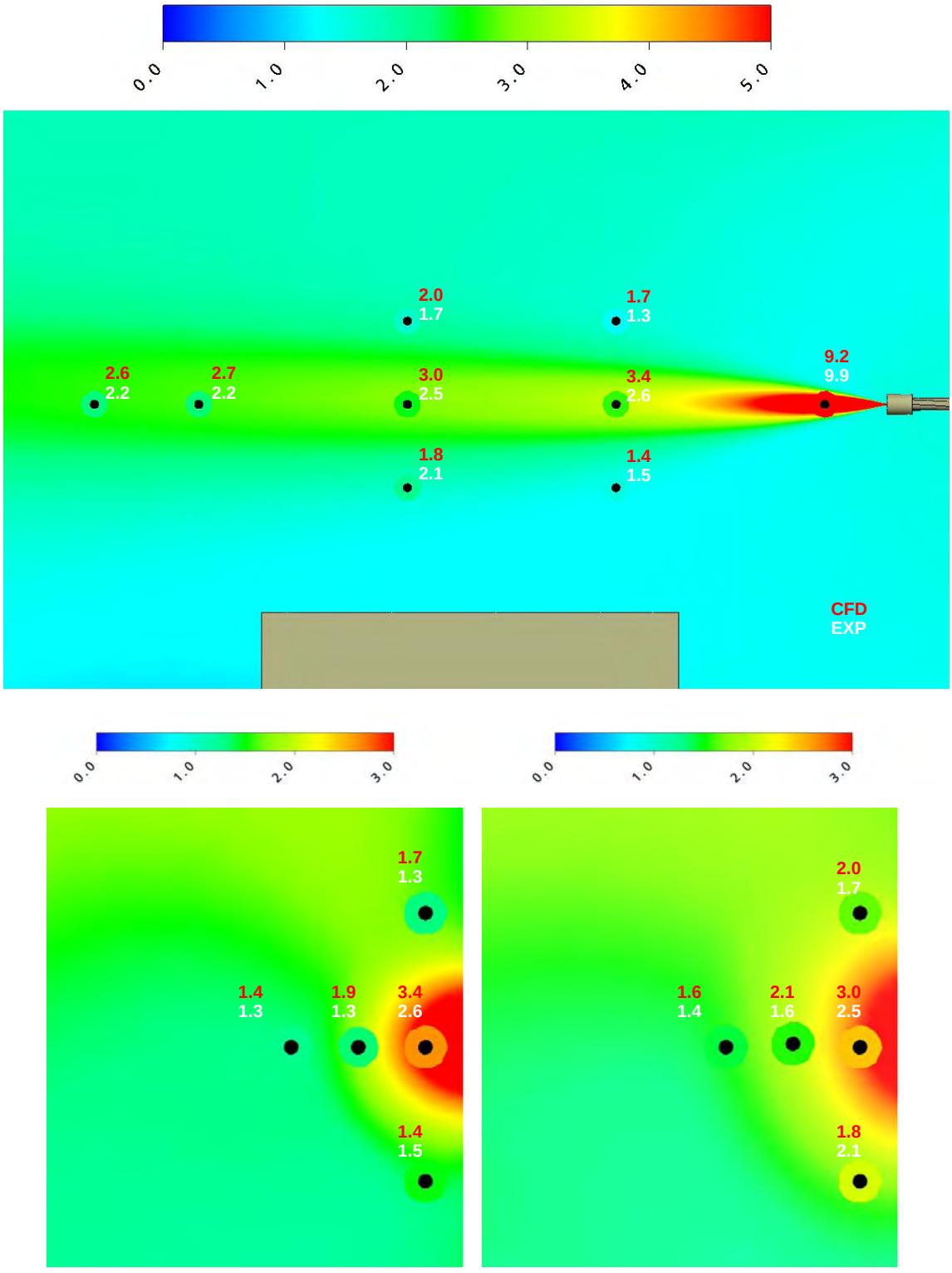

0.65 m from nozzle

1.15 m from nozzle

Figure 11.31 Methane concentrations in % vol/vol for case C2-9: Configuration 2 with a leak rate of 0.86 g/s and a ventilation rate of 6 ach.

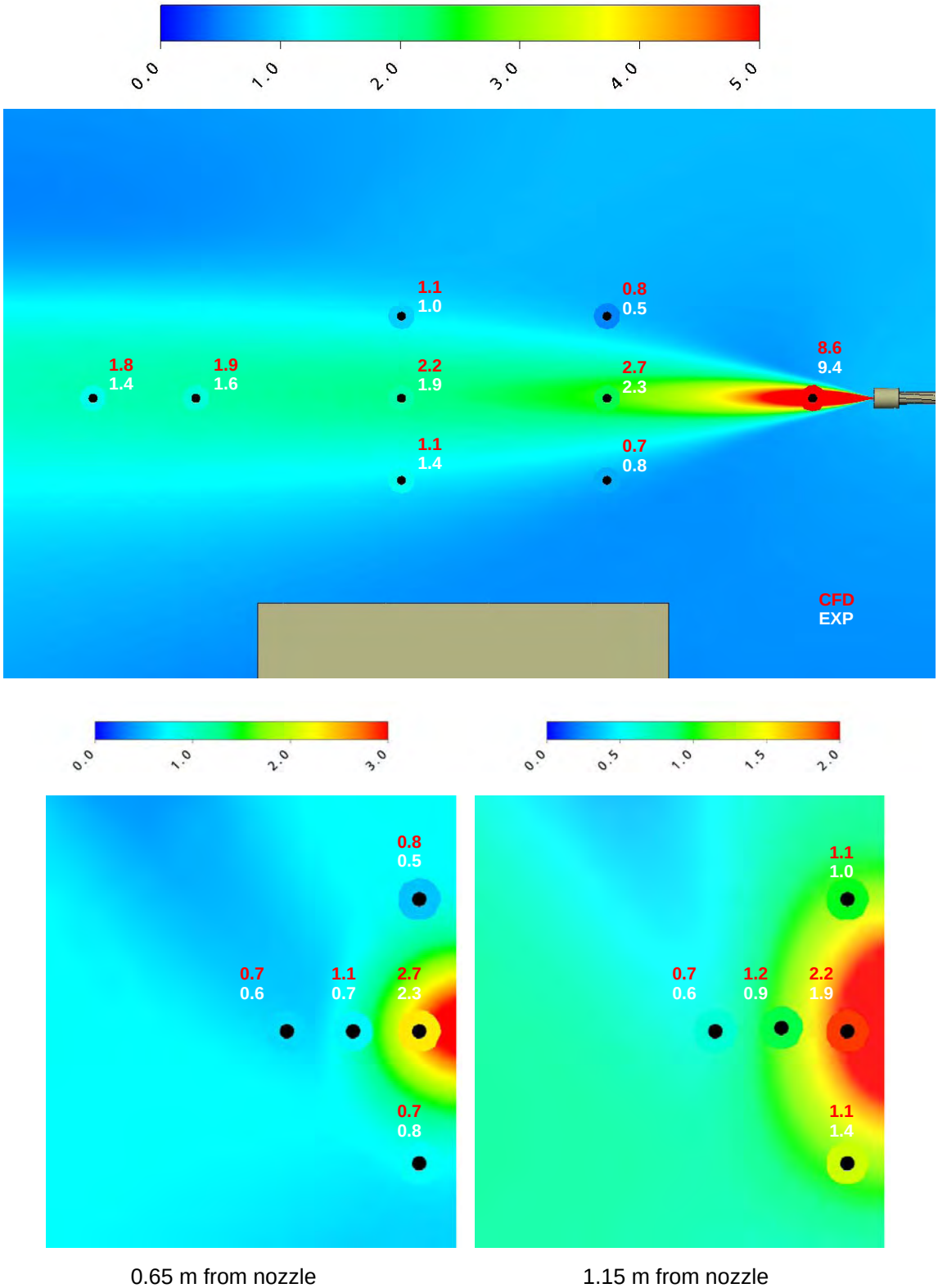

0.65 m from nozzle

1.15 m from nozzle

Figure 11.32 Methane concentrations in % vol/vol for case C2-10: Configuration 2 with a leak rate of 0.86 g/s and a ventilation rate of 12 ach.

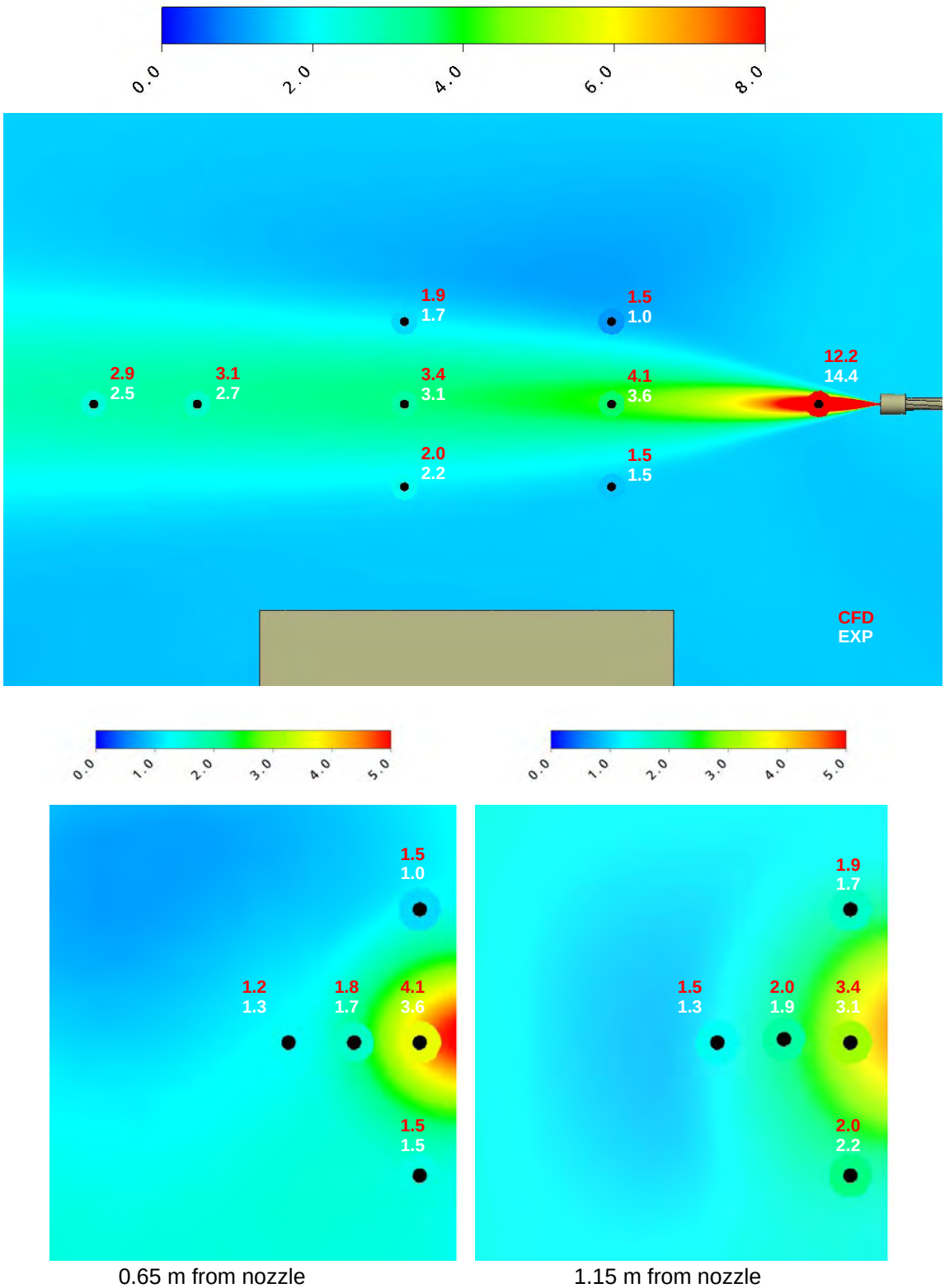

0.65 m from nozzle

1.15 m from nozzle

Figure 11.33 Methane concentrations in % vol/vol for case C2-11: Configuration 2 with a leak rate of 1.72 g/s and a ventilation rate of 12 ach.

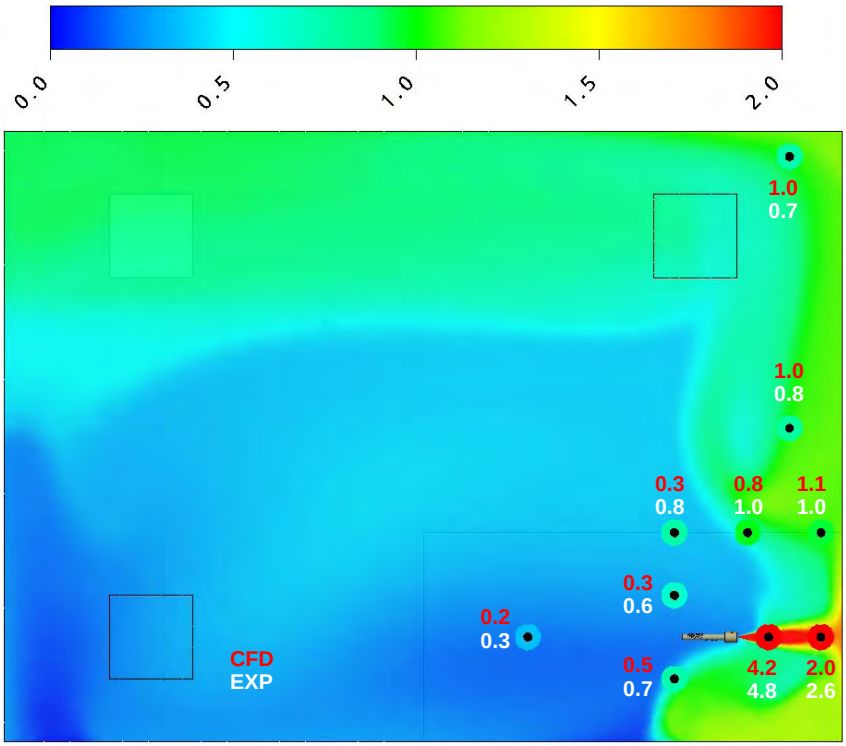

Side View

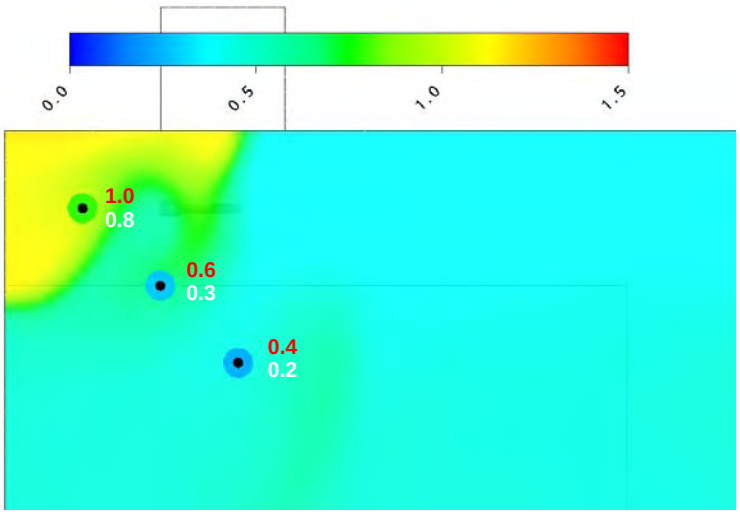

Plan View

Figure 11.34 Methane concentrations in % vol/vol for case C3-3: Configuration 3 with a leak rate of 0.26 g/s and a ventilation rate of 6 ach.

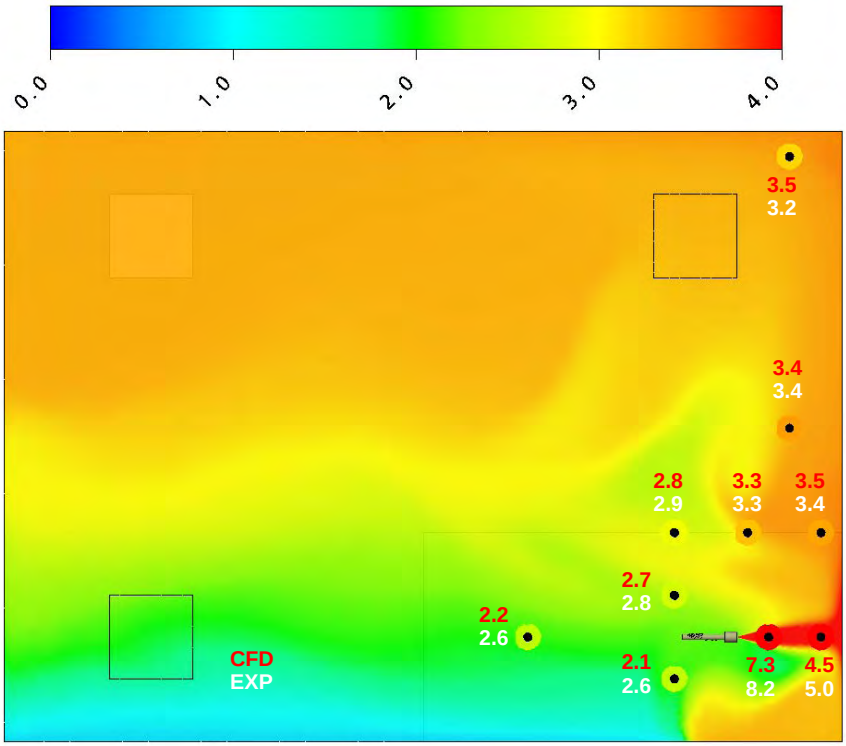

Side View

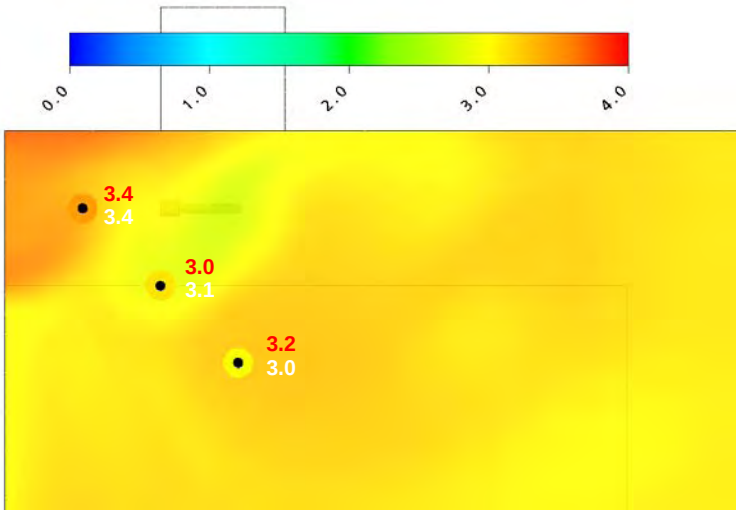

Plan View

Figure 11.35 Methane concentrations in % vol/vol for case C3-4: Configuration 3 with a leak rate of 0.47/s and a ventilation rate of 2 ach.

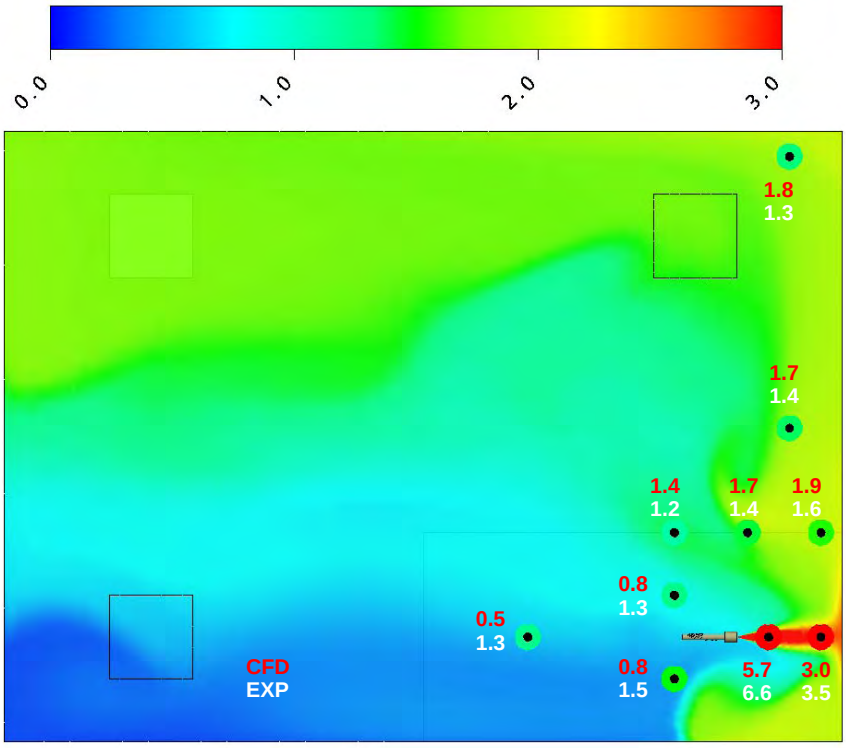

Side View

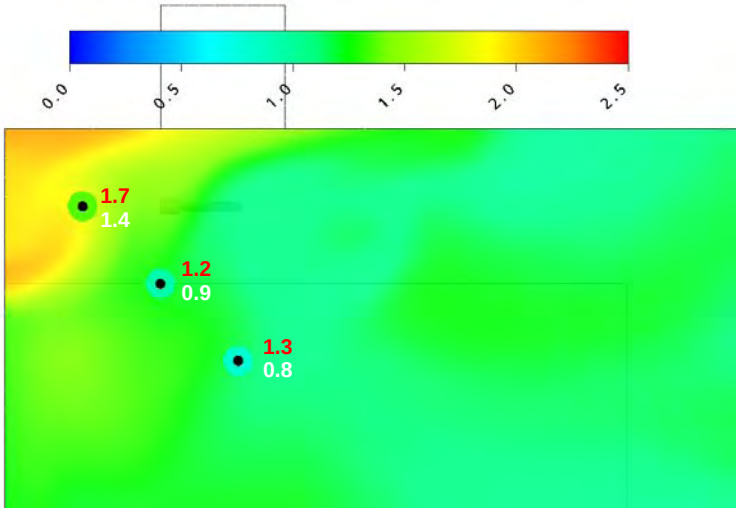

Plan View

Figure 11.36 Methane concentrations in % vol/vol for case C3-5: Configuration 3 with a leak rate of 0.47/s and a ventilation rate of 6ach.

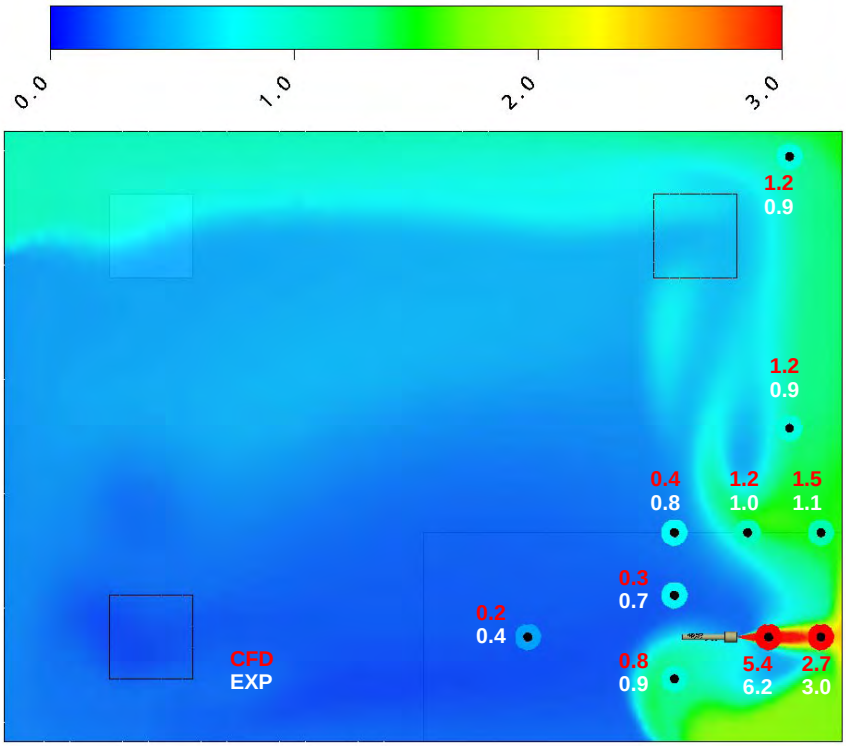

Side View

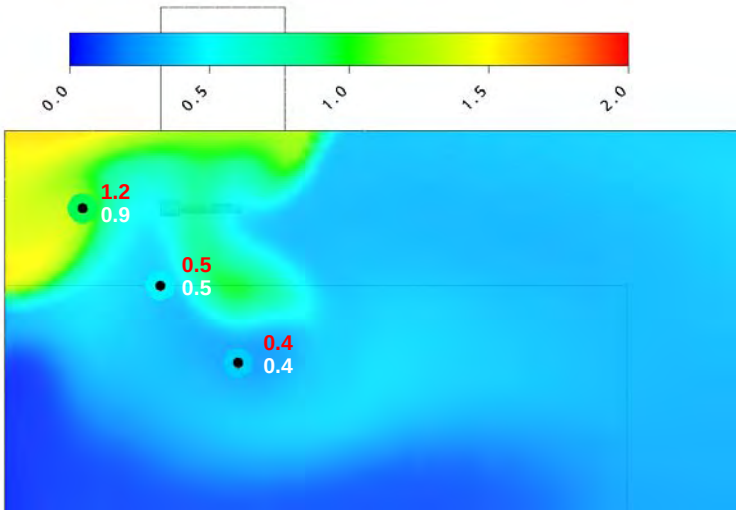

Plan View

Figure 11.37 Methane concentrations in % vol/vol for case C3-6: Configuration 3 with a leak rate of 0.47/s and a ventilation rate of 12ach.

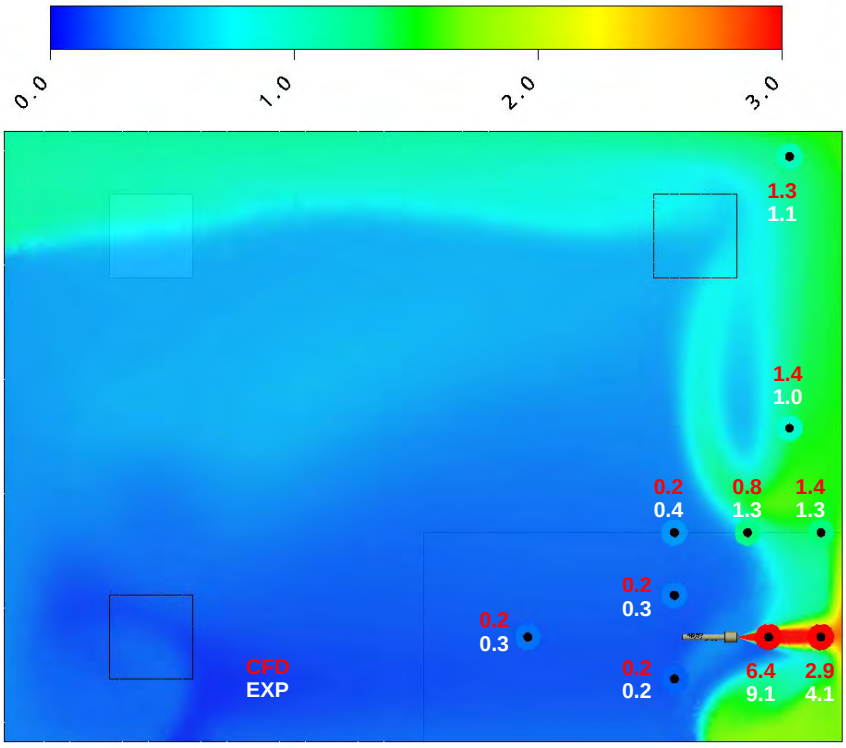

Side View

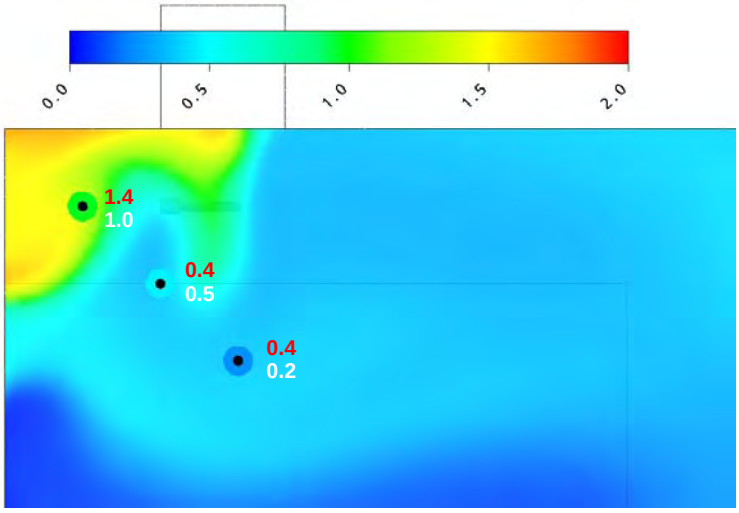

Plan View

Figure 11.38 Methane concentrations in % vol/vol for case C3-7: Configuration 3 with a leak rate of 0.49s and a ventilation rate of 12 ach.

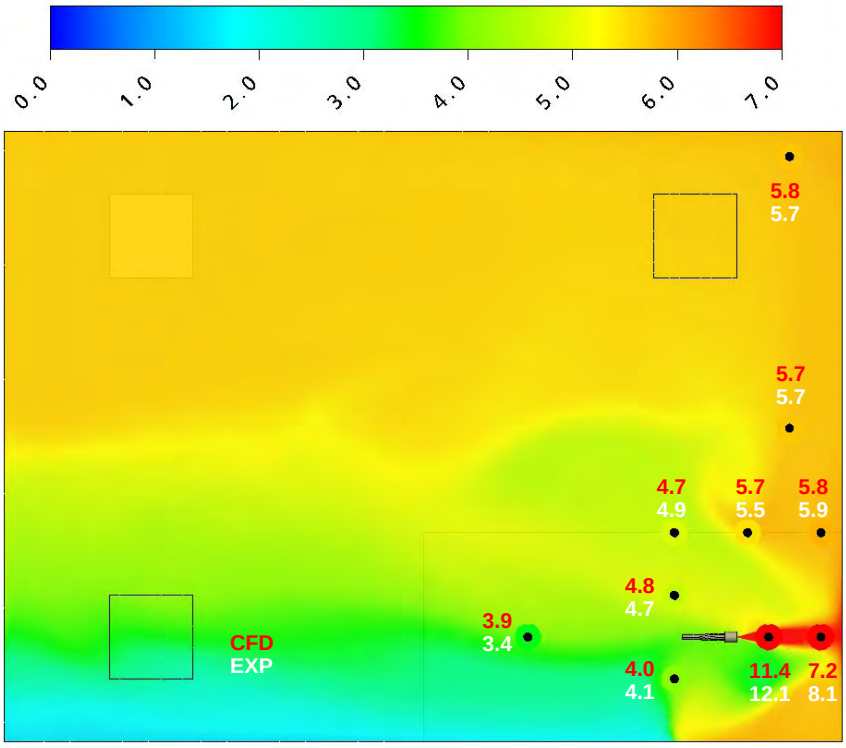

Side View

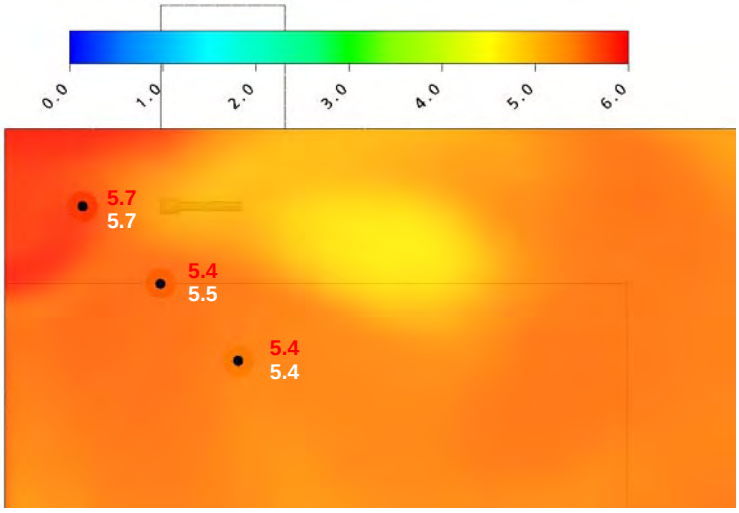

Plan View

Figure 11.39 Methane concentrations in % vol/vol for case C3-8: Configuration 3 with a leak rate of 0.86 g/s and a ventilation rate of 2 ach.

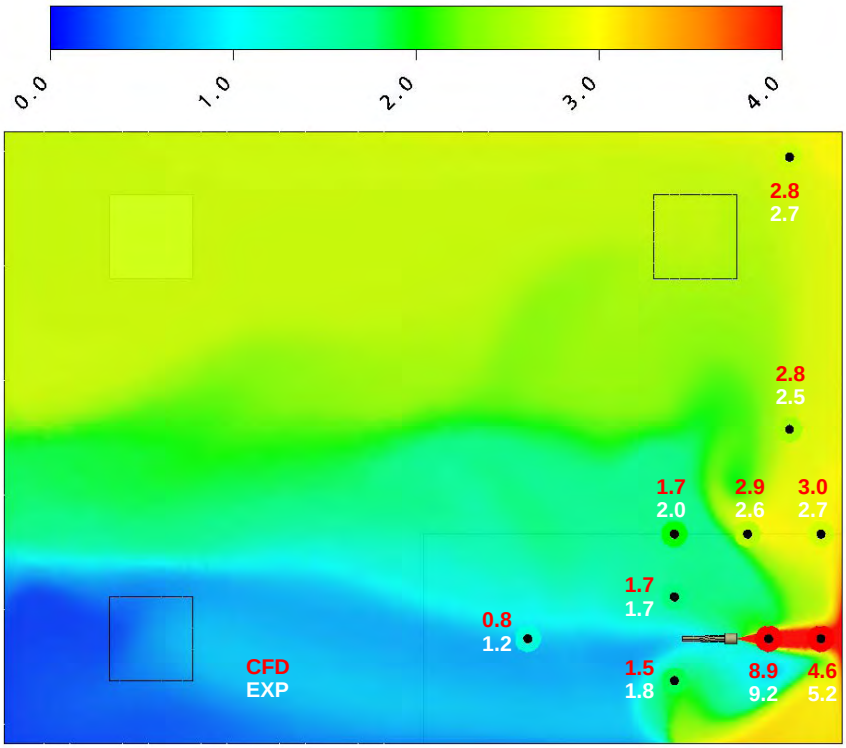

Side View

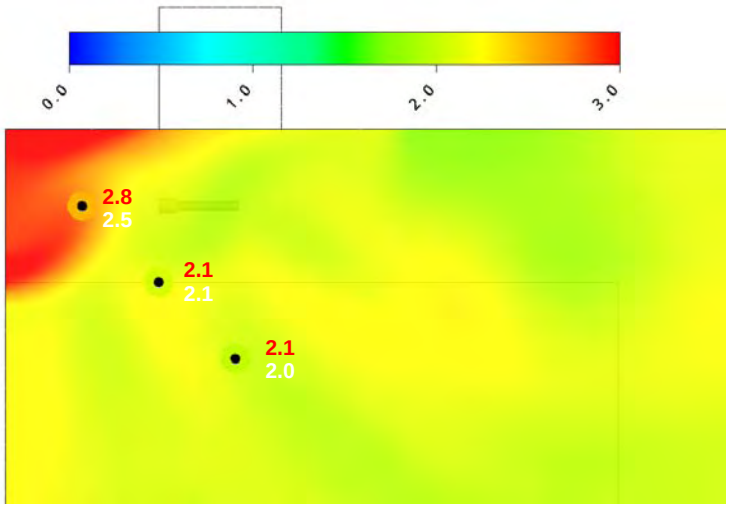

Plan View

Figure 11.40 Methane concentrations in % vol/vol for case C3-9: Configuration 3 with a leak rate of 0.86 g/s and a ventilation rate of 6 ach.

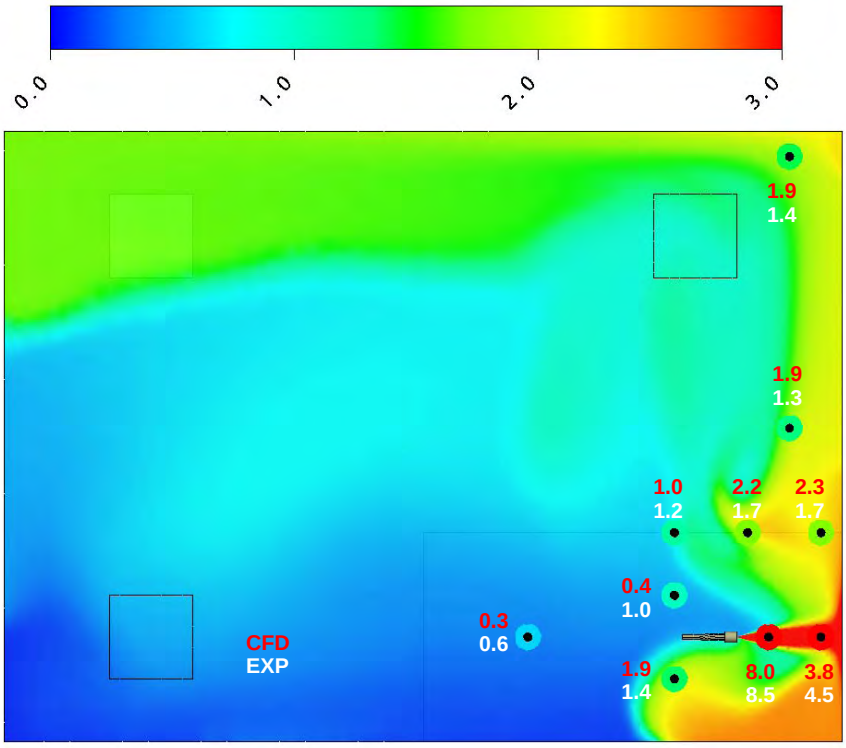

Side View

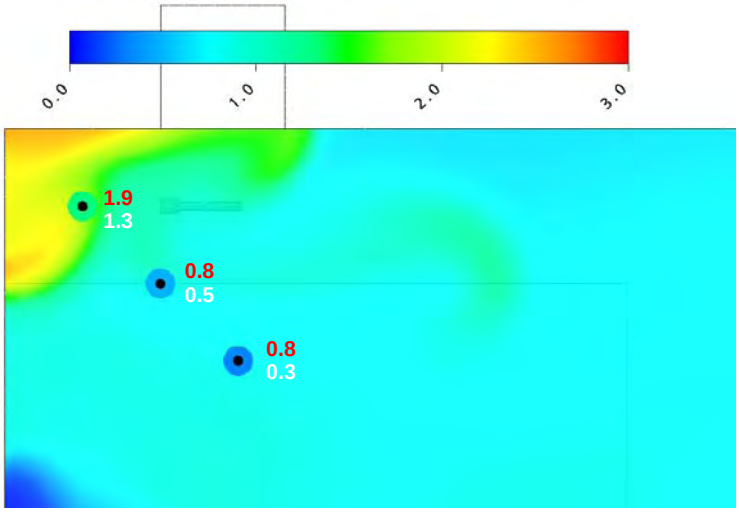

Plan View

Figure 11.41 Methane concentrations in % vol/vol for case C3-10: Configuration 3 with a leak rate of 0.86 g/s and a ventilation rate of 12 ach.

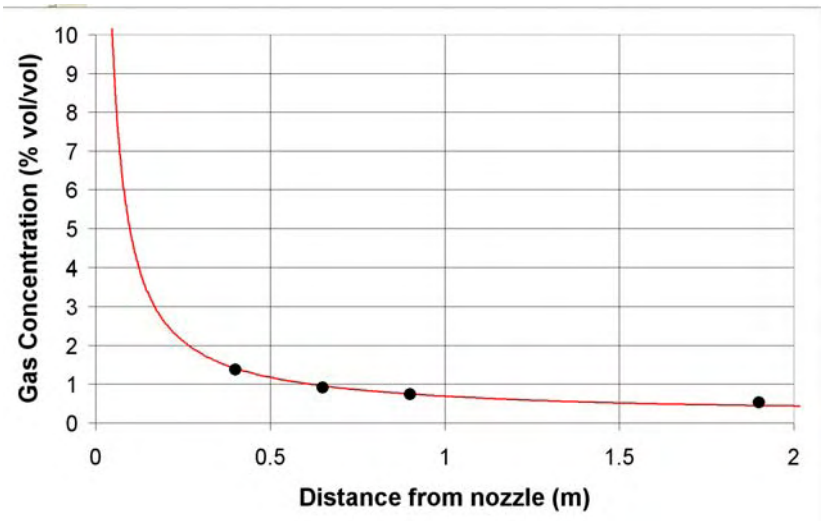

Figure 11.42 Decay of methane concentrations with distance along the jet axis for case C1-1: Configuration 1 with a leak rate of 0.15 g/s and a ventilation rate of 2 ach: – CFD, ● experiments.

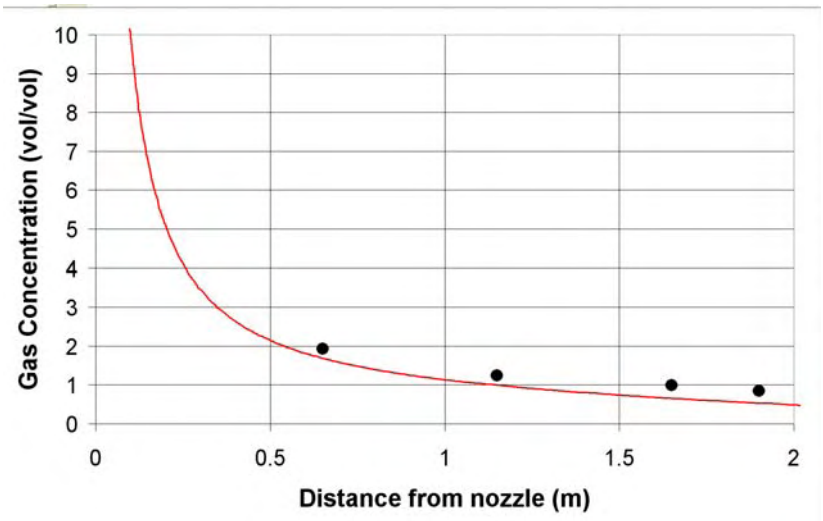

Figure 11.43 Decay of methane concentrations with distance along the jet axis for case C1-2: Configuration 1 with a leak rate of 0.22 g/s and a ventilation rate of 12 ach: – CFD, ● experiments.

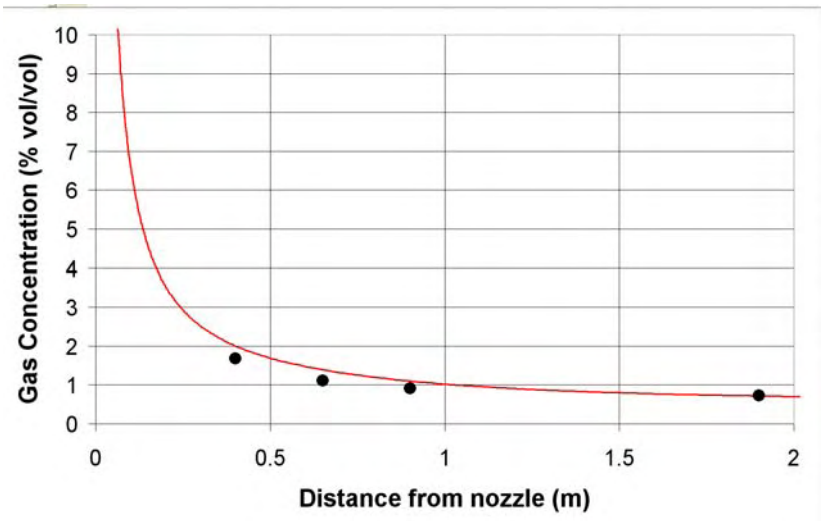

Figure 11.44 Decay of methane concentrations with distance along the jet axis for case C1-3: Configuration 1 with a leak rate of 0.26 g/s and a ventilation rate of 6 ach: – CFD, ● experiments.

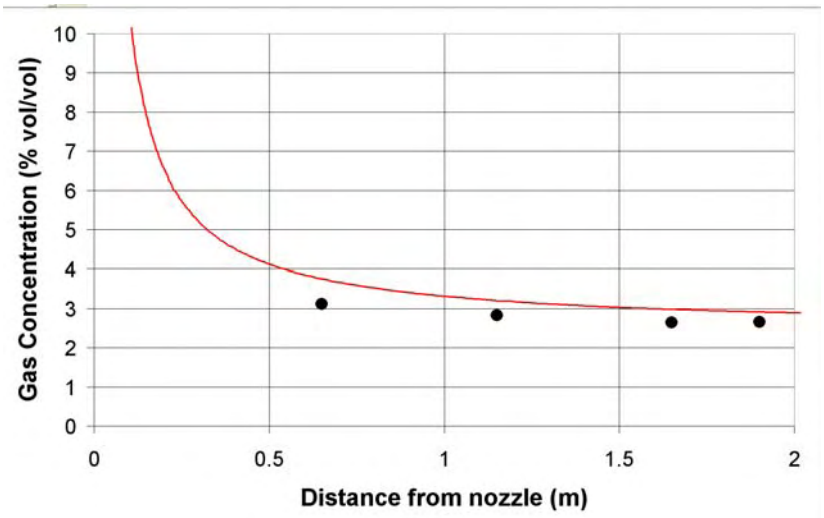

Figure 11.45 Decay of methane concentrations with distance along the jet axis for case C1-4: Configuration 1 with a leak rate of 0.47 g/s and a ventilation rate of 2 ach: – CFD, ● experiments.

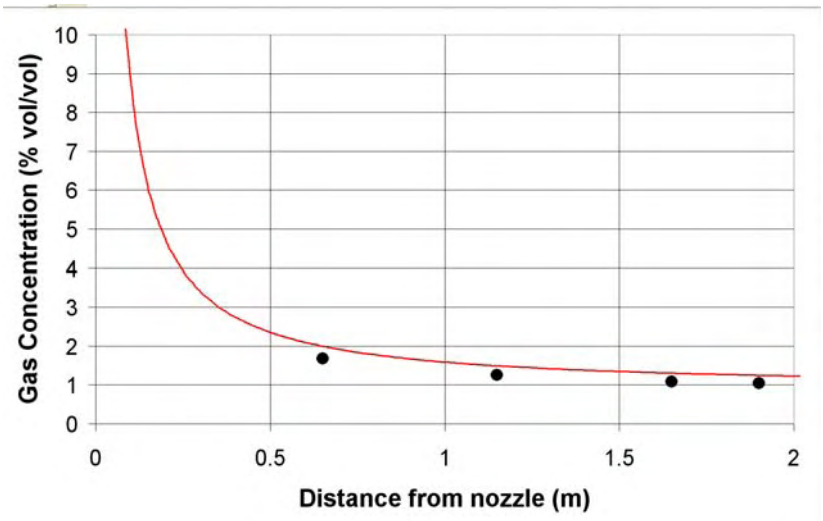

Figure 11.46 Decay of methane concentrations with distance along the jet axis for case C1-5: Configuration 1 with a leak rate of 0.47 g/s and a ventilation rate of 6 ach: – CFD, ● experiments.

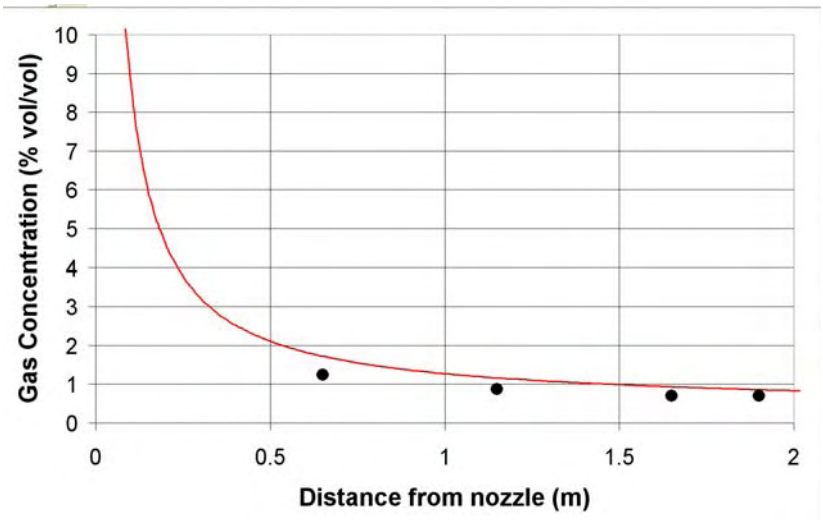

Figure 11.47 Decay of methane concentrations with distance along the jet axis for case C1-6: Configuration 1 with a leak rate of 0.47 g/s and a ventilation rate of 12 ach: – CFD, ● experiments.

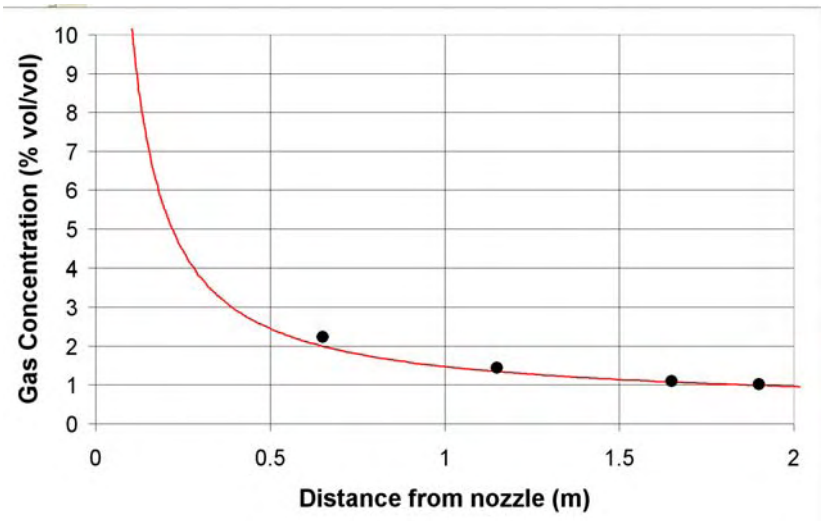

Figure 11.48 Decay of methane concentrations with distance along the jet axis for case C1-7: Configuration 1 with a leak rate of 0.49 g/s and a ventilation rate of 12 ach: – CFD, ● experiments.

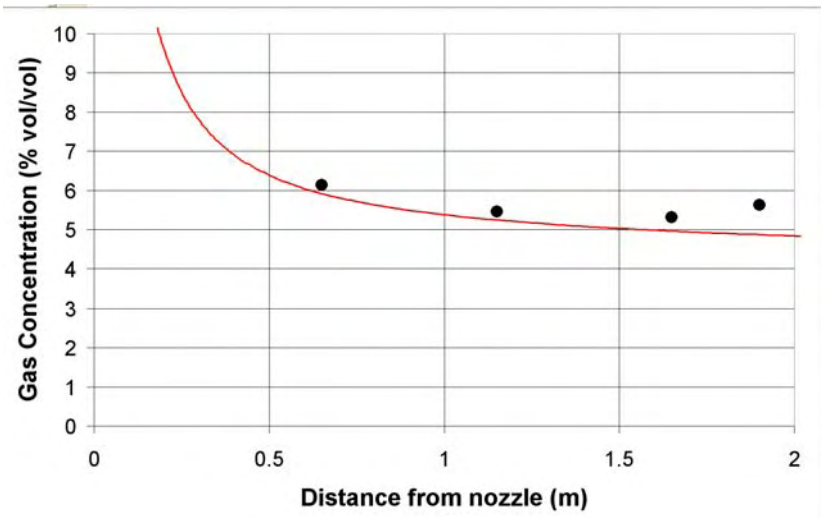

Figure 11.49 Decay of methane concentrations with distance along the jet axis for case C1-8: Configuration 1 with a leak rate of 0.86 g/s and a ventilation rate of 2 ach: – CFD, ● experiments.

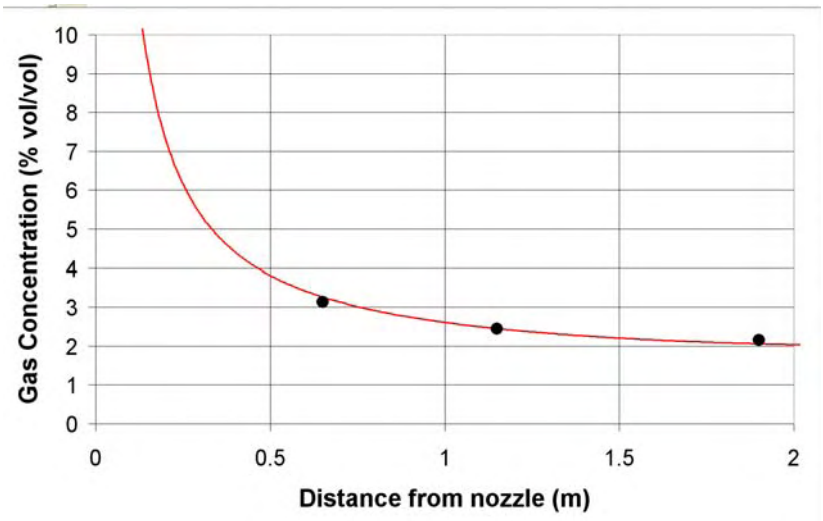

Figure 11.50 Decay of methane concentrations with distance along the jet axis for case C1-9: Configuration 1 with a leak rate of 0.86 g/s and a ventilation rate of 6 ach: – CFD, ● experiments.

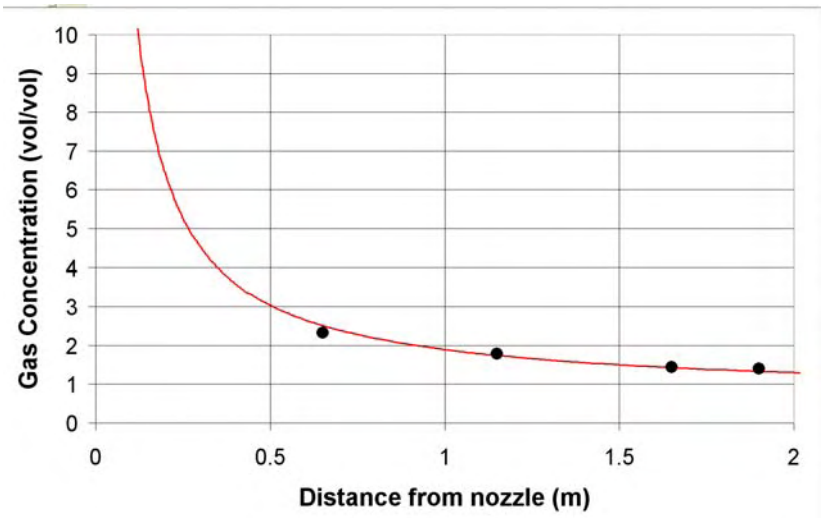

Figure 11.51 Decay of methane concentrations with distance along the jet axis for case C1-10: Configuration 1 with a leak rate of 0.86 g/s and a ventilation rate of 12 ach: – CFD, ● experiments.

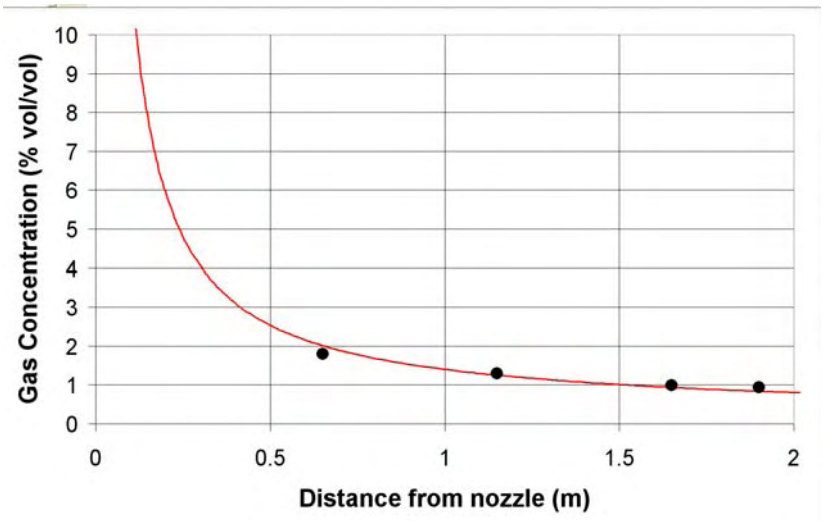

Figure 11.52 Decay of methane concentrations with distance along the jet axis for case C1-11: Configuration 1 with a leak rate of 0.86 g/s and a ventilation rate of 24 ach: – CFD, ● experiments.

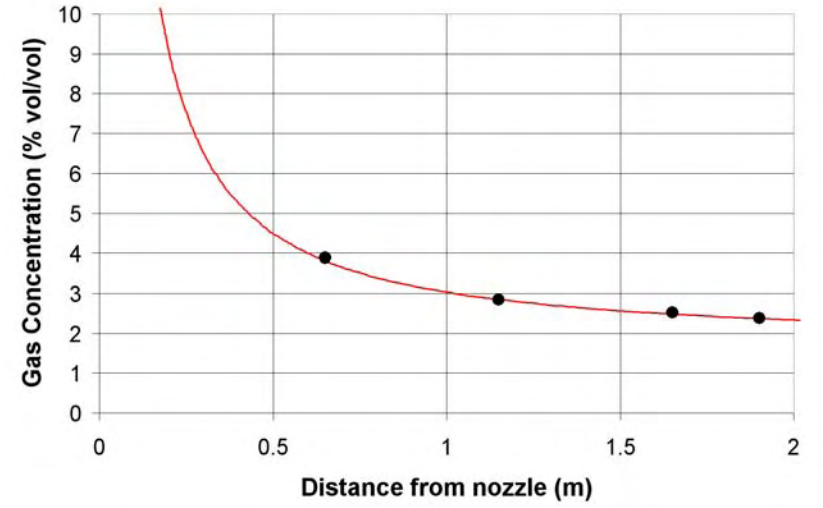

Figure 11.53 Decay of methane concentrations with distance along the jet axis for case C1-12: Configuration 1 with a leak rate of 1.72 g/s and a ventilation rate of 12 ach: – CFD, ● experiments.

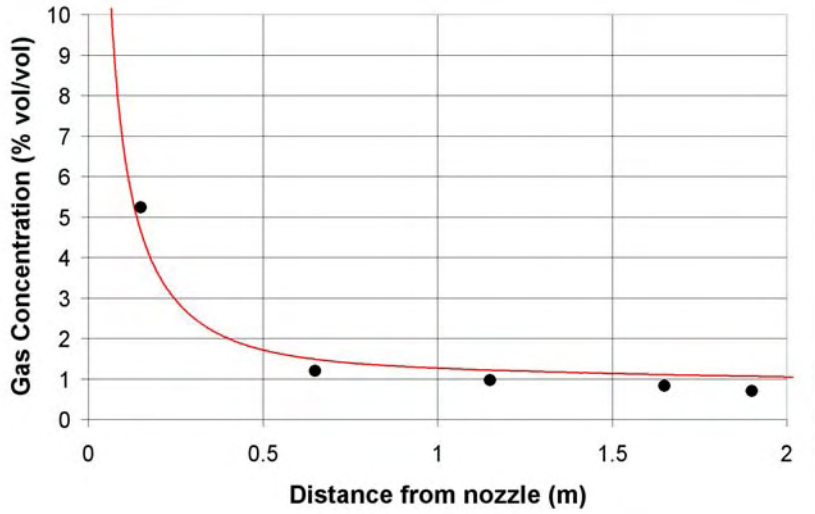

Figure 11.54 Decay of methane concentrations with distance along the jet axis for case C2-3: Configuration 2 with a leak rate of 0.26 g/s and a ventilation rate of 6 ach: – CFD, ● experiments.

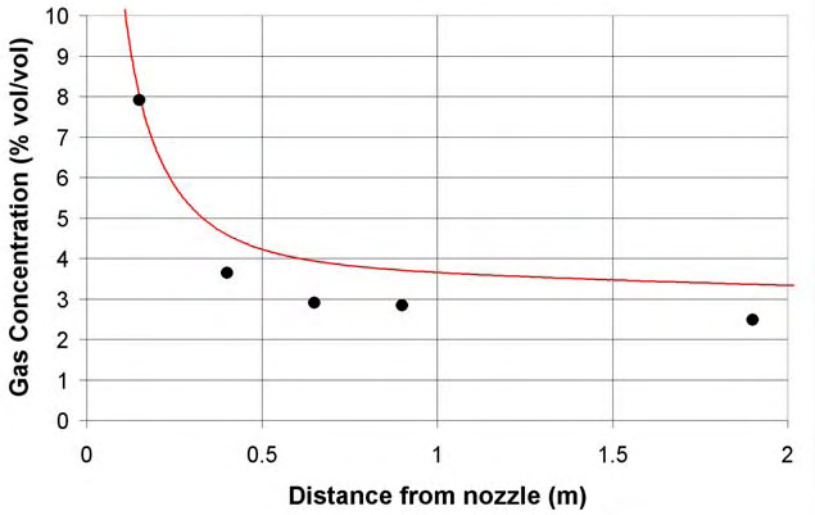

Figure 11.55 Decay of methane concentrations with distance along the jet axis for case C2-4: Configuration 2 with a leak rate of 0.47 g/s and a ventilation rate of 2 ach: – CFD, ● experiments.

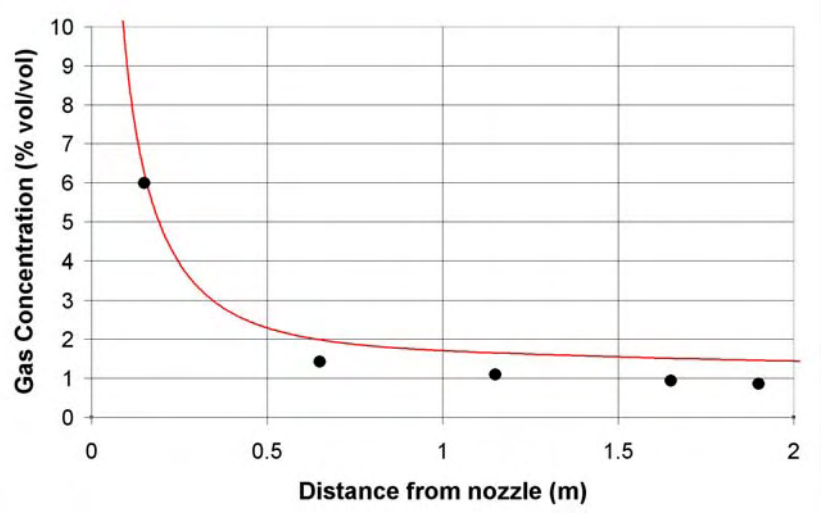

Figure 11.56 Decay of methane concentrations with distance along the jet axis for case C2-5x: Configuration 2 with a leak rate of 0.38 g/s and a ventilation rate of 6 ach: – CFD, ● experiments.

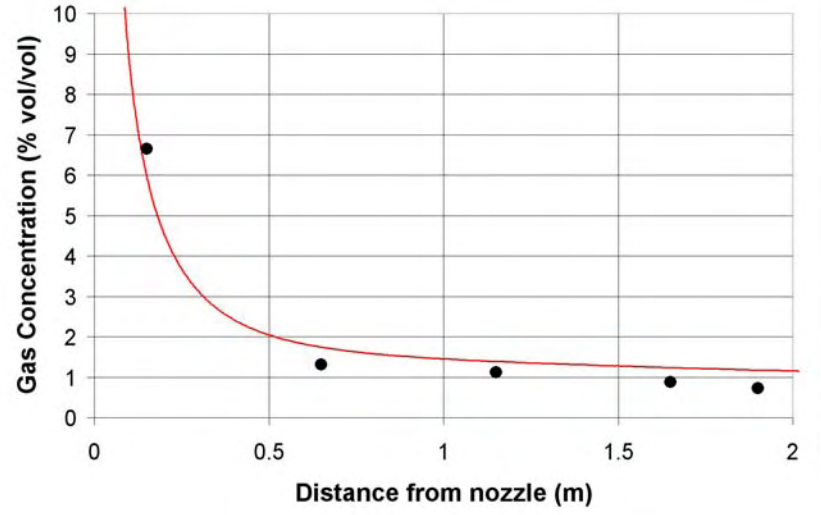

Figure 11.57 Decay of methane concentrations with distance along the jet axis for case C2-6: Configuration 2 with a leak rate of 0.47 g/s and a ventilation rate of 12 ach: – CFD, ● experiments.

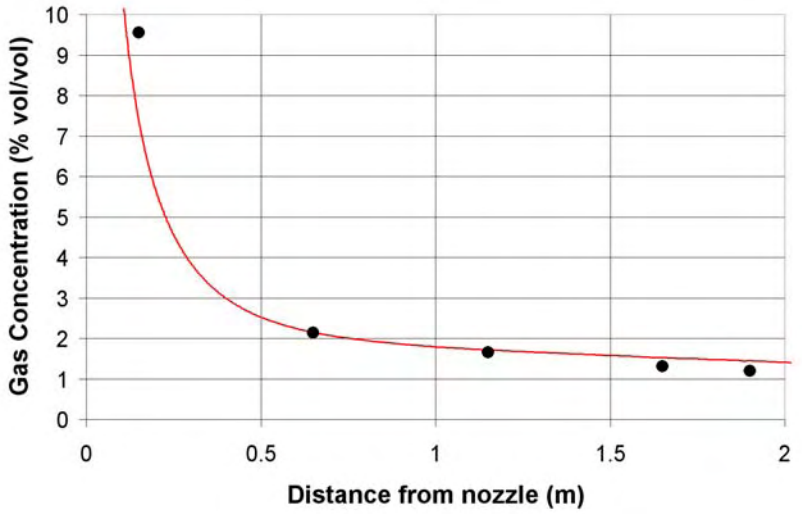

Figure 11.58 Decay of methane concentrations with distance along the jet axis for case C2-7: Configuration 2 with a leak rate of 0.49 g/s and a ventilation rate of 12 ach: – CFD, ● experiments.

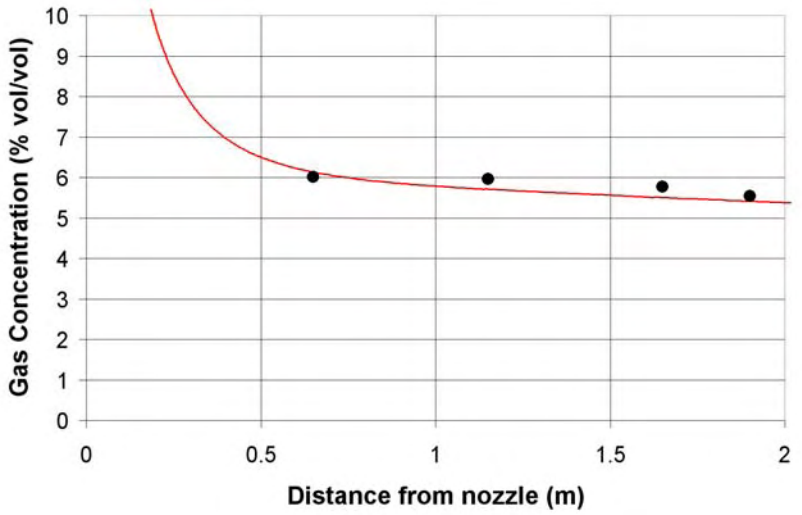

Figure 11.59 Decay of methane concentrations with distance along the jet axis for case C2-8: Configuration 2 with a leak rate of 0.86 g/s and a ventilation rate of 2 ach: – CFD, ● experiments.

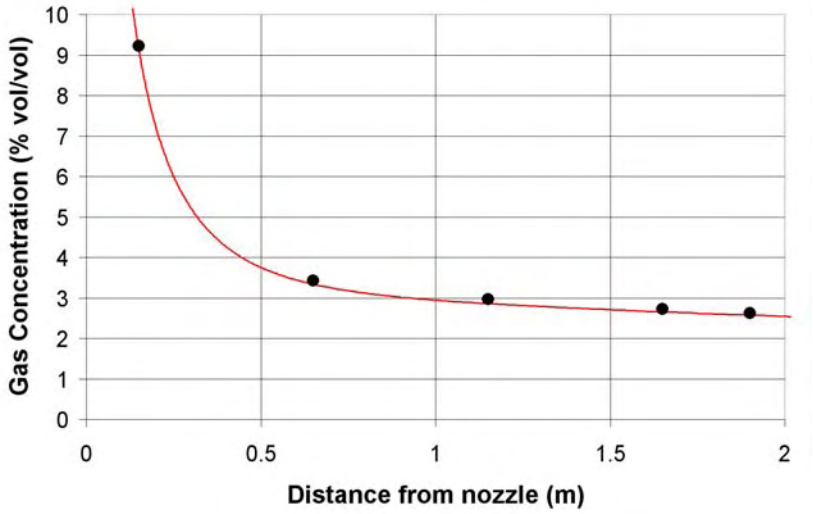

Figure 11.60 Decay of methane concentrations with distance along the jet axis for case C2-9: Configuration 2 with a leak rate of 0.86 g/s and a ventilation rate of 6 ach: – CFD, ● experiments.

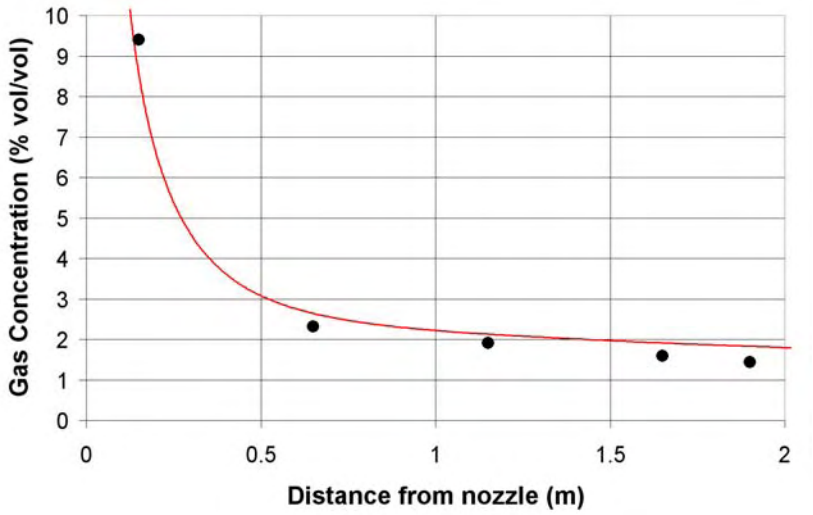

Figure 11.61 Decay of methane concentrations with distance along the jet axis for case C2-10: Configuration 2 with a leak rate of 0.86 g/s and a ventilation rate of 12 ach: – CFD, ● experiments.

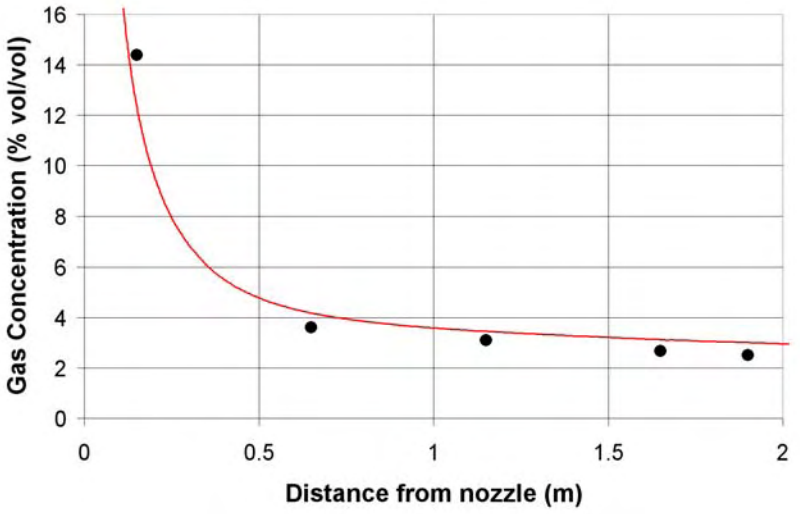

Figure 11.62 Decay of methane concentrations with distance along the jet axis for case C2-11: Configuration 2 with a leak rate of 1.72 g/s and a ventilation rate of 12 ach: – CFD, ● experiments.

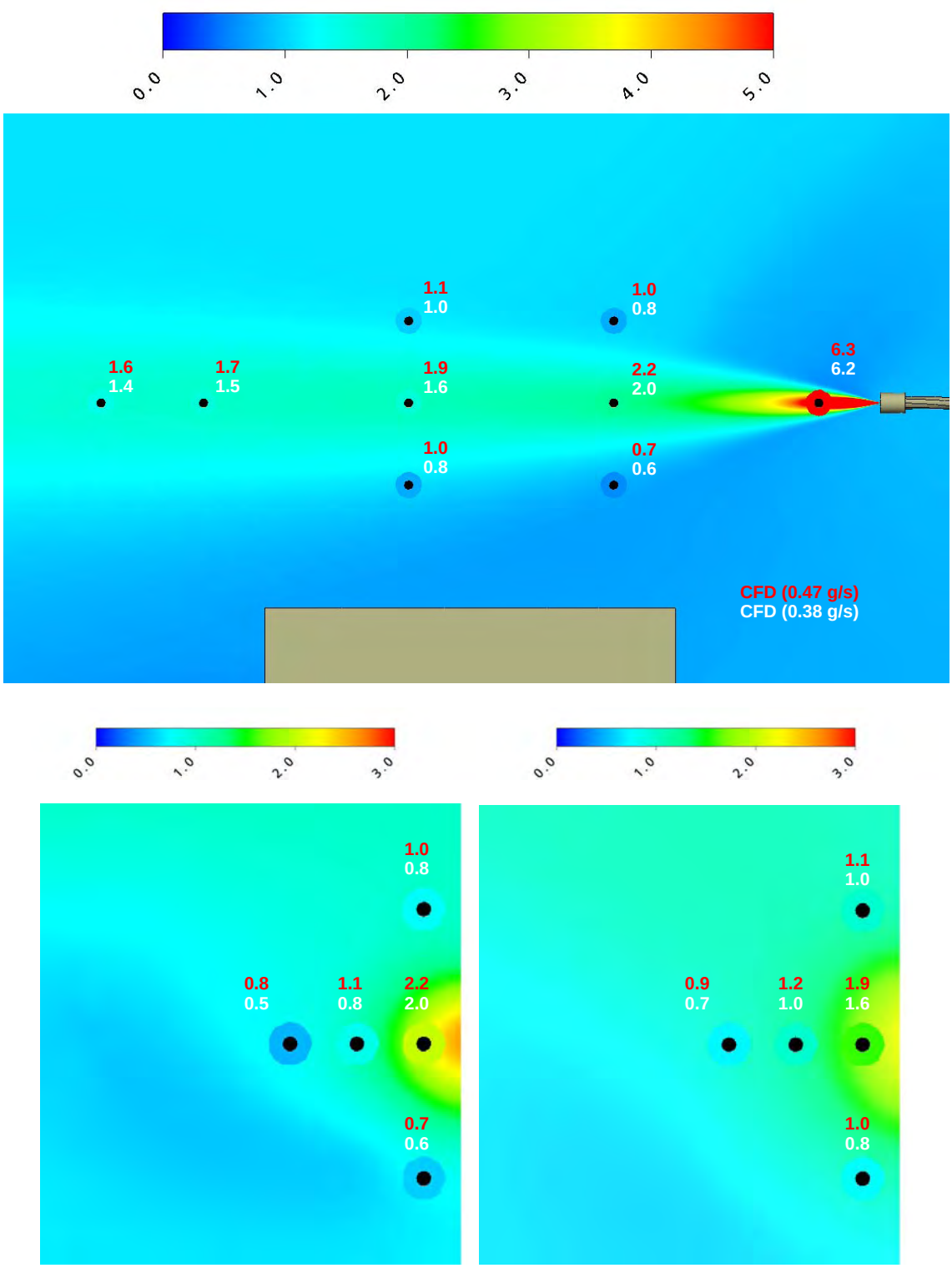

0.65 m from nozzle

1.15 m from nozzle

Figure 11.63 Methane concentrations in % vol/vol for Configuration 2 with a ventilation rate of 6 ach and leak rate of 0.47 g/s and (background contours) compared against 0.38 g/s (spot values). Both sets of results are from CFD calculations.

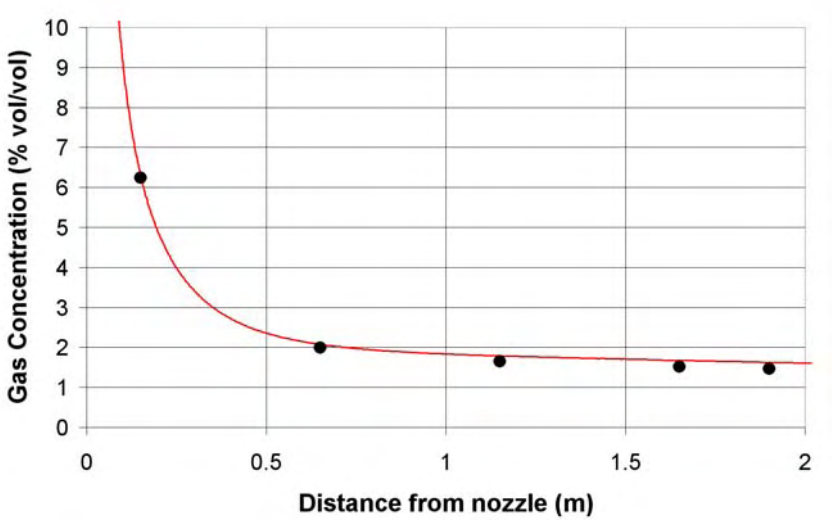

Figure 11.64 Decay of methane concentrations with distance along the jet axis for Configuration 2 with a ventilation rate of 6 ach: – CFD with a leak rate of 0.47 g/s, • CFD with a leak rate of 0.38 g/s.

12 APPENDIX E – FURTHER CFD SIMULATIONS

12.1 INTRODUCTION

Appendix D presented results from a validation study in which CFD model predictions were compared to experimental measurements of gas concentrations resulting from leaks in enclosures. The conclusion from that work was that CFD models are capable of predicting gas releases to an acceptable degree of accuracy. Having established this fact, the aim of the present Appendix is to describe the CFD modelling that has been carried out to explore more widely the behaviour of gas releases in a range of different situations. This includes consideration of enclosures of different size, obstructions in the enclosure of different shape, different orientations of the leak source and the effects of heat sources. The aim of these simulations is to establish what effect these factors have on the resulting gas cloud size, and in particular which factors lead to increased gas cloud volumes.

The first section briefly describes the CFD methodology that has been used in the simulations. This is followed by two sections which document the effect of changing the blockage and leak orientation, and then changing the size of the enclosure. The results presented in these two sections involve essentially isothermal conditions (i.e. all surfaces including walls are assumed to be adiabatic). A summary is then given of all the isothermal simulations, including those made in the earlier validation exercise, which also assumed isothermal conditions. The penultimate section presents the results from non-isothermal simulations: either involving a cold floor or a heated surface in the enclosure. Conclusions are then drawn in the final Section.

12.2 CFD METHODOLOGY

The same overall methodology is used in these tests as presented in Appendix D. This includes use of the pseudo-source approach for the gas leak, the same turbulence and buoyancy modelling approaches and the same "steady" calculation method. Unlike the validation study, grid sensitivity tests have not been rigorously pursued in each case here due to the need to consider such a large number of different scenarios. However, grids have been designed based on the experience gained in the previous validation exercise. Details of the geometry are described on a case-by-case basis below, together with the leak rates and ventilation rates tested and details of any heat sources. The results are presented primarily in terms of the V_z gas cloud volume.

12.3 BLOCKAGES AND LEAK ORIENTATION

In these simulations the sensitivity of the gas cloud volume to changes in the leak orientation and position relative to a blockage in the enclosure are investigated. The same basic enclosure structure is used as that for the validation study (see Figure 12.1). The enclosure is 4 metres wide, 4 metres long and 2.92 metres high with two ventilation inlets on one wall and two outlets on the opposite wall. The inlets and outlets were located diagonally opposite on each wall (upper-left and lower-right) and staggered with respect to each other to prevent the flow "short-circuiting" directly from the inlets to the outlets. The original aim of this set of tests was to produce a design for Configuration 3 in the validation study.

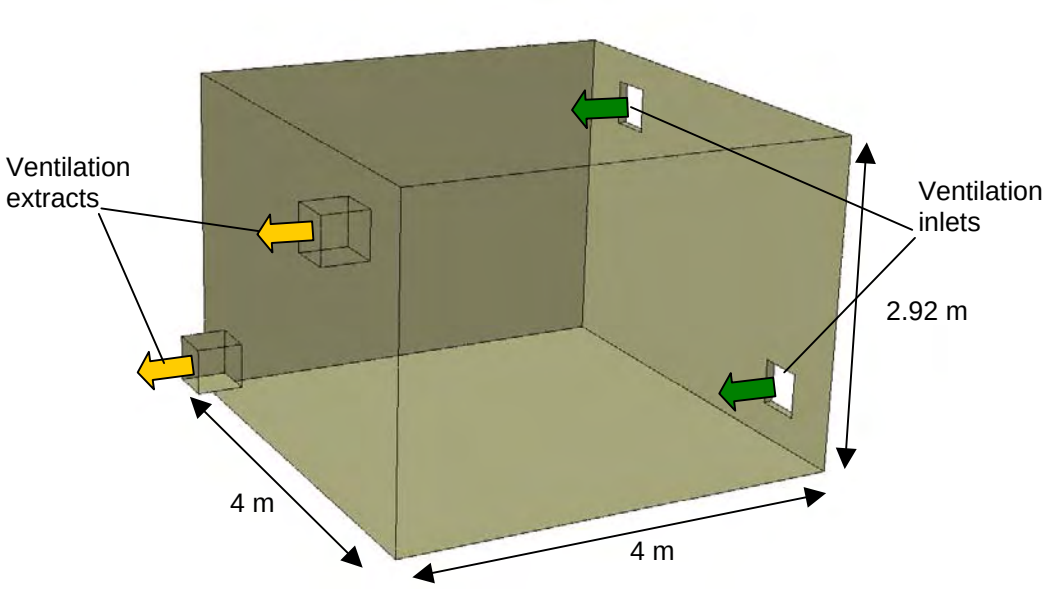

Figure 12.1 Geometry of the basic enclosure without leak source or obstruction

A 2 × 1 × 1 metre rectangular box-shaped obstruction is placed within the enclosure at various different locations. In total 13 different arrangements have been tested, including the 3 cases examined in the previous validation exercise. The tests consist of different combinations of the leak and obstacle locations. Plan, side and perspective views of the configurations are shown in Figure 12.2. In each case, the box obstruction is marked in blue, the nozzle through which the gas was released in red and an arrow marks the initial direction of the gas jet. The mass release rate and ventilation inlets and outlets were identical in all cases.

Cases D1, D2 and D3 are the same as Configurations 1, 2 and 3 described in Appendix D as part of the validation study (specifically tests C1-10, C2-10 and C3-10). cases D4 to D11 are variations on the "worst-case" scenario D3. The penultimate case, D12, is the same as D1 except that the nozzle orientation is reversed so that the jet impinges onto the adjacent wall rather than flowing freely into the centre of the enclosure, and in the final case, D13, the leak is directed at 45° into a corner formed between the box, the wall and the floor.

CFD simulations were undertaken for each of the 13 cases using a "baseline" leak rate of 0.86 g/s and ventilation rate of 12 ach. The V_z clouds produced by each of these configurations are presented in Figure 12.3 and summarised in Table 12.1. Also given in Table 12.1 are three dimensions:

- the distance from the leak source to the nearest wall, following a straight line path along the axis of the jet
- the width of the cavity between the box and the wall in which the leak source is situated (only relevant for cases D3 – D11)
- the maximum gap underneath the box or between the box and the side wall (also only relevant for cases D3 – D11)

See Figure 12.4 for a diagram showing these dimensions for case D4.

The lowest gas cloud volumes are produced when there is sufficient space around the leak source for fresh air to be entrained freely into the jet from all sides and where there is little or no re-entrainment of gas back into the source zone (e.g. case D1).

The presence of a wall on one side close to the leak source, case D2, limits the entrainment of fresh air into the jet. This leads to a doubling of the gas cloud volume V_z compared to case D1.

The largest V_z cloud is produced by case D3, where the nozzle is confined in a cavity 50 cm wide. Here, the nozzle is sufficiently close to the side wall such that the jet impinges at high speed on the wall and produces a flow recirculation within the cavity. Gas surrounding the nozzle is then re-entrained into the jet, giving rise to higher gas concentrations. This mildly buoyant gas mixture remains unaffected by the weak ventilation flow and therefore rises slowly as a plume to the ceiling.

To help identify some generic trends in the results from the other tests, the V_z data is plotted as a bar chart in Figure 12.5. As discussed, the longest bar is clearly case D3 (coloured in black). The two adjacent bars coloured in red (cases D4 and D5) are results from simulations where the leak is maintained in the same position as D3 but the box is moved incrementally further away from the leak to produce a wider cavity. These show that the gas cloud volume is strongly affected by the width of the cavity. As the cavity is widened from 0.5 to 0.75 metres, the V_z falls by one order of magnitude from 0.89 to 0.092 m^3 (cases D3 to D4). While one might expect that as the box is moved further away from the leak the V_z would continue to decrease, there is actually a modest increase in V_z from 0.092 to 0.13 m^3 as the cavity width is increased from 0.75 to 1.0 metres. This demonstrates how sensitive V_z is to the ventilation flow.

The effect of introducing a gap between the box and the adjacent wall, as in case D6, is even more marked. Just by moving the box 20 cm away from the wall reduces the V_z by a factor of 20 (comparing the black and green bars in Figure 12.5). This significant reduction is due to the gas which impinges on to the wall escaping along the open slot at the back of the box rather than recirculating within the cavity.

The V_z is also reduced if the leak source is moved further away from the wall. In case D7 the leak is 1.75 metres from the wall, compared to 0.5 metres in the worst case, D3. This leads to a reduction in the V_z by nearly a factor of 70. When the jet is sufficiently far from the wall, there is a significant amount of fresh air entrained into the jet between the leak source and the wall. As well as diluting the gas cloud, this entrainment also reduces the jet velocity so that by the time the jet impinges onto the wall it has insufficient momentum to produce a flow recirculation in the cavity.

A moderately large V_z is produced in the final case, D13, where the leak source is very close to a three-sided corner formed by the floor, the wall and one side of the box. A three-pronged V_z gas cloud is formed here, flowing away from the leak source in the corners. Gas concentrations are maintained at high levels in these regions due to the limited entrainment possible, owing to the presence of the two side walls. Note the similarity between this case and the free jet running parallel to two walls described in Appendix B.

Case D1

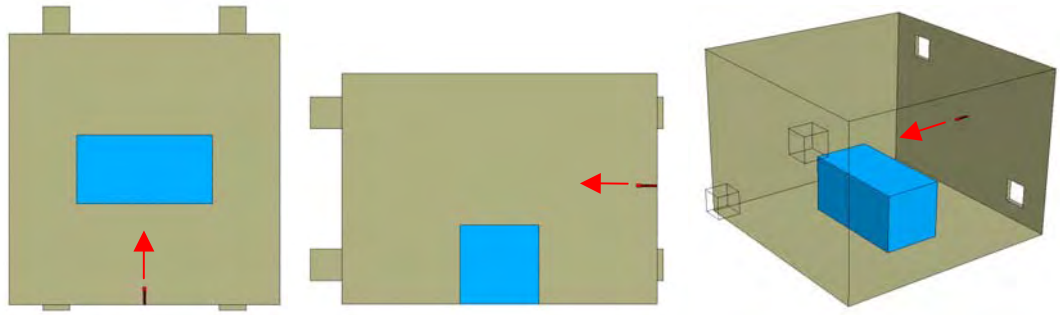

Case D2

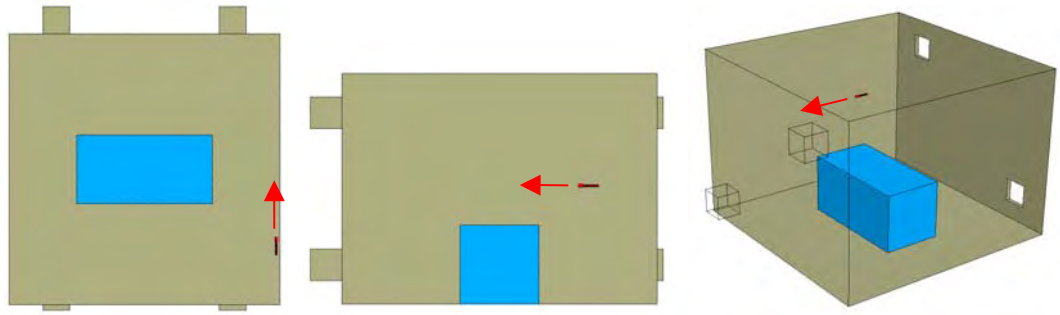

Case D3

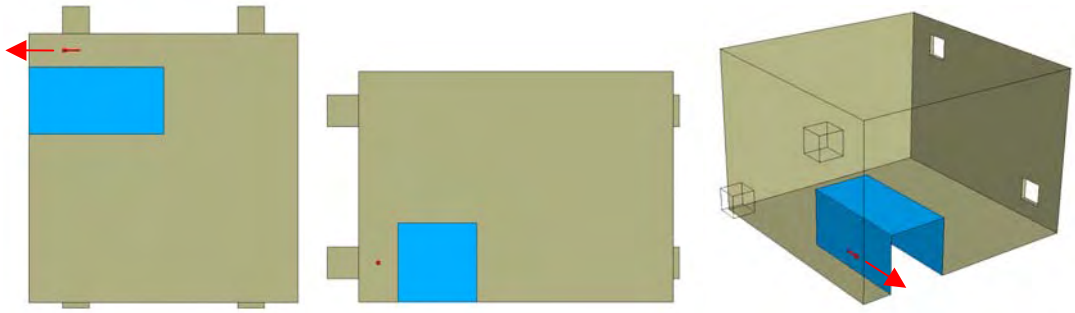

Case D4

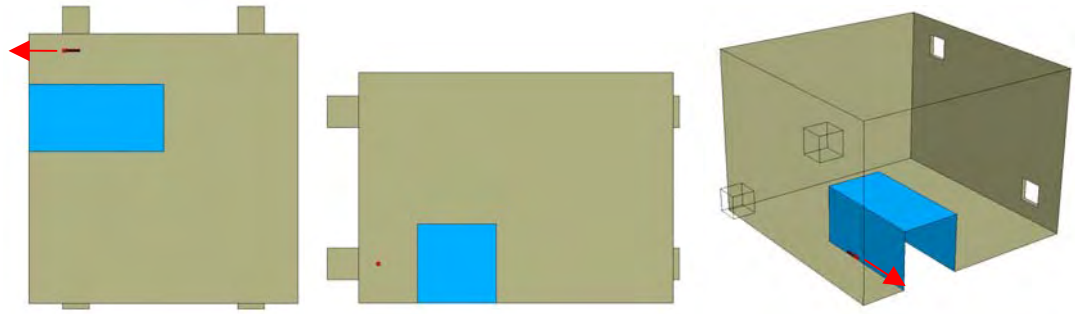

Plan View Side View Perspective

(for figure caption see following page)

Case D5

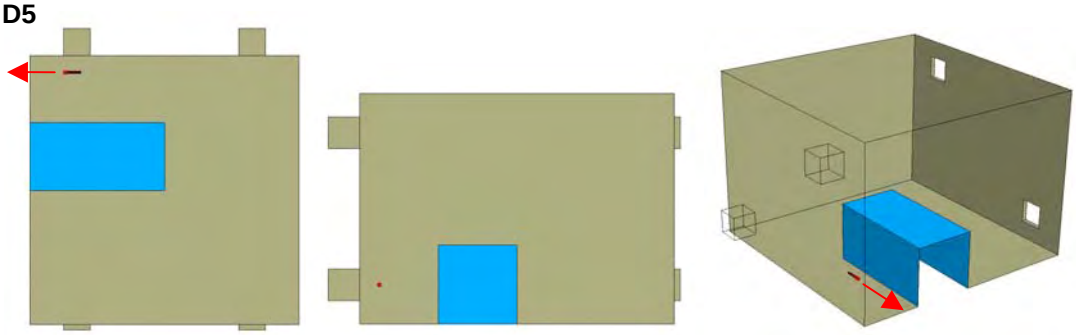

Case D6

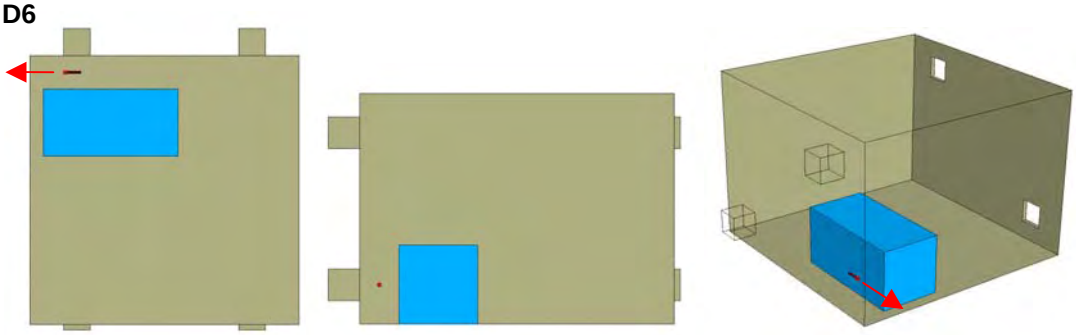

Case D7

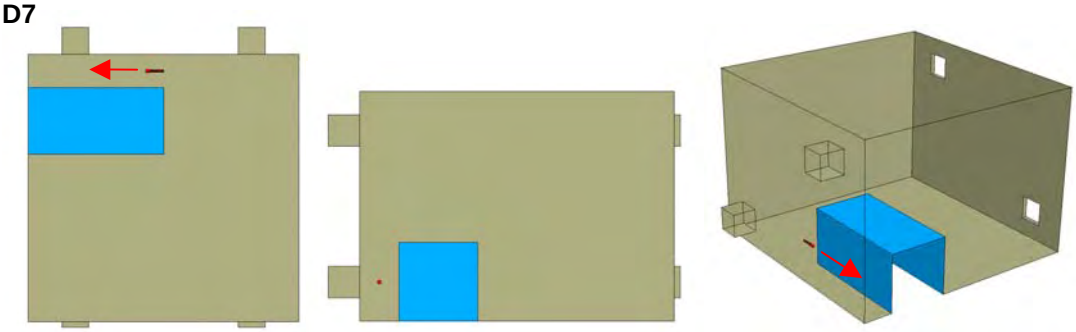

Case D8

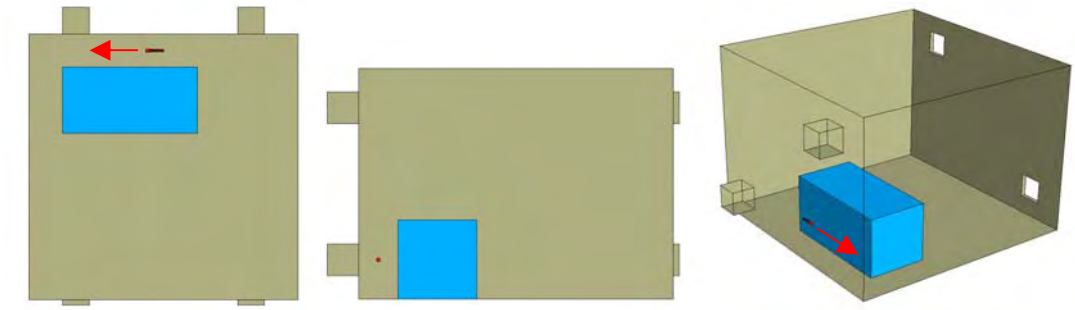

Plan View Side View Perspective

(For Figure caption see subsequent page)

Case D9

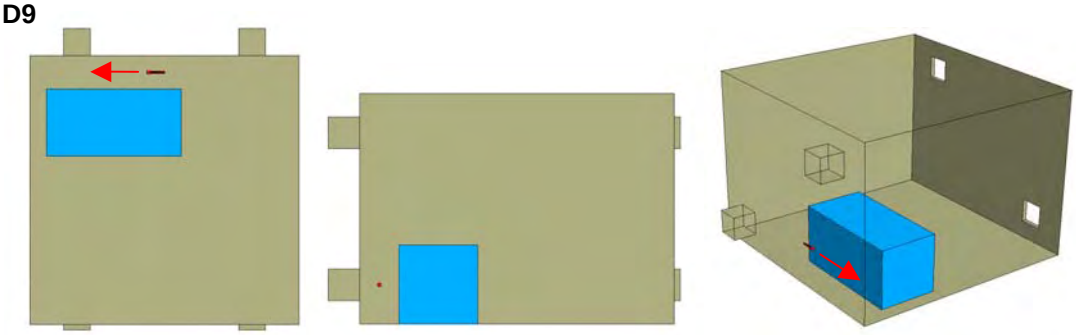

Case D10

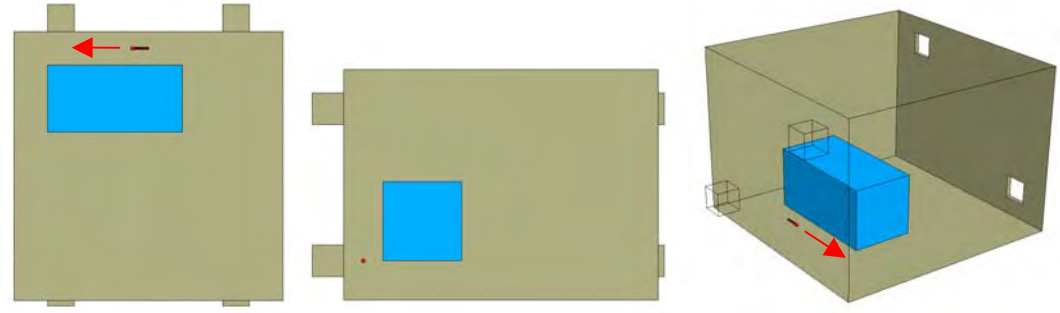

Case D11

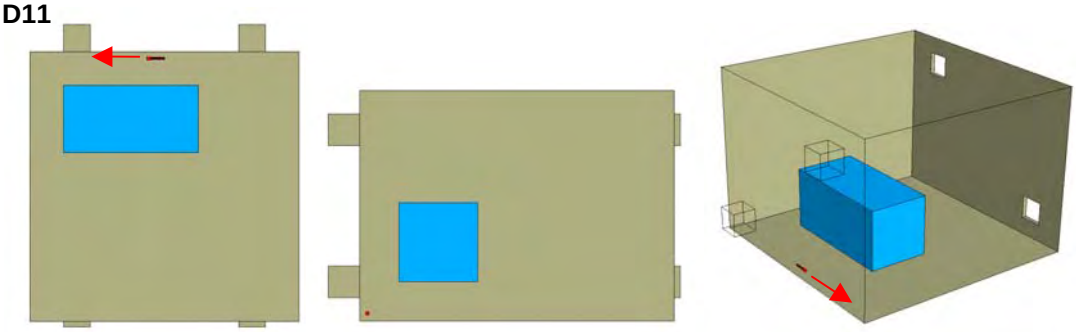

Case D12

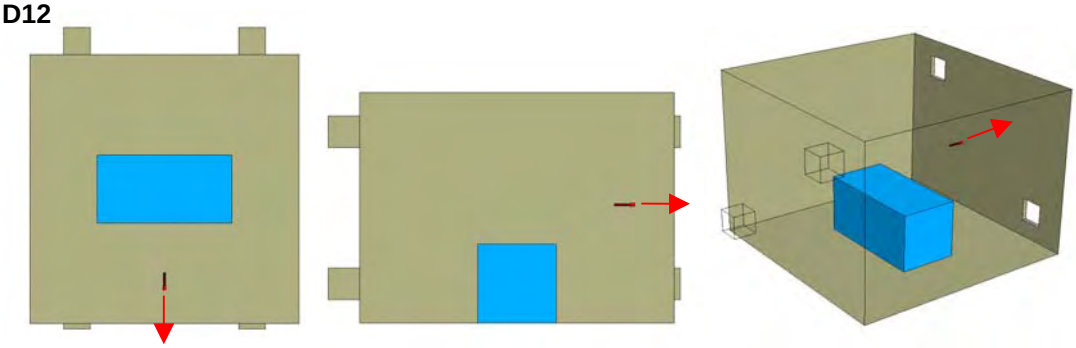

Plan View Side View Perspective

(For Figure caption see subsequent page)

Case D13

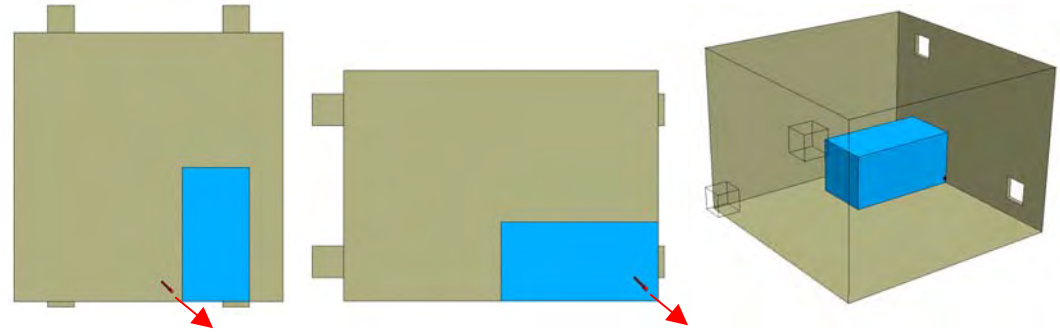

Figure 12.2 Arrangements of the leak and box obstruction (shown in red and blue, respectively) used in each of the 13 sensitivity tests.

Case D1

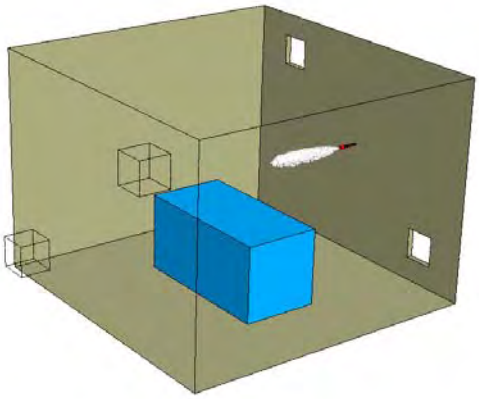

Case D2

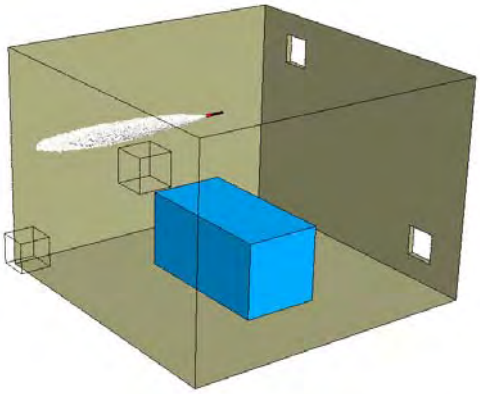

Case D3

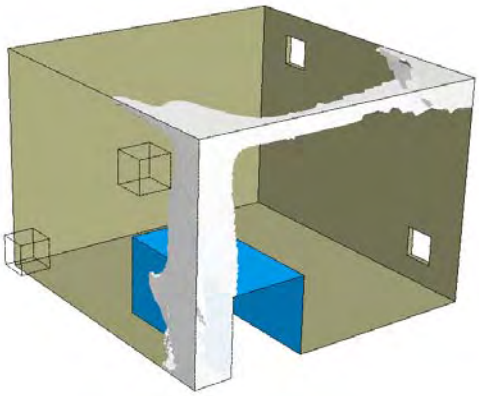

Case D4

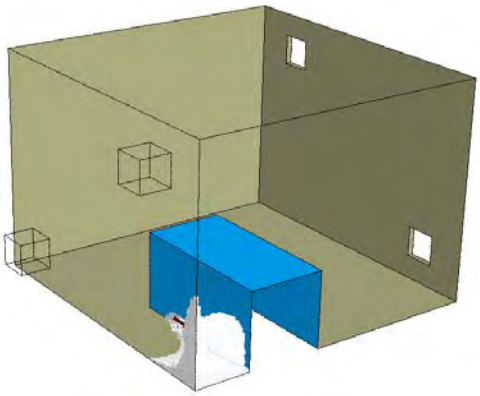

(For Figure caption see subsequent page)

Case D5

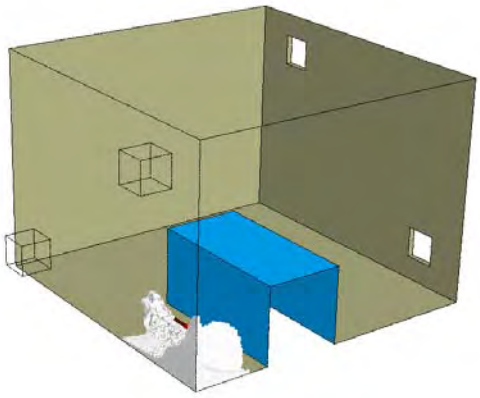

Case D6

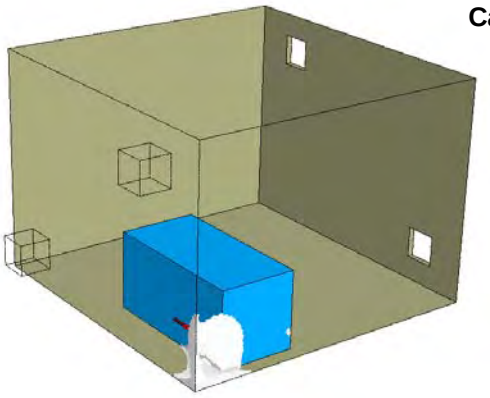

Case D7

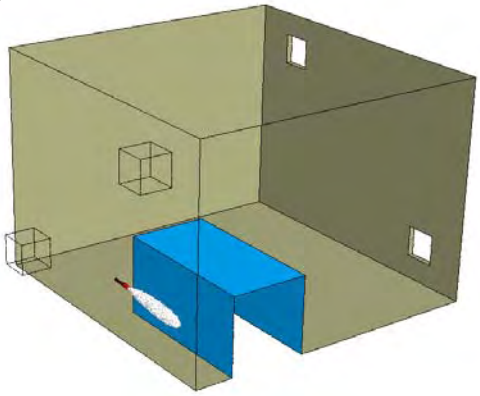

Case D8

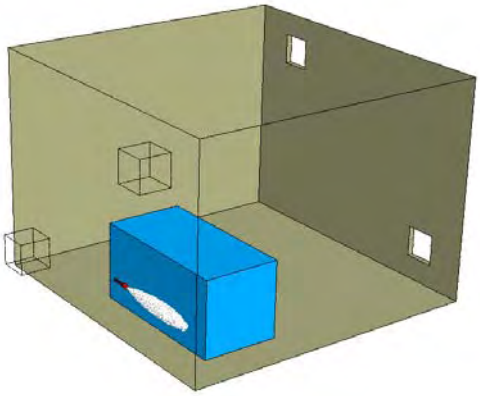

Case D9

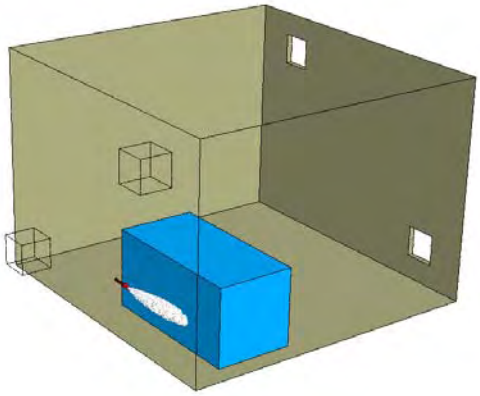

Case D10

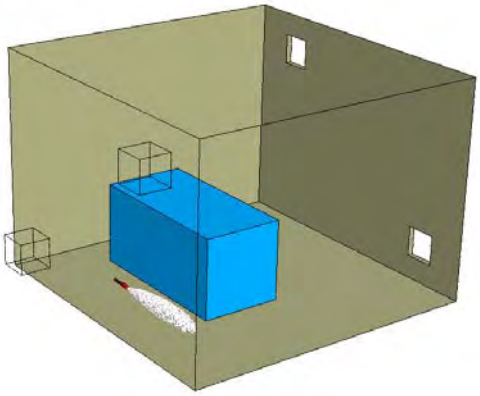

(For Figure caption see subsequent page)

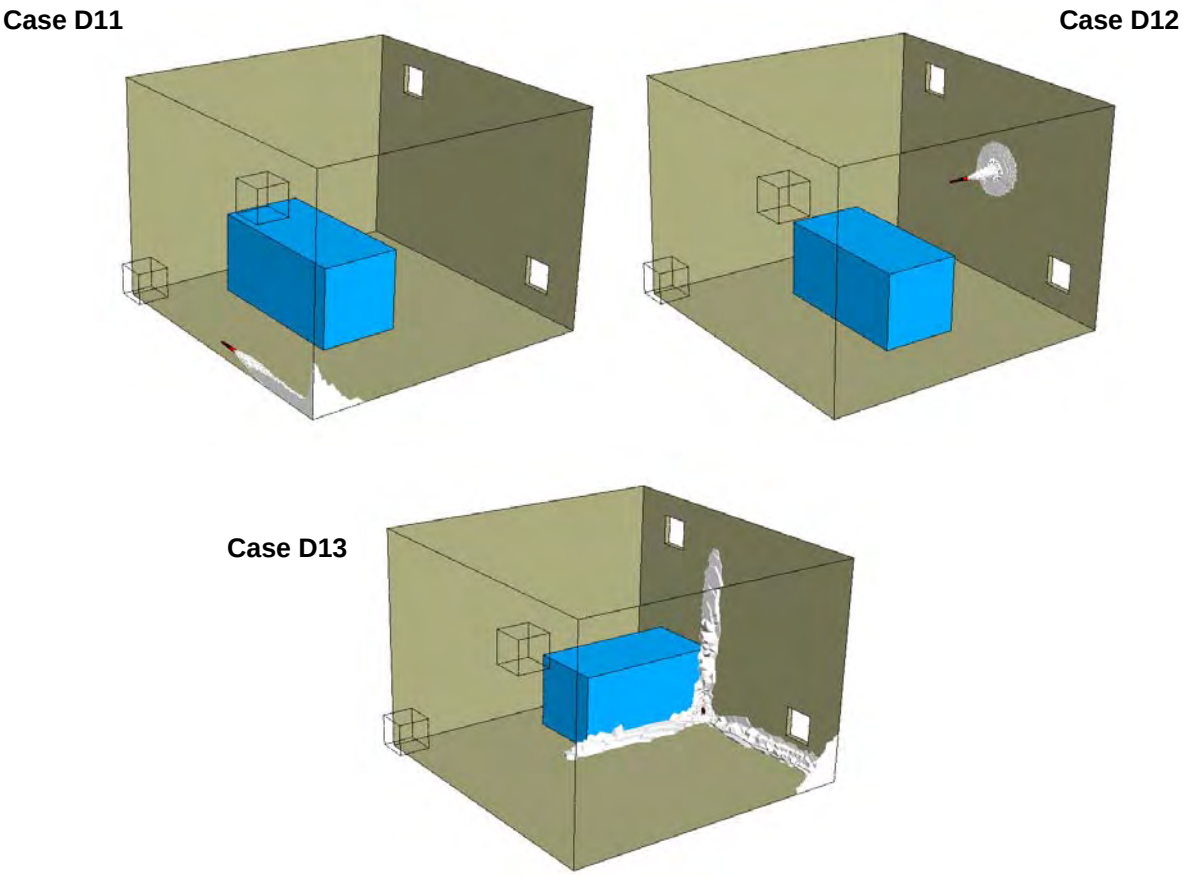

Figure 12.3 V_z clouds (shown in white) produced from a 0.86 g/s release with a ventilation rate of 12 ach in the 13 different leak and blockage configurations.

Table 12.1 Summary of the predicted V_z cloud volume and details of the enclosure geometry

Case	*V_z Cloud Volume (m^3)*	*Nozzle to wall distance (m)*	*Width of cavity containing leak (m)*	*Gap from box to wall/floor (m)*
D1	0.015	3.74	-	-
D2	0.033	3.0	-	-
D3	0.89	0.5	0.5	0.0
D4	0.092	0.5	0.75	0.0
D5	0.13	0.5	1.0	0.0
D6	0.044	0.5	0.5	0.2
D7	0.013	1.75	0.5	0
D8	0.018	1.75	0.5	0.5
D9	0.016	1.75	0.5	0.25
D10	0.028	1.75	0.5	0.5
D11	0.031	1.75	0.5	0.5
D12	0.017	0.5	-	-
D13	0.20	0.26	-	-

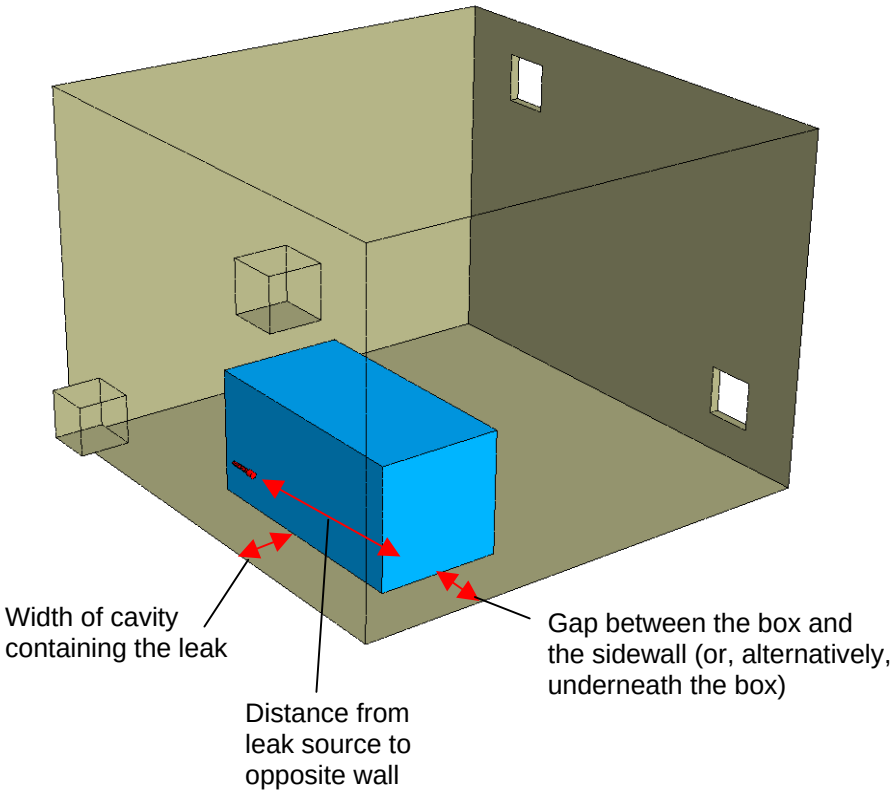

Figure 12.4 Diagram showing the location of the three dimensions given in Table 12.1

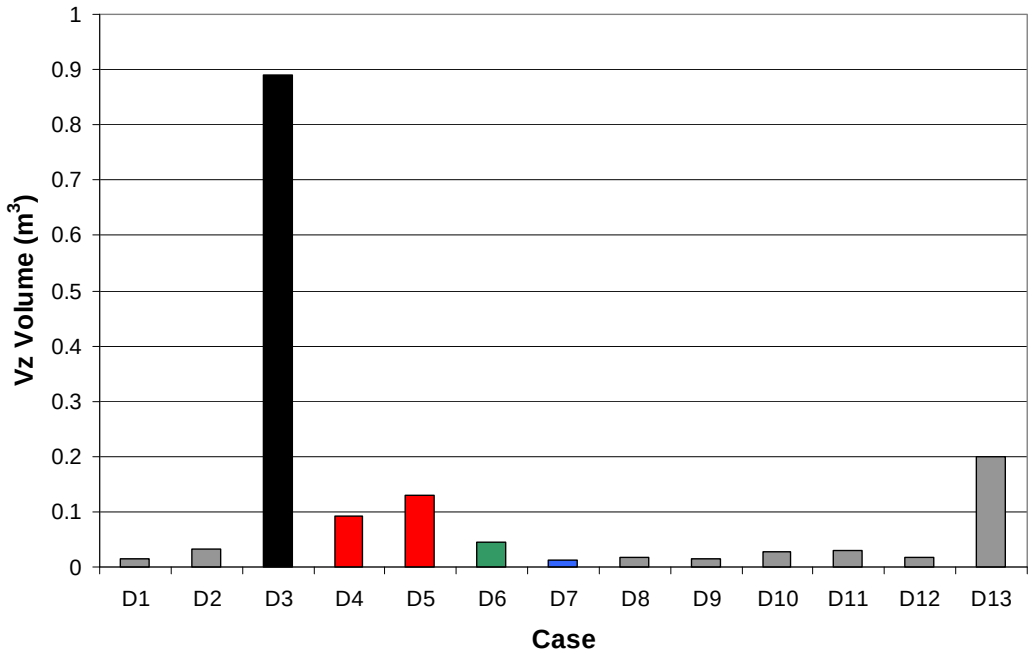

Figure 12.5 Summary of the predicted V_z data for the 13 different blockage and leak orientation tests

12.4 SMALL AND LARGE ENCLOSURES

Gas releases have been modelled in four different sizes of enclosure. The aim of these tests is to cover a number of possible applications, from small gas metering enclosures to a reasonably sized boiler room. The largest space considered (Figure 12.7) is an enclosure 10 m long, 10 m wide and 4.25 m high with a boiler-sized cylindrical obstruction of diameter 2.5 m and length 5 m. The ventilation inlet into the enclosure is a long slot at low level on one wall and the extract is a similarly shaped opening at high level on the opposite wall. The leak source is located on the same wall as the ventilation inlet and this directs the gas jet into the centre of the enclosure. The configuration is roughly equivalent to case D1 considered in the previous section (or Configuration 1 in the validation study) but in a larger space. The small enclosure (Figure 12.7) is a cube of side 2 m with low-level ventilation inlet and high level extract, again with the gas leak situated on the wall with the inlet and with the gas jet directed into the centre of the enclosure. An even smaller enclosure of sides 1 m has also been studied with a similar configuration to those above, as shown in Figure 12.7. In addition to these three enclosures, the results can be compared to those presented in the previous section, where the enclosure had dimensions 4 × 4 × 2.96 m, which from now on will be referred to as a "medium" sized enclosure.

A wide range of CFD simulations have been undertaken for each of these enclosures, covering a range of different ventilation rates and leak rates. Table 12.2 provides a summary of the 28 tests. In this table, the ventilation rate is expressed in terms of both an air-change-per-hour and a volumetric flow rate in litres/s. Also provided is the average gas concentration at the outlet (see Section 6), expressed as percentage of the lower explosive limit (LEL) of methane[8]. The average gas concentration at the outlet is calculated from the flow rate of gas from the leak

[8] *the lower explosive limit of methane is a gas concentration of 4.4% by volume.*

mixed with the given volumetric flow rate of fresh air supplied to the enclosure. In reality, the gas concentration at the outlet is likely to fluctuate above and below this value over time due to the motion of gas in the enclosure, but on average over time it will equal this value. Finally, the table provides the mean volume of the V_z clouds predicted by the CFD model.

Sample views of the V_z clouds for the 0.86 g/s leak with a ventilation rate of 12 ach in the large and medium enclosures are shown in Figure 12.8 together with views of a 0.15 g/s leak and 6.45 ach in the small enclosure and a 0.013g/s leak and 12 ach in the very small enclosure. These results are highlighted with an asterisk in the first column of Table 12.2. In all four plots, the V_z clouds appear as cigar-shaped volumes issuing from the leak source. The ventilation rate in these cases is sufficient to prevent the build up of gas within the enclosure and in all cases the V_z is below the 0.1 m^3 cut-off necessary for the Zone 2 NE criteria. However, in some other cases in which the ventilation rate was lower, or the leak rate larger, the V_z clouds exceeded the 0.1 m^3 limit. These results are highlighted in red in Table 12.2.

The production of a large V_z cloud correlates well with a high average concentration of gas at the outlet. All the results highlighted in red in Table 12.2 with a V_z greater than 0.1 m^3 have a gas concentration at the outlet above 36% LEL. This trend is shown more clearly in Figure 12.9, which plots the V_z cloud volume against the average gas concentration at the outlet. The dotted line in the Figure marks the 0.1 m^3 cut-off. In some tests, the V_z cloud filled nearly the entire enclosure. A notable example is the 0.013 g/s release in the very small enclosure with a ventilation rate of 1 ach, where the V_z volume was 0.80 m^3 (compared to a enclosure volume of 1 m^3). The release rate in this case is equivalent to a pressure of 21 mbarg and a hole size of 0.25 mm^2. It should not be surprising that the V_z is so large here as the ventilation rate of 1 ach equates to only 0.28 litres/s of fresh air and the average concentration at the outlet is well above LEL.

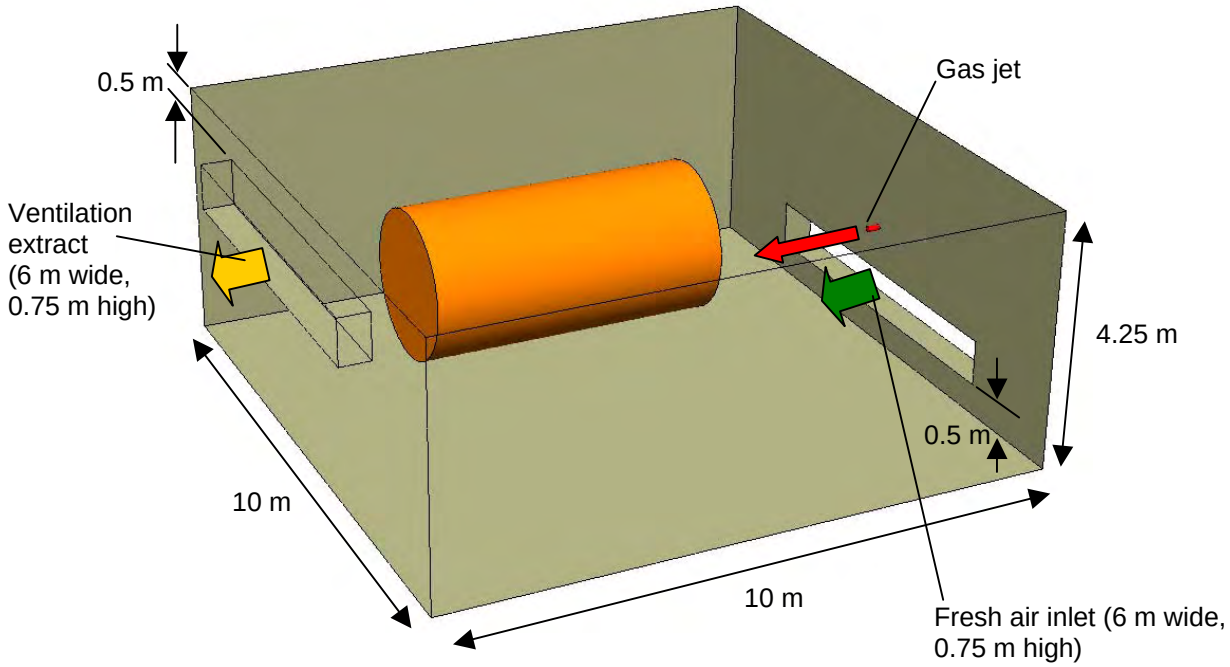

Figure 12.6 Large enclosure showing the location of ventilation inlets and extracts, and the leak source

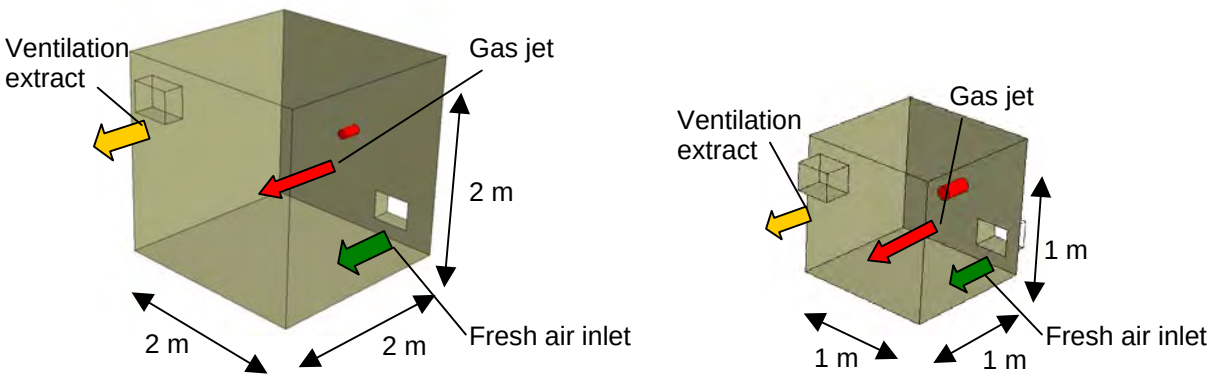

Figure 12.7 Small and very small enclosures (not to scale) showing the location of ventilation inlets and extracts, and the leak source.

Table 12.2 Summary of cases studied with large, medium, small and very small enclosure volumes with the leak directed into the centre of the enclosure

Enclosure	*Enclosure Volume (m^3)*	*Leak Size (g/s)*	*Ventilation Rate (ach)*	*(litres/s)*	*Average conc. at outlet (% LEL)*	*V_z Volume (m^3)*
Large	400	0.47	2	222	7.2	0.0022
Large	400	0.86	6	667	4.4	0.0059
Large*	400	0.86	12	1333	2.2	0.0053
Large	400	1.72	3	333	17.6	0.025
Large	400	2.00	1.72	191	35.7	0.047
Medium	45	0.15	6	75	6.9	0.00048
Medium	45	0.22	12	149	5.0	0.0041
Medium	45	0.26	2	25	35.3	0.024
Medium	45	0.26	6	75	11.9	0.0015
Medium	45	0.47	2	25	64.7	45
Medium	45	0.47	6	75	21.6	0.0082
Medium	45	0.47	12	149	10.8	0.0039
Medium	45	0.49	12	149	11.2	0.0075
Medium	45	0.86	2	25	118.3	45
Medium	45	0.86	6	75	39.4	0.24
Medium*	45	0.86	12	149	19.7	0.015
Medium	45	0.86	24	298	9.9	0.008
Medium	45	1.72	12	149	39.4	0.68
Small	8	0.062	13	29	7.5	0.00020
Small	8	0.086	6.9	15	20.0	0.00051
Small	8	0.15	3.07	6.8	75.0	8
Small*	8	0.15	6.45	14	35.7	0.0095
Small	8	0.22	7.5	17	45.0	0.13
Small	8	0.47	6	13	120	8
Small	8	0.49	8.36	19	90.0	8
Small	8	0.86	22	49	60.0	8
V. Small	1	0.013	1	0.28	160	0.80
V. Small*	1	0.013	12	3.3	13.3	0.00016

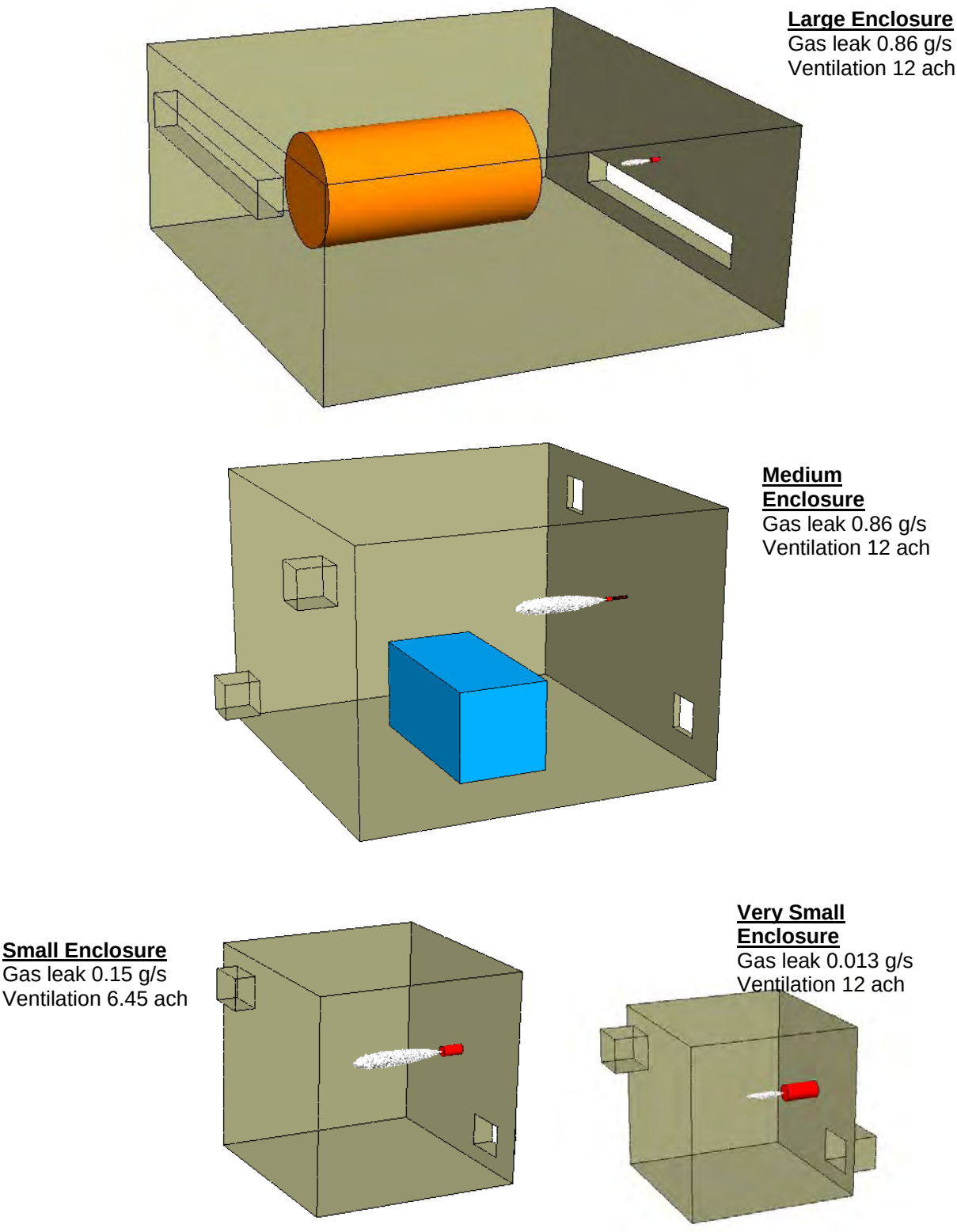

Figure 12.8 V_z clouds (shown in white) for the large, medium, small and very small enclosures. The leak rate and ventilation rate in each case are indicated.

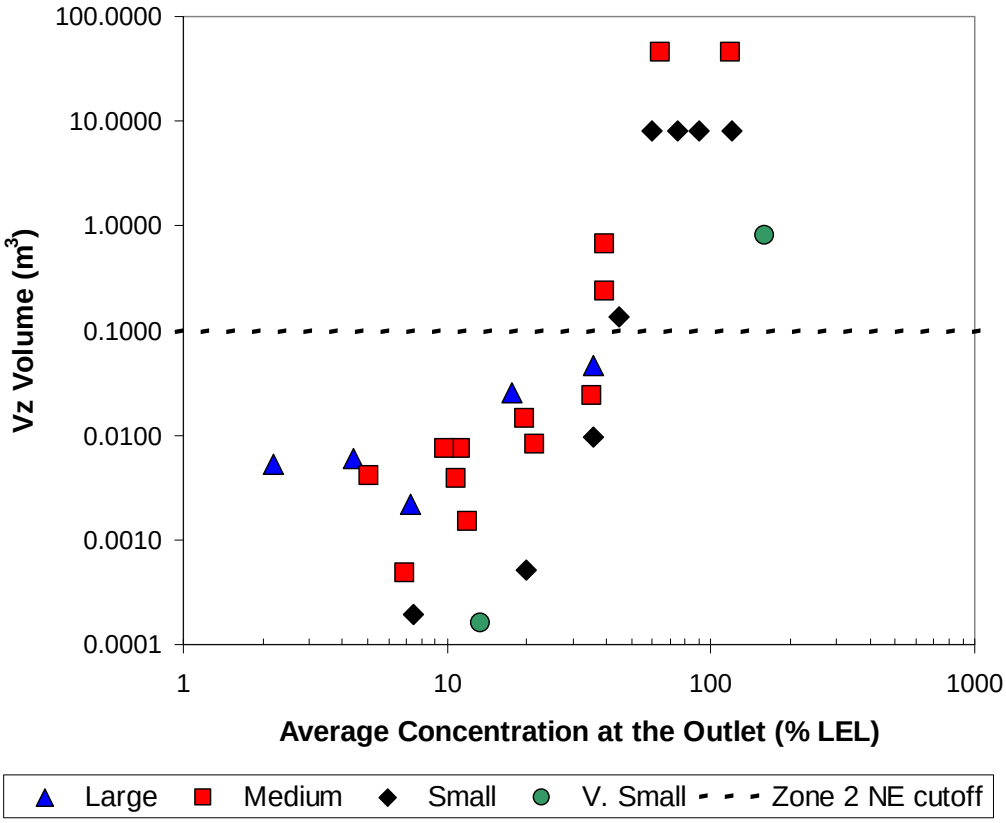

Figure 12.9 Variation of predicted mean V_z volume with the average concentration of gas at the outlet for enclosures of different size in which the gas jet is directed into the centre of the enclosure.

Further tests in the medium and large enclosure have explored the "worst-case" scenario where the leak is situated in a confined region between a box-shaped obstruction and a wall in one corner of the enclosure (similar to case D3 in the previous section or Configuration 3 in the validation study). Figure 12.10 shows the V_z cloud for this configuration in the large and medium enclosures for a leak rate of 0.86 g/s and ventilation rate of 6 ach. Near the source a similar flow pattern is produced in the large enclosure as in the medium-sized enclosure near the source. A flow recirculation is formed in the cavity which leads to the gas becoming dilute more slowly than for the unobstructed releases. However, unlike the medium-sized enclosure where the V_z nearly fills the entire space, the cloud in the large enclosure is confined to a relatively small region near the source. This is probably related to the much higher ventilation rate in absolute terms in the large enclosure than in the medium-sized enclosure (a flow rate of 667 litres/s instead of just 75 litres/s). Table 12.3 summarises the details of all the tests with this configuration and also includes the results previously presented as part of the validation exercise (see Appendix D). The predicted V_z volumes are also plotted against the average gas concentration at the outlet in Figure 12.11, with the previous results (i.e. Figure 12.9) shown in grey for comparison.

The V_z clouds produced from these scenarios where the leak is located in a confined space are all larger than for the previous case in which the gas jet was directed into the centre of the

enclosure. The results indicate that, for the cases considered, in order to produce a V_z smaller than 0.1 m^3 in this configuration it is necessary to have an average gas concentration at the outlet of less than 19% LEL.

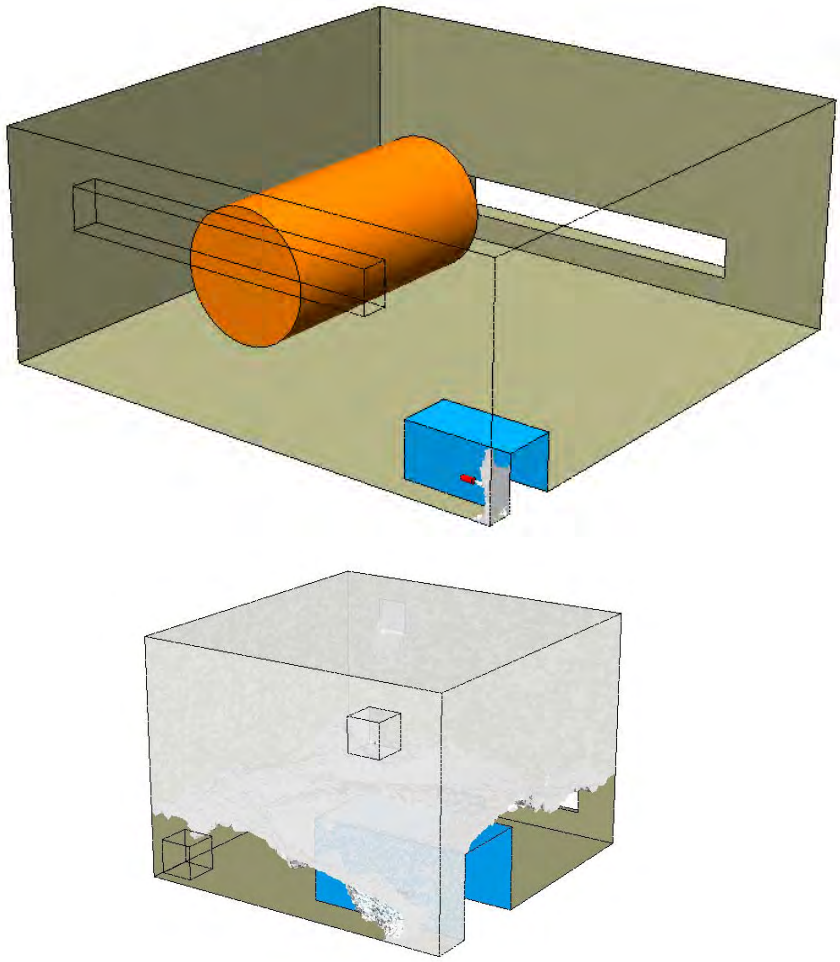

Figure 12.10 V_z clouds for large and medium sized enclosures with the gas released in a confined space in one corner of the enclosure. In both cases the gas release rate is 0.86 g/s and the ventilation rate 6 ach.

Table 12.3 Summary of cases studied with large and medium sized enclosures with the gas released in a confined spaced in one corner of the enclosure

Enclosure	*Enclosure Volume (m^3)*	*Leak Size (g/s)*	*Ventilation Rate*		*Average conc. at outlet (% LEL)*	*V_z Volume (m^3)*
			(ach)	*(litres/s)*		
Large	400	0.86	6	667	4.4	0.026
Medium	45	0.029	2	25	4.0	0.00011
Medium	45	0.26	6	75	11.9	0.0017
Medium	45	0.47	2	25	64.7	44
Medium	45	0.47	6	75	21.6	0.17
Medium	45	0.47	12	149	10.8	0.011
Medium	45	0.49	12	149	11.2	0.020
Medium	45	0.86	2	25	118.3	45
Medium	45	0.86	6	75	39.4	34
Medium	45	0.86	12	149	19.7	0.89

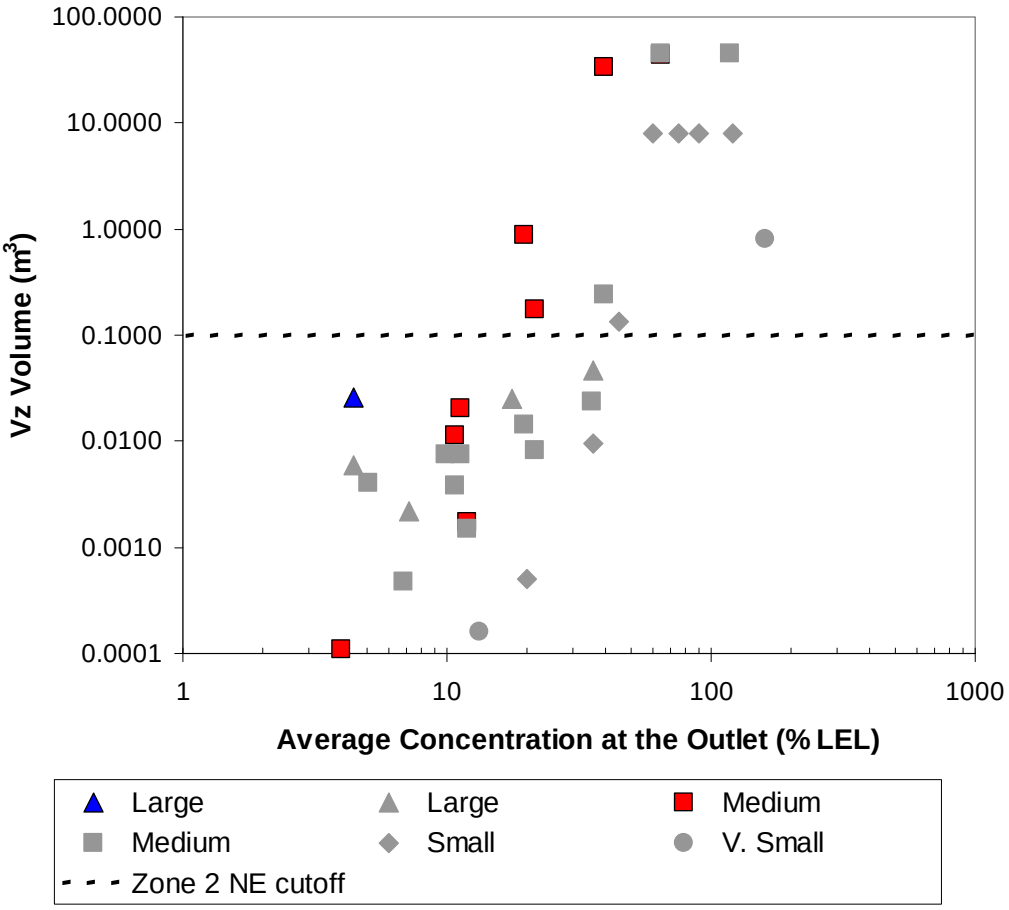

Figure 12.11 Variation of predicted mean V_z volume with the average concentration of gas at the outlet for enclosures of different size. Points shown in grey are for cases where the gas jet is directed into the centre of the enclosure, points in red and blue are for the cases where the leak is situated in a confined space in a corner of the enclosure.

12.5 SUMMARY OF ISOTHERMAL RESULTS

All of the CFD results presented up to this point have considered enclosures in which temperature differences have been very small. Essentially the scenarios can be considered to be isothermal. All surfaces have been assumed to be adiabatic (i.e. perfectly insulated), fresh air has entered the enclosure at 20 °C and the only source of temperature differences in the enclosure has been the leak source, which for the majority of the cases (where the releases have been choked) has been -18 °C. Before continuing to the next Section, in which the effects of heat transfer are investigated, it is useful to summarise all the data collected so far. Figure 12.12 plots all 60 results from the validation tests in Appendix D and the sensitivity tests described above. The shape of the symbols denotes the size of the enclosure (triangle = large, square = medium, diamond = small, circle = very small) and the colours now indicate which configuration was tested: red for Configuration 1 where the gas jet issued into the centre of the enclosure, green for Configuration 2 where the jet ran alongside one of the walls, blue for Configuration 3 where the jet was in a confined space in one corner of the enclosure, and finally grey for any other configurations tested. There are a number of new points on this graph that have been added onto that shown previously in Figure 12.11. Near the centre of the plot are clustered in a vertical line a number of grey squares. These are the results for different blockage and leak orientations which were discussed in Section 12.3. Since the leak and ventilation rates are identical in all these cases (0.86 g/s and 12 ach) the average concentration at the outlet is identical and so they appear in a vertical line. The grey triangle is from a simulation in the large enclosure with leak rate 0.86 g/s, ventilation rate 6 ach and a similar arrangement to Configuration 3 except that the cavity between the box and the wall in which the leak source was located was 1.0 m instead of 0.5 m wide. For this case, widening the cavity by 0.5 m decreased the V_z from 0.026 to 0.012 m^3. The majority of the other new points on the graph are for the medium-sized enclosure, shown as squares, from the validation study (see Appendix D).

The new points on the graph support the observation seen in Figure 12.11, in which V_z increases as the average concentration of gas at the outlet increases. Based on these isothermal results alone it appears that the V_z cloud volume is below 0.1 m^3 in enclosures where the ventilation rate is sufficient to maintain an average gas concentration at the outlet below 19% LEL.

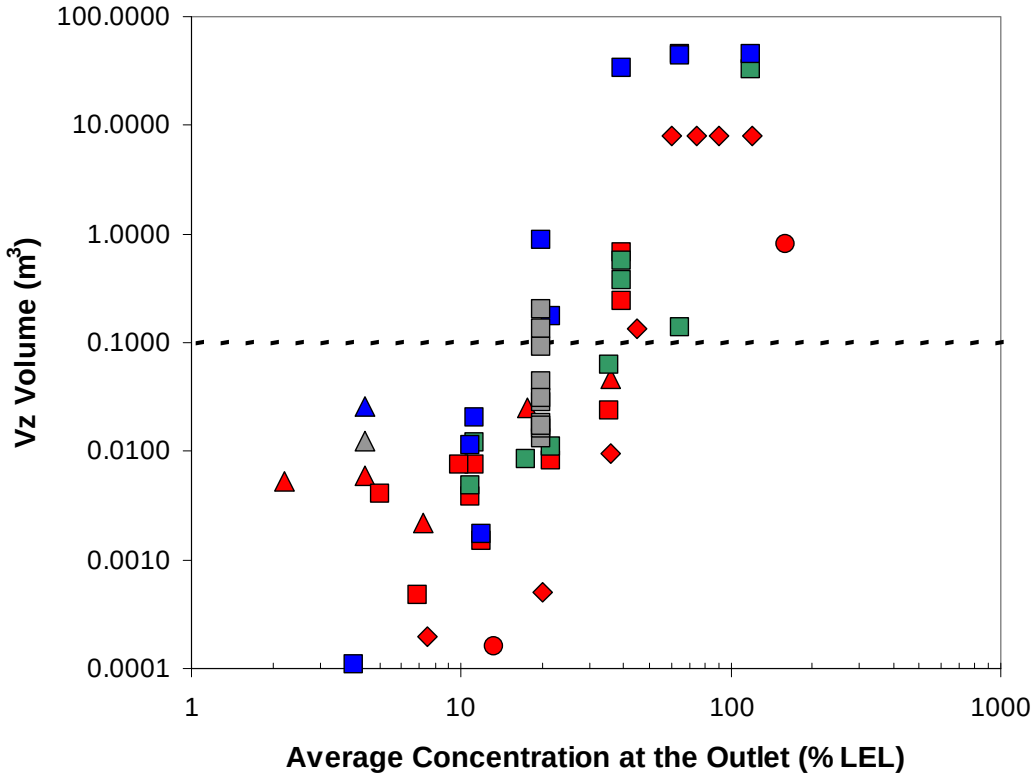

Key

- Shape denotes enclosure size: ▲ = large ; ■ = medium; ◆ = small; ● = very small
- Colours denotes configuration: **Configuration 1, Configuration 2, Configuration 3** Other

Figure 12.12 Summary of CFD results for all isothermal cases

12.6 HEAT SOURCES / SINKS

There are a number of possible sources of temperature differences in enclosures in which gas leaks may occur. Floor slabs are often cooler than walls, fresh air entering the enclosure may be cool or warm relative to the mean enclosure temperature, and boilers or other equipment may present hot or cold surfaces. The purpose of this section is to investigate how these temperature differences may affect the size of a gas cloud produced by a leak. Several scenarios have been examined:

- Cold floors
- Hot boilers and other obstructions with all other enclosure surfaces adiabatic
- Hot boilers with heat loss through the enclosure walls

In CFD models there are two principal ways in which thermal effects can be specified on wall surfaces: either by specifying a constant surface temperature or by specifying a constant heat flux from the surface (a positive flux for hot walls and negative for cold). Previous research (Ivings *et al.*, 2004) has suggested that, using standard CFD models, the former approach can actually under-predict the amount of heat transfer by a factor of two or more. In the tests undertaken here, both prescribed surface temperatures and prescribed heat fluxes are

investigated. Regardless of the approach used in the CFD model to prescribe the thermal conditions, the most important aspect of these tests is to set up realistic, or at least representative, temperature gradients in the enclosure. It has been assumed that a realistic temperature gradient in a boiler room may be for the temperature to increase from 20 °C at low level up to perhaps 30 °C close to the ceiling.

Table 12.4 summarises the 5 cases considered with a cold floor in which the temperature of the floor surface was set at 16 °C while fresh air entered at 20 °C. Four of the tests were undertaken in the medium-sized enclosure and one in the smaller 2-metre-cubed enclosure. The second column in Table 12.4 describes the leak and obstruction configuration. The three configurations are the same as those used in the earlier validation study (see Appendix D): in Configuration 1 the gas jet is directed into the centre of the enclosure, in Configuration 2 the jet flows along a side wall, and in Configuration 3, the jet is located in a confined space between the box and one corner of the enclosure. Details of the leak and ventilation rates are provided in the table. The final two columns are the predicted mean V_z cloud volumes. The results from the tests involving cold floors are provided and, for comparison purposes, the predicted V_z obtained from previous tests with adiabatic floors are also included.

Overall, the presence of a cold floor has a relatively modest effect on the cloud volumes. In some cases the gas cloud increases in size when the floor is cold while in other cases it decreases in size. The most significant differences are for the 0.47 g/s release with a ventilation rate of 12 ach for Configuration 3. In this case there is a three-fold increase in the cloud volume in going from an adiabatic to a cold floor, however in both instances the V_z is still less than 0.1 m^3. Figure 12.13 plots the V_z cloud, the temperature and the density fields for this case. The cooling effect of the floor is confined to a relatively narrow layer and thermal stratification is limited to a height of a few tens of centimetres above the floor at most. The density contours do not show significant differences between the isothermal and cold-floor cases close to the release or in the upper part of the enclosure.

Table 12.4 Summary of CFD simulations with cold floors

Enclosure	***Config.***	***Enclosure Volume (m^3)***	***Leak Size (g/s)***	***Ventilation Rate***		***Average conc. at outlet (% LEL)***	***V_z Volume (m^3)***	
				(ach)	***(l/s)***		***Isothermal***	***Cold floor***
Medium	C2	45	0.86	12	149	19.7	0.033	0.038
Medium	C3	45	0.47	6	75	21.6	0.17	0.092
Medium	C3	45	0.47	12	149	10.8	0.011	0.046
Medium	C3	45	0.86	12	149	19.7	0.89	1.2
Small	C1	8	0.062	6	13	16.1	-	0.00029

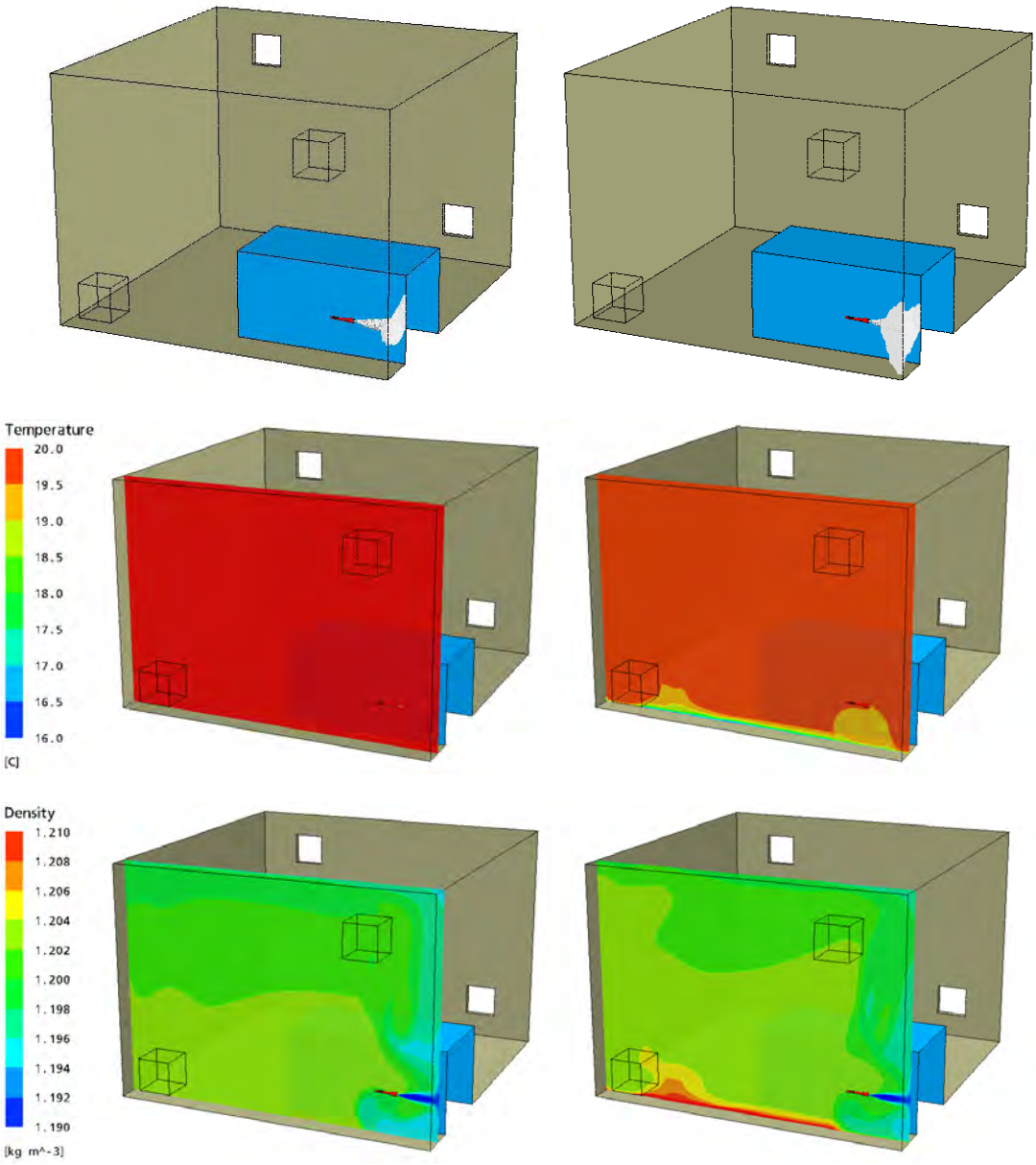

Figure 12.13 Results comparisons for a 0.47 g/s release with ventilation rate of 12 ach showing V_z cloud size (top), temperatures on a vertical plane through the leak source (middle) and density contours (bottom), for an adiabatic floor (left) and 16 °C floor (right)

Further simulations investigated the effect of heat sources in enclosures. A summary of the CFD simulations for these tests is given in Table 12.5. All of these simulations used the large enclosure with a leak source of 0.86 g/s in the Configuration 3 arrangement. Two different ventilation rates were studied: 6 and 12 ach. The boiler surfaces were either given a surface temperature of 70 °C or a prescribed heat flux of 84 W/m^2 in the CFD model. The latter condition is calculated from empirical heat transfer formulae based on the boiler having a surface temperature of 40 °C, an air temperature of 20 °C and the air flowing over the surface having a velocity of 0.15 m/s. Details of the calculation involved in arriving at the prescribed heat flux value are given in Ivings *et al*. (2004). Tests showed that due to the under-prediction of heat transfer when a surface temperature was applied directly in the CFD model, the 70 °C case produced nearly the same net heat flux as the 84 W/m^2 case. In four of the calculations the walls of the enclosure were adiabatic (marked as a dash in Table 12.5), while in the other two calculations, the four side walls of the enclosure were set to either 20 °C or had a heat flux of -2.7 W/m^2. This heat flux was again calculated based on empirical heat transfer formulae. Finally, in one simulation the 2 × 1 × 1 metre box-shaped obstruction near the leak source was given a surface temperature of 40 °C. The final two columns in Table 12.5 compare the predicted V_z cloud volumes for the case where all surfaces are adiabatic and the case where they are given the thermal boundary conditions described in the table. Results for fully-adiabatic conditions were only available for the 6 ach case.

The CFD model predicts a significant increase in the size of the V_z cloud in simulations where the surface of the boiler is hot instead of adiabatic. The V_z rises by a factor of 38, from 0.026 m^3 to around 1.0 m^3, for the 6 ach case with either a 70 °C surface temperature or 84 W/m^2 heat flux. The cause of this increase is strong thermal stratification in the enclosure. Figure 12.14 plots the V_z cloud and temperature contours at various planes in the enclosure. These show that the temperature near the ceiling reaches a maximum of around 27 °C, while at floor level it remains at around 20 °C. Near the gas leak, the relatively high gas concentrations produce a cloud with positive buoyancy. This causes the gas to rise in a plume towards the ceiling from the source region. As the gas rises it encounters air at a higher temperature and eventually the density of the surrounding air becomes less than that of the gas in the plume. The gas at this point has insufficient buoyancy to penetrate further upwards and instead it stops rising and starts to spread horizontally, forming a layer beneath the warm air[9]. This is shown more clearly in Figure 12.15, which plots the cloud of gas above 5 % of LEL, coloured according to height. The gas cloud reaches a maximum height of just over 3 metres before spreading out laterally across the enclosure (the ceiling height in this case is 4.25 m). The layer within the first metre of the ceiling is free of gas. The thermal stratification provides an artificial lid on the upward movement of the gas plume, effectively reducing the height of the enclosure in which dispersion can take place. A more important consequence of the thermal stratification in the upper half of the enclosure is that it will damp the turbulent mixing in the vertical direction, so that dilution of the gas cloud is very much reduced.

Modifying the conditions at the side walls of the enclosure so that instead of being effectively perfectly insulated (adiabatic) they have a constant temperature of 20 °C or a heat flux of -2.7 W/m^2, has little effect on the predicted V_z cloud size (see Table 12.5). A comparison of the predicted temperatures in the enclosure with the adiabatic, 20 °C and -2.7 W/m^2 walls is given in Figure 12.16.

[9] *This flow behaviour is similar to that observed in the atmosphere on high-pressure days when there is a temperature inversion (i.e. a layer in the atmosphere where the temperature increases with altitude). Under these conditions, smog is trapped under the inversion layer leading to a darker grey region of haze at lower level with blue skies above.*

A further simulation was undertaken with the temperature of the box adjacent to the leak source fixed at 40 °C instead of being adiabatic. This led to roughly a five-fold reduction in the size of the V_z cloud. The hot box adjacent to the source produces a convective plume which draws in fresh air from the surroundings. This additional draught of fresh air helps to dilute the gas jet, reducing the gas cloud size.

Table 12.5 shows that at a higher ventilation rate of 12 ach, which for the 0.86 g/s release produces an average outlet concentration of only 2.2 % of LEL, it is still possible to obtain large V_z clouds. In this case, the V_z actually increases slightly from 1.0 to 1.6 m^3 as the ventilation rate is increased from 6 to 12 ach.

All of these results presented in Table 12.5 are for the Configuration 3 scenario in the large enclosure. Two further calculations have been undertaken in different configurations to study the relative importance of the stratification compared to the local confinement experienced by the leak. The first involved only a minor modification to the geometry. The box was moved sideways to increase the width of the cavity containing the leak source from 0.5 to 1.0 metres. This led to a reduction in the V_z from 0.95 to 0.15 m^3. This change in V_z is similar to that observed in the purely isothermal cases examined for the equivalent geometries in the medium-sized enclosure (see Section 12.3), where the V_z reduced from 0.89 to 0.13 m^3.

The second calculation was a repeat of case D2 in Section 12.3 involving a gas release in the medium-sized enclosure with the gas jet directed along one of the walls (the same as Configuration 2 in the validation study), but with the box in the centre of the enclosure now having a surface temperature of 70 °C. Here the size of the V_z cloud was unchanged by the presence of the heat source. The predicted V_z and temperature contours for this case are shown in Figure 12.17. In this case, the high momentum, relatively unconfined release appears to be less sensitive to thermal stratification than in the previous cases in which the jet issued into a confined space and produced a low-momentum plume. This is probably because the turbulent mixing induced by this unconfined jet is effective in overcoming the tendency of the thermal stratification to damp turbulence.

Table 12.5 Summary of CFD simulation in the large enclosure with non-adiabatic conditions

Leak Size	***Ventilation Rate***		***Average outlet conc.***	***Thermal boundary conditions on:***			***V_z Volume (m^3)***	
(g/s)	***(ach)***	***(l/s)***	***(% LEL)***	***Boiler***	***Walls***	***Box***	***Isothernal***	***Thermal***
0.86	6	667	4.4	70 °C	-	-	0.026	1.0
0.86	6	667	4.4	84 W/m^2	-	-	0.026	0.95
0.86	6	667	4.4	84 W/m^2	20 °C	-	0.026	0.89
0.86	6	667	4.4	84 W/m^2	-2.7 W/m^2	-	0.026	1.0
0.86	6	667	4.4	70 °C	-	40 °C	0.026	0.23
0.86	12	1333	2.2	70 °C	-	-	-	1.6

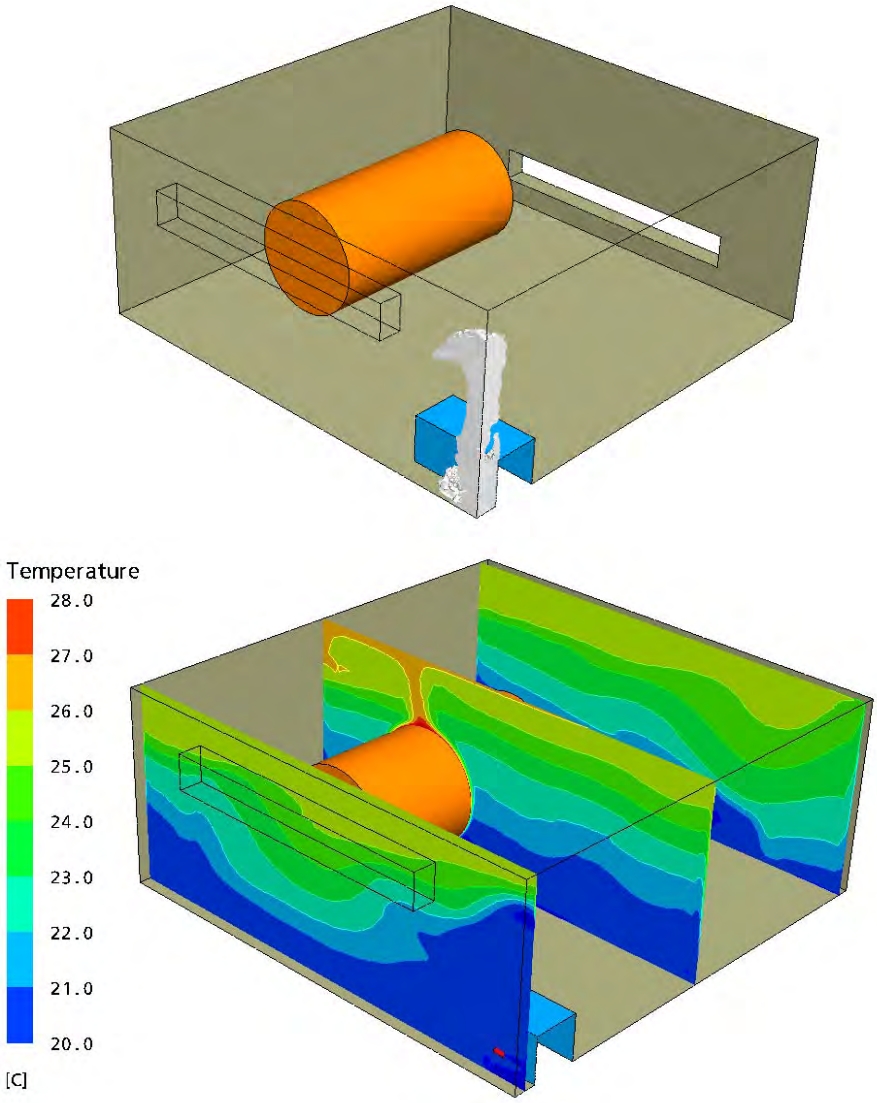

Figure 12.14 CFD predictions for the large enclosure with a constant heat flux of 84 W/m^2 on the boiler surfaces, a gas leak of 0.86 g/s and ventilation rate of 6 ach. The upper plot shows the V_z cloud and the lower plot shows temperature contours at three vertical planes.

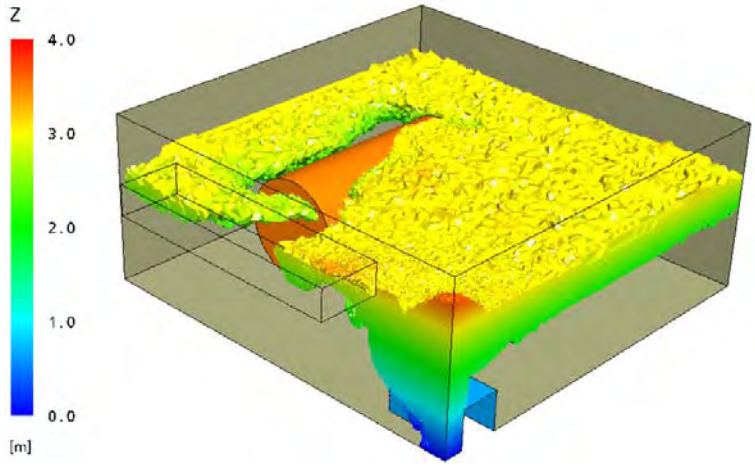

Figure 12.15 CFD predictions of the gas enclosed by an iso-surface at 5 % of LEL for the large enclosure with a constant heat flux of 84 W/m^2 on the boiler surfaces, a gas leak of 0.86 g/s and ventilation rate of 6 ach. The isosurface is coloured by its height above the floor.

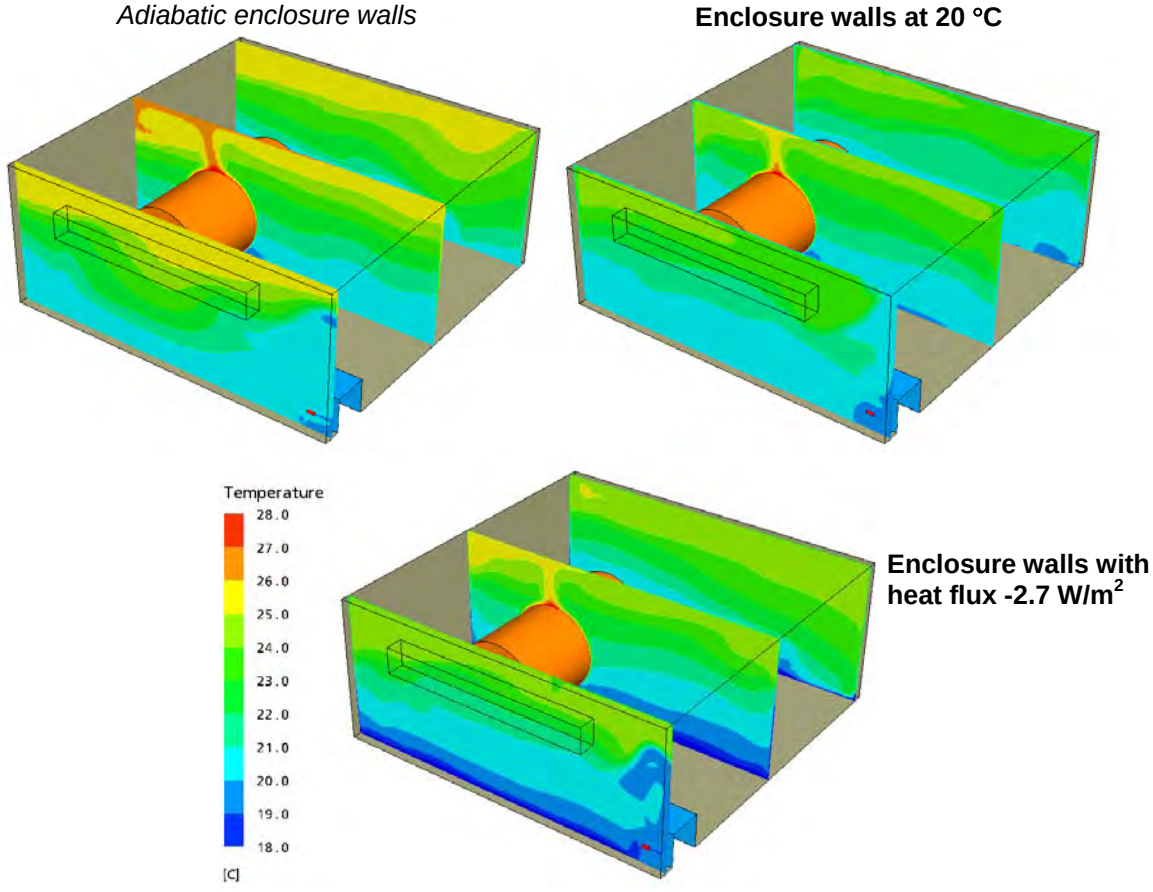

Figure 12.16 Predicted temperatures in the large enclosure with the boiler heat flux of 84 W/m2 and three different thermal conditions on the enclosure walls: adiabatic, 20 °C or -2.7 W/m^2.

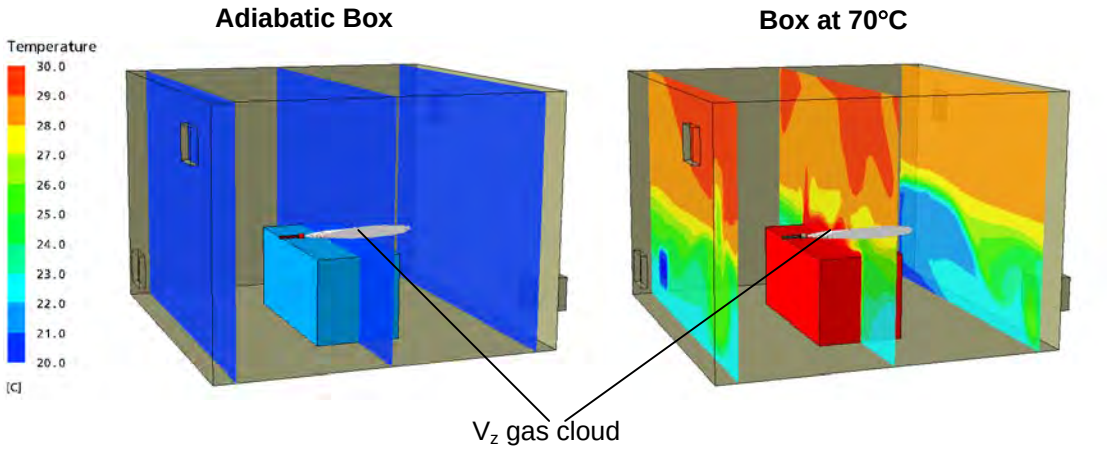

Figure 12.17 Predicted temperature contours and V_z cloud for a 0.47 g/s release in the medium-sized enclosure with a ventilation rate of 12 ach with the central box obstruction adiabatic (left) and with the box having a surface temperature of 70 °C (right).

12.7 SUMMARY AND CONCLUSIONS

The purpose of this part of the project was to perform CFD simulations of gas leaks in enclosures of different size, with obstructions of different shape, for a range of orientations of the leak source, for both isothermal and non—isothermal conditions, to establish what effect these factors have on the resulting gas cloud size, and in particular which factors lead to increased gas cloud volumes.

The results from the CFD simulations suggest that the largest gas clouds are produced when the leak source is located in a tightly confined space. Here, as the jet impinges onto nearby surfaces it produces a local flow recirculation which causes gas to be re-entrained into the source region. This leads to a build-up of gas near the leak which in turn produces a low-momentum buoyant plume of gas rising from the confined space. The worst-case scenario comprises strong thermal stratification with higher temperatures nearer the ceiling. In this case the buoyant gas plume reaches a height where its density matches that of the surrounding warm air whereupon it spreads horizontally in a layer across the enclosure. The thermal stratification strongly damps turbulent mixing in the vertical direction, with the result that the gas cloud is much less effectively diluted than under isothermal conditions. A CFD simulation of this scenario with sufficient ventilation to produce an average gas concentration at the outlet of only 2.2% LEL still produced a V_z cloud in excess of 1 m^3.

The sensitivity of the predicted gas cloud volume to the enclosure size, leak and blockage orientation, ventilation rate and thermal conditions are shown in Figure 12.18, which plots the results for all the cases simulated. The graph shows how the V_z cloud varies as a function of the average gas concentration at the ventilation outlets. The first conclusion from this graph is that there is significant variation in the size of the gas cloud for a given average gas concentration at the outlets; the maximum difference in V_z is roughly four orders of magnitude. This indicates that there is a significant sensitivity in the gas cloud volume to the different conditions tested.

With the exception of the tests involving strong thermal stratification, the results show a general trend for the size of the gas cloud to decrease if the average gas concentration at the outlet

decreases. For these cases, gas clouds less than 0.1 m^3 were produced for an average outlet gas concentration below 19% LEL. However, the presence of strong thermal stratification has been shown to have a marked effect on the size of gas clouds in cases where there was a significant degree of confinement of the release.

Further discussion and interpretation of these results is presented in the main body of the report in Section 6.4.

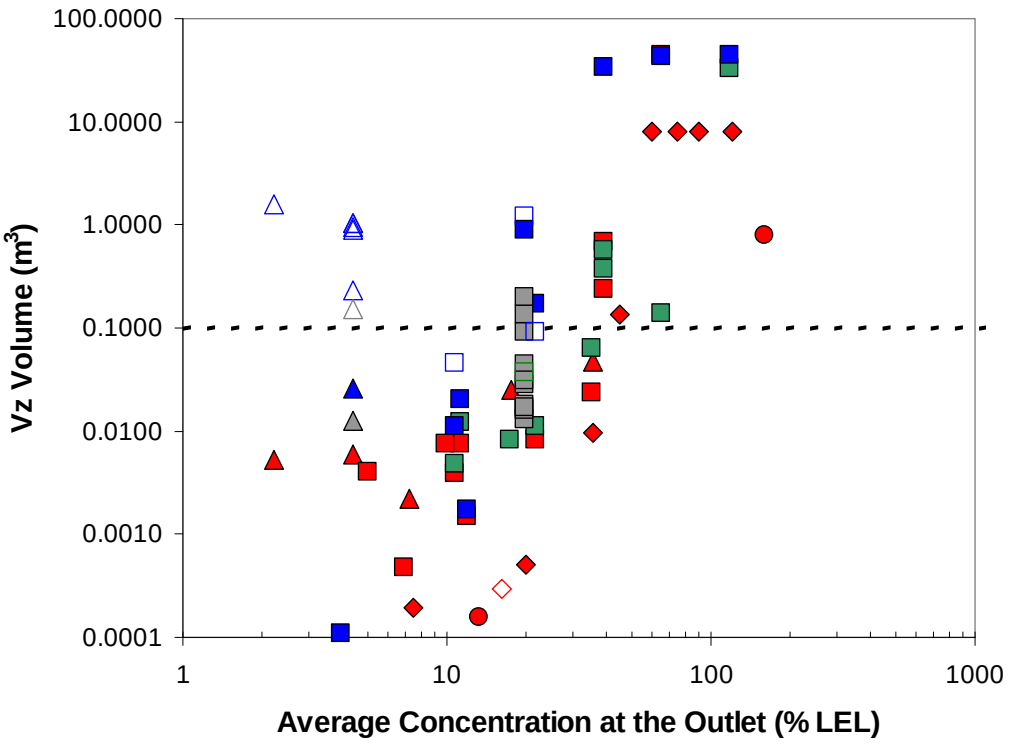

Key

- Shape denotes enclosure size: ▲ = large ; ■ = medium; ◆ = small; ● = very small
- Colours denotes configuration: **Configuration 1,** **Configuration 2,** **Configuration 3** **Other**
- Fill denotes thermal conditions: ▲ = isothermal ; △ = non-isothermal

Figure 12.18 Final summary of all the CFD simulations of gas releases in enclosures

13 REFERENCES

BS 5925:1991 Code of practice for: ventilation principles and designing for natural ventilation. British Standards Institute.

BS EN 60079-10:2003, Electrical apparatus for explosive gas atmospheres, Part 10: Classification of hazardous areas.

BS EN ISO 9300:2005. Measurement of gas flow by means of critical flow Venturi nozzles. British Standards Institution.

Caton, P.G.F. (1976) Maps of hourly mean wind speed over the United Kingdom, 1965 – 1973, Meteorological Office Climatology Memorandum No. 79.

Caton, P.G.F. (1977) Standardized maps of hourly mean wind speed over the United Kingdom and some implications regarding wind speed profiles, Proceedings of the fourth International Conference on Wind Effects on Buildings and Structures, Heathrow 1975, ed K J Eaton, Cambridge University Press.

Chandler, T.J. and Gregory, S. (1976) The climate of the British Isles, Longman, London

CIBSE (1986) Weather and solar data, CIBSE Guide vol A, section A2.

CIBSE (2005) The Chartered Institution of Building Service Engineers, Guide B: Heating, Ventilating, Air Conditioning and Refrigeration.

Communication from the Commission concerning the non-binding guide of good practice for implementing Directive 1999/92/EC of the European Parliament and of the Council on minimum requirements for improving the safety and health protection of workers potentially at risk from explosive atmospheres, /* COM/2003/0515 final */, 25th August 2003, http://eur-lex.europa.eu/LexUriServ/LexUriServ.do?uri=CELEX:52003DC0515:EN:NOT

Cooper, M.G. (2001) A model for jet dispersion in a congested environment, Health and Safety Executive Contract Research Report 396/2001

Cox, Lees & Ang, (1990), Classification of Hazardous locations, The Institution of Chemical Engineers.

CP3 (1972) Code of basic data for the design of buildings, Part 2 Wind loads. British Standards Institute.

Craft, T.J., Launder, B.E. (2001) "On the spreading mechanism of the three-dimensional turbulent wall jet", J. Fluid Mech., Vol 435, pp 305 – 326

Dangerous Substances and Explosive Atmospheres Regulations (2002), SI 2002/2776

Ewan, B.C.R. and Moodie K. (1986) Structure and velocity measurements in under-expanded jets. Combustion Science and Technology, 45: p. 275-288.

Gant, S.E. and Ivings M.J. (2005) CFD Modelling of Low Pressure Jets for Area Classification, Health & Safety Laboratory report HSL/2005/11, Buxton, UK.

Harris R J (1983), Gas Explosions in Buildings and Heating Plant, British Gas

IEC 60079-10 (2002) Electrical apparatus for explosive gas atmospheres, Part 10: Classification of hazardous areas

IGEM/SR/25 (2000), Hazardous area classification of natural gas installations, The Institution of Gas Engineers and Managers

IP15 (2003) Area classification code for installations handling flammable fluids: Model code of safe practice in the petroleum industry Part 15, ISBN 978 0 85293 418 1

Ivings, M. J., Lea, C. J. and Ledin, H. S. (2004), Outstanding safety questions concerning the analysis of ventilation and gas dispersion in gas turbine enclosures: best practice guidelines for CFD, Health & Safety Laboratory Report CM/03/12

Lewis, M.J. (1998), Extension of a simple model for analysis of high pressure gas release to include impingement on plans surfaces, Health and Safety Laboratory report, CM/98/01, Buxton, UK.

List, E. J. (1982) Mechanics of Turbulent Buoyant Jets and Plumes, HMT; The Science & Application of Heat and Mass Transfer. Vol. 6, Turbulent Buoyant Jets and Plumes, pp 1-68. Rodi W. editor.

Meteorological Office (1975) Maps of mean and extreme temperature over the United Kingdom, 1941 – 1970, Meteorological Office Climatology Memorandum No. 73.

Meteorological Office (1976) Averages of temperature for the United Kingdom, 1941 – 1970, Meteorological Office Publications Met 0 883.

McMillan A. (1998), Electrical Installations in Hazardous Areas, Butterworth-Heinemann

14 NOMENCLATURE

a	Constant
a	Speed of sound
A_1, A_2,A_3, A_4	Area of openings
A_w	Effective equivalent area
C	Air change rate
c_c	Centreline gas concentration (vol/vol)
C_d	Discharge coefficient
c_{out}	Average gas concentration at the outlet (vol/vol)
$D1$	Diameter
f	Correction factor
K	Constant
k	Safety factor
L	Axial length scale
LEL_m	Lower explosive limit (kg / m^3)
M	Molecular weight
M_1	Mach number
$\dot{m}$	Mass release rate
P	Pressure
P_*	Critical pressure
P_a	Ambient pressure
Q_{ent}	Entrained air volume flux
Q_w	Volume flow rate
r	Radial distance
R	Radial length scale
R	Universal gas constant
T	Temperature
u	Wind speed
u_m	Wind speed at reference height
V_0	Enclosure volume
v_1	Velocity
VE_1	Measure of ventilation effectiveness
$\dot{V}$	Ventilation rate
V_{stoich}	Equivalent stoichiometric volume
V_z	Gas cloud volume
z	downstream distance
ρ	Density
ρ_{amb}	Ambient density
ΔC_p	Differential mean pressure coefficient
γ	Ratio of specific heats
Subscripts	
0	Stagnation condition
1	Exit condition

HSE

Health and Safety Executive

Area classification for secondary releases from low pressure natural gas systems

The ATEX Workplace Directive (1999/92/EC) has been implemented in the UK as the Dangerous Substances and Explosive Atmospheres Regulations (DSEAR) 2002 and by similar regulations in other EU member states. These regulations require area classification to be carried out where there may be a risk of explosion due to the presence of flammable substances in the form of gases, vapours, mist or dust. Any equipment used to ensure safe operation in a classified hazardous area falls within the scope of the regulations. The regulations have major implications for all non-domestic natural gas installations. Whilst area classification has been applied to high-pressure natural gas installations in the past, it is now necessary to consider it for all pressures including distribution pressure.

Hazardous areas are classified into zones based on the frequency of the occurrence and the duration of an explosive gas atmosphere. In the case of a secondary release, the relevant zone is zone 2 and is defined as a place where an explosive atmosphere is not likely to occur in normal operation but, if it does occur, will persist for a short period only. In areas where the ventilation can be regarded as 'high' relative to the leak size, BS EN 60079:10 recommends that the area classification is zone 2 but of negligible extent (NE) such that no action is thus required to control sources of ignition within it.

This report and the work it describes were funded by the Health and Safety Executive (HSE). Its contents, including any opinions and/or conclusions expressed, are those of the authors alone and do not necessarily reflect HSE policy.

RR630

www.hse.gov.uk